

Investigating the link between acute myeloid leukaemia and the dysregulation of liver metabolism

By

Rebecca Sarah Maynard, MSci

A thesis submitted for the degree:

Doctor of Philosophy

Centre for Metabolic Health

Faculty of Medicine and Health

The University of East Anglia, Norwich, UK

Date of Submission: 1st October 2024



University of East Anglia

This copy of my thesis has been supplied on condition that anyone who consults it is understood to recognise that its copyright rests with the author and that use of any information derived there from must be in accordance with current UK Copyright Law. In addition, any quotation must include full attribution.

Declaration

I declare that the contents of this thesis entitled 'Investigating the link between acute myeloid leukaemia and the dysregulation of liver metabolism' was undertaken and completed by myself, unless otherwise acknowledged and has not been submitted in an application for another degree or qualification in this or any other university or institution.

This thesis is approximately 51,000 words in length.

A handwritten signature in black ink, appearing to read 'Rebecca Sarah Maynard', written in a cursive style.

Rebecca Sarah Maynard

Acknowledgements

The last three years have passed a lot quicker than I expected, with many highs and lows. I'm proud of the work I've done and know I wouldn't have been able to do it without the amazing people around me. I would first like to thank my supervisors Stuart and Kris; you've been fantastic mentors imparting so much guidance and encouragement, with what I'm sure was much needed patience.

I would also like to thank my lab-mates in the Rushworth lab group, especially Charlotte and Kat for the regular supply of edible moral (baked goods). Everyone in the group pitched in and helped with experiments, answered my dumb questions, and were sounding boards for my experimental plans. Thanks also go to everyone who started and/or ended this with me at the BCRE particularly Beth as a friend both in and out of the lab. Bob's was an excellent place to learn, research and make friends, the PhD has been what it was because of the people there.

Thank you to the patients who donated their blood to research so that it could be used in this study. Thank you to Dr Beraza, Dr Ruiz, and Dr Le Gall who each performed techniques outside of the remit of the Rushworth group. Thank you to the staff at the BCRE and DMU who keep the facilities going. And thank you to the many mice, who gave everything they had and without which I wouldn't have a thesis.

I would like to thank my parents, Alison and Richard, and my brothers, Joshua and Daniel, who have supported me wholeheartedly through this process. Thanks, must also go to Dougie and Camilla who generously put me up for my last month of writing. Finally, I want to thank Jamie, you have stood by me throughout the crazy ups and downs of this PhD. You all have listened to me getting excited, sad and ridiculously stressed over science. You've supported my long days and working weekends, told me to take breaks when I haven't seen the need and encouraged me to push through when the end was in sight.

Abstract

Acute myeloid leukaemia (AML) is a highly proliferative, metabolically plastic haematological malignancy. There is currently no cure and even after treatments patients often relapse. AML is addicted to fatty acid (FA) for proliferation, survival, and treatment resistance. Bone marrow (BM) adipose tissue is utilised and depleted by AML, although AML can also access FA from peripheral blood. The liver is the master regulator of FA metabolism in the body via storage, *de novo* generation and secretion back into the blood. Signals from tissues around the body modify hepatocyte FA metabolism, increasing or decreasing availability of serum FA. In this thesis I investigate how BM AML induces changes to FA metabolism in the liver.

This study shows that AML induces systemic metabolic changes within a murine model. During BM AML progression, mice lost bodyweight, and proportional weight of the inguinal and gonadal fat pads, and serum FA were elevated. Bulk RNA sequencing showed that AML engraftment significantly reduced expression of FA metabolism and peroxisome proliferator-activated receptor (PPAR) pathways in the liver, this was confirmed by gene and protein analysis in the livers of engrafted mice. Treatment of primary murine hepatocytes with media conditioned by AML cells further showed downregulated gene expression, FA uptake and respiration. Furthermore, analysis of mouse serum and conditioned media showed increased hepatocyte growth factor (HGF) and IL-1 β , which also downregulated FA metabolism *in vivo* and *in vitro*. Moreover, knockdown (KD) of *Hgf* in AML blasts mildly restored FA metabolism gene expression and reduced blast FA uptake *in vivo*. *Ppara* expression was also downregulated and, as HGF has been shown to act on PPAR α , AML engrafted mice were treated with the PPAR α agonist fenofibrate. Treatment reduced tumour burden, mildly restored liver FA metabolism gene expression, and increased serum FA. These findings show that AML secreted HGF downregulates liver FA metabolism via a PPAR α dependent mechanism.

Access Condition and Agreement

Each deposit in UEA Digital Repository is protected by copyright and other intellectual property rights, and duplication or sale of all or part of any of the Data Collections is not permitted, except that material may be duplicated by you for your research use or for educational purposes in electronic or print form. You must obtain permission from the copyright holder, usually the author, for any other use. Exceptions only apply where a deposit may be explicitly provided under a stated licence, such as a Creative Commons licence or Open Government licence.

Electronic or print copies may not be offered, whether for sale or otherwise to anyone, unless explicitly stated under a Creative Commons or Open Government license. Unauthorised reproduction, editing or reformatting for resale purposes is explicitly prohibited (except where approved by the copyright holder themselves) and UEA reserves the right to take immediate 'take down' action on behalf of the copyright and/or rights holder if this Access condition of the UEA Digital Repository is breached. Any material in this database has been supplied on the understanding that it is copyright material and that no quotation from the material may be published without proper acknowledgement.

Table of Contents

Declaration	i
Acknowledgements	ii
Abstract	iii
Table of Contents	iv
List of publications and conferences	viii
List of Figures	x
List of Tables	xiii
Abbreviations	xiv
List of genes and alternate names	xvii
1. Introduction	1
1.1 Haematopoiesis	1
1.2 The bone and bone marrow	4
1.3 Cells of the BM microenvironment	7
1.3.1 Bone marrow stromal cells	7
1.3.2 Osteo lineage cells	9
1.3.3 Adipocytes	10
1.3.4 Endothelial cells	12
1.3.5 Macrophages	13
1.3.6 Megakaryocytes	14
1.3.7 Haematopoietic stem cell niche	14
1.4 Haematological malignancies	17
1.4.1 Lymphoma	17
1.4.2 Multiple Myeloma	18
1.4.3 Leukaemia	19
1.4.4 Acute Lymphoid Leukaemia	19
1.4.5 Acute Myeloid Leukaemia	20
1.4.5.1 Acute Myeloid Leukaemia Treatment	21
1.4.5.2 The AML niche	23
1.5 AML metabolism	26
1.5.1 Glycolysis	26
1.5.2 Mitochondrial transfer	27
1.5.3 Amino acid metabolism	28
1.5.4 Fatty acid metabolism	29
1.6 The Liver	32

1.6.1	Cells of the Liver.....	33
1.6.1.1	Kupffer cells.....	35
1.6.1.2	Stellate cells	35
1.6.1.3	Hepatocytes.....	36
1.6.1.3.1	Detoxification	36
1.6.1.3.2	Protein synthesis and storage	37
1.6.1.3.3	Immune response	38
1.6.1.3.4	Metabolism	39
1.6.2	Liver FA Metabolism for energy to the rest of the body	40
1.6.2.1	Fatty acids	40
1.6.2.2	Uptake and synthesis.....	41
1.6.2.3	Storage and export	43
1.6.2.4	Ketogenesis.....	44
1.6.2.5	Cancer mediated alteration of liver FA metabolism	45
1.7	Research models.....	47
1.8	Rationale	49
1.9	Hypothesis.....	50
1.10	Aims and objectives	50
2.	Materials and methods	51
2.1	Materials.....	51
2.2	Animal models	54
2.2.1	Animal maintenance	54
2.2.2	Animal Procedures	54
2.2.2.1	Body weights and food consumption.....	55
2.2.2.2	Intravenous injections	55
2.2.2.3	Intraperitoneal injections	55
2.2.2.4	Oral gavage	55
2.2.2.5	Live <i>in vivo</i> imaging	56
2.2.2.6	Schedule 1 sacrifice.....	56
2.3	Murine tissue collection	57
2.3.1	Bone marrow isolation	57
2.3.2	Liver isolation.....	58
2.3.3	Fat pad isolation	58
2.3.4	Blood and serum isolation.....	58
2.4	Cell culture	59
2.4.1	MN1 and HOXA9/MEIS1 cells	59

2.4.1.1	<i>Hgf</i> knockdown	60
2.4.2	Conditioned media.....	60
2.4.3	Primary mouse hepatocytes	60
2.4.4	AML12s	61
2.4.5	Cell cryo preservation	62
2.4.6	Isolation of human serum.....	63
2.4.7	Cell counting.....	64
2.5	Molecular Biology	65
2.5.1	Long chain fatty acid uptake	65
2.5.2	FATP2 protein expression	65
2.5.3	Flow cytometry	66
2.5.4	Preparation of BM for flow cytometry	66
2.5.5	Preparation of liver immune cells for flow cytometry	66
2.5.6	Bulk RNA sequencing.....	67
2.5.7	Liquid chromatography mass spectrometry	67
2.5.8	Seahorse Metabolic flux analysis.....	68
2.5.9	Proteome profiler array	70
2.5.10	ELISA kits.....	70
2.5.11	PCR.....	70
2.5.11.1	RNA extraction.....	70
2.5.11.2	Quantification of extracted RNA	71
2.5.11.3	CDNA synthesis.....	71
2.5.11.4	Real time quantitative PCR	72
2.5.11.5	Gene expression.....	73
2.6	Quantification and statistics	74
3.	AML progression in the BM induces systemic metabolic changes and weight loss.....	75
3.1	Introduction.....	75
3.2	Establishing a model of AML induced weight loss and reduction of fat deposits.....	76
3.3	AML alters availability and composition of FA in the peripheral blood	92
3.4	Summary	96
4.	AML in the bone marrow alter FA metabolism in the liver.....	97
4.1	Introduction.....	97
4.2	Bulk RNA sequencing confirms aberrant metabolic pathways in the livers of mice engrafted with AML.....	99

4.3	Genes associated with FA metabolism are downregulated in the livers of AML engrafted mice.	103
4.4	Engraftment of AML reduces murine FATP2 protein expression <i>in vivo</i>	108
4.5	AML downregulates FA metabolism genes in a cell-cell independent manner.	113
4.6	AML conditioned media reduces primary hepatocyte OCR.	121
4.7	AML conditioned media reduces primary hepatocyte FA uptake.	125
4.8	Summary.	129
5.	AML secreted HGF inhibits PPARα mediated liver FA metabolism.	130
5.1	Introduction.	130
5.2	AML secreted HGF and IL-1 β downregulates FA metabolism genes in hepatocytes.	131
5.3	HGF reduces hepatocyte FA uptake and metabolism.	141
5.4	<i>In vivo</i> stimulation with HGF or IL-1 β downregulates FA metabolism genes in mouse livers.	147
5.5	AML HGF KD rescues liver FA metabolism <i>in vivo</i>	151
5.6	AML secreted HGF acts on PPAR α to reduce liver FA metabolism.	159
5.7	PPAR α agonism impairs AML progression by rescuing liver FA metabolism.	163
5.8	Summary.	170
6.	Discussion.	171
6.1	General discussion.	171
6.2	Key findings.	172
6.2.1	AML alone induces systemic metabolic alteration in a murine model.	172
6.2.2	BM resident AML downregulates liver FA metabolism.	174
6.2.3	AML secreted HGF downregulates liver FA metabolism via a PPAR α mechanism.	176
6.2.4	HGF KD in AML blasts has a restorative effect on AML induced downregulation of liver FA metabolism.	178
6.2.5	PPAR α agonism slows AML engraftment and rescues liver FA metabolism.	179
6.3	Limitations.	181
6.4	Future work.	184
6.5	Conclusions.	187
7.	References.	188

List of publications and conferences

Maynard, R., Hampton, K., Ruiz, P., Polski-Delve, A., Fowler-Shorten, D.J., Altera, A., Markham, M., Le Gall, G., Flint, T., Hellmich, C., Smith, J.G., Bowles, K.M., Beraza, N. and Rushworth, S.A. **(2024)**. Leukemia reprograms hepatic fat metabolism to support tumor proliferation. *Manuscript submitted to Cell reports*.

Markham, M., **Maynard, R.**, Bell, G., Hampton, K., Fowler-Shorten, D.J., Polski-Delve, A., Altera, A., Taylor, R. Hellmich, C., Bowles, K.M., and Rushworth, S.A. **(2024)**. Repolarisation of M2 macrophages via cGAS-STING activation enhances phagocytosis of acute myeloid leukaemia. *Manuscript submitted to Blood cancer discovery*.

Wojtowicz, E.E., Hampton, K., Moreno-Gonzalez, M., Utting, C.L., Lan, Y., Ruiz, P., Beasy, G., Bone, C., Hellmich, C., **Maynard, R.**, and Acton, L., et al, **(2024)**. Low protein diet protects the liver from Salmonella Typhimurium-mediated injury by modulating the mTOR/autophagy axis in macrophages. *Communications Biology*.

Fowler-Shorten, D.J., **Maynard, R.S.**, Hampton, K., Altera, A., Markham, M., Ehikioya, M., Wojtowicz, E.E., Bowles, K.M., Rushworth, S.A. and Hellmich, C., **(2024)**. Acute myeloid leukemia driven IL-3-dependent upregulation of BCL2 in non-malignant hematopoietic stem and progenitor cells increases venetoclax-induced cytopenias. *Haematologica*.

Blood cancer alters lipid metabolism in the liver. **Oral presentation University of East Anglia Centre for Metabolic Health Postgraduate Conference. 2024. Best oral presentation award.**

AML directs free fatty acids to the bone marrow by altering liver metabolism via cytokine release. **Poster presentation. European Haematology Association Research Conference 2024.**

Jibril, A., Hellmich, C., Wojtowicz, E.E., Hampton, K., **Maynard, R.**, De Silva, R., Fowler-Shorten, D.J., Mistry, J.J., Moore, J.A., Bowles, K.M. and Rushworth, S.A., **(2023)**. Plasma cell-derived mtDAMPs activate the macrophage STING pathway, promoting myeloma progression. *Blood*.

AML reprograms lipid metabolism by downregulating fatty acid uptake in hepatocytes. **Oral presentation. Norwich Cancer Research Network Symposium 2023.**

Acute Myeloid Leukemia Reprograms Lipid Metabolism by Downregulating CD36 Expression in Hepatocytes. **Poster presentation. European Haematology Association Annual Congress 2023. Young EHA travel award.**

STING Agonists Activate Macrophage STING and Synergizes with Anti-CD47 to Enhance Phagocytosis of Acute Myeloid Leukemia. **Poster presentation. European Haematology Association Annual Congress 2023. Young EHA travel award.**

Acute myeloid leukaemia alters lipid metabolism in the liver. **Oral presentation. University of East Anglia Faculty of Medicine and Health Postgraduate conference 2023.**

Maynard, R.S., Hellmich, C., Bowles, K.M. and Rushworth, S.A., (2022). Acute myeloid leukaemia drives metabolic changes in the bone marrow niche. *Frontiers in Oncology*.

STING Agonists Activate Bone Marrow Macrophages and Synergise with Anti-CD47 Blockade Improving Survival in Animal Models of Acute Myeloid Leukemia. **Poster presentation. American Society of Haematology Annual Meeting 2022.**

Investigating macrophage activation in repression of acute myeloid leukaemia expansion. **Poster presentation. University of East Anglia Faculty of Medicine and Health Postgraduate conference 2022.**

List of Figures

Figure 1.1 Hierarchical tree of haematopoiesis.	3
Figure 1.2 Transition of red to yellow bone marrow.....	4
Figure 1.3 The bone marrow microenvironment.....	6
Figure 1.4 Lipolysis pathway.....	11
Figure 1.5 Interactions in the HSC niche regulate HSC.....	16
Figure 1.6 AML remodels and reprogrammes the BM niche.	25
Figure 1.7 Metabolism of glucose, amino acids, and fatty acids.....	31
Figure 1.8 Liver microanatomy.....	34
Figure 1.9 Liver lipid metabolism.	46
Figure 2.1 Bone marrow isolation.	57
Figure 2.2 Isolation of human serum.....	63
Figure 2.3 Cell viability counting via Trypan blue exclusion.....	64
Figure 2.4 Seahorse metabolic flux mitostress kit.	69
Figure 3.1 MN1 cell engraftment did not cause mouse weight loss.....	77
Figure 3.2 Food intake was not altered by MN1 injection.	78
Figure 3.3 MN1 engraftment did not alter fat pad weight.....	79
Figure 3.4 Peripheral blood metabolic markers were not altered by MN1 engraftment	80
Figure 3.5 HOXA9/MEIS1 BM engraftment did not cause significant weight loss.	82
Figure 3.6 Food intake was not altered by HOXA9/MEIS1 engraftment.	83
Figure 3.7 Fat pad weight was altered by HOXA9/MEIS1 engraftment.	84
Figure 3.8 Total food restriction (tfr) did not alter bodyweight loss in HOXA9/MEIS1 engrafted mice.....	86
Figure 3.9 HOXA9/MEIS1 engraftment induced fat pad weight loss.....	87
Figure 3.10 HOXA9/MEIS1 engraftment did not alter blood metabolic markers. ...	88
Figure 3.11 Mice engrafted with AML lose weight during late stages of tumour progression.....	90
Figure 3.12 Late stages of AML engraftment cause loss of adipose tissue weight.	91
Figure 3.13 MN1 engraftment increased serum FFA.	92
Figure 3.14 Serum long chain fatty acids were elevated in AML engrafted mice...	93
Figure 3.15 AML did not induce a metabolic stress response.	95

Figure 4.1 Bulk RNAseq shows alteration in mouse liver gene expression in response to AML.....	100
Figure 4.2 FA metabolism pathways among the most significantly downregulated in mice engrafted with AML.	101
Figure 4.3 Genes associated with fatty acid metabolism pathways are dysregulated in mice engrafted with AML.....	102
Figure 4.4 MN1 cells have very low engraftment in the liver.	103
Figure 4.5 Proteins/genes associated with FA metabolism.	104
Figure 4.6 Genes associated with FA metabolism are down regulated in the liver of mice engrafted with AML.	105
Figure 4.7 MN1 engraftment downregulates liver FA metabolism genes within 2 weeks of engraftment.	107
Figure 4.8 Immunofluorescence-stained liver histology samples for FATP2.....	109
Figure 4.9 Immunofluorescence-staining of liver histology samples for Fatp2 and CD45.	110
Figure 4.10 FATP2 protein levels are decreased in mice engrafted with AML.....	112
Figure 4.11 FA metabolism is down regulated in primary murine hepatocytes cultured with MN1 cells in transwells.	114
Figure 4.12 FA metabolism genes were altered in primary murine hepatocytes treated with AML conditioned media.	116
Figure 4.13 FA metabolism genes were not altered in AML12 liver cells treated with AML conditioned media.	118
Figure 4.14 FA metabolism genes were altered in primary murine hepatocytes treated with AML conditioned media.	120
Figure 4.15 Seahorse metabolic flux mitostress kit was used to assess oxygen consumption rate.	122
Figure 4.16 Oxygen consumption rate was altered in primary murine hepatocytes treated with AML conditioned media.	124
Figure 4.17 Primary murine hepatocytes differentially take up LCFA BODPIY C12 in response to AML conditioned media.	125
Figure 4.18 Visibly less LCFA-BODIPY C12 taken up by hepatocytes pretreated with AML conditioned media.	126
Figure 4.19 LCFA-BODIPY C12 uptake is decreased in primary hepatocytes treated with AML conditioned media.	128

Figure 5.1 Cytokines associated with FA metabolism are elevated in response to AML.....	133
Figure 5.2 Primary murine hepatocyte FA metabolism genes are downregulated by IL-1 β and HGF.....	134
Figure 5.3 Low dose of IL-1 β downregulates primary hepatocyte FA genes.	135
Figure 5.4 Mouse IL-1 β monoclonal antibody (mAb) did not rescue FA metabolism genes in hepatocytes.....	137
Figure 5.5 Low dose HGF downregulates primary hepatocyte FA genes.	138
Figure 5.6 Crizotinib rescued FA metabolism expression in HGF treated primary hepatocytes.	140
Figure 5.7 Stimulation with HGF reduced LCFA BODIPY C12 uptake in primary hepatocytes.	142
Figure 5.8 HGF stimulation reduced OCR in primary hepatocytes.	143
Figure 5.9 Serum HGF is significantly increased in mice engrafted with AML	144
Figure 5.10 HGF is elevated in the serum of some AML patients.....	145
Figure 5.11 Mice stimulated with HGF and IL-1 β did not have altered liver FA metabolism genes.....	148
Figure 5.12 Repeated stimulation of HGF and IL-1 β downregulated FA metabolism genes in mouse livers.	150
Figure 5.13 Crizotinib treatment did not restore mouse liver FA metabolism.....	152
Figure 5.14 HGF KD was used to assess alterations in tumoural FA uptake.....	154
Figure 5.15 HGF KD reduced tumoural LCFA uptake.	156
Figure 5.16 HGF KD partially rescued liver FA metabolism gene expression.....	158
Figure 5.17 <i>Ppara</i> expression is downregulated by AML and HGF <i>in vivo</i>	161
Figure 5.18 <i>Ppara</i> downregulated in primary hepatocytes by AML conditioned media and recombinant HGF.....	162
Figure 5.19 Agonism of <i>Ppara</i> rescues some FA metabolism gene expression in primary hepatocytes stimulated with AML conditioned media or HGF.....	165
Figure 5.20 Fenofibrate is not toxic to MN1 cells.....	165
Figure 5.21 Fenofibrate treatment reduces AML engraftment and neutral lipid storage.	166
Figure 5.22 Fenofibrate treatment rescues liver FA metabolism genes.....	167
Figure 5.23 Fenofibrate treatment restored serum FFA in mice engrafted with AML.	169

List of Tables

Table 2.1 Reagents used, with manufacturer and catalogue ID.	51
Table 2.2 Primers used in RT-qPCR analysis	72
Table 2.3 qPCR SYBR-Green Quantstudio 7 programming	73
Table 5.1 Patient details for collected samples.	146

Abbreviations

Acadm	Acyl-Coenzyme A dehydrogenase medium chain
ALL	Acute lymphoblastic leukaemia
AML	Acute myeloid leukaemia
AML 12	Alpha male liver cells – 12 weeks
ATGL	Adipose triglyceride lipase
ATP	Adenosine-5'-triphosphate
BLC-2	B-cell lymphoma-2 protein
BM	Bone marrow
BMAT	Bone marrow adipose tissue
BMSC	Bone marrow stromal cells
BSA	Bovine serum albumin
CAR	CXCL12-abundant reticular
CAR-T	Chimeric antigen receptor T-cells
CLP	Common lymphoid progenitor
CMP	Common myeloid progenitor
CPT1a	Carnitine palmitoyltransferase 1A
CXCL12	Stromal cell-derived factor 1
CXCR4	C-X-C chemokine receptor type 4
DGAT	Diacylglycerol acyltransferase
DMEM	Dubecco's modified eagle's medium
DMSO	Dimethyl sulfoxide
ECM	extracellular matrix
EDTA	Ethylenediaminetetraacetic acid
ER	Endoplasmic reticulum
FA	Fatty acid
FABP	Fatty acid binding proteins
FAO	FA β -oxidation
FATP	Fatty acid transport proteins
FBS	Foetal calf serum
FFA	Free fatty acids
G-CSF	Granulocyte colony stimulating factor
GM-CSF	Granulocyte-macrophage colony stimulating factor
GMP	Granulocyte-monocyte progenitors

HDL	High-density lipoproteins
HGF	Hepatocyte growth factor
HIF1α	Hypoxia-inducible factor-1 α
HMGCS2	3-hydroxymethylglutaryl CoA synthase
HOXA9	Homeobox Protein A9
HSC	Haematopoietic stem cells
HSL	Hormone sensitive lipase
HSPC	Haematopoietic stem and progenitor cells
IL	Interleukins
IP	Intraperitoneal
IV	Intravenous
KD	Knockdown
LCFA	Long chain fatty acid
LD	Lipid droplets
LDL	Low-density lipoproteins
LepR	Leptin receptor
Lin⁻	Lineage negative
LMPP	Lymphoid-primed multipotent progenitor
LSC	Leukaemic stem cells
LSK	Lineage negative, CD117 positive, Sca1 positive
LXR	Liver X receptors
mAb	Monoclonal antibody
MACS	Magnetic-activated sorting
MEM	Minimum essential medium
MEP	Megakaryocyte-erythrocyte progenitor
MEIS1	Meis Homeobox 1
MGL	Monoglyceride lipase
MK	Megakaryocyte
MN1	Meningioma
MM	Multiple myeloma
MOI	Multiplicity of infection
MPP	Multipotent progenitor cells
MSC	Mesenchymal stem cells
NAFLD	Non-alcoholic fatty liver disease
NK	Natural T-killer

OCR	Oxygen consumption rate
OXPHOS	Oxidative phosphorylation
PBS	Phosphate-buffered saline
PI3K	Phosphatidylinositol 3-kinase
PLIN	Perilipin
PPAR	Peroxisome proliferator-activated receptor
RNAseq	RNA sequencing
ROS	Reactive oxygen species
RT-qPCR	Real time quantitative PCR
SCF	Stem cell factor
SLC	Solute carrier family
SLC27A2	Solute carrier family 27, member 2
SREBP-1c	Sterol regulatory element binding protein-1c
TCA	Tricarboxylic acid
TFR	Total food restriction
TGF-β	Transforming growth factor beta
TNF	Tumour necrosis factor
TNT	Tunnelling nanotubules
VEGF	Vascular endothelial growth factor
VLDL	Very low-density lipoproteins

List of genes and alternate names

Gene names have been listed with alternate names where the gene may be commonly known by another name. The final column contains the gene symbol in the format for human genes. Throughout the thesis standard gene and protein nomenclature has been followed as: human genes are written in all capitals and italicised and proteins are all capitals in standard font. For mice genes have been written with only the first letter capitalised and italicised. For mouse proteins they are written in all capitals and standard font.

<u>Gene name</u>	<u>Alternate Names</u>	<u>Gene Symbols</u>
3-Hydroxy-3-Methylglutaryl-CoA Synthase 2		<i>HMGCS2</i>
Activated Leukocyte Cell Adhesion Molecule		<i>CD166</i>
Acyl-CoA Dehydrogenase Medium Chain		<i>ACADM</i>
Albumin		<i>ALB</i>
B-Cell Lymphoma 2		<i>BCL-2</i>
Carnitine Palmitoyltransferase 1A		<i>CPT1A</i>
CD3 Gamma Subunit Of T-Cell Receptor Complex		<i>CD3</i>
CD33 Molecule		<i>CD33</i>
CD47 Molecule		<i>CD47</i>
Chondroitin Sulfate Proteoglycan 4		<i>MCSP, NG2</i>
C-X-C Chemokine Receptor Type 4	Fusin	<i>CXCR4</i>
E-Selectin		<i>CD62E, SELE</i>
Fatty Acid Binding Protein 4		<i>FABP4, AP2</i>
Fms Related Receptor Tyrosine Kinase 3		<i>FLT3, CD135</i>

Glyceraldehyde-3-Phosphate Dehydrogenase		<i>GAPDH</i>
Granulocyte Colony Stimulating Factor	Pluripoietin	<i>G-CSF</i>
Granulocyte-Macrophage Colony Stimulating Factor		<i>GM-CSF</i>
Hepatocyte Growth Factor	Scatter Factor	<i>HGF, SF</i>
Hepatocyte Nuclear Factor 4 Alpha		<i>HNF4α</i>
Homeobox Protein A9		<i>HOXA9</i>
Interleukin 1 beta	Catabolin	<i>IL1B, IL-1β</i>
Interleukin 3	Hematopoietic Growth Factor	
Interleukin 6		<i>IL-6</i>
Interleukin 7		<i>IL-7</i>
KIT Ligand	Stem Cell Factor	<i>KITLG, SCF</i>
KIT Proto-Oncogene Receptor Tyrosine Kinase		<i>CD117, KIT, c-KIT</i>
Leptin Receptor		<i>LEPR, CD295</i>
Lipocalin 2		<i>LCN2, NGAL</i>
Mechanistic Target of Rapamycin Kinase		<i>mTORC1</i>
Meis Homeobox 1		<i>MEIS1</i>
Melanoma Cell Adhesion Molecule		<i>CD146, MCAM</i>
Meningioma		<i>MN1</i>
Nuclear Receptor Subfamily 1 Group H Member 3	Liver X Receptor-Alpha	<i>LXR, NR1H3</i>
Patatin Like Phospholipase Domain Containing 2	Desnutrin	<i>PNPLA2, ATGL</i>
Perilipin		<i>PLIN</i>

Phosphatidylinositol-4,5-Bisphosphate 3-Kinase Catalytic Subunit Alpha		<i>PI3K</i>
Proliferator-Activated Receptor Alpha		<i>PPARα</i>
RUNX Family Transcription Factor 2	Osteoblast-Specific Transcription Factor 2	<i>RUNX2</i>
Scavenger Receptor	Fatty Acid Translocase	<i>CD36, FAT</i>
Solute Carrier Family 1 Member 5		<i>SLC1A5</i>
Solute Carrier Family 2 Member 1	Glucose Transporter Type 1	<i>GLUT1, SLC2A1</i>
Solute Carrier Family 27 Member 2	Long-Chain Fatty Acid Transport Protein 2	<i>SLC27A2, FATP2</i>
Sterol Regulatory Element Binding Transcription Factor 1		<i>SREBP-1C</i>
Stromal Cell-Derived Factor 1	Chemokine Ligand 12	<i>CXCL12, SDF1</i>
Syndecan 1		<i>CD138, SDC1</i>
Thyroid Peroxidase		<i>TPO</i>
Transforming Growth Factor Alpha		<i>TGFα</i>
Transforming Growth Factor Beta 1		<i>TGFβ-1</i>
Tumor Protein P53		<i>TP53</i>
Vascular Endothelial Growth Factor		<i>VEGF</i>

1. Introduction

1.1 Haematopoiesis

Haematopoiesis is the process by which all the blood cells in the body are produced. It is a hierarchical differentiation process starting with haematopoietic stem cells (HSC) and ending in mature blood cells (1). It is an incredibly complex but organised process which occurs in three main waves during human development. During the earliest stages of development there are no HSC, and the primitive wave begins in the yolk sac as blood islands. At this stage, cells such as erythroid, megakaryocytes and macrophages are produced. These provide the red blood cells, platelets and primitive immunity. The second wave of haematopoietic development occurs with the production of vasculature, taking place in the haemogenic endothelium of the yolk sac. It is at this stage that erythromyeloid progenitors are produced. These first two waves make up HSC independent haematopoiesis, while also providing the necessary signals for HSC emergence (2-4). These signals and the emergence of HSC signal the third wave of haematopoietic development, forming the aorta-gonads-mesophryon region. After this point haematopoietic stem and progenitor cells (HSPC) home to the foetal liver, which remains the principal location of haematopoiesis until later stages of gestation (5). It is only later that HSC relocate to the bone marrow (BM), where the majority of haematopoiesis occurs for the rest of a person's life (6). During times of haematopoietic stress, it is possible for haematopoiesis to also occur in the spleen and liver (7). This allows the body to rapidly respond to increased demand for blood cells.

The HSC are at the heart of haematopoiesis, defined by their ability for self-renewal and pluripotency that allows them to produce all the blood cell types (8). In average, healthy individuals (70kg), these HSC produce an estimated 1×10^{12} mature blood cells a day (9). In adults, these long-term HSC reside in specific hypoxic niche microenvironments and remain mostly non-replicative and quiescent (10). However, under stress stimuli, such as infection or severe blood loss, quiescent HSC are activated to begin cell cycling and increase progenitor cells for expansion of circulating blood cells (11). This is a complex and highly regulated system, balancing the requirements for blood cells, while maintaining pro-survival quiescence.

HSC are at the apex of the haematopoietic tree as the most potent cells (Figure 1.1). The HSC pool is heterogeneous, with the cells diverse in their range of self-renewal ability and differentiation potential. The pool is comprised of long-term, intermediate, and short-term HSC as well as multipotent progenitor cells (MPP) (12, 13). HSC undergo a series of lineage commitments which gives rise to haematopoietic progenitor cells (HPC). These include the common myeloid progenitor (CMP) and lymphoid-primed multipotent progenitor (LMPP) cells (13). These progenitor cells both contribute to granulocyte-monocyte progenitors (GMP), which further differentiate to granulocytes; neutrophils, basophils, eosinophils, monocytes, and macrophages (8, 14). LMPPs also give rise to common lymphoid progenitors (CLP) which further differentiate to produce T-lymphocytes, natural T-killer (NK) cells, or B-lymphocytes that can differentiate into antibody producing plasma-cells and memory B-lymphocytes (8, 15). CMPs differentiate to the megakaryocyte-erythrocyte progenitor (MEP) cells that result in megakaryocytes, for the production of thrombocytes, and erythrocytes (7, 8). This is a simplified model of the haematopoietic tree, with increasing evidence that HSC are able to bypass the traditional pathways directly generating more mature cells. As such, it has been seen that there is more of a continuum of differentiation, where terminally fated blood cells emerge from undifferentiated HSPC, without the traditional steps of differentiation required (16). This may confer advantages for rapid responses to stimuli.

Due to their role in producing all subsequent blood cells, it is vitally important that HSC have the correct niche within the bone marrow to enable them respond to stimuli. The HSC niche is kept hypoxic by arterial blood being relatively deoxygenated when it gets to the BM. The low oxygen tension maintains quiescence in HSPC by keeping oxidative stress low (17). These conditions stabilise transcriptional regulators such as hypoxia-inducible factor-1 α (HIF-1 α) protein, which regulates the hypoxia response, and the related downstream effectors (18). Hypoxia pushes glycolysis as the main source of adenosine-5'-triphosphate (ATP) for HSC which confers survival advantages, such as surviving a hypoxic episode that most other cells would not (19). Taken together, this shows us that to understand the process of haematopoiesis, we must also understand the niche within which it occurs.

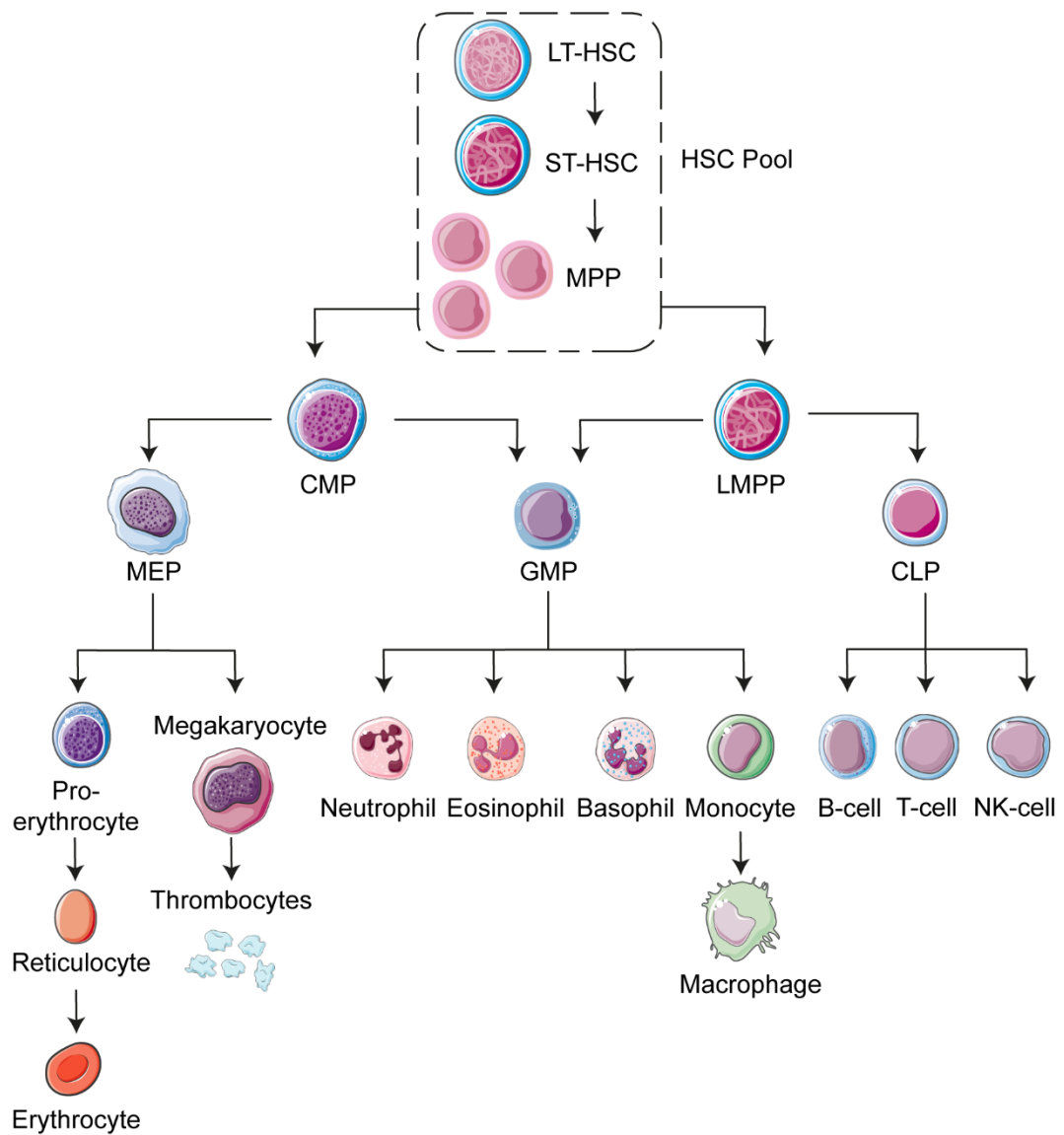


Figure 1.1 Hierarchical tree of haematopoiesis.

Haematopoiesis is the perpetual self-renewal and production of mature blood cells from immature haematopoietic stem cells (HSC). Long-term HSC are quiescent and rarely differentiate and so they remain contained within a pool of HSC. The pool also includes more mature HSC, such as short-term HSC and multipotent progenitor cells (MPP). These cells can further differentiate towards progenitors, such as common myeloid (CMP) and common lymphoid (CLP) progenitors, which go on to develop the various types of blood cells required by the body. During a strong stress response, it is possible for cells to bypass the multi-step differentiation pathway. LMPP -lymphoid multipotent progenitor, MEP -megakaryocyte-erythrocyte progenitor, GMP -granulocyte-monocyte progenitors, NK-cell –natural killer cells.

1.2 The bone and bone marrow

The bones of our body are made up of two main components; the hard outer layer, known as the cortical bone and the more porous, spongy inner structure, called the trabecular bone. Together this structure provides the rigidity required for the skeleton to support our body, but also provides the niche for the BM (20). The BM is a complex tissue which is soft and spongy and fills the space of the trabecular bone. It is made up of blood, vessels, nerve tissue, and a heterogeneous population of cells (21). The main two forms of the BM are red and yellow marrow. The Red marrow is comprised of cells which are directly required for, or supportive of, haematopoiesis (22). The yellow marrow is primarily made up of adipocytes and serves as a storage reserve for fats, which can be metabolised for energy during times of stress or starvation. As we age the ratio of red to yellow marrow shifts as the yellow marrow displaces the red marrow (Figure 1.2) (23).

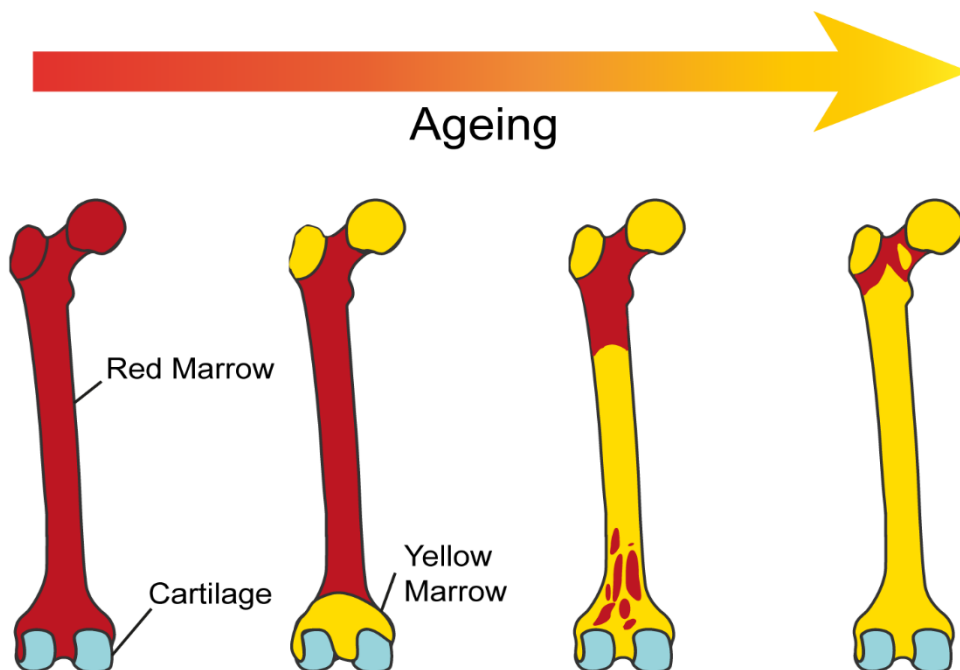


Figure 1.2 Transition of red to yellow bone marrow.

Schematic diagram of age-related bone marrow conversion. During aging adipocyte rich yellow marrow displaces red marrow, reducing the volume of haematopoietic tissue. (Adapted from Chiarelli, et al. 2021).

The BM is connected to the peripheral blood via a network of vascular sinuses. In flat bones, this is through vessels entering the BM via small or large nutrient canals (Figure 1.3A). Long bones are supplied via nutrient canals consisting of nutrient veins and the main nutrient artery which enters the BM cavity longitudinally through the centre of the bone. Branches off the canal supply the rest of the BM via thin-walled arterioles and capillaries. These accumulate to form specialist vascular sinuses, which can be venous or arterial (24). Venous sinuses are comprised of thin-walled endothelial cells without a basement membrane. The venous sinuses drain via collecting venules which return the blood to the centre of the cavity. This results in a circular blood flow process, with blood entering through the central cavity and being moved peripherally, before drainage back to the centre cavity (25). Innervation of the bone is distributed similarly to the nutrient arteries by both myelinated and non-myelinated nerve cells. The nerves run through the arterials and innervate the vessels all the way through to the haematopoietic tissue within the BM. This allows regulation of both haematopoiesis and bone formation via the central nervous system (26). Taken together, this shows a high level of structural complexity within the BM.

The BM cavity comprises four main niches: central, perisinusoidal, endosteal, and sub-endosteal (27). Histology and functional assays show that HSC and MPP predominantly reside in the perivascular/sinusoidal niches and are closely associated to the surface of the bone (28-30). Increasingly mature cells home to the central and perisinusoidal regions with the most mature, differentiated cells at the latter (31). The complexity of the organisation within the BM allows for more efficient haematopoiesis (Figure 1.3B).

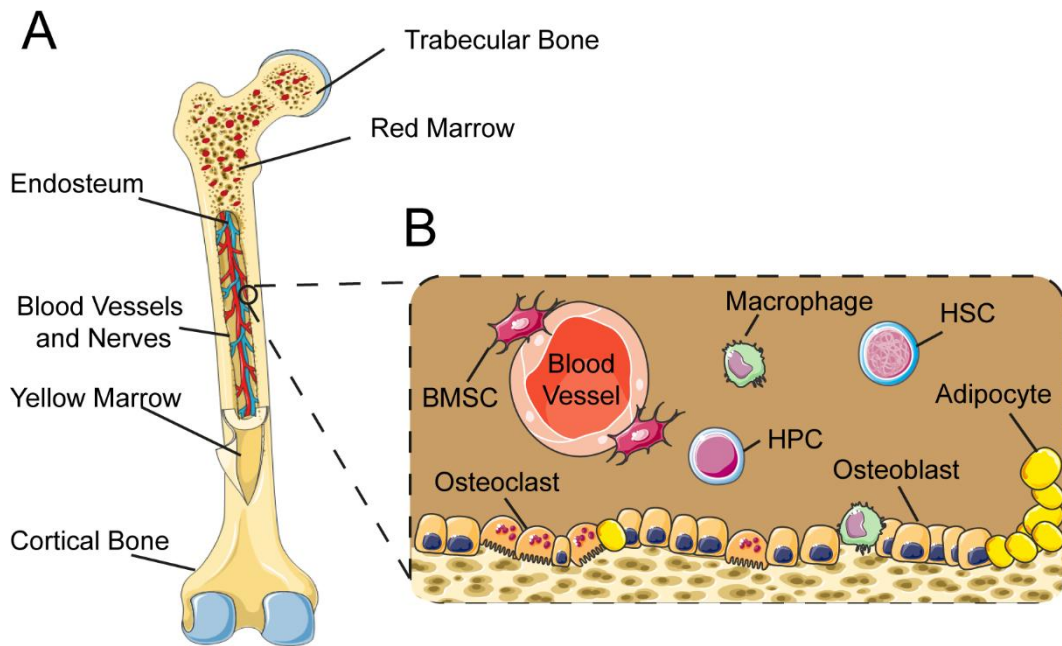


Figure 1.3 The bone marrow microenvironment.

(A) The unique mechanical anatomy of the bone is provided by the cortical and trabecular bone. The endosteum encases blood vessels, nerves, and the red marrow. Yellow marrow fills the remaining porous space. (B) Haematopoietic stem cells (HSC) and Haematopoietic progenitor cells (HPC) reside in the endosteal or sinusoidal niche, with more mature cells in more oxygenated niches. They remain close to the blood vessels and other BM cells such as osteoblasts, osteoclasts, macrophages, adipocytes and bone marrow stromal cells (BMSC). These cells provide the support and signals to maintain haemostasis.

1.3 Cells of the BM microenvironment

The BM microenvironment is highly complex with different niches and cavities maintaining different roles in haematopoiesis (32). It has therefore been a key area of research for infection and malignancy over recent years. Several studies have looked at the interactions between malignant haematological cells and non-haematopoietic cells within the BM, and how these aid in the survival and proliferation of these malignant cells (33-35).

The multitude of cells within the BM microenvironment play an important role in supporting HSPC quiescence and the process of haematopoiesis. The makeup of the niches within the BM creates optimal environments for HSPC proliferation and differentiation potential (27). Recent studies have shown that HSPC reside in a perivascular niche, where cells such as mesenchymal stem cells (MSC) and endothelial cells secrete factors to support the maintenance of HSPC (36, 37). It is also known that other cells of the BM microenvironment are able to directly and indirectly affect the HSC niche (11, 38). These interactions ensure that the niche is correct for the demands on the HSC for blood cells.

1.3.1 Bone marrow stromal cells

Bone marrow stromal cells (BMSC), also known as mesenchymal stem cells, have a varied role in the BM microenvironment. They are identified by markers such as CD146 and are found around the vasculature and sinusoids of the BM (38, 39). They are a multipotent cell type which is imperative to the BM as they have the ability to repopulate tissues such as adipose tissue, cartilage, muscle, tendon, ligament and, bone. To do this BMSC have the potential to differentiate into the required cells such as osteoblasts, adipocytes, and chondrocytes (40, 41). BMSC and their daughter cells are important for creating a supportive microenvironment for HSPC. BMSC have an autocrine and paracrine effect on HSPC via the release of factors such as Interleukins (IL)-1, -6, -7, -8, -11, -14 and, -15, stem cell factor (SCF), Transforming growth factor beta (TGF- β), and leukaemia inhibitory factor (41-43). These are essential to the homeostasis of haematopoiesis.

Two key factors that BMSC release are SCF and stromal cell-derived factor 1 (CXCL12). When these are conditionally deleted from BMSC *in vitro*, HSC are depleted or lost, thus highlighting the importance of BMSC in haematopoiesis (44). SCF is crucial for HSC maintenance and can be secreted in a soluble form or presented as membrane bound. It acts to regulate proliferation when it binds to its receptor CD117 on the HSC (45-47). It has also been shown to be essential for culturing HSC *in vitro* (46). CXCL12 released by BMSC is an important chemokine for promoting the retention of HSC to the niche. It acts by binding and activating the C-X-C chemokine receptor type 4 (CXCR4) on the HSC (36). Without this interaction there is a reduction of the number of HSC in the BM (48). CXCL12 has also been shown to play a role in relocation of the HSC to the peripheral blood or spleen (49). These further indicate the importance of BMSC within the BM niche for the maintenance of haematopoietic homeostasis.

BMSC can be further divided into distinct populations with different functional roles in regulating HSC (50). Three of the studied populations are CXCL12-abundant reticular (CAR) cells, NG2⁻, leptin receptor (LepR)⁺ stromal cells, and NG2⁺ leptin receptor (LepR)⁻ stromal cells (51). As is suggested in the name, CAR cells produce CXCL12. They have the capacity to differentiate into osteoblasts and adipocytes (52) and a depletion of CAR cells results in lower numbers of HSC due to less SCF and CXCL12 (36, 39). NG2⁻, LepR⁺ cells differ from CAR cells as they are unable to differentiate into osteoblasts (53). These cells form perisinusoidal niches and regulate HSC proliferation by inhibiting HSC cycling (53, 54). NG2⁺, LepR⁻ maintain HSC quiescence within the arteriole niche (54). The distribution between the niches is dependent on the activation of HSC cycling (44). The commonality of SCF and CXCL12 expression dictate that these cell types are all BMSC.

Taken together the above information shows the importance of BMSC within the BM microenvironment. Both with their role in maintaining the HSC niche and cycling, but also in their ability to differentiate into other cells required for haematopoietic homeostasis.

1.3.2 Osteo lineage cells

Osteo lineage cells are one of the cell types that BMSC cells can differentiate into. These include immature and mature osteoblasts, and osteocytes (44). These cells are important for the regulation of bone formation. Osteoblasts are responsible for the formation of new bone and as such, are found at the surface of them (20). Differentiation of BMSC to osteoblasts requires the transcription factor RUNX2 to be switched on (55). The major role of mature osteoblasts is formation of new bone, via proliferation and matrix maturation, they also play a role in haematopoiesis (56). HSC are found close to osteoblasts unlike more mature progenitor cells which are located further away (57). Increased numbers of osteoblasts have been linked to increased long-term HSC (58, 59), and development of other cell types. Osteoblast progenitors have been found to support the differentiation of B-lymphocytes via the release of IL-7 (60, 61). Immature osteoblasts are denoted by their higher *Runx2* expression. Studies have shown that these cells mediate haematopoiesis-enhancing activity, including HSC regulation via CD166 (62). (56). Mature osteocalcin positive osteoblasts produce DLL4, a notch ligand, which is essential for the development of CLP to T-lymphocytes (63). Together these studies show the important role osteoblasts may have in HSC maintenance and the production of mature lymphocytes.

Osteoblasts further differentiate into osteocytes. This occurs when osteoblast become embedded within the new bone matrix. These cells are important for detecting mechanical stresses, triggering a signal cascade to osteoblasts and osteoclasts (64, 65). Osteocytes still have an important role in haematopoiesis support, despite being embedded in the bone. They play a role in supporting stromal cells, as well as being indicated in the HSPC migration response to granulocyte colony stimulating factor (G-CSF) (66). These studies indicate the importance of osteocytes in the migration and support of HSPC and mature blood cells.

Osteoclasts also play an important role in the BM microenvironment. However, they are not derived from BMSC, they are produced from GMP (67, 68). These cells are important for maintaining the balance of bone formation. This is a dynamic process which requires the formation of new bone by osteoblasts and subsequent resorption by osteoclasts (69, 70). This makes them important for the maintenance of the HSC niche.

1.3.3 Adipocytes

BMSC also differentiate into adipocytes, the most abundant of the stromal cells. They can occupy up to 70% of adult long bone cavities, making up the BM adipose tissue (BMAT) (71). Interestingly, BMAT can form up to 10% of the adipose tissue in healthy humans (72). As stated in 1.2, the yellow marrow, which is mostly adipocytes, increases its volume during aging. Increases in yellow marrow are also seen in osteoporosis (73) and obesity (74). The main transcription factors pushing BMSC to differentiate into adipocytes, in a process called adipogenesis, are peroxisome proliferator-activated receptor (PPAR) γ and CCAAT/enhancer-binding protein alpha (75). BM adipocytes are required as an energy store and source, as well as playing a role in endocrine function and bone metabolism (72, 76). It is important that they are able to store high levels of fat, as this regulates bone metabolism. The fat is stored as lipid droplets (LD) of triglycerides. These undergo the catabolic process of lipolysis into free fatty acids (FFA) and glycerol (77) (Figure 1.4). Therefore, adipocytes play an important part in the BM microenvironment, with multiple roles.

Adipocytes are also important for the regulation of HSPC. They negatively regulate granulopoiesis via cell-cell interaction with neuropilin-1 (78). Adipocytes secrete various factors such as cytokines and adipokines. For example, studies show that Lipocalin 2 produced by adipocytes blocks differentiation of erythroid progenitors (79), and TGF- β 1 inhibits HSC cell cycling (42). It has been shown that the number of HSC is negatively correlated with the number of adipocytes in the BM (80). More recent studies have indicated that adipocytes may be able to directly maintain HSC populations and promote their regeneration, especially after high stress conditions (81). Adipocytes can secrete SCF (82), CXCL12, IL-3 and, IL-8 (83), all of which have been characterised to play a role in HSC maintenance. Under stress conditions adipocytes can donate FFA as a source of energy to HSC for β -oxidation. This is achieved via increased expression of lipolysis genes in the adipocytes, such as *Pnpla2* (84), or expression of fatty acid (FA) uptake proteins on HSC, such as *Cd36* and fatty acid transport proteins (*Fatp*), which are encoded for by some of the solute carrier family (SLC) genes (85). These genes are upregulated during a stress response, such as infection, to maximise HSC ATP production, and increase proliferation and differentiation to respond to the stimuli (86). It is inconclusive what all the roles of the adipocytes are within the BM. This is due to the difficulties in

isolating and culturing adipocytes from humans and mice. Further studies will be required to fully elucidate the role of adipocytes in the BM microenvironment.

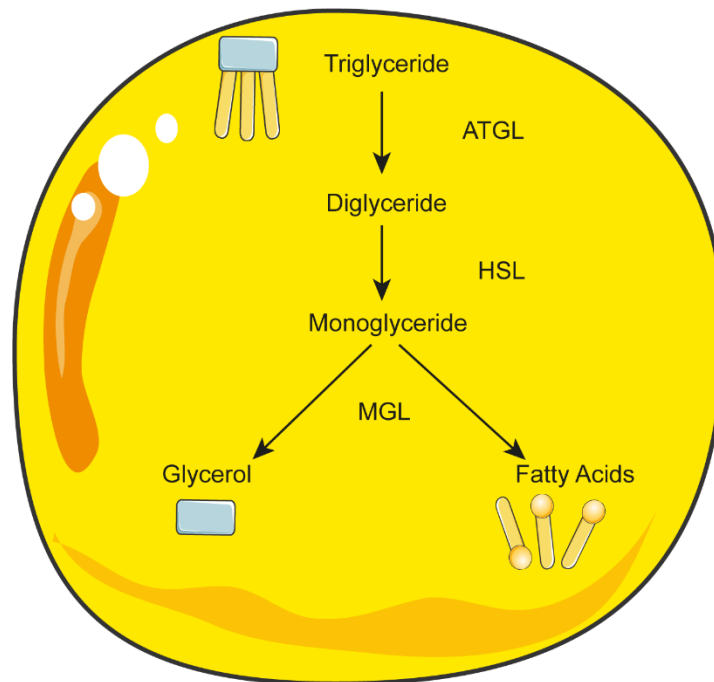


Figure 1.4 Lipolysis pathway.

Triglycerides are broken down in steps by adipose triglyceride lipase (ATGL), hormone sensitive lipase (HSL), and monoglyceride lipase (MGL). The result is glycerol and fatty acids.

1.3.4 Endothelial cells

Endothelial cells are also derived from BMSC and make up the lining of the blood vessels. They are major regulators of metabolism, oxygen availability and homeostasis by forming these connecting networks throughout the BM (37). They are able to modulate cell trafficking by creating a barrier, allowing mature cells into the peripheral blood while preventing circulating mature red blood cells and platelets from unnecessarily entering the BM (87). Endothelial cells make up part of the perivascular niche, alongside BMSC, that HSC reside in, and therefore are able to play a role in HSC trafficking and quiescence (88). Due to the varied vasculature in the BM, different vessels have different properties (89). More permeable vessels at the sinusoids allow for trafficking of mature and immature leukocytes to and from the BM. The high permeability in these areas increases the HSC exposure of reactive oxygen species (ROS), this enriches migration and differentiation, while compromising the HSC capacity for self-renewal. On the other hand, less permeable vessels maintain a lower ROS, which promotes HSC quiescence (90). This therefore shows that endothelial cells can influence HSC and their location dictates the state of the HSC.

Endothelial cells express markers and release key cytokines to regulate HSC. These include the expression of *E-SELECTIN*, which is unique to endothelial cells and modulates quiescence (91). Endothelial cells also release G-CSF, IL-6 and granulocyte-macrophage colony stimulating factor (GM-CSF), upon stimulation by proinflammatory cytokines, all of which are known to regulate HSC maintenance (92). Additionally endothelial cells release the factor pleiotrophin and express vascular adhesion molecule 1, which act to retain HSC within the BM (93, 94). These show the importance of endothelial cells, and the vessels they make up, within the BM microenvironment.

1.3.5 Macrophages

Macrophages are a mononuclear haematopoietic cell type derived from CMP (Figure 1.1). They play a critical role in the immune response, with functions in both the innate and adaptive immune systems (95). Macrophages have a number of roles within the immune system, from phagocytosis of microbes and parasites to clearance of cell debris from cells undergoing apoptosis or cell modification (96). Macrophages also activate B and T-lymphocytes through the secretion of cytokines, chemokines, and cell-cell interaction (97). Macrophages can be activated to play a pro- or anti-inflammatory role, allowing them to aid in regeneration or destruction of tissues (95).

Most tissues have tissue resident macrophages, and this is true for the BM (98). It has been indicated the BM resident macrophages are important for HSC modulation. BM macrophages induce niche supporting cells to produce the homing signal CXCL12 and studies have shown that depleting these macrophages results in increased circulating HSPC, due to a depletion of niche-specific CXCL12 (96, 99). However, macrophages are also able to release G-CSF, which suppresses CXCL12 expression, thus causing HSC mobilisation (66). This process is linked with macrophage clearance of neutrophils and suppression of granulopoiesis within the BM, as accumulation of these cells can cause an inflammatory response in the BM, liver, and spleen (100). This process occurs with circadian rhythms to maintain homeostasis. When macrophages phagocytose neutrophils it suppresses IL-23, a key regulator in G-CSF and IL-12 dependent neutrophil differentiation (101). This process induces HSC mobilisation via the reduction of niche CXCL12 by circadian rhythms and Liver X receptors (LXR) signalling (102). This process curbs granulopoiesis and mobilises HSC in the BM. Taken together these studies show an important role of BM macrophages in haematopoiesis by regulation of granulopoiesis and trafficking of HSC.

1.3.6 Megakaryocytes

Megakaryocytes (MKs) are the largest cells in the BM, and they differentiate from HSC. As well as the largest, MK cells are one of the rarest cell types in the BM, accounting for up to 0.1% of the cells (103). MKs are the cells which produce thrombocytes/platelets and are therefore located centrally, near the sinusoids, to allow thrombocytes to enter into circulation quickly (45). MKs also play an important role in bone formation and the maintenance and quiescence of HSC. Like other cells of the BM, MKs release CXCL4 to maintain HSC pools. Removal of MKs has been shown to cause HSC proliferation and differentiation (104), further supporting the role of MKs in the maintenance of HSC. Another cytokine released by MKs is Thyroid Peroxidase (TPO). Not only is TPO required for the differentiation of HSC to MKs, but it has also been shown to play an important role in the regulation of HSC (105). TPO has been shown to support HSC quiescence and competitive transplants experiments showed that removal of the cytokine or its receptor from the niche reduced the capacity to reconstitute the BM (106, 107). Furthermore, *Tpo* knockout mice have been shown to have age progressive loss of HSC and increased HSC cell cycling (108). These studies, providing evidence that TPO released by MKs is required for HSC numbers and maintenance within the healthy BM. Interestingly, MKs can also have an indirect effect on HSC via the release of adiponectin, which acts on osteoblasts (109). MKs have the ability to maintain HSC pools via negative regulation to keep a quiescent state.

1.3.7 Haematopoietic stem cell niche

The haematopoietic stem cell niche is important for the regulation and maintenance of HSC. It dictates the state of quiescence or proliferation that the HSC is in (11). The cells described above all make up the composition of the HSC niche, each sending signals in the form of secreted factors and membrane bound proteins. The niche is made up of progenitor cells from all of the lineages, as well as the mature cells.

Figure 1.5 shows that stromal cells interact with the HSC via release of IL-6, IL-8, SCF and, CXCL12 (36, 43). These cells can also differentiate into osteoblasts, which produce IL-7 and CD166 which promote B-lymphocyte differentiation and haematopoietic-enhancing activity, respectively (60, 62). Adipocytes release FFA for

the HSC to use as an energy source for differentiation (77). They also release TGF- β 1 which inhibits HSC cell cycling (42). Endothelial cells express *E-SELECTIN* to regulate quiescence, as well as pleiotrophin which acts to retain the HSC within the niche. Macrophages promote the expression of *CXCL12* within the HSC niche (99). However, macrophages and endothelial cells also produce G-CSF which induces migration of HSC from the niche (66, 92). All these interactions help to maintain homeostasis of haematopoiesis and contribute to the highly complex HSC niche.

Despite the perivascular location, the HSC niche is hypoxic due to the blood becoming relatively deoxygenated by the time it reaches the BM (38). This hypoxic condition is favourable for HSC quiescence, minimising oxidative stress. Thus, in steady state, HSC rely on anaerobic glycolysis for their metabolic source of ATP (110). This retains low mitochondrial mass and function. Balancing the processes of mitochondrial biogenesis and mitophagy to maintain low mitochondrial ROS to keep HSC homeostasis (11). This changes during a stress response, such as infection. During stress the BM becomes more acidic due to an increased production of lactate, a by-product of glycolysis (111), however it has also been shown that lactate can be fed into the tricarboxylic acid (TCA) cycle, alongside pyruvate, for oxidative phosphorylation (OXPHOS) production of ATP (112). The BM is also full of adipocytes, which contain triglycerides stored in LD. These can be released as glycerol and FFA (77). These can be used by the HSC for β -oxidation and downstream ATP production. FA β -oxidation (FAO) occurs within the mitochondria and breaks down the FA into acetyl-CoA which can be fed into the TCA cycle (113). HSC are able to acquire these FA from adipocytes by upregulating FA transport genes such as the scavenger receptor CD36 and FATP (85, 114). Another way in which the HSC are able to increase their metabolism during a stress response, is the acquisition of more mitochondria. This is achieved via three main methods: tunnelling nano-tubules, via gap junctions, or extracellular vesicles (19, 115). These interactions aid the HSC in responding to a stress response and proliferating at an increased rate, to meet the demand for more blood cells. This shows the importance of the BM microenvironment and the complexity of the HSC protein expression and secretome to maintain homeostasis.

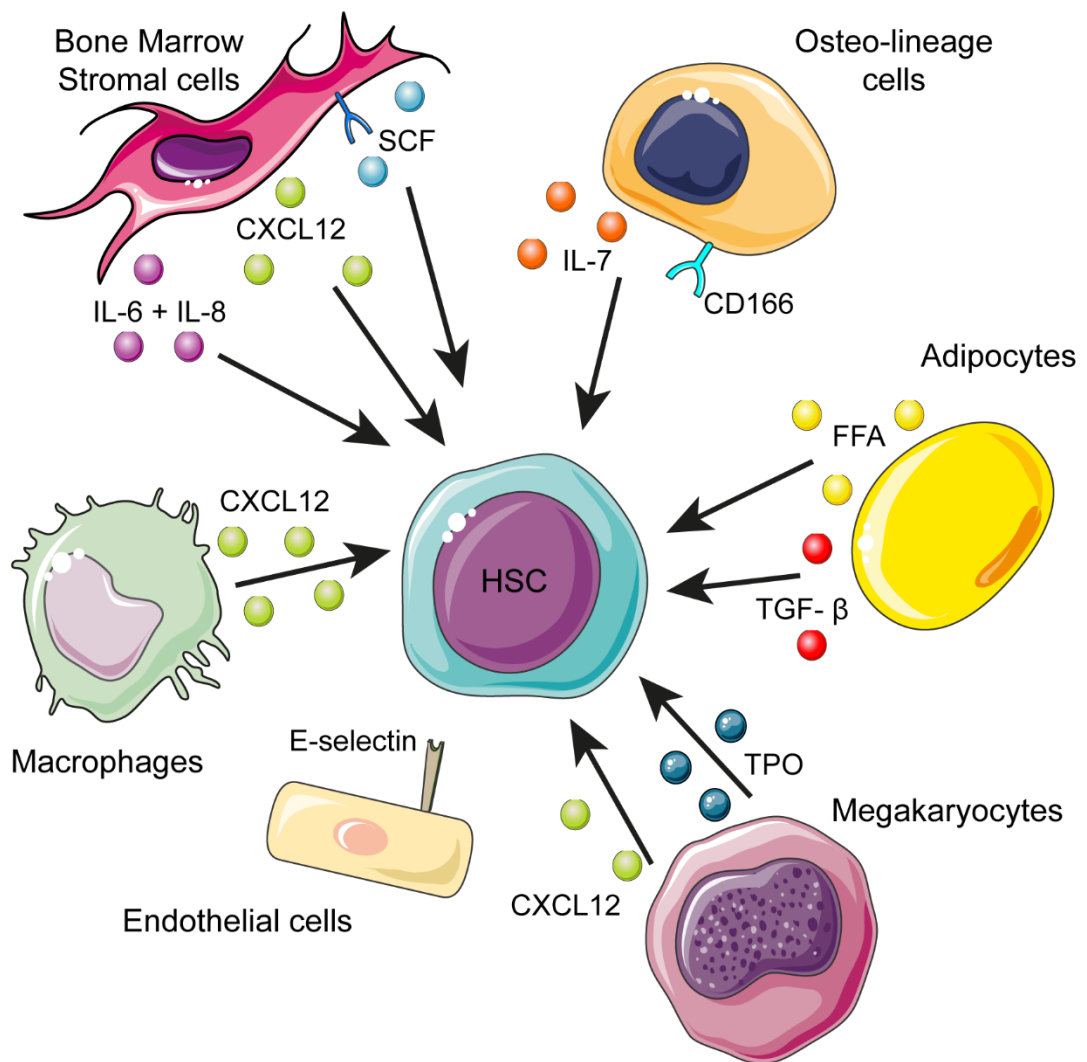


Figure 1.5 Interactions in the HSC niche regulate HSC.

BMSC can produce IL-6 +8, CXCL12, and SCF which act on the HSC to maintain homeostasis and home them to the niche. Osteoblasts act on HSC to induce B-cell production via IL-7 and CD166. Adipocytes release FA as a source of energy for the HSC. They also release TGF-β, which negatively regulates haematopoiesis. Megakaryocytes secrete both CXCL12 and TPO to maintain HSC quiescence. The E-selectin membrane bound protein on endothelial cells regulates HSC quiescence. Like BMSC, macrophages also secrete the chemokine CXCL12, homing HSC where they are required.

1.4 Haematological malignancies

There are a range of different haematological malignancies which include cancers of the blood, BM, and lymphatic system. It is predicted that 'one in every 16 men and one in every 22 women will develop it [blood cancer] at some point in their lives' (116), making it a very common cancer type, which typically increase in incidence with aging (117). These cancer types have been at the forefront of research into understanding the molecular mechanisms of tumour progression. Within the last 30 years there has been great improvement in the treatment of some of these malignancies with the introduction of more targeted and personalised therapies such as combination regimes and Chimeric antigen receptor (CAR) -T cells (118, 119). However, some malignancies, such as acute myeloid leukaemia (AML), are more challenging and have seen less progression in treatment options and continue to have poor prognosis (120). Although there have been some advances it is still imperative the research continues for all these malignancies. Better understanding of disease development, pathogenesis and interplay within the BM niche will allow for further research for treatments with better tolerance and effectiveness.

1.4.1 Lymphoma

Lymphomas are a blood cell malignancy that arises from T or B-cell lymphocytes. The malignant lymphocytes accumulate within the lymph nodes or other organs that are haematologically active, such as the BM and spleen. Like most malignancies, the exact cause of lymphoma is unknown although risk factors such as aging, infections such as Epstein-Barr virus, and a family history can predispose a patient, increasing the likelihood of the cancer (121). The two main categories of lymphoma are Hodgkin and non-Hodgkin lymphoma. The former is denoted by the presence of Reed-Sternberg cells, which are abnormally large lymphocytes that contain multiple nuclei (122). Whereas non-Hodgkin lymphoma is a group of over 60 different subtypes. The different subtypes of lymphomas can be indolent or aggressive and vary in their prognosis (123). The prognosis of patients depends on the type of lymphoma, the stage of the malignant progression, and the frailty of a patient as this dictates the type of treatment they can tolerate. Typically, treatment options include chemotherapy, radio therapy, immunotherapies, such as CAR-T cells, and stem cell transplant (121).

Research into lymphomas continues to be important, advances in our understanding of how the disease works will continue to open up possible drug targets. Studies have shown that lymphoma is able to manipulate healthy immune cells, for example it recruits regulatory T-cells to aid in immune evasion and causes T-cell exhaustion (124). Tumour secretion of IL-10 has been shown to polarise macrophages to an M2 phenotype. The M2 macrophages promote angiogenesis and suppress anti-tumoural immunity (125). These findings helped to inform the use of Lenalidomide in the treatment of some lymphomas. The drug has been shown to enhance T-cell and natural killer cells in the removal of lymphoma cells. It has also been shown to suppress angiogenesis and inhibit the production of other cytokines such as IL-6 and TNF- α which contribute to systemic inflammation and tumour cell survival (126). Further research into the genesis and mechanisms of lymphoma are imperative for the continued improvements to treatments and patient outcomes.

1.4.2 Multiple Myeloma

Multiple myeloma (MM) is a cancer of the plasma cells within the BM. It is initiated in memory B-cells, leading to an over production of abnormal antibodies. The malignant cells remain protected within the BM, where they continue to proliferate at a high rate and take over the cavity (127). These cells secrete an over production of antibodies which can lead to viscous blood, as well as posing a risk of kidney damage (128). MM is an age associated malignancy with approximately 35% new patients presenting at 75 years or older and the median age of diagnosis is 69 (129). The 5-year prognosis for patients is varied, especially due to age, but averages at 61.1% (130). The BM is integral for the development and progression of MM. For example, BMSC secrete IL-6, a pro-inflammatory cytokine that promotes MM proliferation and survival (131). MM can interact with the niche via expression of the surface protein *CD138*, allowing the cells to bind to the extracellular matrix, which further mediates adhesion to other MM cells and growth (132). These are examples of how MM utilises the niche to further progress the disease.

Fortunately, treatment for MM has greatly improved within the last decades. There are a range of treatment options which can be tailored to the patient. Often the first line regime includes a combination of drugs, with the most common combinations being bortezomib, lenalidomide, and dexamethasone, or daratumumab,

lenalidomide, and dexamethasone. It is also possible for some patients to receive autologous stem cell transplantation, which can provide a long remission period (133). Although there are several possible lines of therapy, patients often become resistant to them, which is termed relapse or refractory MM. For those who have exhausted treatment options, CAR T-cell therapy is a rapidly developing and encouraging therapy option which may slow down the disease progression (134). It is an immunotherapeutic approach which involves the genetic manipulation of the patients T-cells to express chimeric antigen receptors that are specific to the target antigen of choice on the cancer cell. This acts to reprogramme the patient's immune system and redirect T-cells to attack the tumour (135). Although promising, patients may still become resistant to the treatment, or it can be toxic and lead to intolerable side effects (136). Ongoing research continues to investigate better mechanisms and targets to improve treatment options.

1.4.3 Leukaemia

Leukaemias are another subtype of blood cancers that can arise from lymphoid or myeloid lineage, leading to high genetic variability within the classification (137). They are classed as the invasion of non-functioning, abnormally differentiated haematopoietic blasts into the BM, blood, and other haematopoietic organs (138). Leukaemias overtake the BM via rapid uncontrolled proliferation, displacing normal haematopoietic cells. This can cause anaemias and immunodeficiency to levels that can be life-threatening. They are classified as chronic or acute, which is denoted by the rate with which the leukaemia progresses. Thus acute leukaemias having a more rapid progression than the chronic leukaemias (139).

1.4.4 Acute Lymphoid Leukaemia

Acute lymphoid leukaemia (ALL) arises from immature B or T- cells. It is a malignancy which predominantly affects younger patients who have ~80% survival rate, however, older patients have decreased survival of ~50% (140). ALL is highly reliant on the BM microenvironment, hijacking normal cellular interactions. ALL blasts adhere to BMSC and cause morphological and cell-cycling alterations, conferring a more protective environment for the blasts (141). For example, BMSC can express asparagine

synthetase which aids in preventing apoptosis of the blasts ALL by asparagine treatments (142). ALL also utilises the expression of *CXCR4* receptors to aid in homing to the BM cells (143). B-ALL secretes inflammatory factors such as IL-1 β , IL-12 and tumour necrosis factor (TNF) α , which disrupt healthy haematopoiesis by creating a proinflammatory microenvironment (144). Although it has been shown that T-ALL does not rely as heavily on the BM microenvironment for expansion, it does cause substantial remodelling to compartments of the BM such as the endosteal niche. This results in a loss of supporting cells and hinders healthy haematopoiesis (145). This highlights the importance of interactions between the BM microenvironment and the secretions from blasts in the progression of ALL.

1.4.5 Acute Myeloid Leukaemia

Acute myeloid leukaemia (AML) is a highly proliferative malignancy that arises from the myeloid progenitors of the haematopoietic hierarchy (146). It is an aggressive malignancy due to it being sustained by leukaemic stem cells (LSC), which, like HSC, can produce high numbers of cells and can cause relapse via their ability to evade chemotherapy (147). AML is a disease which is predominantly diagnosed in elderly patients with the average age of diagnosis at 71. It has a poor prognosis; in 2021 a study by Sasaki et al showed that the 5-year survival rate between 2010-2017 in the USA was only 28% (148). Even younger patients who are able to undergo intensive chemotherapy are likely to relapse due to LSC and other malignant cells which are able to 'hide' within the protective niches of the BM microenvironment (149).

There is extensive heterogeneity within AML, and it is therefore important to understand the genomic landscape, interactions with the microenvironment and other prognostic factors when deciding treatment regimens or researching potential new treatments. Techniques such as next-generation sequencing have helped to identify the frequency and spectrum of AML mutations that patients present with (146, 150). Like other cancers, AML can arise from mutations in tumour suppressor genes such as TP53, leading to dysregulation of transcription and thus increased proliferation of nonfunctional blasts. It has also been shown that AML can arise from mutations, such as in the *FLT3* gene, which confers a proliferative and survival advantages. Or AML can arise from chromosomal rearrangements, such as *RUNX1:RUNX1T1* (150-154).

AML often has sub-clonal populations that can lead to selection of clones which evade chemotherapies or proliferate at much higher rates (155).

Along with the heterogeneity of AML, symptoms also vary between patients. Common symptoms include weakness and fatigue, bruising, and bleeding (156). Even in recent years more symptoms of AML are being considered. One of these is cachexia, which is the excessive body wasting due to stored fats, proteins and carbohydrates being used for energy. It was previously believed that the intensive treatment with chemotherapy was causing the weight loss, however studies are now suggesting that it is also a direct effect of the AML (157, 158). Due to the variance of symptoms, AML must be confirmed with a number of protocols. Initial bloods tests would include low or abnormal lymphocyte counts as an indicator of AML. Confirmation is achieved by flow cytometry and Wright-Giemsa staining of BM samples (159). If the BM contains 20% or more AML blasts a diagnosis is given (160).

1.4.5.1 Acute Myeloid Leukaemia Treatment

Unfortunately, treatment for AML has been vastly unchanged in recent decades. Treatment is divided into two phases: induction and consolidation. Most induction regimens involve chemotherapy which is aggressive and poorly tolerated by patients (161). The standard induction regime is two cycles of daunorubicin and cytarabine, and consolidation often involves further chemotherapy. Allogenic haematopoietic stem cell transplant can be given as a consolidation treatment to patients under 60 with standard disease risk (162-164). Intensive chemotherapy regimens are associated with high morbidity and mortality, they are myelosuppressive and increase risk of treatment associated infections and toxicities (163). Despite treatment options there is still a high rate of relapse and older more frail patients are unable to tolerate the aggressive nature of the treatments. Researchers continue to investigate new, more targeted therapies to improve treatment tolerability and patient survival.

The introduction of targeted therapies has advanced the treatment of AML. These are especially beneficial to older patients who can take them in combination with lower dose chemotherapy that they are not normally able to tolerate (162). Examples of targeted drugs include FLT3 inhibitors (specific for patients with this mutation), such as Crenolanib and Sunitinib, which block FLT3 protein synthesis. This prevents

the downstream cascade which regulates survival, proliferation and differentiation (165). Newly approved targeted treatments also include Sorefinib, Midostaurin and Quizartinib. Another example is B-cell lymphoma-2 protein (BCL-2) inhibitors such as Venetoclax and Navitoclax (166). The BCL-2 protein is a key anti-apoptotic protein which is often expressed in haematological malignancies and is associated with tumour progression and increased chemo-resistance. BCL-2 inhibitors target the protein to activate the mitochondrial apoptotic pathway, inducing tumour cell death (167). This is a great advancement for frail patients and those over 75, as it has been shown to be effective in combination with lower doses of chemotherapy, such as azacitidine (168). Although this protocol can reduce tumour volume and improve survival, it is not possible to reach remission (162). These drugs are toxic and some mutations, such as BCL-2, lead to resistance to these treatments. With a host of side effects leading to some patients opting for a palliative approach.

Immunotherapies are another treatment type which has seen advances in the last decades. These therapies work to boost the immune system and aid the bodies response to the tumour. Bispecific antibodies are an example of immunotherapies used for the treatment of AML. These are a construct of 2 antibodies which act by binding to a surface receptor on the AML cell, such as CD33, and then binding a protein on an immune cell, such as CD3 on T-cells. The clinical name of this example is JNJ-67571244 however, there are many more being researched and tested. This brings the cells together and enables the immune system to aid in the clearance of the AML cells (169-172). Like other treatments, these cause side effects and are unable to achieve complete remission. As such, researchers continue to investigate molecular mechanisms of AML survival and proliferation. Other potential aspects of the disease which may be considered for future AML treatments include interactions between the BM microenvironment and AML cells, and other organs within the system.

1.4.5.2 The AML niche

Research has shown that AML, and other haematological malignancies, remodel the BM microenvironment to make it more permissive for tumour expansion. AML drives changes in BMSC, adipocytes, endothelial cells, and even macrophages. These act to promote proliferation, survival, and resistance to treatment (173). Many studies have shown that AML is unable to effectively proliferate outside of its microenvironment (21, 33, 174-176). AML does not directly deplete HSC but expansion within the BM and remodelling of the niche impairs normal haematopoietic function, leading to the characteristic cytopenias often seen at diagnosis (177).

As described in 1.3.7 BMSC are important for the support of HSC. These cells can be manipulated by the AML blasts to aid in their survival and proliferation (Figure 1.6). It has been shown that BMSC confer protection against chemotherapies and drug induced apoptosis via cell-cell interactions (178-180). Furthermore, AML has been shown to induce a senescent phenotype in BMSC and the secretion of senescent associated secretory phenotype. The accumulation of senescent cells within the BM has been shown to drive AML development as *in vivo* depletion of senescent cells prolonged animal survival by slowing tumour progression (181). Senescence is accumulated as a natural form of aging, and it is possible that tumour development only occurs after age-associated senescent changes are initiated (182). Or it is possible that malignant clone presence in the BM drives the senescent changes. Albeit it is probably a combination of both, with age-associated senescence occurring naturally and creating a more favourable environment for progenitor cells which acquire mutations. In turn these malignant cells may speedup this age-associated processes (183). Another example of AML hijacking normal HSC function is the utilisation of the CXCR4/CXCL12 signalling axis between the blasts and the BMSC to home to the BM (184). As with HSC, if this axis is blocked, AML cells mobilise to the peripheral blood (185, 186). These interactions highlight the importance of BMSC in development and progression of AML, and the importance of understanding them for discovering targetable interactions for treatment.

Our laboratory has also shown the importance of the BM microenvironment in AML progression. The group has shown that BM adipocytes support the proliferation of AML. The AML blasts can reprogram metabolism within the adipocytes to induce lipolysis, releasing FFA for FOA within the blasts preventing apoptosis (33). This is

achieved by subsets of leukaemia which upregulate CD36 which is a process hijacked from healthy HSC (85). The proximity to adipocytes also increases the expression of fatty acid binding protein (*FABP*)-4 (Figure 1.6C). The FFA released from the adipocytes have been identified to activate transcriptional programmes which support leukaemia cell survival (187), and inhibition of these processes has been revealed to impair the anti-apoptotic effect BM adipocyte impart on the AML blasts (188). Interestingly it has also been shown that by compromising the adipocyte niche, AML disrupts myelo-erythropoiesis (189). These indicate the important role of BM adipocytes in supporting AML metabolism and survival and will be further discussed in 1.5.4.

Endothelial cells support the AML microenvironment through their role within the sinusoids of the BM protecting the AML, as well as providing a route for metastasis via the peripheral blood (190). AML cells mediate their adhesion to and activation of endothelial cells by secreting cytokines such as TNF- α and IL-1 β (191). Furthermore, interactions between the AML blasts and endothelial cells induces angiogenesis via the Notch/Dll4 pathway (192). When cultured with endothelial cells, proangiogenic factor vascular endothelial growth factor (VEGF) induced expression and secretion of *Gm-csf*, a known stimulator of AML proliferation (Figure 1.6A) (193). Thus, endothelial cells and their support of AML cells is an interesting area of research for the treatment of AML.

The interactions between AML and macrophages have been widely reported to benefit survival and immuno-avoidance. One way in which AML avoids phagocytosis is the expression of the surface marker CD47, a 'don't eat me' marker which interacts with SIRP α on macrophages (Figure 1.6B). This prevents the morphological changes required for macrophage phagocytosis and has recently been utilised as a therapeutic target for AML and other tumours (194-196). It has been further reported that AML induces the infiltration of macrophages into the BM and spleen, creating a pro-inflammatory state. These infiltrating macrophages are polarised to tumour associated macrophages which are directly correlated with survival *in vivo* and shown to be increased in human patients in comparison to controls (197). Targeting these macrophages has shown promising results, with activation of the LC3 associated phagocytosis pathways suppressing AML expansion and prolonging survival *in vivo* (198). AML interactions with macrophages is an interesting area of research with continued investigated into how these cells further support the AML niche.

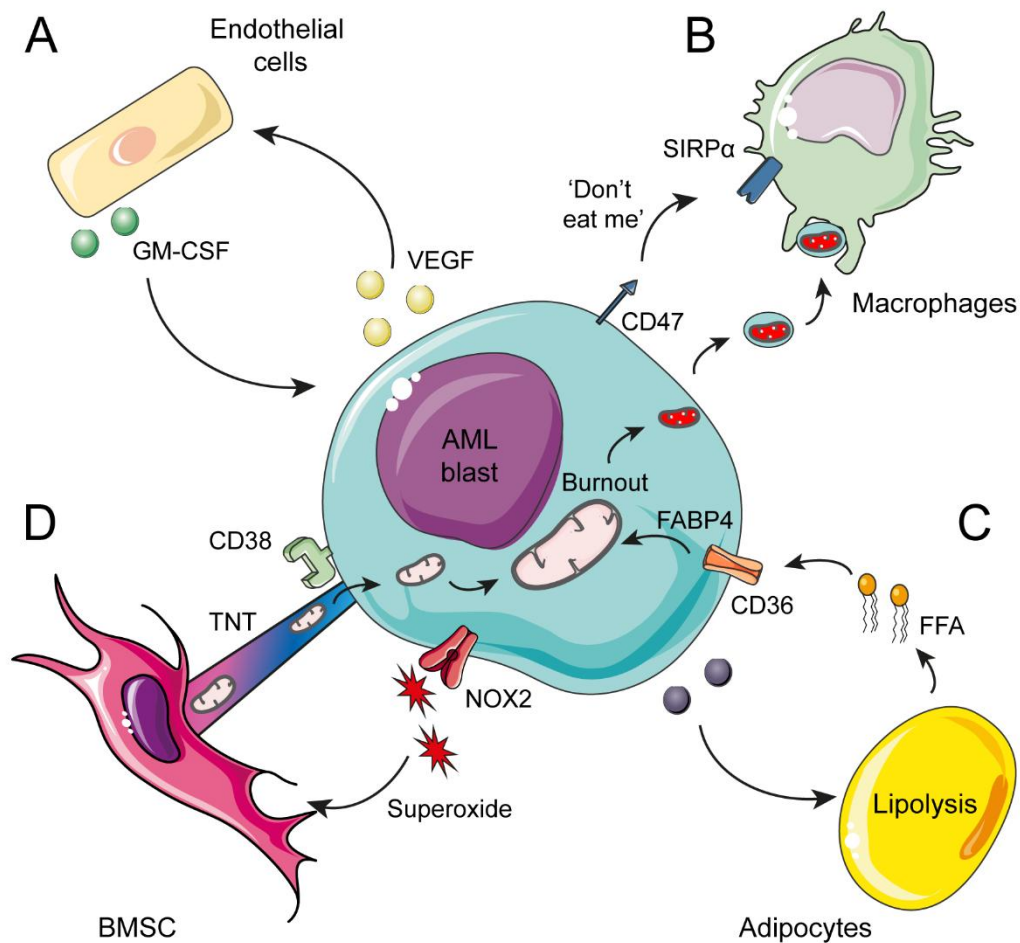


Figure 1.6 AML remodels and reprogrammes the BM niche.

AML manipulates the cells within the BM microenvironment to increase proliferation and obtain metabolites. (A) AML releases VEGF which stimulates endothelial cells to release the pro AML proliferation factor GM-CSF. (B) AML expresses CD47, the don't eat me signal that interacts with SIRP α on macrophages. AML also offloads burnt out mitochondria for mitophagy to macrophages, preventing induction of apoptotic pathways. (C) AML manipulates adipocyte lipolysis and increases FFA uptake by increasing the scavenger receptor CD36 and subsequent shuttling to the mitochondria by FABP4. (D) AML replenishes the mitochondria it offloads by inducing TNT to acquire more mitochondria from BMSC. Release of Superoxides via NOX2 and interactions between CD38 and the stromal cells regulates TNT formation.

1.5 AML metabolism

Due to the highly proliferative nature of AML, it requires a huge amount of energy for progression of the disease. While AML remodels the BM niche to make it more permissive, it is also known to hijack other healthy HSC processes such as metabolic remodelling of the niche (114). This remodelling and energy requirement by AML is an important area of study as it highlights exploitable targets for therapies.

1.5.1 Glycolysis

Glycolysis is an anaerobic process converting glucose into pyruvate and further into lactate, yielding relatively low levels of ATP (Figure 1.7). As described above, HSC normally reside within the hypoxic niche and use glycolysis as the main source of metabolism. This reduces the risk of oxidative stress and limits the production of ROS, aiding to keep the cells quiescent (11). In the 1950's Warburg proposed that cancer cells rely on glycolysis for energy production (199). While this has since been disproved for AML, which primarily relies on OXPHOS, glycolysis is still used by AML both for energy and other pathways that feeds into it (200). It is said that AML is 'addicted' to glucose and over activates the mTORC1 signalling pathway to promote glycolysis. The success of glycolysis inhibitors, on AML, is determined by the activity levels of mTORC1 (201). AML cells overexpress *GLUT1* to increase uptake of glucose from the blood, which has been shown in both cell lines and primary patient samples to confer cell survival and drug resistance (202). Downregulation of *GLUT1* by mutations of AMPK perturbed glycolysis and suppressed disease progression (203). Glycolysis is also important for biosynthesis pathways such as serine biosynthesis, the pentose-phosphate pathway for ribonucleotide synthesis and one-carbon metabolism to generate NADH (204). This highlights the importance of glycolysis as more than just as bioenergetic role in AML, providing further evidence for it as an exploitable pathway for treatment.

1.5.2 Mitochondrial transfer

Mitochondria are central to the metabolism of FA, carbohydrates and amino acids. They are known as the powerhouse of the cell and are the location of OXPHOS, the TCA cycle, and β -oxidation (Figure 1.7) (205). AML has a metabolic bias towards OXPHOS. ATP is produced via electron transport from NADH or FADH₂ down the electron transport chain of protein complexes I, II, III and, IV. This occurs within the inner mitochondrial membrane. NADH and FADH₂ are produced during glycolysis, FAO, and the TCA cycle (206). OXPHOS produces significantly more ATP than glycolysis, making it significantly more efficient when a cell needs to proliferate.

AML have an increased mitochondrial mass to keep up with the high energy demand and have the ability to increase mitochondrial mass by up to 14% in a co-culture environment with BMSC (207). To achieve this, AML blasts hijack the HSC stress response in order to acquire more mitochondria from the BMSC within the niche (114). There are multiple mechanisms by which this can occur, such as transfer by extracellular vesicles, through Gap junctions upon cell-cell interactions or via leukaemia derived tunnelling nanotubules (TNT) (208). AML generates superoxide via NADPH oxidase-2 to create oxidative stress in BMSC stimulating transfer of mitochondria by AML derived TNT (209). CD38 plays a significant role in mitochondrial transfer from BMSC via cell adhesion and anchor points for the TNT (Figure 1.6D). It is possible to inhibit CD38 with a monoclonal antibody, already used in the treatment of multiple myeloma. *In vivo* use of the anti-CD38 antibody Daratumumab inhibits disease progression by altering the metabolic profile of MM indicating that this may be effective treatment for AML (210-212). Increased ROS mediates the opening of connexin channels at Gap junctions via phosphatidylinositol 3-kinase (PI3K) activation. It has been shown that mitochondrial transfer can be achieved through Connexin 43, which further acts to promote adhesion of LSC to the BMSC and induce TNT formation (115, 213). The increase in ROS not only impairs normal haematopoiesis, where HSC rely on low ROS for health and quiescence, but also drives leukaemogenesis. This is a notable problem with some traditional chemotherapies, such as cytarabine and daunorubicin, which increase ROS to induce apoptosis. Even though the AML cannot withstand constant high levels of ROS, it creates genetic instability and favours AML, promoting chemotherapy resistance and survival (207). This further exemplifies the importance of understanding the metabolic profile of AML.

Due to the increased accumulation and use of mitochondria, AML also accumulates dysfunctional mitochondria and metabolic waste products. These will trigger intracellular apoptotic pathways if not efficiently removed. AML blasts achieve this via the release of extracellular vesicles and apoptotic bodies which are subsequently phagocytosed by macrophages (Figure 1.6B) (198). Mitophagy has also been shown to confer treatment resistance against BCL-2 antagonists such as venetoclax, via the increase in expression of mitophagy mediating genes such as *Mfn2* and *p62*. Targeting these pathways impaired the packaging, degradation and autophagy of mitochondria, resensitising AML to BCL-2 antagonists (214, 215). Mitochondrial import and export are key for the progression of AML and continue to be an attractive target for therapeutics.

1.5.3 Amino acid metabolism

AML cells have been shown to increase their uptake of amino acids (aa) to keep up with the reliance on metabolic requirements, as well as other processes such as activating signalling pathways and protein biosynthesis (Figure 1.7) (216). Glutamine is important for many cell functions and as such it is the most abundant aa in the body. It is used as a substrate for the TCA cycle, antioxidant production, cell signalling, and is required for the production of lipids, nucleotides, and other aa (110). Low levels of glutamine have been linked with reduced oxygen consumption indicating that glutamine deprivation inhibits OXPHOS (217). Glutamine is imported into AML blasts via SLC1A5 and undergoes glutaminolysis to produce glutamate and α -KG for the TCA cycle. Knockdown (KD) of this transporter protein results in increased apoptosis of AML blasts (218). Furthermore, the BCL-2 antagonist venetoclax has been shown to cause the loss of proteins involved in the process of using glutamine for the TCA cycle, which further sensitises the blasts to the drug (219). Reduced aa uptake can also be a rate-limiting factor for AML proliferation as they are the building blocks for proteins and the amide group for *de novo* nucleotides (220). These highlight the importance of aa in the energy supply chain within AML, highlighting the potential therapeutic benefits in targeting this.

1.5.4 Fatty acid metabolism

To keep up with the demand for ATP, AML blasts also utilise β -oxidation of FFA. Similar to HSC in a stress response, they access the FFA from the abundant adipose within the body (85). While glucose and lactate contribute roughly half of the TCA cycle carbon, FA and aa are suggested to contribute the remainder (111). During lipolysis of adipocytes, triglycerides are hydrolysed and secreted as FFA and glycerol (84). The FFA are used in β -oxidation in the mitochondria and peroxisomes where they are broken down into acetyl-CoA to feed into the TCA cycle for subsequent ATP synthesis (Figure 1.7) (221).

Not only are FA an energy source but they also serve to regulate metabolism as ligands for transcription factors and enzyme complexes. These mediate cellular processes such as survival, proliferation, migration, and metabolism (222). A group of transcription factors which are both activated by and alter FA metabolism are PPAR (223). The family of PPAR α , β , and γ are known as lipid sensors and all play a key role in lipid homeostasis as well as other functions. PPARs have large ligand binding cavities, allowing them to bind a range of endogenous and synthetic ligands. This includes essential FA which agonise transcription of genes involved in glucose and lipid homeostasis (224, 225). The PPAR act to increase FA metabolism by stimulating FAO and lipid uptake to increase the available substrates (226). They achieve this by increasing the expression of *FATP*, *FABP*, and *CD36* (227-231).

AML relies on adipocytes and FA as an energy source for survival and proliferation (232). Like healthy haematopoietic cells, AML can access FA from the peripheral blood as well as inducing lipolysis of adipocytes. It has been shown that elevated serum FFA is an indicator of pre-leukaemia to leukaemia progression (233). However, with such a great demand for FA, AML can further remodel the niche to increase accessible FA. IL-6 signalling can increase the expression of *Cd36* on blasts, as well as some subsets of AML having increased baseline *Cd36* expression. This further promotes FFA as a source of energy and homes them to the adipocytic niche (234, 235). The recently developed inhibitor of CD36 SMS121 has been shown to impair FA uptake and reduced survival of blasts *in vitro* (236). Our group has also reported that AML has increased *FABP4* expression, further enhancing the uptake and shuttling of FFA into the cell and to the mitochondria (33). Furthermore, AML has been shown to act on adipocytes via the release of growth differentiation factor 15.

This has been shown to remodel mature BM adipocytes to small adipocytes by inhibiting calcium channels which increases lipid breakdown within the BM (237). Thus, the increased uptake of FFA increase FAO to feed into the TCA cycle and further increase OXPHOS. FFA metabolism has also been shown to play a role in relapsed AML where it is utilised in instances where initial treatment reduced the availability of aa metabolism (219). Tabe et al further showed that inhibition of FOA improved AML sensitivity to cytarabine (238). These indicate the reliance of AML of fatty acids for survival and proliferation, making it an attractive pathway to target new therapeutics.

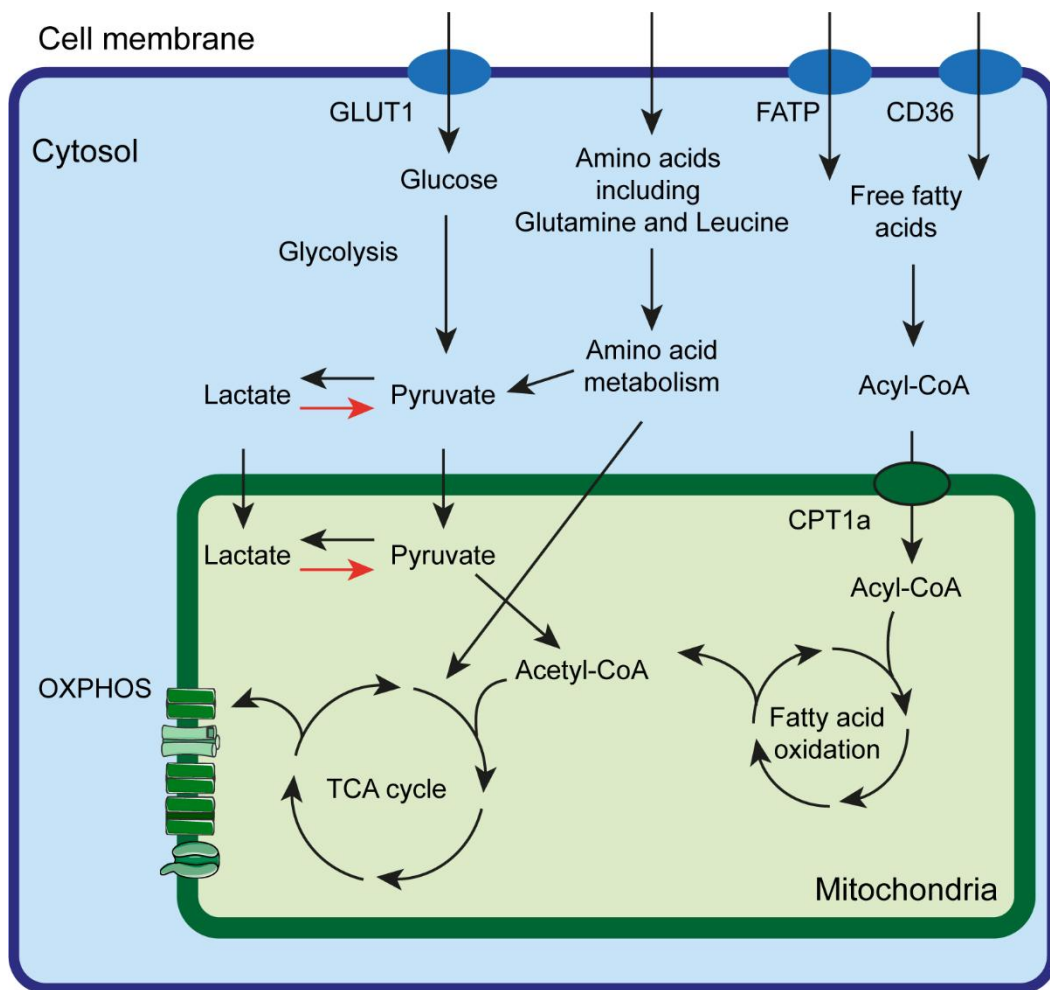


Figure 1.7 Metabolism of glucose, amino acids, and fatty acids.

AML utilises as many metabolites as it can to produce ATP. Cells import glucose through GLUT1 which undergoes glycolysis into pyruvate. Pyruvate can be converted into and generated from lactate, both in the cytosol and within the mitochondria. Amino acids can also be converted into pyruvate. Within the mitochondria, pyruvate is metabolised to Acetyl-CoA and enters the TCA cycle. Amino acids are also required as substrates for the TCA cycle. Fatty acids are transported into the cytosol by proteins such as CD36 and FATP. During β -oxidation they are converted into Acyl-CoA which is transported into the mitochondria by carnitine palmitoyltransferase 1A (CPT1A). Here fatty acid oxidation continues and feeds Acetyl-CoA into the TCA cycle. The end stage of this metabolism is oxidative phosphorylation down the electron transport chain within the mitochondrial membrane.

1.6 The Liver

The liver is a vital organ within the body with a myriad of roles including metabolism, detoxification, bile production, immunity, and storage of nutrients (239). As the key metabolic hub for the body, the liver is important for metabolism of carbohydrates, lipids, and protein. It regulates blood glucose and FFA as well as the safe excretion of urea (239). The liver detoxifies endogenous and exogenous substrates such as metabolic biproducts, toxins, and drugs into less harmful products which can be excreted via the bile or urine (240). Bile is produced by hepatocytes and stored in the gall bladder and is vital for the emulsification of fats in the small intestine for digestion and absorption (241). The tissue resident macrophages, called Kupffer cells, are important for the immunity of the liver, phagocytosing pathogens, non-functional cells, and debris (242). The cells of the liver are the major stores of essential vitamins and minerals such as Vitamins A, B12, D, E, and K, along with Iron and copper. These can be released to maintain balance for cellular functions (243).

The liver plays an essential role in the regulation of FA homeostasis by acting as the primary metabolic hub for synthesis, storage and breakdown of fats. It processes and distributes FA in accordance with the demands of the body. The liver converts excess dietary proteins and carbohydrates into FA and triglycerides (244). The liver stores the FA and triglycerides as LD or exports them via the peripheral blood to other tissues. It regulates serum FA by producing lipoproteins to transport fats throughout the body (245-247). The ability to process FA effectively and in accordance with the demands of the body is imperative to homeostasis. Dysregulation of these processes can lead to metabolic disorders such as non-alcoholic fatty liver disease (NAFLD), characterized by excessive accumulation of lipids in the liver (248, 249). The regulation of FA by the liver also impacts the progression of malignancies via reprogramming the availability of FA for the malignant cells. For example, Flint et al show that IL-6 secreted by pancreatic and colorectal cancers acts on the liver to alter FA metabolism, increasing tumour burden (250). The interplay between liver lipid metabolism and cancers highlights a central role for the liver in cancer progression.

1.6.1 Cells of the Liver

The unique cellular composition of the liver enables the diverse functions it provides to the body. The functional units of the liver are hepatic lobules, the hexagonal structure which surrounds the central veins with portal triads in each of the corners. The portal triad contains a hepatic artery, portal veins, and common bile duct. Sinusoids radiate from the central vein, joining the hepatic vein, and are lined with endothelial cells and Kupffer cells. Between these cells and the most abundant cells of the liver, hepatocytes, is the space of Disse, where stellate cells reside (Figure 1.8) (251). The structure and composition of hepatic lobules are central to the role of the liver.

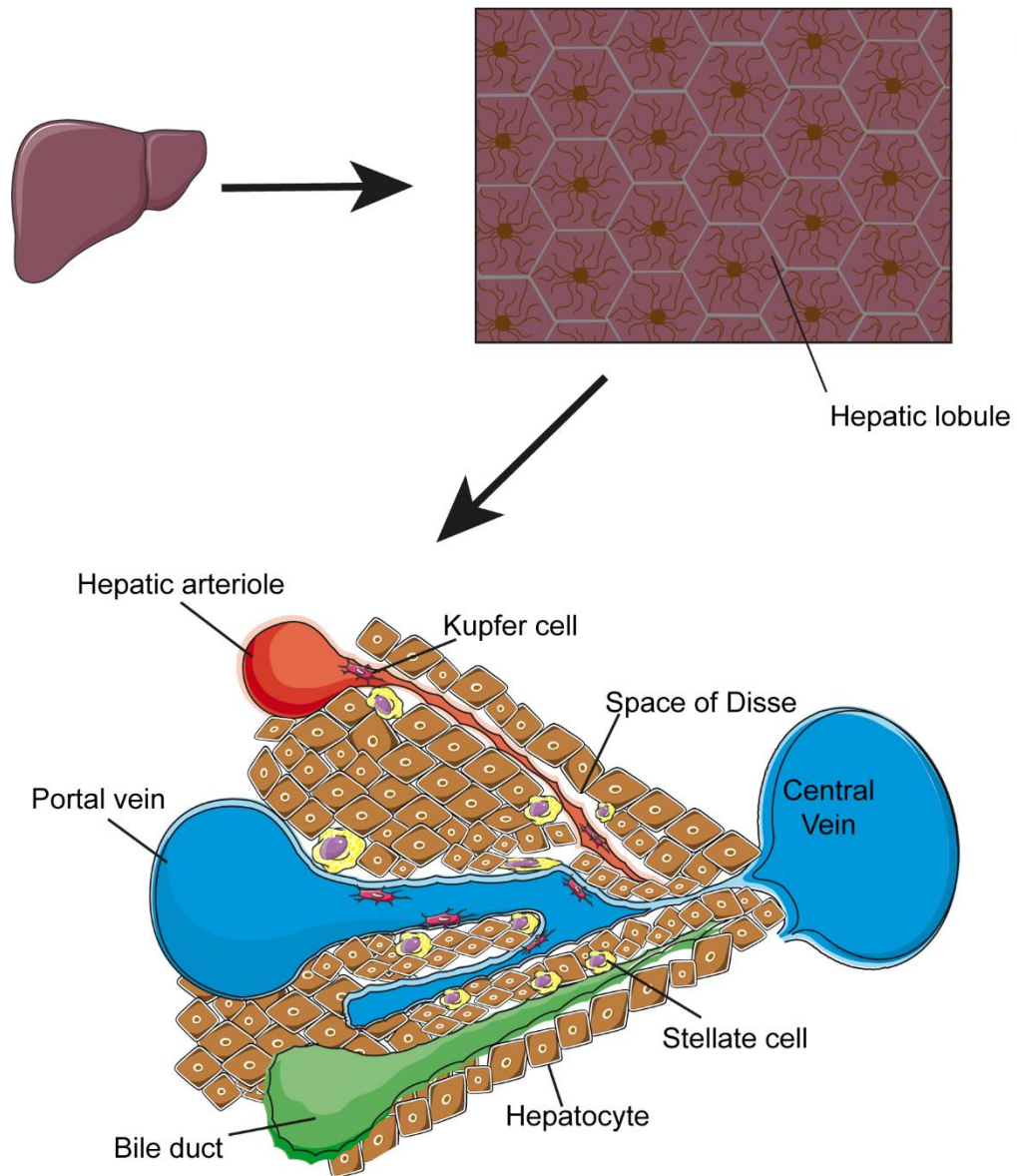


Figure 1.8 Liver microanatomy.

The functional units of the liver are called hepatic lobules. Roughly hexagonal in shape, each corner contains the portal triad. This is comprised of a hepatic arteriole, portal vein and bile duct. Blood drains to the central vein in the middle of the lobule. Vessels are made up of endothelial cells without a basement membrane and are surrounded by plates of hepatocytes. The space between the hepatocytes and endothelial cells is home to the stellate cells and is called the space of Disse. Tissue resident macrophages called Kupffer cells are found within the vessel walls alongside the endothelial cells.

1.6.1.1 Kupffer cells

Kupffer cells are tissue resident macrophages and are located within the lumen of the liver sinusoids attached to the endothelial cells which make up the walls of the vessels (97, 252). Under steady state they are a long lived, self-renewing cell population that locate to the liver during developmental haematopoiesis. During stress stimuli, if these cells are depleted, they can be replenished by circulating monocytes from the BM HSC (253). Kupffer cells have different structures and functions dependent on their location in the hepatic lobule. Periportal Kupffer cells are larger and have a greater phagocytic activity due to being closer to the portal vein where bacteria, debris, and endotoxins first enter the liver from the gastrointestinal tract (254, 255). Centrilobular Kupffer cells are smaller and produce superoxide radicals and pro-inflammatory IL-6 to combat deeper injury and infection into the lobule (256, 257). The cells have surface features such as microvilli to increase their surface area and increase endocytic activity (255). Kupffer cells play a major role in haematopoiesis as they clear senescent cells including red blood cells from the peripheral blood and recycle the globulin chains, iron, and bilirubin (258). Furthermore, Kupffer cells are important for FA regulation in the liver, which will be discussed in 1.6.2.

1.6.1.2 Stellate cells

Hepatic stellate cells are pericytes and thus sits between the hepatocytes and the endothelial cells within the space of Disse (259). Stellate cells account for roughly 10% of the liver resident cells and are currently thought to be of mesenchymal origin, albeit research is ongoing to confirm this (260). Under steady state, stellate cells are considered to be quiescent., however they play a crucial role in homeostasis. Stellate cells are the major site of vitamin A storage in perinuclear LD which is essential for the healthy function of the immune system (261, 262). They also secrete growth factors to regulate hepatocyte turnover, and their contractile ability is required for vaso-regulation (259). During a stress response, stellate cells are activated by TGF β and platelet derived growth factor signalling and become myofibroblast-like stellate cells (263). They contribute to tissue repair and are the major source of extracellular matrix (ECM) within the liver. If the stimulus is chronic, the stellate cells can be activated for long periods of time and continue to produce ECM. This can lead to

scaring and increases the risk of developing tumours (264). Interestingly it has been shown that stellate cells play a role in haematopoiesis. During development they produce SCF which homes HSC to the liver niche for foetal haematopoiesis. When *Scf* was knocked down in stellate cells there was a reduction of HSC in this niche (265). They are also proposed to have a role in liver immunity as they may act as antigen presenting cells and release cytokines and chemokines, aiding in immuno suppression (266). Although comparatively few in number, stellate cells play an important role within the liver.

1.6.1.3 Hepatocytes

Hepatocytes are the primary cells of the liver, making up ~80% of the total mass. They are large polyploid cells containing high mitochondrial and endoplasmic reticulum (ER) mass. Within the hepatic lobule they are organised in plates around the sinusoids and supported by a collagen network. Hepatocytes are separated from the blood vessels by the space of Disse, which drains the lymph into the portal tract (267). The endothelial cells of the sinusoids do not form basement membrane thus minimising the barriers between the hepatocytes and the blood travelling through the lobules. Blood from the hepatic artery is rich in oxygen and blood from the portal circulation is nutrient rich. As blood moves through the lobule cells utilise the oxygen and nutrients. As the blood drains to the central vein, it becomes less oxygenated and has an increase in metabolic waste products. The gradients of oxygen and nutrients through the lobule creates zones of hepatocytes with varying metabolic functions based on the composition of the blood they receive (268). Hepatocyte metabolism provides the energy for the other processes required of them including metabolic homeostasis, detoxification, protein synthesis and storage, and hormone regulation, so confer the majority of the roles of the liver (269).

1.6.1.3.1 Detoxification

Hepatocytes are the detoxifying agents of the body. They metabolise and neutralise endogenous and exogenous substrates such as toxins, drugs, and alcohol. Once toxins reach the liver via drainage from the intestinal venous blood they undergo two phases of detoxification which are oxidation, reduction, and hydrolysis, followed by conjugation to water soluble forms for excretion (270). One of the methods of toxin

excretion is via the bile. It is secreted by hepatocytes into canaliculi that flow in the opposite direction to the sinusoids. The bile excretes toxins and waste into the faeces and is also involved in intestinal functions such as emulsifying fats (241). The role of detoxification is important for drug delivery and absorption, therefore making hepatocytes a key area of research across many biological fields. Isolated primary hepatocytes from humans and animal models, and immortalised cell lines are widely used to investigate the pharmacokinetics of drugs and can be used to predict *in vivo* reactions (271, 272). The cytochrome P450 is part of the superfamily of haemoproteins which are necessary for drug metabolism and predominantly found in the liver. Genetic polymorphisms in these genes causes altered drug metabolism, resulting in patients reacting differently to the drugs (273). This highlights the importance of hepatocytes when developing new treatments regardless of the desired target cell.

1.6.1.3.2 Protein synthesis and storage

Another important function of hepatocytes is the synthesis and storage of proteins. They are responsible for 85-90% of circulating protein volume (269). The main proteins produced and secreted by hepatocytes are albumin, transferrin, and clotting factors (274). Albumin is the most abundant secreted protein and is required for blood volume maintenance and thus the osmotic pressure of the blood, it is also a non-specific hormone binding protein (275). Hepatocytes produce specific and non-specific hormone binding proteins for lipophilic hormones. Their circulation in the blood contributes to tissue specific distribution of the hormones (276). Another group of proteins produced by the liver are clotting factors which are required for the coagulation of blood including fibrinogen and prothrombin (277). Impaired expression, synthesis and secretion of clotting factors leads to disorders such as haemophilia and thrombosis (278, 279). Hepatocytes are also key for protein storage. They can act as a reservoir of aa derived from diet or protein turnover. This store can be used for synthesis of new proteins or for metabolism during fasting states (280). Hepatocytes also produce ferritin for iron storage so that they can regulate the balance between availability and toxicity (281). This shows the importance of hepatocytes in protein synthesis and storage for normal physiological functions.

1.6.1.3.3 Immune response

Although not generally considered an immune cell, it has been shown that hepatocytes do play a role in immunity. They release acute phase proteins in response to local or system infection. In response to cytokines produced by activated immune cells such as IL-1 α , IL-6, and TNF- α , hepatocyte transcription is altered (282). It has been shown that in response to IL-6 secretion of normally high proteins like albumin and fibronectin are reduced, while secretion of acute phase proteins like haptoglobin and fibrinogen are increased (283). Attenuation of the acute phase can lead to increased liver injury, indicating a hepatoprotective role of the acute phase proteins (284). Interestingly, the cytokine hepatocyte growth factor (HGF) can counteract many of the acute phase proteins and inhibit haptoglobin, increasing production of albumin and transferrin (285). Hepatocytes also express both cell surface and cytoplasmic pattern recognition receptors (284), these receptors may play a role in mediating liver protective signalling. For example, toll like receptor 2 on hepatocytes has been shown to help attenuate the inflammatory response caused by trypanosomes (286). Conversely it is apparent that hepatocytes are required for immune tolerance. With blood coming from the intestines, hepatocytes are subjected to elements from the gut microbiota as well as other pathogens and debris. It is therefore important that an immune response is not mounted against non-hazardous molecules (287). The basement membrane lacking sinusoids allows for direct cross talk between hepatocytes and T-cells. Antigen presenting hepatocytes have been shown to induce apoptosis in T-cells thus mitigating an immune response (288). Despite activating the immune response, the sheer volume of blood that passes around the hepatocytes puts them at risk of pathogens. For example, hepatitis viruses are able to induce endocytosis via the Na⁺ taurocholate co-transporting polypeptide. The virus replicates within the cells and hijack the vesicular components to be released and utilises the secretory ability of the liver to enter the peripheral blood and infect other cells (289). Exposure to these viruses can lead to liver damage and subsequent diseases (290). This demonstrates the importance of immunity within the liver for homeostasis.

1.6.1.3.4 Metabolism

Metabolism is at the heart of hepatocyte functions. Not only is it required for the other processes carried out by the hepatocytes, but it is essential for homeostasis of circulating metabolites. They maintain the balance between required uptake and toxicity to the tissues of the body (269). Like other cells, hepatocytes utilise glycolysis, FAO, aa metabolism, the TCA cycle, and OXPHOS to produce energy. As such, mitochondria are indispensable to their function. Due to their energy demand hepatocytes are one of the most at-risk cells of cellular function being impaired during stress, such as infection or disease. Disruption to metabolism can lead to the pathogenesis of disease such as insulin resistance, diabetes, and NAFLD (291). To meet the demands of the hepatocytes, their mitochondria can adapt to the changing demands via biogenesis or fusion (292). Dysregulation of these processes can be caused by consistent excess nutrient intake and cause oxidative stress via ROS production. This results in dysfunctional mitochondria and promotes FA uptake by the hepatocytes, leading to lipo-toxicity, inflammation, and further insulin resistance (291). This exemplifies the importance of metabolic balance with hepatocytes and their potential for pathogenesis.

Hepatocytes are highly important for the balance of blood glucose and the pathways involved have to be carefully regulated. They have the capacity to store glycogen during a fed state and undergo glycogenesis in response to starvation. Insulin is released by pancreatic β cells after food intake and initiates uptake of glucose upon binding to receptors. This increases glycolysis and glycogen deposition within the hepatocytes (293). They can store up to 100g in glycogen polysaccharides, making them a huge store (294). Hepatocytes remove over 50% of insulin from the blood before it reaches the peripheral tissues (295). As blood glucose declines with uptake, pancreatic α cells secrete glucagon which stimulates gluconeogenesis from glycogen stores and increases hepatocyte glucose output (296). Hepatic insulin resistance is of growing concern to the medical community. It is linked with diseases such as NAFLD, Diabetes type II and cardiovascular diseases. Insulin resistance is the inability of insulin to inhibit glucose output by hepatocytes, while continuing to induce lipogenesis (297). This emphasises the critical role hepatocytes play in efficiently regulating metabolism in the body.

Another highly important role of hepatocytes, and one of the major focusses of this study, is lipid metabolism, storage, and secretion which will be further expanded on in the next sections. Hepatocyte lipid processing is also important for the uptake and secretion of lipid soluble vitamins. Deficiencies in these vitamins can lead to increased risk of haemorrhage (vitamin K), osteomalacia (vitamin D), as well as being a marker of poor outcomes for comorbidities (298, 299). Hepatocyte lipid handling is also important for producing phospholipids for cellular membranes (300). High rates of endo- and exocytosis within the hepatocyte make this a vital role for healthy function. Cholesterol is important for membrane fluidity and can be synthesised by hepatocytes for cells around the body, however excess dietary and *de novo* cholesterol can lead to membrane dysfunction and is linked with pathogenesis of diseases such as atherosclerosis (269, 301). Metabolic regulation is imperative to the function of hepatocytes and necessary for availability of metabolites for the rest of the body's tissues.

1.6.2 Liver FA Metabolism for energy to the rest of the body

Fatty acids are essential for bodily functions such as energy production, composition of cellular membrane, and signalling molecules. The liver plays a pivotal role in regulating FA availability and metabolism. As described above, hepatocytes require fatty acids for their own metabolic and structural maintenance. But also have an essential role in ensuring availability of metabolic substrates for the rest of the body.

1.6.2.1 Fatty acids

The liver is the master regulator of FA metabolism, and it is therefore important to understand the types of FA that we take in via diet, the breakdown of FA and the different forms FA are stored in. FA consist of a hydrocarbon chain with a carboxyl group on one end (222). They can be sub-divided into saturated and unsaturated, the former has no double bonds within the chain, this creates a straight chain of FA which can be packed tightly with other saturated FA chains, resulting in them being solid at room temperature. High intake of saturated FA is closely associated with a higher

risk of cardiovascular disease and low grade inflammatory disorders (302). Unsaturated FA contain one or more double bonds, which creates kinks in the chain, thus resulting in liquid form at room temperature. (303). It is important to have enough FA in the diet as they have a varied role beyond metabolism for energy. They are also important for the formation of cell membranes and signaling molecules such as hormones (222). However, it is important to consume them in moderation in order to limit onset of fat associated disease (304).

The liver breaks down, stores and synthesises FA from the diet and from other stores in the body (269). The most abundant form of FA storage in the body is triglycerides. These are formed via esterification of three FA to a glycerol backbone. This method of storage is highly efficient and can be broken down quickly, via lipolysis, for energy or synthesising other molecules (244). The liver can store large amounts of triglycerides and other forms of FA but also disperses FA around the body for storage in adipocyte tissue and for use by other cells (305). The cells of the body can utilise different length FA for different purposes. For example, cells can preferentially use medium chain (6-12 carbons) FA for FAO as they enter the mitochondria without transport through protein channels, unlike longer FA which are more regularly used for storage and synthesis of cell membrane or signalling molecules (306, 307). The use and storage of different FA highlights the importance of the liver in its role as master regulator of FA metabolism and maintaining homeostasis.

1.6.2.2 Uptake and synthesis

One of the key components of lipid homeostasis is the hepatocytes' ability to take up dietary fats as well as *de novo* synthesis of fatty acids (Figure 1.9). The bile secreted into the intestines binds with monoglycerides and FA from hydrolysed dietary triglycerides. These passively diffuse into intestinal enterocytes, where they are re-esterified, and the digested fats and lipoproteins are packaged into chylomicrons. These are transported in the blood and lymph before lipoprotein lipases extract the fatty acids from chylomicrons and they are taken up by transport proteins such as CD36, FATP 2, 4, and 5 (269).

As previously mentioned, cholesterol is integral for cell function. Not only do hepatocytes release cholesterol in low-density lipoproteins (LDL) with triglycerides but they also remove excess LDL from the bloodstream (308) via activation of the

low-density lipoprotein receptor by surface proteins such as ApoE on LDL (309). Reverse cholesterol transport can also return cholesterol to the liver via high-density lipoproteins (HDL) to limit the potential damage caused by excess circulating FA (310). Hepatocytes can *de novo* synthesise cholesterol from Acetyl-CoA produced in the metabolism of carbohydrates, fats and proteins, in the mevalonate pathway (311). This process and lipogenesis can be stimulated by the IKK: NF- κ B axis, making it an attractive pathway to target in the development of steatosis (312). They are also capable of other forms of lipogenesis. Excess dietary carbohydrates undergo glycolysis to produce pyruvate for Acetyl-CoA which enters the TCA cycle. Acetyl-CoA is carboxylated to form malonyl-CoA before being elongated by fatty acid synthase to form the FA palmitate for storage or secretion (313).

FA uptake and synthesis regulation by the presence of excess dietary fats and carbohydrates work in a feedback loop. Excess dietary metabolites increase uptake which facilitates increased expression of FA metabolism genes. As the metabolites are removed from the blood so too is the expression stimulus, resulting in reduced expression and protein production (269). One example of this is the PPAR signalling pathway, as discussed in 1.5.4. FA in the hepatocytes activate the PPAR transcription factors which target expression of FA uptake proteins such as *Cd36*, *Fatps* and *Fabps* (227). CPT1a protein catalyzes the transport of long-chain FA into the mitochondria and is also a target gene of PPAR α , as well as genes associated with peroxisomal and mitochondrial β -oxidation (314). PPAR α directly and indirectly influences lipogenesis by interacting with a DR-1 element within the Sterol regulatory element binding protein-1c (SREBP-1c) promoter or via cross regulation of SREBP-1c by the LXR signalling pathway. SREBP-1c is one of the insulin dependent transcription factors of lipogenesis (315). Kupffer cells can also be involved in signalling increased FA uptake and lipogenesis via cell-cell signalling or the release of IL-6 and TNF- α (316, 317), highlighting the role of tissue resident macrophages in lipid homeostasis. Uptake and synthesis of FA by hepatocytes is tightly regulated to maintain homeostasis at cellular and systemic level.

1.6.2.3 Storage and export

It is important that hepatocytes can store and release FA. This prevents lipo-toxicity and allows for secretion of FA for other tissues to store or use as an energy source (Figure 1.9). However, aberration in this process has been linked with metabolic diseases (318). LD are the organelles which store neutral lipids during periods of energy excess while serving as a reservoir in energy deficit (319). Of the FA in the liver 15-30% come from uptake of dietary fats, up to 30% is from *de novo* synthesis, and the remainder is recycled FA from adipose tissue (320). In addition to its other roles, insulin activates transcription factors, such as SREBP-1c, to enable the expression of lipogenic genes to store excess carbohydrates (321). The FA produced from these can be esterified by enzymes such as diacylglycerol acyltransferase (DGAT)2, so they can be stored in LD (322). Reviewers' state that the first to describe LD were R. Altmann in 1890 and E. B. Wilson in 1896 (318). However, they were described as inert fat droplets, leading to very limited research into them for almost a century until 1991. It was then that Greenberg et al described the LD protein they called perilipin (PLIN), a protein highly involved in LD formation and lipid metabolism (323). LD contain a core of neutral lipids surrounded by a phospholipid monolayer with membrane bound proteins. The FA core contains neutral lipids such as triglycerides and cholesterol esters (324). The process of packaging neutral lipids into LD is still being determined. One model suggests that FA accumulate within the phospholipid bilayer of the ER when they are synthesised and esterified by enzymes such as DGAT 1 which esterifies FA which have the potential to cause toxicity in the ER (325). Once the critical concentration of FA has been reached, the bilayer is deformed and budding of the LD is triggered and they acquire proteins such as PLIN that targets the organelles to the cytoplasm. The LD can also acquire enzymes from the ER that mediate triglyceride synthesis and thus continues to grow the LD (325). Investigation into the proteome of LD is challenging due to the difficulties in purifying them. However, some studies have shown that PLIN 2 and 3 are conserved (318). These have also been seen to be implicated in diseases with increased LD formation like NAFLD (326) and cancers such as breast cancer (327) and renal cancers (328), and may be an interesting target for treatment of these diseases going forward.

While it is important for hepatocytes to store the FA, it is equally important that they can export them. LD must be catabolised, and dietary fats secreted in very low-density lipoproteins (VLDL). Breakdown of LD can occur by two different

mechanisms, either through the action of lipases on the surface of the LD or the trafficking of the LD to a lysosome (329). PLIN proteins must undergo chaperone mediated autophagy before lipolysis can occur (330). ATGL is one of the key studied lipases, and through binding its co-activator it initiates triglyceride hydrolysis (331). Its importance has been highlighted in murine models where liver specific knockout resulted in accumulation of LD in hepatocytes (332). After hydrolysis FA undergoes exocytosis out of the cell where fusion with the cell membrane allows release of the FA (333). Lipophagy occurs when LD are engulfed by a lysosome to form autophagosomes and is induced by *HNF4 α* downstream gene expression (246). Lysosomal acid lipases and the RAB family of GTPases are required for degradation of the neutral lipids. (333) FFA can subsequently be taken up by neighbouring cells or carried in the blood by albumin (275) or via VLDL. The construction of VLDL also occurs at the ER and branches off before LD formation via interaction with carboxylesterase-1 (334). A large portion of the dietary FA taken up by hepatocytes is released in VLDL for use or storage in other tissues such as muscle and adipose tissue (Figure 1.9)(269). ApoB100 is required for the production of VLDL during its production within the ER, the VLDL is formed around it. FA accumulate in the ER either from dietary fats, *de novo* synthesis, or trafficked from the breakdown of LD. VLDL are transferred to the Golgi, where they continue to grow and are then trafficked to the cell membrane and undergo exocytosis into the sinusoid to be circulated to other tissues (324). Dysregulation of lipid accumulation and secretion is implicated in numerous diseases, a hallmark of these disease is oxidative stress in the liver. When trafficking of FA is impaired, β -oxidation is increased, generating increased cellular ROS, leading to further liver damage (335). This highlights requirement of functional lipid trafficking for hepatocyte function.

1.6.2.4 Ketogenesis

During fasting/starvation state ketone bodies are produced by the process of ketogenesis. They are an alternative energy source in a carbohydrate deficient state, and a conduit to remove excess acetyl-CoA from FAO (336). During fasting, high glucagon induces lipolysis of adipocytes, increasing FA available to hepatocytes. Ketone bodies are produced to cope with the excess acetyl-CoA and insufficient TCA intermediaries to keep up with the demand (Figure 1.9) (336). The primary ketone bodies produced are acetoacetate, beta-hydroxybutyrate, and acetone. Ketogenesis

occurs in the mitochondria of hepatocytes and is driven by 3-hydroxymethylglutaryl CoA synthase (HMGCS2) which is transcriptionally regulated downstream of PPAR in response to high FA levels (337, 338). Liver specific *Hmgcs2* knockout results in increased LD formation and steatosis (339). (337) Interestingly hepatocytes produce ketone bodies but do not have the capabilities to utilise them as they lack the ketolytic mitochondrial enzyme succinyl-CoA:3-oxo-acid CoA-transferase (340). Hepatocytes export ketone bodies into the blood via solute carrier family 16, member 6, and they are taken up by target cells via monocarboxylate transporters. The ketone bodies are re-oxidised into acetyl-CoA for use in the TCA cycle or lipogenesis (341). It is of note that studies show that ketone bodies have a tumour suppressing affect. A ketone diet has been shown to aid in the suppression of pancreatic cancer and gliomas, as well as resensitising *in vivo* AML models to PI3K inhibitors (342-344). Ketogenesis is necessary for homeostasis and minimises lipid toxicity in hepatocytes. It is also an increasingly attractive target in cancer treatments.

1.6.2.5 Cancer mediated alteration of liver FA metabolism

Liver FA metabolism is clearly important for the normal physiological functions of the body. However, the tightly regulated process can be hijacked to benefit the proliferation and expansion of various cancers. Altered lipid metabolism is a hallmark of many malignancies, as well as cachexia prior to treatments (345, 346). Although limited research is currently being published in investigating alterations to liver specific metabolism, systemic alterations are a good indicator due to the central role of the liver in metabolism. Lipidomic studies have indicated systemic or liver lipid dysregulation in breast cancer (347), prostate cancer (348), colorectal cancer (250, 349), ovarian cancer (350), and pancreatic cancer (351). This process can occur by cell-cell interaction or cytokine release that can also act on the liver to alter FA metabolism (352). More research needs to be done to further elucidate alteration to liver FA metabolism by cancers. This research has the potential to find novel therapeutic targets and in doing so exemplifies the importance of interrogating whole organism metabolism in cancer studies.

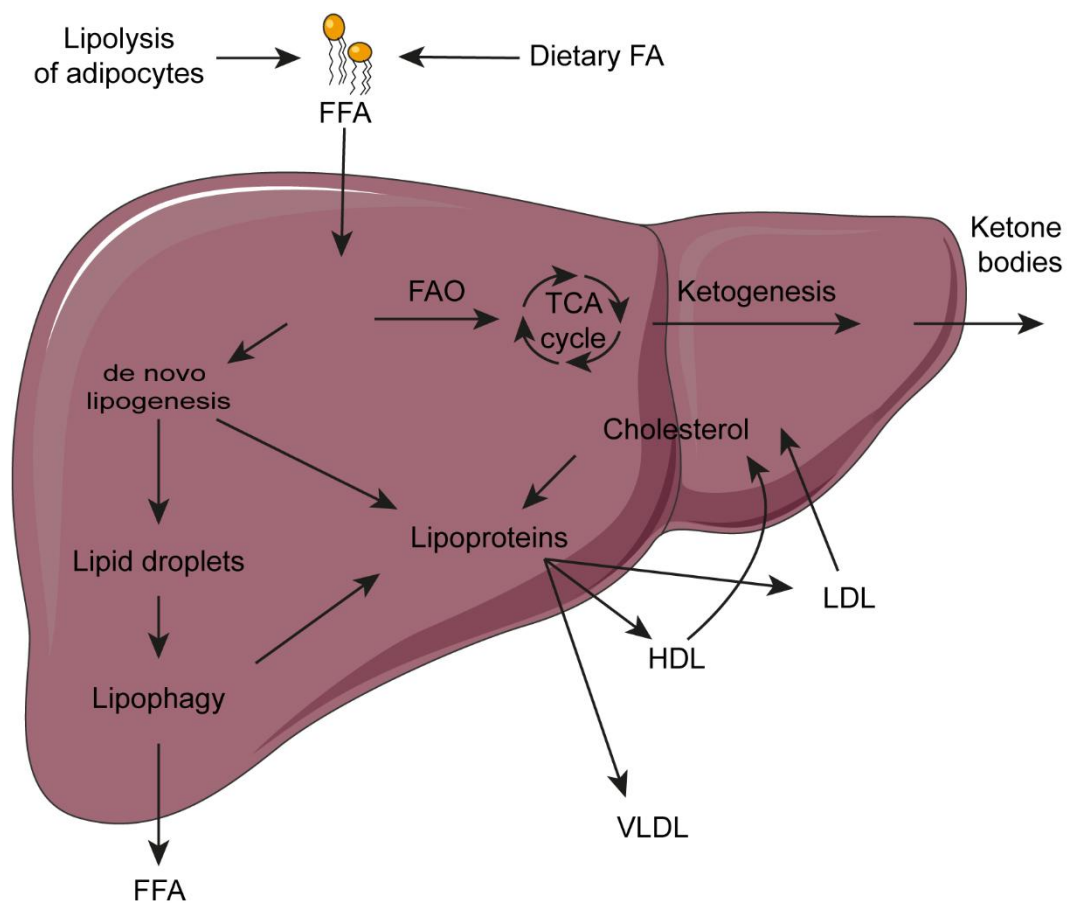


Figure 1.9 Liver lipid metabolism.

The liver obtains FFA from dietary fats or from lipolysis of adipocytes. Once in the hepatocytes they are either used as an energy source or undergo lipogenesis. In low energy states the lipids are packaged into lipoproteins, VLDL, HDL, or LDL for the rest of the body to use or store. These can then be taken up by the liver again if necessary. Cholesterol can be recycled from these for cellular functions or further lipoprotein secretion. In a high energy state lipid can be stored as LD. During increased demand or toxicity lipophagy breaks down LD and FA can be released as FFA or by used to make lipoproteins. In a starvation state hepatocytes utilise ketogenesis. From this ketone bodies are secreted for other tissues to use.

1.7 Research models

In research it can be challenging to model and investigate a disease. It is difficult to model complex organs *in vitro*, and, although technology is advancing, it is harder still to model interactions between organs *in vitro*. Therefore, many complex diseases, that affect the whole system, are researched in model organisms such as drosophila flies, zebra fish, and mice (353). Where possible, scientists perform experiments *in vitro* or mathematically model them in order to reduce the use of animals and inform *in vivo* experiments, as the experiments inevitably cause harm to them (354). In this study the interactions between cells in the BM and cells in the liver are being investigated. Mouse BM and livers closely resemble human anatomy and physiology (355), making them the best suited small animal model for this study. Mice are relatively cheap to house and reproduce quickly. This has allowed for many mouse strains to be bred for research. Wild-type mice may be inbred to reduce variability and can further be used for genetic modification to model specific diseases (356, 357).

To research AML different mouse models have been produced. Mice may be genetically engineered to expressed AML associated genes, resulting in spontaneous development of the disease (358). Another model of AML in mice is via the transplantation of BM. This can use patient derived xenografts (PDX), which are taken directly from a human patient and best reflect the heterogeneity of AML (359). However, they are often difficult to access and therefore retroviral transduction of mouse HSPC cells with genes associated with AML can be used to transplant into a new mouse and develop AML. These genetic alterations can be linked to an inducible control so that they are only activated with external intervention for precision studies into the development and progression of AML (360).

In this study the two main AML cell lines used are HSPC cells which have been transfected to over express the meningioma (*MN1*) or homeobox protein A9 (*HOXA9*) and meis homeobox 1 (*MEIS1*) genes. The MN1 gene and its protein play a role on cell growth and development (361). Over expression of MN1 has been implicated in AML as over production of the MN1 protein results in increase proliferation of immature myeloid cells, which are impaired from differentiating into mature blood cells. Patients with the MN1 mutation often have a poor prognosis with higher relapse rates and poor response to standard chemotherapies (362, 363). By inducing this

gene over expression in mice HSPC, it is possible to closely resemble human AML within the murine system (364). Studies have shown that a large proportion of AML cases involve overexpression of MN1, and it is often associated with specific AML subtypes including inversion of chromosome 16 (365). Meanwhile HOXA9 encodes for transcription factors involved in haematopoietic development and MEIS1 encodes for complementary co-factors (366). The combined overexpression of these genes in HSPC has been shown to cause uncontrolled proliferation of immature myeloid cells. This results in an aggressive form of AML with poor prognosis for patients (367). Both genetic abnormalities are associated with poor outcome for patients, they have both been tested in mouse models to mimic the disease (368). Therefore, this study utilised over expression models of MN1 and HOXA9/MEIS1.

1.8 Rationale

AML remains an incurable malignancy with poor prognosis for patients. Although novel therapeutics and more targeted treatments have become available over recent years, the treatment outcomes have remained largely unchanged. It is therefore imperative that we continue to investigate new mechanisms and targets for novel therapeutics. Studies have shown that AML is highly reliant on its ability to source metabolites for survival and proliferation. This has been shown to be targetable within the BM niche. Studies have indicated the possibilities of blocking or downregulating metabolic mechanisms such as induction of lipolysis of adipocytes or transfer of mitochondria from stromal cells. Through its ability to hijack healthy haematopoietic mechanisms, it has been shown that AML depletes the BM of stored metabolic resources. However, it is also important to look at the system as a whole and how AML is able to access a continuous source of metabolites from around the body. This is especially important as AML patients often present with non-specific symptoms such as drastic weight loss. This sustained loss of weight is detrimental to the patients, causing increased frailty and lead to poor outcomes. The liver is the master regulator of FA metabolism in the body, and thus important to investigate. Under healthy conditions the liver can store FA or release them into the blood stream as demand necessitates.

This study will investigate the interaction between AML and the liver, specifically focusing on the potential to alter FA uptake and metabolism, and how that might impact on AML disease progression. The research will explore how AML alters the liver's FA uptake and metabolism, further examining the mechanism by which AML increases the availability of FA in the serum.

1.9 Hypothesis

I hypothesise that during its progression, AML induces a cachectic state and acts on the liver to perturb FA metabolism. I further hypothesise that AML secretes factors such as HGF into the peripheral blood, which acts on the liver to downregulate FA uptake and metabolism, resulting in higher serum FA availability for AML use.

1.10 Aims and objectives

1. To define changes in systemic FA metabolism during AML proliferation.
2. To determine whether AML acts on the liver to dysregulate FA metabolism and uptake, at a gene, protein and functional level.
3. To investigate the mechanism of AML induced changes in liver FA metabolism and whether it can be rescued.

2. Materials and methods

2.1 Materials

All reagents and materials used in this study are described in the section below. Reagents were obtained from the indicated manufacturers.

Table 2.1 Reagents used, with manufacturer and catalogue ID.

Abcam (Cambridge, UK), Agilent (Santa Clara, USA), ATCC (Virginia, USA), (BioLegend (San Diego, CA, USA), Bio-technique (Minneapolis, USA), Fisher Scientific (Hampton, New Hampshire, USA), Invitrogen (Waltham, USA), Linton Instrumentation (Diss, UK), Medisave UK Ltd (Weymouth, UK), Merck Millipore (Burlington, MA, USA), Miltenyi Biotec (Bergisch Gladbach, Germany), National Diagnostics (Atlanta, USA), PCR Biosystems (London, UK), Peprotech (Rocky Hill, NJ, USA), Promega (Madison, WI, USA), Qiagen (Hilden, Germany), R&D Systems (Minneapolis, USA), Sigma Aldrich (St Louis, MO, USA), Sarstedt (Nümbrecht, Germany), SwissLumix (Lausanne, Switzerland), ThermoFisher (Waltham, MA, USA), Tocris (Minneapolis, USA), Vector Laboratories Ltd (Peterborough, UK), and Worthington Biochemical (Lakewood, USA).

Product	Manufacturer	Catalogue ID
Alexa Fluor™ Plus 647 Phalloidin	Invitrogen	A30107
BODIPY™ 493/503	ThermoFisher	D3922
Foetal Bovine Serum	FisherScientific	1550356
Penicillin-Streptomycin	FisherScientific	15276355
1ml syringe	Fisher Scientific	15489199
20ga/33mm polypropylene animal feeding tubes	Linton Instrumentation	FTP-20-33
26-gauge butterfly needle	Medisave UK Ltd	2674829
26-gauge needle	Fisher Scientific	12349169
27-gauge needle	Fisher Scientific	10204444
AML 12 cell line	ATCC	CRL-2254
Bioluminescent Fatty Acid Luciferin (FA-SS-Luc)	SwissLumix Sarl	GL61203
Bovine serum albumin	Sigma Aldrich	A7906
Calcium Chloride - CaCl₂	Sigma Aldrich	C1016
CD117 MicroBeads, mouse	Miltenyi Biotec	130-091-224
CD45 Antibody, anti-mouse, REAfinity™, FITC	Miltenyi Biotec	130-110-658

Collagen type 1	Fisher Scientific	354236
Collagenase type 1	Worthington Biochemical	LS004196
Corticosterone Parameter Assay Kit	R&Dsystems	KGE009
Crizotinib	Tocris	4368/10
DAPI	ThermoFisher	62248
Dexamethasone	Sigma Aldrich	D4902
D-Luciferin	Fisher Scientific	8829
DMEM F12 Medium	ThermoFisher	10565018
DMEM Medium	ThermoFisher	10566016
DMSO	Fisher Scientific	BP231-100
EDTA	Sigma Aldrich	E9886
EDTA tubes	Sarstedt	6.265 374
Ethylenediaminetetraacetic acid calcium disodium salt hydrate	Sigma Aldrich	E9886
Fenofibrate	Tocirs	4113
Formalin	Sigma Aldrich	1004960700
Free Fatty Acid Assay Kit - Quantification	abcam	ab65341
Glucose	Sigma Aldrich	389374
Goat anti-Rabbit IgG (H+L) Cross-Adsorbed Secondary Antibody, Alexa Fluor™ 568	Invitrogen	A-11011
HCS LipidTOX™ Deep Red Neutral Lipid Stain, for cellular imaging	Invitrogen	H34477
Histo-clear	National Diagnostics	HS-200
Hoechst 33342 solution	Invitrogen	62249
Human HGF ELISA Kit - Quantikine	R&D Systems	DHG00B
Insulin-selenium-trensferrin	Sigma Aldrich	I1884
IsoFlo - Isoflurane	DMU	in house
L-Glutamine	Sigma Aldrich	G7513
Lineage Cell Depletion Kit, mouse	Miltenyi Biotec	130-110-470
LS columns	Miltenyi Biotec	130-042-401
mAb IL-1β	bio-techne	MAB401
Magnesium sulphate - MgSO₄	Sigma Aldrich	M2643
MEM Medium	ThermoFisher	11095080
Mouse & Rat HGF ELISA Kit - Quantikine	R&D Systems	MHG00

Mouse IL-1 beta/IL-1F2 ELISA Kit - Quantikine	R&D Systems	MLB00C
Mouse Sca1 – APC	Miltenyi Biotec	130-102-343
Mouse/Rat HGF Quantikine ELISA Kit	R&Dsystems	MHG00
Normal Goat Serum	abcam	ab7481
Palmitic acid	Sigma Aldrich	P5585
Polybrene Infection / Transfection Reagent	Sigma Aldrich	TR-1003-G
Polyethylene glycol 400	Sigma Aldrich	528877
Potassium Chloride - KCl	Sigma Aldrich	P9541
Potassium phosphate monobasic - KHPO₄	Sigma Aldrich	P9791
primers for RT-qPCR	See Table 2.2	
Proteome Profiler Mouse XL Cytokine Array	R&Dsystems	ARY028
qPCRBIO SyGreen Mix Lo-ROX	PCRBIO SYSTEMS	PB20.11-01
Recombinant Human IL6	PeptoTech	200-06
Recombinant Mouse G-CSF	Biologend	574604
Recombinant Mouse HGF	Biologend	771601
Recombinant Mouse IL-1β	Biologend	575102
Recombinant Mouse IL3	PeptoTech	213-13
Recombinant Mouse SCF	PeptoTech	250-03
ReliaPrep™ RNA Miniprep Systems	Promega	Z6012
Seahorse XF Cell Mito Stress Test Kit	Agilent	103015-100
Seahorse XFp Base Medium	Agilent	1033335-100
SHCLNV Hgf KD	Sigma Aldrich	SHCLNV, TRCN0000336131
SLC27A2/FATP2 murine Polyclonal Antibody	Invitrogen	PA5102343
Sodium bicarbonate - NaHCO₃	Sigma Aldrich	S5761
Sodium chloride - NaCl	Sigma Aldrich	S3014
Triglyceride Assay Kit - Quantification	abcam	ab65336
Triton X-100	Sigma Aldrich	9036-19-5
Trypan Blue Solution	Sigma Aldrich	T8154
Tween-80	Fisher Scientific	T164-500
UltraScript® cDNA Synthesis Kit	PCRBIO SYSTEMS	PB30.11-02

2.2 Animal models

All *in vivo* work was performed in accordance with the regulations of the UK Home Office and the Animal Scientific Procedures Act 1986 under the project licence PP0023671 (Dr Stuart Rushworth). Experiments were planned to follow the 3R's of replacement, reduction, and refinement, to ensure experiments were well planned out. Only using the number of mice truly necessary and ensuring all drugs and reagents had been tested *in vitro* prior to any *in vivo* work.

2.2.1 Animal maintenance

Animals were housed in the containment level 3 facility, Disease Modelling Unit at the University of East Anglia. This study used wildtype C57Bl/6 mice, purchased from Charles River (UK). Breeding pairs were set up with mice between 6 and 8 weeks old and kept for no more than 6 months. Pups were weaned at 3 weeks old and utilised in experiments aged 8-14 weeks. C57Bl/6 mice are the most widely used inbred mouse strain as they maintain good breeding records. These mice were used to study changes in liver metabolism in response to AML. Mice were regularly weighed to ascertain whether AML caused weight loss. The blood and BM were collected from mice to confirm AML cell engraftments. The blood was also collected to obtain serum for detection of altered FFA in response to AML. The inguinal and gonadal fat pads were collected to indicated fat loss due to the disease progression. Finally, the liver was collected for analysis of the changes in gene expression associated with FA metabolism.

2.2.2 Animal Procedures

All animal procedures were performed by myself under my UK Home Office personal licence I32269130, with help from Dr Stuart Rushworth (ICD3874DB), Dr Charlotte Hellmich (IE10ADD51), Miss Katherine Hampton (I211627388), Mr Dominic Fowler-Shorten (I84770732) and Miss Alyssa Polski-Delve (108750454). Training for the procedures was given by Mr Richard Croft (IGEBEF87) and Mrs Anya Croft (L8A2ACED).

2.2.2.1 Body weights and food consumption

During the experiments mice were individually weighed prior to treatments and weighed daily throughout experiments to monitor for adverse effects and record weight loss due to AML engraftment. For some experiments food consumption was weighed to ascertain whether food intake altered during AML progression. This was performed by providing a fresh cage at the beginning of the experiment followed by weighing the food daily. Intake was calculated per mouse per day.

2.2.2.2 Intravenous injections

For the AML models, MN1 or HOXA9/MEIS1 AML cells were isolated from culture and resuspended in phosphate-buffered saline (PBS). FFA-SS-luciferin was dissolved in dimethyl sulfoxide (DMSO) and diluted in PBS for injections. Mice were warmed in a heat chamber for 10 minutes at 37°C to obtain vasodilation. Then transferred to a bench-top holding cone and 200µl of the suspension was injected into the lateral tail vein via a sterile 27-gauge needle, pressure was applied to aid clotting. Mice were briefly monitored in a fresh cage and returned to their home cage.

2.2.2.3 Intraperitoneal injections

Mice were given D-Luciferin, recombinant murine HGF, and IL-1 β by Intraperitoneal (IP) injections. Mice were restrained and 200µl of the treatment solution was injected into the peritoneum via a 26-gauge needle. Mice were monitored in a fresh cage and returned to their home cage.

2.2.2.4 Oral gavage

In different experiments a single dose of Crizotinib and 7 consecutive days of fenofibrate were administered by oral gavage (by Dr Rushworth). Both were prepared in 10% DMSO, 5% Tween80, 40% polyethylene glycol 400 and 45% deionised water. Suspensions were prepared fresh each day. 200µl of the suspensions were administered by scruff restraint, via 20ga/33mm polypropylene animal feeding tubes. Mice were monitored and returned to home cages.

2.2.2.5 Live *in vivo* imaging

To analyse the tumour burden and uptake of FFA by the tumour, bioluminescent imaging of live mice was used. This was enabled as the murine AML cells (MN1) expressed the luciferase construct (2.4.1) To assess FA uptake of the tumour MN1^{+FF}_{KD HGF} or MN1^{+FF con HGF} (2.4.1.1) engrafted mice were IV injected with 3mg/kg FFA-SS-luc and left for 5 minutes at room temperature for optimal detection of the luciferase signal. Mice were anaesthetised using isoflurane using a chamber filled at a flow rate of 2-4%. Once loss of consciousness was confirmed, mice were transferred to the Bruker In-Vivo Xtreme and imaged with a bioluminescent exposure of 5 minutes, followed by x-ray and light images. To further analyse the tumour of these mice, they were IP injected with 150mg/kg of D-luciferin while still under the effect of anaesthesia. The mice were then left for 5 minutes in the Bruker In-Vivo Xtreme with continued anaesthesia. Imaging was taken with the bioluminescent exposure for 1 minute, followed by the x-ray and light images. Mice were transferred to their home cages for recovery post imaging. The bioluminescent detection was achieved by the formation of oxyluciferin from luciferin catalysed by the luciferase in the modified MN1 cells. Bioluminescence analysis was performed using ImageJ software and edited to merge the bioluminescent and x-ray images for figures.

2.2.2.6 Schedule 1 sacrifice

Mice were humanely sacrificed at the endpoint of each experiment or if a mouse was showing any signs of adverse effects from any of the procedures. These include sudden weight loss (10% in 24hrs), sustained weight loss (20% in 64hrs), reduced motility, piloerection and hunched postures. Two schedule one methods were used to confirm death of the animals. Firstly, asphyxiation by a rising concentration of CO₂. This was followed either by cervical dislocation or, when blood was required, exsanguination via a jugular slit.

2.3 Murine tissue collection

2.3.1 Bone marrow isolation

Mouse BM was isolated from the tibias and femurs of mice. This was achieved by dissecting the legs and removing any muscle, tendons and ligaments. Bones were then cut in half and individually placed into a 0.5ml microcentrifuge tube with a hole in the bottom. This was placed into a 1.5ml microcentrifuge tube (Figure 2.1). These tubes were centrifuged at maximum speed for 5 seconds, allowing the cells from each bone to be collected at the base of the 1.5ml microcentrifuge tube. The BM pellets were resuspended in 1ml magnetic-activated sorting (MACS) buffer (1X PBS pH7.4, 0.5% BSA and 1mM Ethylenediaminetetraacetic acid (EDTA)), per mouse.

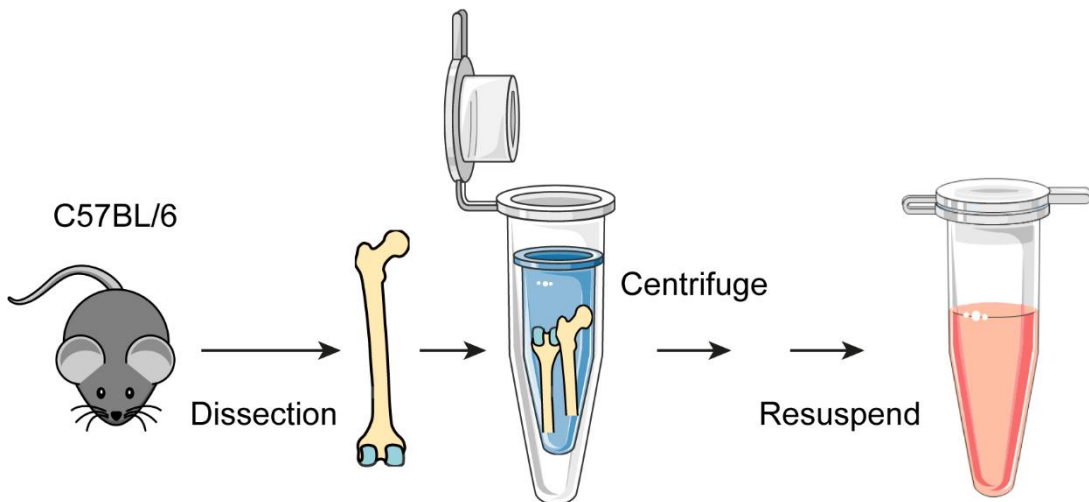


Figure 2.1 Bone marrow isolation.

Tibias and femurs were dissected from mice after sacrifice. Bones were cut in half and placed in a 0.5mL microcentrifuge tube with a hole in the bottom, and then into a 1.5mL microcentrifuge tube. Centrifugation was followed by resuspension of the BM pellet.

2.3.2 Liver isolation

Livers were isolated from the mice by a small incision through the skin and muscle, just below the sternum. This allowed the liver lobes to be gently pushed through the incision. Lobes were cut out, while avoiding damage to the gallbladder, to avoid leakage of products which would damage the tissue. Lobes for gene analysis were immediately put into cryopreservation tubes on dry ice and placed into the -80°C freezer at the earliest convenience. When cells were required for further isolation for flow cytometry or cell culture assays, a lobe was placed into a 1.5ml Microcentrifuge with 1X PBS, before later preparation. For sectioning and immunofluorescent staining of livers, a lobe was placed into a histology cassette and submerged in buffered formalin (4% formaldehyde, 4 gr/L NaH₂PO₄, 6.5 gr/L Na₂HPO₄; pH 6.8,) for 24hours followed by dehydrating and embedding in paraffin wax for sectioning.

2.3.3 Fat pad isolation

Inguinal and Gonadal fat pads were isolated by dissection. The mouse skin was carefully removed from the hind legs and reflected. Fat from the outside of the thigh area was scraped from the skin, making the inguinal portion. The gonadal fat pads were isolated by a further incision above the sex organs of the mouse. That fat compartment removed from here made up the gonadal portion. These portions were then weighed and normalised to the bodyweight of the mouse for further analysis.

2.3.4 Blood and serum isolation

Blood was collected during the Schedule 1 procedure (2.2.2.6). For blood parameters peripheral blood was collected into EDTA coated tubes to prevent clotting. To measure blood glucose and ketones content, 3µl was placed onto a testing strip for respective handheld devices. To acquire serum the peripheral blood was collected into 1.5ml microcentrifuges to encourage clotting, aiding in further isolation of the serum. Samples were left at room temperature for 20 minutes followed by centrifugation at 300g for 10 minutes. Serum was carefully collected and stored at -20°C for later analysis.

2.4 Cell culture

Culture of cells was carried out in incubators set to 5% CO₂ at 37°C.

2.4.1 MN1 and HOXA9/MEIS1 cells

MN1 and HOXA9/MEIS1 cells were generated as AML cell lines for this project. For both lines lineage (lin⁻) negative cells were isolated by negative selection using the Lineage Cell Depletion Kit, per the manufacturer's instructions, from C57BL/6 BM. Lin⁻ cells were further enriched with CD117 magnetically labeled beads for MACS. After incubation with the beads for 30 minutes at 4°C, cells were centrifuged at 300xg for 5 minutes and resuspended in 3ml of MACS buffer. The cells were loaded onto a LS column prewashed with MACS buffer attached to a magnet. The column was washed three times with MACS buffer and the CD117⁺ cells were flushed from the LS column by removal from the magnet and plunging the column. Cells were finally sorted for SCA1-APC on a FACSMelody by Dr Edyta Wojtowicz (Erlham Institute, Norfolk, UK). The cells were expanded in DMEM containing 10%FBS plus 1% penicillin-streptomycin (pen/strep) supplemented with mSCF (100ng/ml), mIL3 (10ng/ml) and hIL6. Once established the cells were retrovirally infected by coculture with PSF91MN1iGFP for *MN1* over expressing cells, or MIH-HA-HoxA9iGFP and MIY-HA-Meis1a for *HOXA9/MEIS1* cells in the presence of polybrene (10µg/ml) for 3 days. Cells were maintained in DMEM, 10% FBS and 1% pen/strep, further supplemented with mSCF (100ng/ml), mIL-3 (10ng/ml) and hIL-6 (10ng/ml). Media was replaced every other day.

MN1 cells were further infected (using the same method as above) with the firefly (FF) construct pCDH-luciferase-T2A-mCherry for *in vivo* imaging, kindly provided by Professor Irmela Jeremias (Helmholtz Zentrum München, Munich, Germany). Transduced cells were kindly cell sorted using the mCherry fluorescence by Dr Edyta Wojtowicz (Erlham Institute, Norfolk, UK).

2.4.1.1 *Hgf* knockdown

MN1 cells (10^5) were cultured in DMEM and 10% FBS. Cells were transduced with a lentiviral shRNA for murine *Hgf* (sequence target GGTAAGGAGGCAGCTATAAA, clone TRCN0000336131), or a scrambled shRNA at a multiplicity of infection (MOI) of 0.1, 1, 5, and 10 in the presence of polybrene (0.1%) for 24 hours, media was topped up for the following 2 days to maintain nutrient levels. In subsequent days 1% pen/strep was added to the media. After 5 days the KD was confirmed by real time quantitative polymerase chain reaction (RT-qPCR) and the most successful, an MOI of 1, and the cells were then maintained in the standard AML culturing media outlined above. The generated cells were termed MN1^{+FF KD HGF} or MN1^{+FF con HGF}.

2.4.2 Conditioned media

AML cells were cultured in the absence of the cytokines normally in the maintenance media for 24hrs at a density of 1×10^6 cells/ml. The cell suspension was transferred to a falcon tube appropriate for the volume and centrifuged at 300g for 5 minutes to pellet the cells. The supernatant was transferred to a new tube and the pellet discarded. The supernatant was further centrifuged at 10,000g for 5 minutes to remove any further particles. The supernatant was then stored for use as conditioned media. For experiments this was cultured on murine hepatocytes and control media only contained 5% FBS rather than the usual 10%. This simulated the growth phase of the AML cell lines utilising the FBS during the conditioning process.

2.4.3 Primary mouse hepatocytes

Primary murine hepatocytes were isolated and plated by Dr Beraza and Dr Ruiz. They were acquired from C57BL/6 mice aged 8-12 weeks. A stock medium was made with ddH₂O with glucose (0.02M), NaCl (0.12M), KCl (4mM), and NaHCO₃ (0.024M), the night before and kept at room temperature overnight. On the day of the experiment the KHPO₄ (0.2M) and MgSO₄ (0.15M) were added to the stock media.

Media was buffered to pH7.4 and warmed to 37°C. Livers were perfused with the stock buffer containing EDTA (0.2mM) until it ran clear, followed by incubation with the stock media for 1 hour. Livers were then incubated in the stock media with the addition of collagenase type1 and CaCl₂ (1.3mM) buffer. Following perfusion, the liver is placed in MEM media and cells released with the aid of tweezers. The isolated hepatocytes were then washed 3 times with MEM, FBS, glutamine and pen/strep and plated in Collagen type I coated plates at a concentration of 2x10⁵ cells/ml. After 2 hours, media was changed to a MEM only media, until experimental use the next day.

In vitro experiments with these cells used conditioned media, recombinant murine HGF, IL-1 β , or G-CSF, Crizotinib, mAb IL-1 β , and fenofibrate prior to further downstream analysis.

2.4.4 AML12s

The alpha mouse liver 12 (AML12) cell line was purchased from ATCC (USA). They are hepatocytes isolated from the normal liver of a 12 week old male mouse and are regularly used as a good model for studies of the liver (271). AML12's were cultured in DMEM F12 supplemented with 10%FBS, 1% pen/strep, 10 μ g/ml insulin, 5.5 μ g/ml transferrin, 5 μ g/ml selenium, and 40 μ g/ml dexamethasone. To split the cells media was removed and put to one side, before washing the cells with PBS. Enough Trypsin was added to the culture flask to cover the cells adhered to the bottom, and incubated for 10 minutes until the majority of the cells have lifted from the flask. The suspension was diluted 1:4 with media and centrifuged for 5 minutes at 130g. Cells were seeded into flasks at a density of 2x10⁵ cells/ml with 1:6 ratio of the old media added to fresh culture media. It was found that AML12 cells cultured best with some old media most likely due to the factors they secrete creating a better environment. Cells were fed every other day and split when density was high enough to completely crowd the flask.

2.4.5 Cell cryo preservation

Cell lines were cryopreserved for long term storage at 5×10^6 cells/ml concentration in their maintenance media with the addition of 10% DMSO. Cells were then transferred to cryotubes and slowly preserved in a Mr Frostey™ Freezing Container in a -80°C freezer. The Mr Frostey™ Freezing Container cools at $-1^{\circ}\text{C}/\text{minute}$, which is optimal for cell cryopreservation. After 24hrs the cryovials were moved to liquid nitrogen storage

To thaw the cells cell culture media was firstly warmed to 37°C . Once up to temperature, the cryovials were brought from liquid nitrogen storage, on dry ice, and held in a water bath at 37°C until partially defrosted. Roughly 1ml of the prewarmed media was added to the cryovial slowly and the cell suspension transferred to a T75 tissue culture flask, with a further 10ml of the media added, diluting the DMSO. After 24hrs the suspension was moved into a 15ml falcon tube and centrifuged at 300g for 5minutes. The supernatant was discarded, and the pellet resuspended in fresh, prewarmed media and cultured accordingly.

2.4.6 Isolation of human serum

Non-malignant and malignant human peripheral blood samples were collected from the Norfolk and Norwich University Hospital by Dr Charlotte Hellmich. Studies were carried out with the approval from the United Kingdom Research Authority research ethics committee (LRCEref07/H0310/146) and patients donated with informed consent. Vacutainer blood centrifuge tubes were used to collect the blood and centrifuged at 3000g for 10 minutes, allowing the translucent gel layer to separate the serum and the blood cells (Figure 2.2). The serum fraction was aliquoted and stored at -80°C freezer for further use.

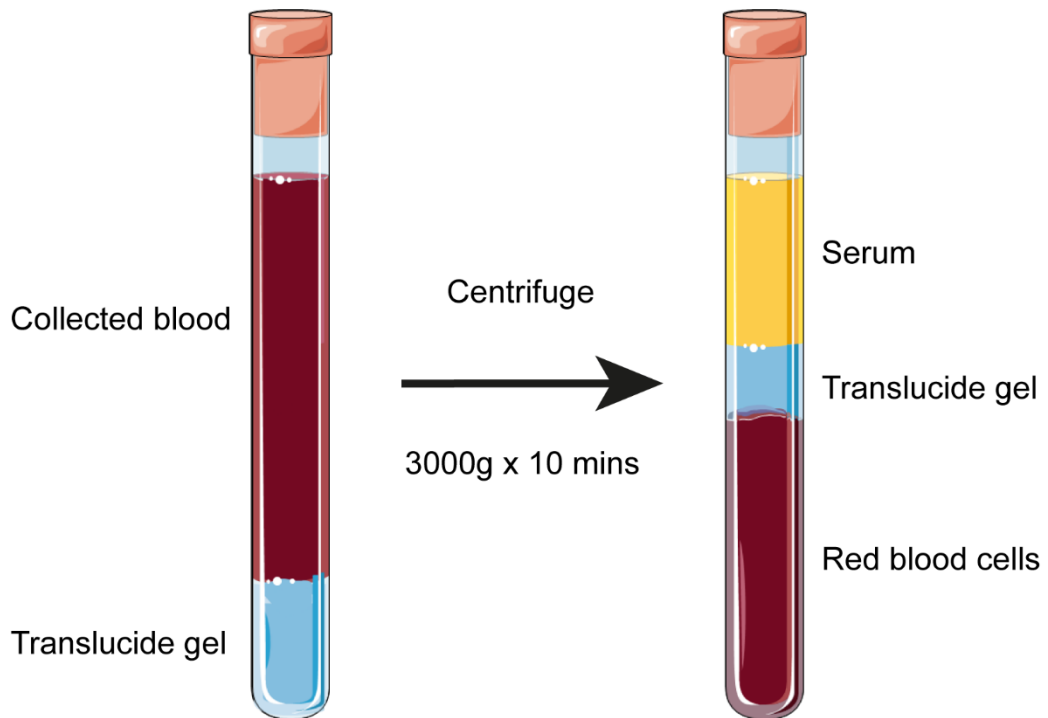
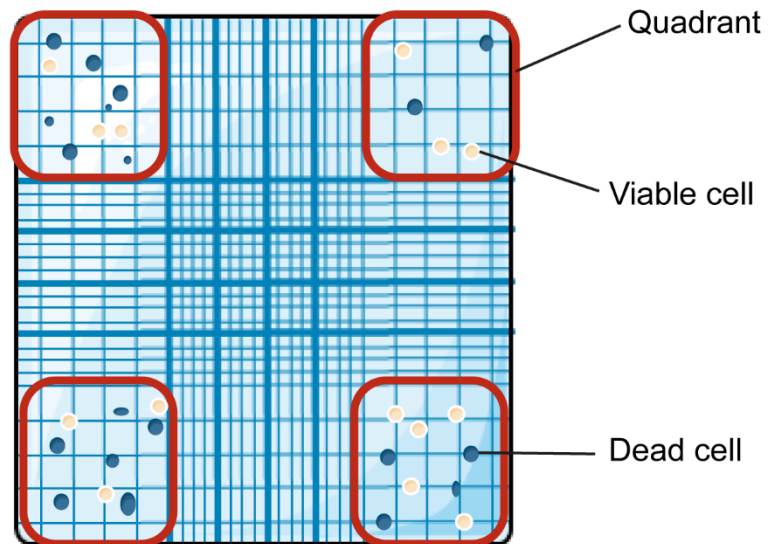


Figure 2.2 Isolation of human serum.

Patient serum was collected in a blood centrifugation tube and spun at 3000g for 10 minutes. Translucide gel separated the serum and the red blood cells allowing serum to be removed easily and stored.

2.4.7 Cell counting

Trypan Blue is commonly used in an exclusion assay to determine the viable cells in a sample. Viable cells are able to exclude Trypan Blue via the intact cellular membrane, whereas non-viable cells rapidly take up the Trypan Blue. Cell suspensions were diluted with Trypan Blue and MACS buffer as appropriate for efficient counts. The mix was then pipetted onto a haemocytometer, and the viable cells counted. The four outer quadrants were counted, averaged, and the cells/ml calculated (Figure 2.3).



$$\text{Cell number (cells/mL)} = \left(\frac{\text{Viable cell number}}{\text{Number of quadrants counted}} \right) \times \text{Dilution factor} \times 10^4$$

Figure 2.3 Cell viability counting via Trypan blue exclusion.

Haemocytometer layout shows the outer quadrants that were counted (red) with the viable (white) and dead (blue) cells. The equation for the cell number per mL is underneath.

2.5 Molecular Biology

2.5.1 Long chain fatty acid uptake

FA uptake by primary murine hepatocytes was analysed with the addition of conditioned media or recombinant murine cytokine addition as described above. After 16-hours cells were further incubated with a long chain fatty acid (LCFA) 4,4-Difluoro-5,7-Dimethyl-4-Bora-3a,4a-Diaza-s-Indacene-3-Hexadecanoic Acid (BODIPY™ FL C16) (1 μ M) for 1 hour. Cells were then washed with PBS, followed by a 15-minute fixative incubation with buffered formalin. Wells were washed 3 times with PBS, followed by blocking and permeabilizing with PBS, 0.5% BSA, 0.1% Triton X100 for 15 minutes. Further 3 washes with PBS were followed by staining with PBS, 0.5% BSA, 1:800 Phalloidin 647, and 5 μ M Hoechst 33342, for 20 minutes, followed by another 3 washes in PB. Wells were left in 200 μ l PBS for imaging on the EVOS 5000 imaging system. Images were taken on the DAPI, FITC, and Texas Red wavelengths using the Bio Tek Cytation 7 and analysed using the CellProfiler Analyst software. Merged images were further used for presentation.

2.5.2 FATP2 protein expression

Isolated mouse livers were embedded in paraffin wax and sectioned at 4 μ m thickness. Sections were dewaxed with histo-clear and re-hydrated with decreasing concentrations of ethanol before quenching with deionised water. Endogenous peroxidases were blocked for 10 minutes in methanol and 3% hydrogen peroxide. Antigen retrieval was performed by microwaving slides for 10 minutes in citrate buffer pH6 and cooled for 10 minutes. After washing with PBS, sections were blocked in PBS with 1% BSA, 10% goat serum, and 0.1% triton X-100 for 1 hour at room temperature. Slides were incubated overnight at 4°C in PBS with 1% BSA and 1:100 SLC27A2/FATP2 antibody. The secondary antibody (1:1000) and conjugated CD45 (1:100) were incubated for 1 hour the following day after PBS washes. Slides were mounted using Vectashield with DAPI. Images were taken on DAPI, FITC, and Texas Red wavelengths and analysed using the CellProfiler Analyst software. Merged images were used for presentation.

The antibody is specific to aa residues 61-112 of the protein. Although the manufacturer has named the polyclonal antibody SLC27A2, this is the gene name and it is binding to FATP2, the protein SLC27A2 encodes for. Therefore, subsequent analysis has been referred to as analysis of FATP2 protein expression

2.5.3 Flow cytometry

Flow cytometry was used in this study to determine the level of engraftment in mice injected with murine AML cells (MN1 or Meis/HOXA9). This relied on the GFP tag included in the transduction of these cell lines. The BD FACSymphony A1 located at the Bob Champion Research and Education Building at the University of East Anglia was used for this study. It has four lasers (405, 488, 561 and 637nm) enabling it to detect up to 16 colours at a time. For this study no antibodies or compensations were required as only the one laser was in use for the detection of the GFP tag.

2.5.4 Preparation of BM for flow cytometry

Flow cytometry was used to analyse mouse BM for the AML cell engraftment per mouse. Cell suspensions from 2.3.1 were passed through a 40µm filter followed by a cell count (2.4.7). The volume for 2.5×10^6 was transferred to a FACS tube and topped up to 300µl before being run through the cytometer. As both MN1 and HOXA9/MEIS1 AML cells are GFP tagged (2.3.1), no further antibodies were required.

2.5.5 Preparation of liver immune cells for flow cytometry

Liver immune cells were isolated from lobes set aside after sacrifice (2.3.2) in PBS. The lobe was further cut into smaller pieces using sterilised scissors before digestion in PBS supplemented with 0.5% BSA, 0.1% glucose, to make liver perfusion buffer (LPB), with further addition of 1mg/mL collagenase Type IV at 37°C for 30 minutes on a shaker. Red blood cells were lysed using red blood cell lysis buffer for 5 minutes on ice before quenching with LPB. The lobes were then passed through a 70µm filter, and the suspension centrifuged at 300g for 10 minutes. The pellet was resuspended

in LPB, while in a separated falcon a Percoll gradient was prepared. Percoll was layered at 70% and 40%, followed by a layer of LPB. The resuspended cells were carefully layered on top of the gradient and centrifuged at 800g for 20 minutes at 4°C. Immune cells could then be collected from between the 40% and 70% Percoll layers with a pipette. The immune cells were washed with LPB and centrifuged at 300g for 10 minutes at 4°C before resuspension in MACS buffer. Cells were run through a flow cytometer to investigate the presence of AML cells in the liver. As both MN1 and HOXA9/MEIS1 AML cells are GFP tagged (2.4.1), no antibodies were required.

2.5.6 Bulk RNA sequencing

Livers from control, MN1 engrafted and Meis/HOXA9 (n=3) were removed as described 2.2.3.2 and the RNA extracted (2.4.7.1). RNA samples were sent off to NOVOGene sequencing (UK) for bulk RNA sequencing (RNAseq). mRNA sequencing was returned with KEGG pathway enrichment as well as raw data for further analysis.

2.5.7 Liquid chromatography mass spectrometry

Liquid chromatography mass spectrometry was performed by Dr Le Galle and Miss Hampton. Serum isolated from control mice or mice engrafted with MN1 or HOXA9/MEIS1 cells were used for analysis of LCFA. 10 µl serum was incubated in 490 µl ice-cold methanol at -20°C for 15 mins. Samples were centrifuged (14800 rpm, 5 mins) and supernatants filtered using 0.45µm PTFE filters. 50µl of the serum extract was mixed with 20 µL of a solution of nonadecanoic acid as internal standard mix (25 ppm). All the samples were transferred to autosampler vials containing 150 µl inserts and prior to LC-MS/MS analysis. FA were purchased from Sigma-Aldrich. Stock solutions of each metabolite were prepared in methanol (1mg/mL) and stored at -20°C. Calibration standards were prepared by pooling all relevant analytes for each method at eight concentrations and adding the internal standard at 25 µg/ml. Calibration standards were prepared by serial diluting each master mix in methanol, creating 8 standards with concentrations ranging from 0 - 10,000 ng/mL for palmitic, steric, oleic, linoleic acids and arachidonic acids and 0- 2,000 ng/ml for linolenic and eicosapentaenoic acids. Metabolite quantification was performed using liquid

chromatography-tandem mass spectrometry (LC-MS/MS) comprising of Waters Acquity UPLC system and Xevo TQ-S Cronos mass spectrometer controlled by MassLynx 4.1 software. For the detection of LCFA, the electrospray ionisation operated in negative mode and chromatographic separations were performed with a CORTECS T3 2.7 μm (2.1 x 30 mm) analytical column. A sample of 5 μl was injected at a flow rate of 1.3 ml/min. Eluent A (0.2 mM ammonium formate, 0.01% formic acid, water) and eluent B (0.2 mM ammonium formate, 0.01% formic acid, 50% isopropanol in acetonitrile) ran at a constant rate of 1.3 mL/min. The gradient began at 50% B before a linear increase to 98% B occurred at 1.20 min. This was held for 0.5 min before a linear decrease in gradient back to 50% B occurred between at 1.70 min. The gradient was held at 50% B for another 5 mins. The analytical column temperature was maintained at 60°C. Calibration standards were run at the beginning and end of each analytical queue. Chromatogram peak analysis was performed by the accompanying Waters® TargetLynx™ application manager. The analyte: internal standard response ratio was used to create calibration curves and quantify each metabolite in Microsoft Excel.

2.5.8 Seahorse Metabolic flux analysis

The Seahorse XFp Analyser was used to measure the metabolic activity of primary murine hepatocytes using the XFp Cell Mito Stress Kit. This was carried out with help from Miss Katherine Hampton. Cells were seeded onto the Seahorse XFp culture plate at a density of 1×10^4 cells per well and stimulated for 16hr with either conditioned media or recombinant murine HGF (10 $\mu\text{g}/\text{mL}$). The XFp flux cartridge was hydrated with XF Calibrant overnight at 37°C. Media was removed from the wells of the culture plate and replaced with 180 μl Seahorse base medium supplemented with pyruvate (1mM), Glutamine (2mM) and Palmitic acid (100 μM).

The XFp Cell Mito Stress Kit measures the oxygen consumption rate (OCR), giving a reading for oxidative phosphorylation, as well as basal extracellular acidification rate (ECAR), for a measure of glycolysis. The machine uses time injections of Oligomycin (2 μM), carbonyl cyanide-4- (trifluoromethoxy) phenylhydrazone (FCCP) (1 μM), and Rotenone (0.5 μM) in accordance with the manufacturer's instructions. Respectively these drugs act on metabolism to inhibit ATP synthase to reduce OCR, target the inner mitochondrial membrane to increase OCR, and again reduce OCR

via inhibition of complex 1 and 3 in the electron transport chain. This assay produces measurements for the basal and maximum respiration of cells (Figure 2.4). These values were calculated by subtracting the non-mitochondrial OCR from the basal and maximal readings. The data was normalised to the number of cells seeded and analysed using Microsoft Excel and GraphPad Prism software version 10.3.1.

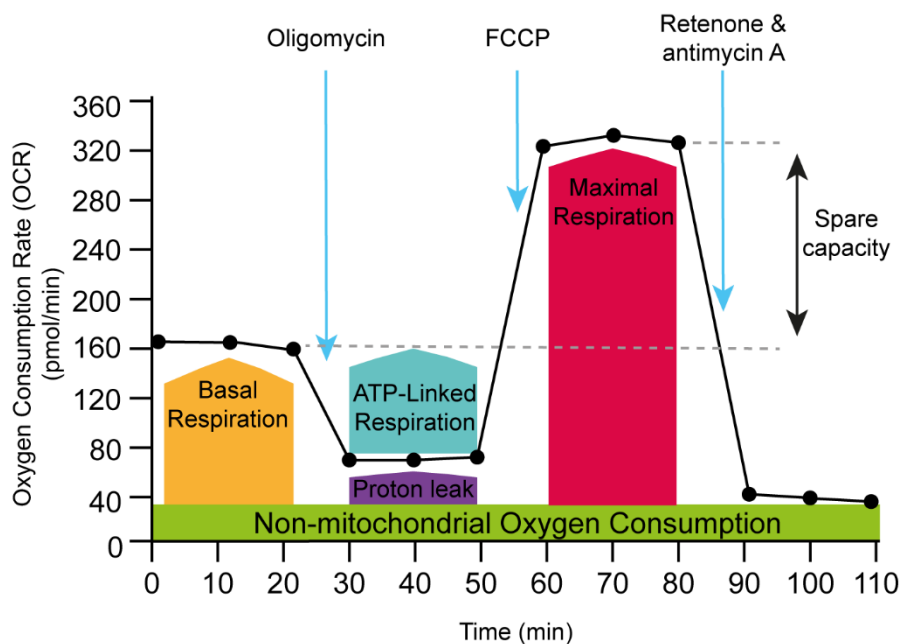


Figure 2.4 Seahorse metabolic flux mitostress kit.

Schematic of seahorse metabolic flux mitostress test. Samples were injected with Oligomycin, FCCP, and Rotenone at timed intervals. The OCR was measured before and after each drug injection, allowing for measurements of maximal and basal respiration to be calculated.

2.5.9 Proteome profiler array

To analyse the cytokine and chemokines released by the AML cell lines MN1 and HOXA9/MEIS1, *in vivo* and *in vitro*, the Proteome Profiler Mouse XL Cytokine Arrays were used. This kit allowed for the detection of 111 secreted cytokines from the AML cell lines in the serum of engrafted mice or in conditioned media. The kit utilises capture and control mouse antibodies, pre-spotted in duplicate on a nitrocellulose membrane. Serum and conditioned media were for the arrays, following the manufacturer's protocol. The membranes were analysed using the G:BOX Chemi XRQ system and quantified using ImageJ.

2.5.10 ELISA kits

Pre-coated ELISA kits were used to analyse the serum levels of mouse HGF, IL-1 β , FFA, corticosterone, and triglycerides. As well as human HGF levels. Serum was isolated from mice as described in 2.3.4 and human serum was collected as outlined in 2.4.6. Kits were performed per the manufacturer's protocol and measurements were taken using the Bio Tek Cytation 7 and analysis was performed using GraphPad Prism software version 10.3.1.

2.5.11 PCR

2.5.11.1 RNA extraction

RNA was extracted for gene expression analysis of livers isolated from mouse experiments, primary hepatocyte experiments and to confirm *Hgf* KD in MN1 cells. For *in vivo* studies, livers from mice were snap frozen after sacrifice and homogenised using a Precellys 24 tissue homogenizer. For *in vitro* experiments cells could be used immediately at the end point. The ReliaPrep RNA cell miniprep system was used for this. RNA lysis was achieved by the addition of TG+BL lysis buffer, the volume varied depending on cell number according to the manufacturer's protocol. Samples were stored in lysis buffer at -20°C until further required. Upon thawing, the appropriate volume of isopropanol was added and mixed well by vortexing for 20 seconds. The lysates were loaded into the ReliaPrep mini-columns and centrifuged

at 13,000g for 30 seconds, before washing with 500µl of RNA wash solution and centrifuged at 13,000g for 30 seconds. The columns were then washed with 200µl Column Wash solution followed by 500µl of RNA wash solution and spun at 13,000g for 30 seconds each time. A final wash step with 300µl of RNA Wash Solution was performed and the samples were spun at 13,000g for 2 minutes. Columns were then placed into the 1.5ml elution tubes and the correct volume of nuclease free water was added (depending on the initial cell numbers used). The samples were centrifuged at 13,000g for 1 minute and the isolated RNA was stored at -20°C until use.

2.5.11.2 Quantification of extracted RNA

The isolated RNA from each sample was quantified using the ThermoFisher NanoDrop Spectrophotometer. After blanking the machine with 1µl of nuclease free water, 1µl of each sample was analysed for the RNA content in ng/mL. The purity level of the samples was also measure using the absorbance threshold of nucleic acids, the was calculated as a ratio of the maximum at 260nm against absorbance at 280nm. Acceptable purity level was a 260/280 ratio between 1.7 and 2.3

2.5.11.3 CDNA synthesis

The extracted RNA within the purity levels was used to synthesis cDNA by reverse transcription using the PCR BIO systems cDNA ultrascript kit. For each sample a 10µl reaction a master mix was made up containing 2µl of 5X cDNA Synthesis Mix, 0.5µl of 20X RTase per samples. Next each sample was diluted to obtain an equal concentration with nuclease free water, making up to a volume of 7.5µl. Then 2.5µl of the master mix was added. The PCR tubes were placed into a Bio-Rad Thermocycler and run on a pre-defined program with 30 minutes at 42 °C, 10 minutes at 85 °C, to denature the RTase, and then a return to 4°C until the samples were removed and stored at -20 °C until used.

2.5.11.4 Real time quantitative PCR

RT-qPCR was performed on a ThermoFisher ABI QuantStudio 7 Flex, using PCRBIOSystems SYBR-green technology to analyse gene expression. Primers were obtained from Qiagen or Sigma-Aldrich (Table 2.2). For the KiCqStart® SYBR Green primers, forward and reverse primers were first combined using 5µl of each and diluted in 90µl of nuclease free water.

Table 2.2 Primers used in RT-qPCR analysis

<u>QuantiTect SYBR-Green Primers (Qiagen)</u>		
Gene	Primer Assay Name	GeneGlobe ID
<i>Acadm</i>	Mm_Acadm_1_SG QuantiTect Primer Assay	QT00111244
<i>Gapdh</i>	Mm_Gapdh_3_SG QuantiTect Primer Assay	QT01658692
<i>Hmgcs2</i>	Mm_Hmgcs2_1_SG QuantiTect Primer Assay	QT00169029
<i>Ppara</i>	Mm_Ppara_1_SG QuantiTect Primer Assay	QT00137984
<u>KiCqStart® SYBR-Green Primers (Sigma-Aldrich)</u>		
Gene	Gene ID	RefSeq ID
<i>Cd36</i>	12491	NM_001159555
<i>Cpt1a</i>	12894	NM_013495
<i>Hgf</i>	15234	NM_010427
<i>Slc27a2</i>	26458	NM_011978

2.5.11.5 Gene expression

To analyse the gene expression in liver samples, primary hepatocytes and MN1 cells, RT-qPCR was performed with SYBR-green technology and diluted cDNA of the samples. A master mix was made with 0.5µl of the primer, 2.5µl of SYBR-Green Mix. 3µL of the master mix was plated onto a 384-well plate, followed by 2µL of cDNA. Once plated, the plate was sealed and centrifuged at 300g for 1 minutes. It was placed into the ABI QuantStudio 7 Flex and run on a pre-programmed cycle seen in Table 2.3. The cycle threshold (Ct) value for each gene of interested was normalised to the housekeeping gene Glyceraldehyde 3-phosphate dehydrogenase (*Gapdh*), which is present in every cell and rarely altered by other genetic changes. Relative expression was determined first by subtracting the Ct value of GAPDH from the Ct value of gene of interest, this is the ΔCt . The $\Delta\Delta\text{Ct}$ was then calculated by subtracting the average control ΔCt from the ΔCt of each condition. The fold change was then calculated by $2^{-\Delta\Delta\text{Ct}}$. Each sample was replicated at least four times.

Table 2.3 qPCR SYBR-Green Quantstudio 7 programming

Step	Cycles	Temperature	Time
Pre-amplification	1	95°C	2 minutes
Amplification	45	95°C	15 seconds
		60°C	10 seconds
		72°C	10 seconds
Melt curve	1	95°C	5 seconds
		65°C	1 minute
		97°C	Continuous
Cooling	1	40°C	30 seconds

2.6 Quantification and statistics

All analysis in this study was carried out using FlowJo software version 10.8.1, GraphPad Prism software version 10.3.1, CellProfiler Analyst software, ImageJ, and Microsoft Excel. Statistical analysis was performed without an assumption of normal distribution due to the variability of data, especially seen when carrying out *in vivo* studies. Therefore, comparisons for 2 groups were performed using a Mann-Whitney U test and for comparisons between more than 2 groups the Kruskal-Wallis H test with Tukey's multiple comparison test was used. Differences between compared groups were considered significant when the probability, p, value was less than 0.05 (*P < 0.05, **P < 0.01, ***P < 0.001, ****P < 0.0001, ns = non-significant). Results are shown with each sample, with the standard deviation. The sample sizes (n) represent the replicates. No statistical protocols were used to determine the sample size ahead of experiments.

3. AML progression in the BM induces systemic metabolic changes and weight loss.

3.1 Introduction

AML has been well characterised within the BM microenvironment. Continued research highlights the metabolic plasticity of the disease. This has been shown both to aid in the progression of the tumour but also to aid in chemotherapy resistance (369). It is well documented that AML scavenges and utilises as many different metabolic sources as it can (209, 219, 235). It has further been shown that AML overtakes the BM, limiting the space for other cells such as adipocytes (33, 370, 371). It is therefore important that research continues to investigate the key mechanisms by which AML is able to acquire metabolites, with a wider view than the immediate niche. Cachexia is characterised as severe loss of bodyweight, specifically a loss of muscle mass, with or without a loss of fat. It has been described in patients with AML and has largely been attributed to chemotherapy treatment. However, more recent research has been indicating that patients may be entering a cachexic state, including the loss of fat, prior to treatment (157, 158, 372). Currently, little research has been performed to understand the mechanism by which this is occurring.

AML utilises FA metabolism both as an energy source and as building blocks for other metabolic processes. It has been characterised that AML increases the expression of scavenger receptors such as CD36, as well as increased expression of FABPs to further improve uptake of FA (33, 236). Like HSC, AML blasts can also access FFA from the peripheral blood flow to the BM (25, 85). This source of metabolites from outside of the BM has not been widely investigated in regard to any BM malignancy. However, it could be a key area in understanding how AML accesses FA when the adipose of the BM has been depleted.

In this chapter I aim to confirm a model of weight loss linked to fat pad weight reduction in response to AML engraftment. This is not a model of cachexia as analysing both changes of fat and muscle mass are outside of the scope of this project. I will determine the methodology for weight loss and any involvement of food intake. Furthermore, I will investigate how this state alters the FA makeup of the peripheral blood serum and thus the availability to AML. Finally, I will ascertain whether the stress response plays a role in these metabolic changes.

3.2 Establishing a model of AML induced weight loss and reduction of fat deposits

The first model used to investigate whether AML induces fat weight loss in mice was the MN1^{GFP+} cells, these were developed by retrovirally infecting healthy murine HSPC with PSF91MN1iGFP to overexpress the MN1 oncogene (as described in the methods). 11 female C57Bl/6 mice aged 8-12 weeks were tail vein injected with 1×10^6 MN1 cells. Mice were monitored and weighed daily. The monitoring checked for the first observable symptoms of AML engraftment. These first signs of illness include, but are not limited to, hunched posture, lethargy, walking up on their toes, and in severe cases hind leg paralysis. At 5 week the first mouse started to show signs of illness, and all 11 mice were sacrificed (Figure 3.1A). Bone marrow was isolated from each mouse and flow cytometry was used to confirm MN1 engraftment by isolating the GFP⁺ population (Figure 3.1B & C). There was a range of engraftment from 0.07%-82.7% of the BM. Within this range there was a jump from 4.9% to 34% and therefore a threshold for engraftment was set at >5%, resulting in 4 mice low engrafted and 7 mice engrafted with MN1 cells. The MN1 cells may not have engrafted as well into the 4 mice for a variety of reasons, these mice are not immuno compromised and the dose of malignant cells may not have been sufficient to overcome the immune system. Alternatively, injections may have missed the vein and subcutaneous injection into the tail is less likely to achieve engraftment. The body weight of each mouse was normalised to their bodyweight 5 days prior to sacrifice. MN1 engraftment did not cause weight loss in mice when compared to non-engrafted mice (Figure 3.1D)

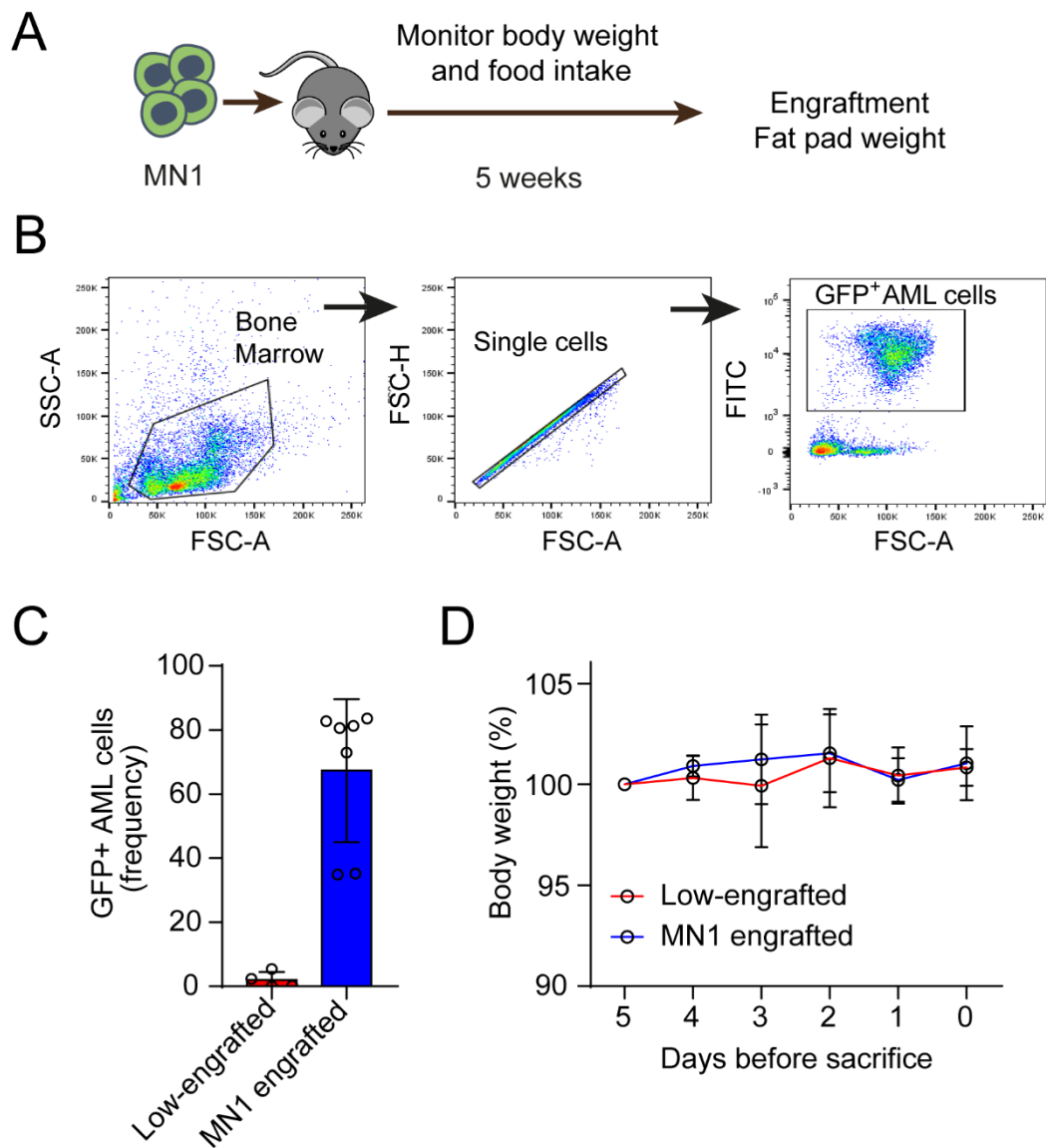


Figure 3.1 MN1 cell engraftment did not cause mouse weight loss.

A) Schematic of experiment. 11 C57Bl/6 mice were tail vein injected with MN1 cells (1×10^6) and monitored for 5 weeks. When the first mouse showed signs of illness, all mice were sacrificed. B) Flow cytometry was used to analyse the GFP⁺ MN1 cells in the BM. Mice were then grouped into low engrafted (n=4) for >5% and MN1 engrafted (n=7) C) The bone marrow analysed for engraftment. D) Mice were weighed daily. Weights are normalised to 5 days prior to sacrifice. Data are expressed as mean \pm SD.

During the 5 weeks that mice were being monitored and the food in each cage was also weighed. Food intake per cage was calculated per mouse in each cage and normalised to 5 days prior to sacrifice (Figure 3.2). Food intake remained the same in all four cages. However, due to all mice receiving MN1 cells and there being variability across the cages for which mice engrafted, it is not possible to ascertain whether MN1 engraftment alters food intake during tumour progression.

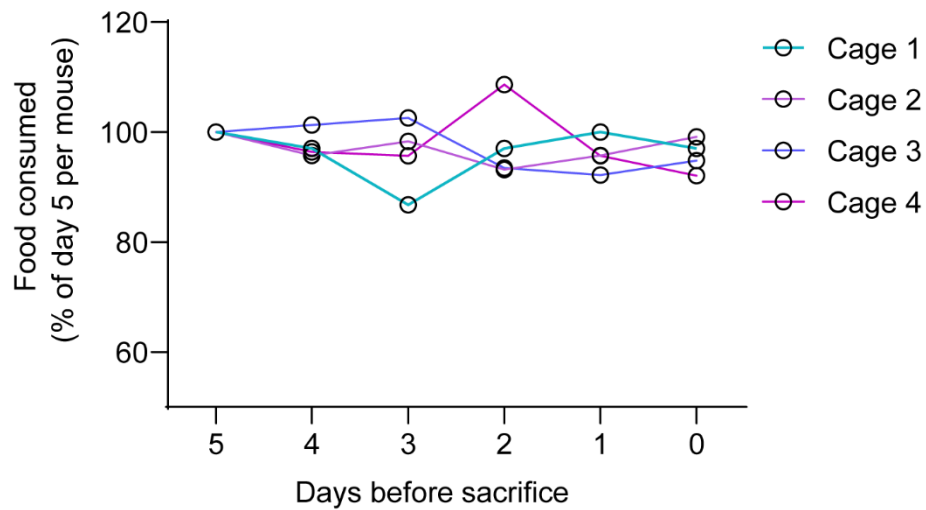


Figure 3.2 Food intake was not altered by MN1 injection.

The average food intake per mouse in each cage remained stable during the progression of the experiment when normalised to 5 days prior to sacrifice (cage 1-3 n=3, cage 4 n=2).

To further analyse if MN1 engraftment alters metabolism in mice, the inguinal and gonadal fat pads were dissected out of the mice, within 20 minutes of sacrifice. The gonadal fat pads and the pair of inguinal fat pads for each mouse was weighed and normalised to the weight of the mouse on the day of sacrifice. When compared to non-engrafted mice there was no significant change to the proportional weight of the fat pads in engrafted mice (Figure 3.3).

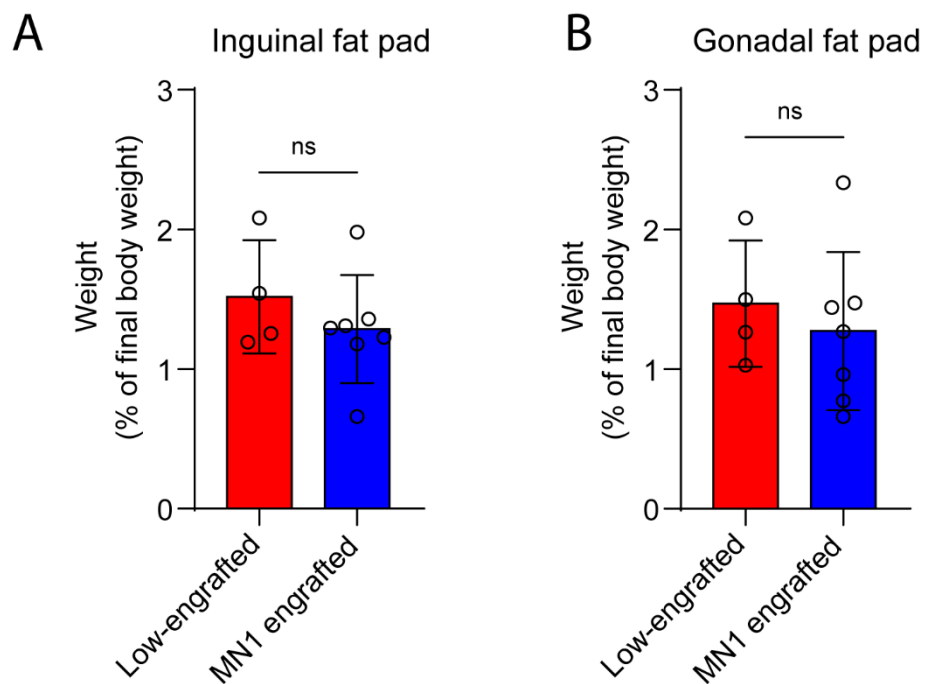


Figure 3.3 MN1 engraftment did not alter fat pad weight

Mice engrafted with MN1 cells (n=7) did not have significantly different A) Inguinal or B) Gonadal fat pad weights, as a percentage of their final body weight, in comparison to mice that did not engraft with MN1 cells (n=4). Data are expressed as mean \pm SD. ns= non-significant using Mann-Whitney U test.

Next, peripheral blood collected at sacrifice was assessed for metabolic markers. The level of ketones and glucose were tested and showed no significant difference between the mice that engrafted with MN1 cells and those that did not (Figure 3.4). However, it should be noted that it is unclear when each individual mouse last ate, and therefore is inconclusive as to whether AML does not alter ketone or glucose levels in the peripheral blood.

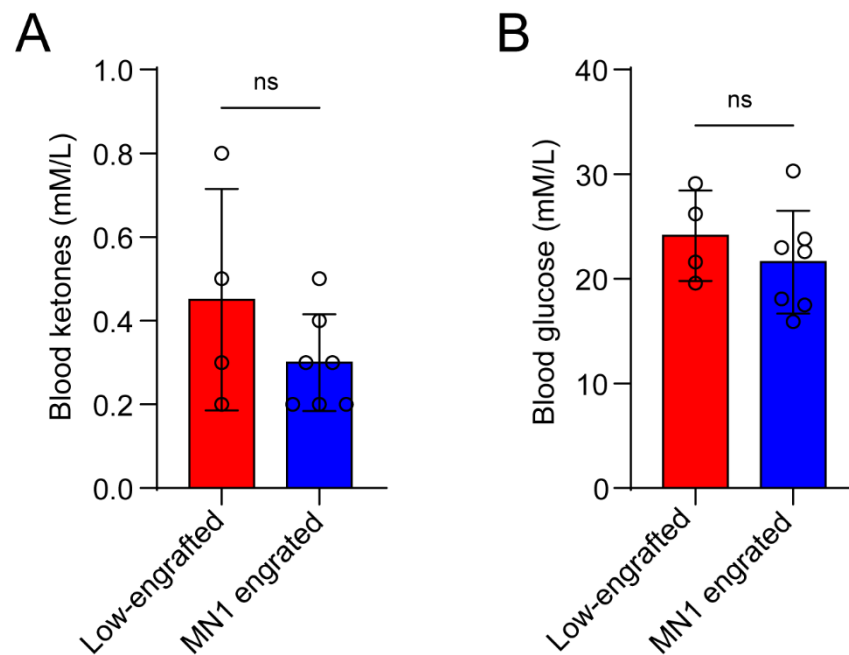


Figure 3.4 Peripheral blood metabolic markers were not altered by MN1 engraftment

Peripheral blood taken, at sacrifice, from MN1- engrafted (n=7) and non-engrafted (n=4) was tested for A) ketones and B) glucose. Data are expressed as mean \pm SD. ns= non- significant using Mann-Whitney U test.

The data from this experiment suggest that IV injecting mice with MN1 cells and sacrificing all mice upon the first mouse exhibiting illness, is not a sufficient model for weight loss and fat pad reduction caused by AML. Therefore, further experiments were required to investigate whether AML alters the systemic metabolism in mice.

The next model used to interrogate the project was utilising the HOXA9/MEIS1^{GFP+} cells which, like the MN1 cells, were developed from healthy murine HSPC by retrovirally infecting them with MIH-HA-HoxA9 and MIY-HA-Meis1a to over express the AML associated oncogenes (as described in the methods). Improvements were made to the previous experimental design by adding non-injected control mice. 12 C57Bl/6 mice (8-12weeks) were IV injected with 1×10^6 HOXA9/MEIS1 cells and were housed in separate cages to the 6 control mice. Bodyweight and food intake was recorded, and all mice were sacrificed upon the first mouse showing signs of illness (Figure 3.5A). Bodyweight for each mouse was normalised to 5 days prior to sacrifice. There is a downward trend in the weight of mice with HOXA9/MEIS1 when compared to controls, although when a Mann-Whitney U test was performed for the final day, this was not statistically significant (Figure 3.5B). Engraftment of the AML cells was confirmed by flow cytometry (Figure 3.5C). All 12 injected mice had GFP⁺ HOXA9/MEIS1 cells in the bone marrow.

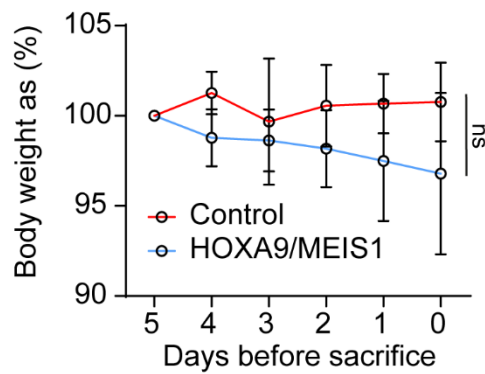
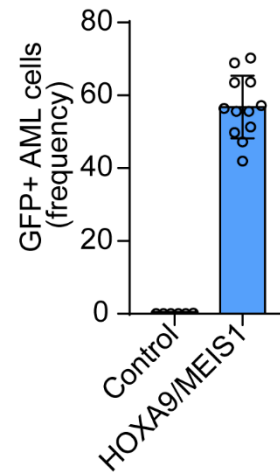
A**B****C**

Figure 3.5 HOXA9/MEIS1 BM engraftment did not cause significant weight loss.

A) Schematic of experiment. 12 C57Bl/6 mice were injected with HOXA9/MEIS1 cells (1×10^6) and 6 control C57Bl/6 mice were monitored for 5 weeks. When the first mouse showed signs of illness, all mice were sacrificed. B) Mouse bodyweight was recorded daily and normalised to 5 days prior to sacrifice. C) Engraftment of HOXA9/MEIS1 was confirmed in the bone marrow of injected mice. Data are expressed as mean \pm SD. ns= non- significant using Mann-Whitney U test.

The experimental design with controls and AML mice in separate cages allows for the comparison of food intake between the experimental groups (Figure 3.6). The chow for each cage was weighed each day and the intake per mouse in the cage was calculated. Weights were normalised to 5 days prior to sacrifice and indicate that mice with HOXA9/MEIS1 engraftment consumed slightly less food than control mice the day prior to sacrifice. Using a multiple Mann-Whitney test with false discovery rate analysed via a two-stage set-up, it was seen that there was no significant difference in the food consumed by control mice and HOXA9/MEIS1 mice.

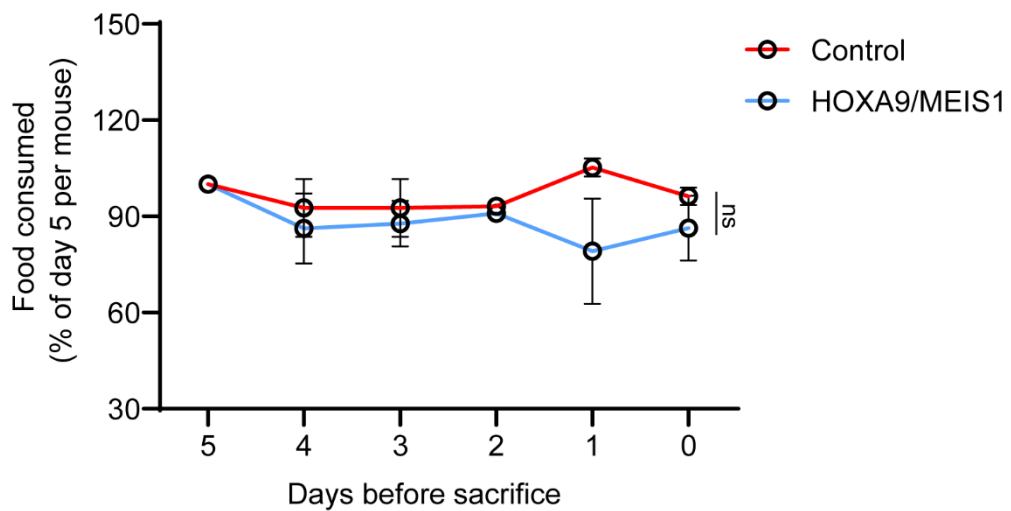


Figure 3.6 Food intake was not altered by HOXA9/MEIS1 engraftment.

Food intake per mouse normalised to the intake 5 days prior to sacrifice for control mice (n=6) and HOXA9/MEIS1 mice (n=12). Data are expressed as mean \pm SD. ns= non- significant using multiple Mann-Whitney U test for false discovery rate using the two-stage-set up method.

Next the fat pads from the mice were dissected and weighed. When normalised to the bodyweight of the mouse on the day of sacrifice. When compared to control mice, the inguinal fat pads of mice engrafted with HOXA9/MEIS1 are significantly lighter (Figure 3.7A). However, there is no significant difference between the groups when comparing the gonadal fat pads (Figure 3.7B).

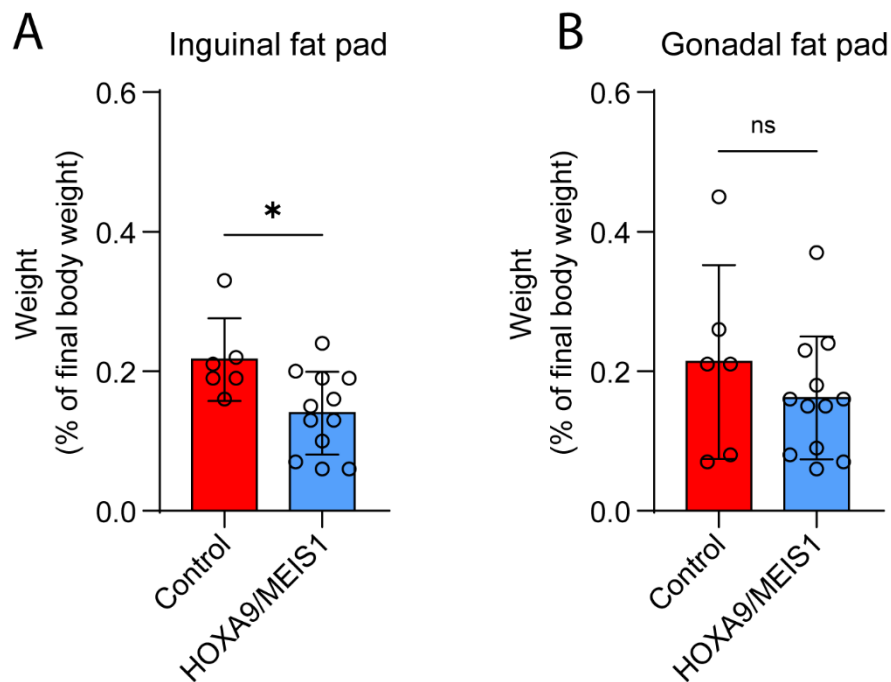


Figure 3.7 Fat pad weight was altered by HOXA9/MEIS1 engraftment.

A) Inguinal and B) Gonadal fat pads were dissected out of control (n=6) and HOXA9/MEIS1 mice (n=12) and normalised to the bodyweight at sacrifice. Data are expressed as mean \pm SD. Statistical significance was calculated using a Mann-Whitney U test. ns = non-significant, and * $p < 0.05$.

These data show that AML can induce metabolic changes in inguinal fat pad weight in mice. Moreover, the data shows that mice with AML have a trend to losing weight as the tumour progresses, but this may be due to variable food intake. Further experiments are required to confirm the model.

It is unclear that changes observed in this model were due to the AML alone or from altered food intake. This is important for investigating metabolic markers such as ketones and glucose in the blood. To ensure that metabolic changes are not impacted by mice consuming food at different times, mice underwent total food restriction. For this experiment 5 control mice and 12 HOXA9/MEIS1 mice were monitored for 29 days. Mice were then moved into individual clean cages and underwent total food restriction (tfr) for 16 hours. This was followed immediately by sacrifice (Figure 3.8A). Body weight of both experimental groups was normalised to 6 days prior to sacrifice and although both groups dropped ~10% bodyweight, there was no significant difference between the groups (Figure 3.8B). Upon sacrifice the bone marrow was assessed by flow cytometry to confirm engraftment of HOXA9/MEIS1 cells (Figure 3.8C). These data suggest that any weight loss is independent of food intake but still do not indicate AML induced weight loss.

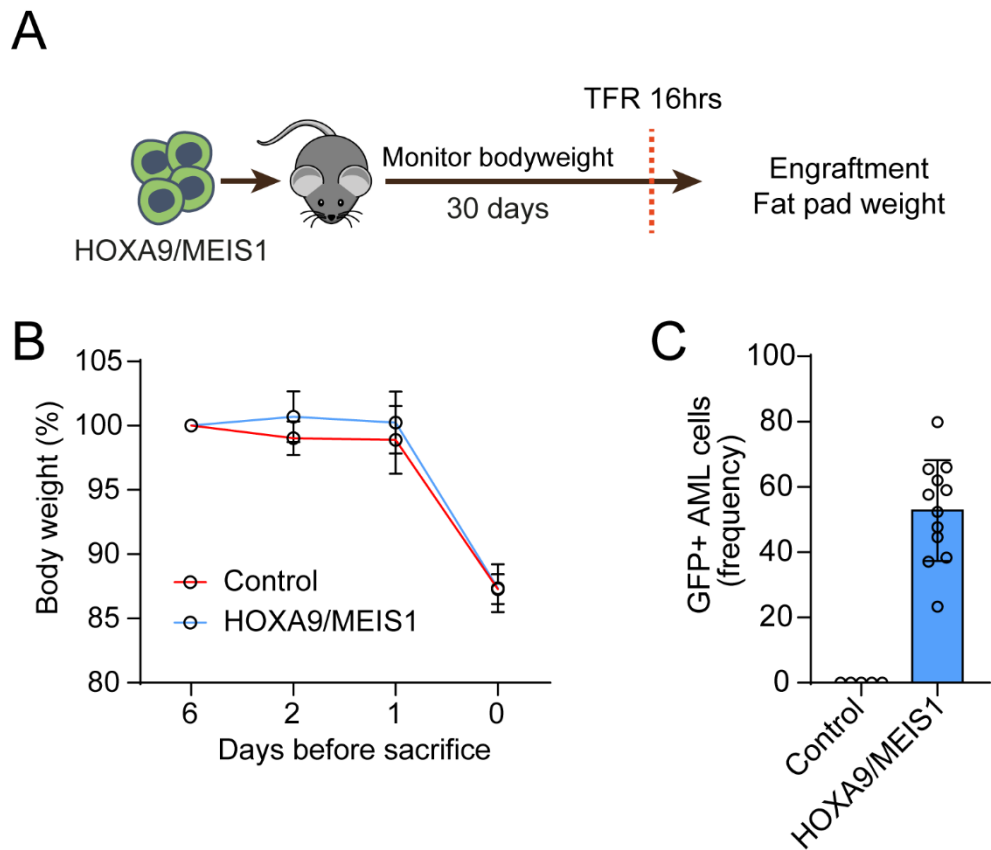


Figure 3.8 Total food restriction (tfr) did not alter bodyweight loss in HOXA9/MEIS1 engrafted mice.

A) Schematic of experiment. 12 C57Bl/6 mice were injected with HOXA9/MEIS1 cells (1×10^6) and 5 control C57Bl/6 mice were monitored for 29 days followed by 16hours of total food restriction before sacrifice. B) Mouse bodyweights were recorded and normalised to 6 days prior to sacrifice. C) Engraftment of HOXA9/MEIS1 was confirmed in the bone marrow of injected mice. Data are expressed as mean \pm SD.

Following this the fat pads were dissected from each mouse and the weight normalised to the body weight at time of sacrifice. Similar to the previous model, there was a significant reduction in the size of the inguinal fat pads for mice engrafted with HOXA9/MEIS1 (Figure 3.9A). However, the same was not seen in the gonadal fat pads (Figure 3.9B). This suggests that the adipose tissue weight loss is a response to the AML rather than just the total food restriction.

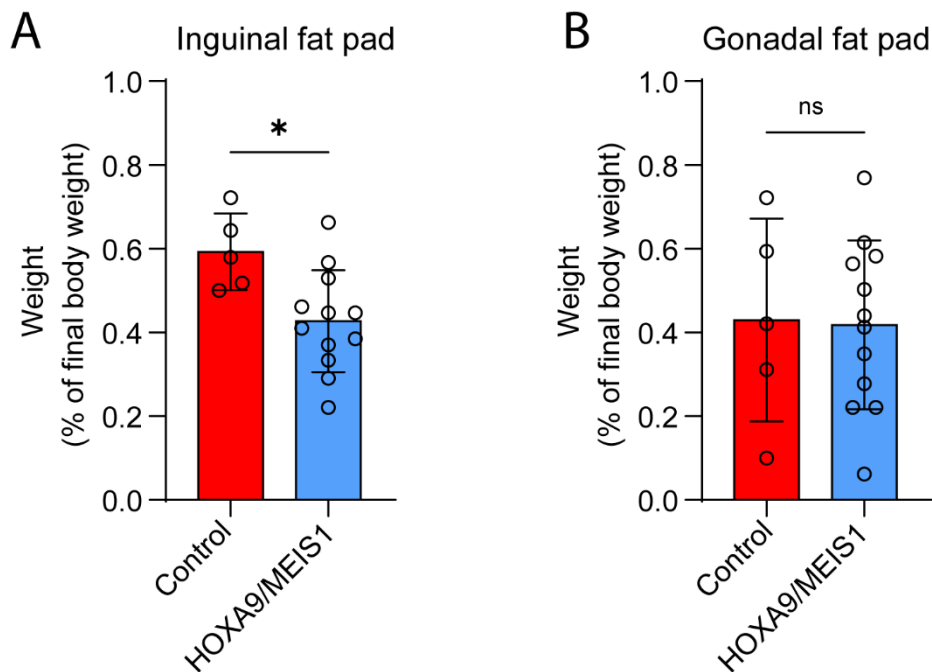


Figure 3.9 HOXA9/MEIS1 engraftment induced fat pad weight loss.

A) Inguinal and B) Gonadal fat pads were dissected out of control (n=5) and HOXA9/MEIS1 mice (n=12) and normalised to the bodyweight at sacrifice. Data are expressed as mean \pm SD. Statistical significance was calculated using a Mann-Whitney U test. ns = non-significant, and * $p < 0.05$.

Finally, the peripheral blood, taken at sacrifice, was analysed for the blood ketones and glucose (Figure 3.10). Both measurements showed no significant difference in the metabolic markers. This suggests that AML engraftment does not alter the ketones or glucose levels in the blood. This further implies that the latest food intake of each mouse is unlikely to be a factor when investigating systemic metabolic changes.

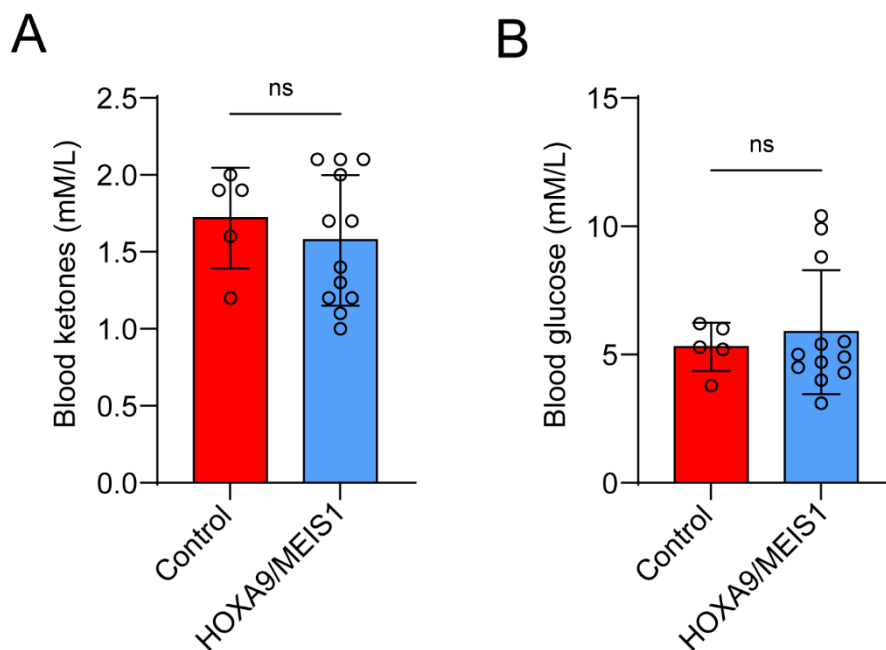


Figure 3.10 HOXA9/MEIS1 engraftment did not alter blood metabolic markers.

A) Ketones and B) Glucose levels were analysed in the peripheral blood of (n=6) and HOXA9/MEIS1 mice (n=12) following 16hrs of tfr. Data are expressed as mean \pm SD. Statistical significance was calculated using a Mann-Whitney U test. ns = non-significant.

Taken together these data from this tfr experiment shows that HOXA9/MEIS1 engraftment does not induce weight loss when mice even with food restriction, nor does it alter the circulating levels of ketones and glucose. It can be suggested that HOXA9/MEIS1 engraftment induces lipolysis of the inguinal fat pads, irrespective of food intake. However, the model is not sufficient in confirming AML causes systemic metabolic changes and weight loss including reduction of fat pad mass.

The previous models show that mice have a trend of losing weight during tumour progression, however, this has not been significant or consistent. The data show that AML may cause loss of fat pads and does not alter the circulating levels of glucose and ketones. So far it has been shown that this is despite animals maintaining their intake of food. It is also important to state that animals were sacrificed when the first animal showed signs of disease.

In the next experiment I changed the protocol to sacrificing the mice only when they individually started showing signs of illness. The utilised both IV injections of MN1 and HOXA9/MEIS1 cells (1×10^6). There were initially 10 mice in each AML group and the control group. The mice were caged per condition and weighed daily. The food intake was recorded for each cage and then calculated per mouse. (Figure 3.11A). Upon sacrifice the BM was analysed for the GFP⁺ AML population by flow cytometry (Figure 3.11B). After 7 weeks any remaining AML injected mice were sacrificed and excluded from data analysis as no AML engraftment was observed. This resulted in 10 controls, 7 MN1 injected mice, and 9 HOXA9/MEIS1 injected mice. When the bodyweight of the mice was normalised to the bodyweight 5 days prior to sacrifice, it can be seen that both AML models lost a significant amount of weight in comparison to control mice (Figure 3.11C). The food intake per mouse was calculated and normalised to 5 days prior to sacrifice (Figure 3.11D). It can be seen that mice maintained their intake leading up to sacrifice. Taken together these data show that as the tumour progresses mice lose bodyweight and that this is likely independent of food consumption.

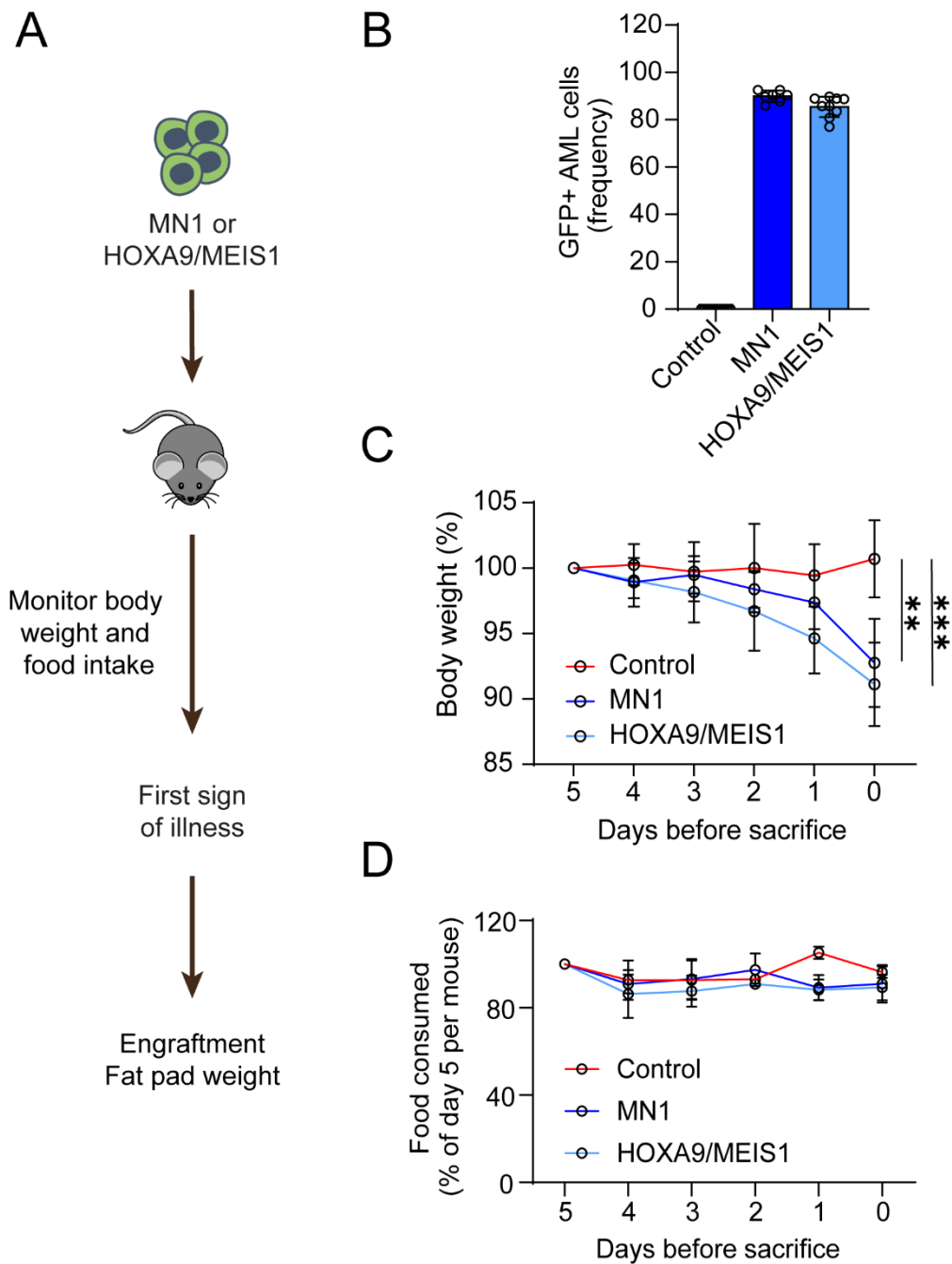


Figure 3.11 Mice engrafted with AML lose weight during late stages of tumour progression.

A) Schematic of experiment. C57Bl/6 control mice (n=10), or mice injected with MN1 (n=7), or HOXA9/MEIS1 (n=9) cells (1×10^6) were monitored daily. Mice were monitored individually and sacrificed at the first sign of illness. B) Engraftment of was confirmed using flow cytometry of the GFP⁺ AML population. Body weight C) and food intake D) were normalised to 5 days prior to sacrifice for each mouse each day. Data are expressed as mean \pm SD. Statistical significance was calculated using Kruskal-Wallis H test with Tukey's multiple comparison test. ** p < 0.01, and *** p < 0.001.

Upon sacrifice fat pads were dissected from each mouse and their weights normalised to the bodyweight on the day of sacrifice (Figure 3.12). Data shows that both MN1 and HOXA9/MEIS1 engraftment induced significant weight loss in both fat pads when compared to controls. This suggests that late stages of AML tumour progression induces lipolysis of adipose tissue.

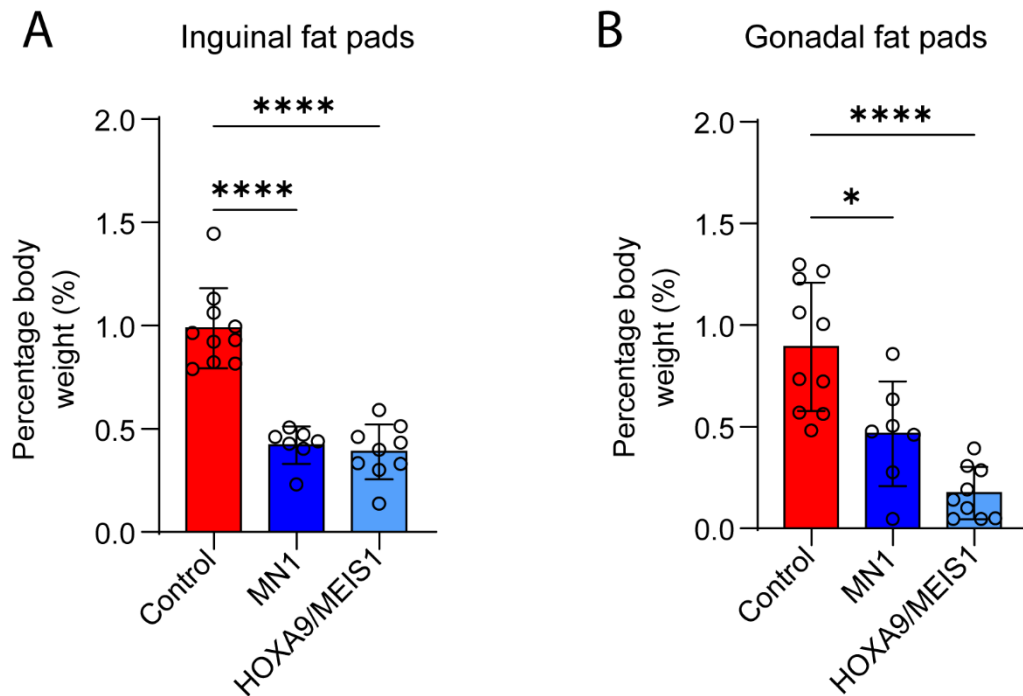


Figure 3.12 Late stages of AML engraftment cause loss of adipose tissue weight.

Mice engrafted with MN1 (n=7) or HOXA9/MEIS1 (n=9) cells had significantly reduced A) Inguinal or B) Gonadal fat pad weights, as a percentage of their final body weight, in comparison to control mice (n=10). Data are expressed as mean \pm SD. Statistical significance was calculated using Kruskal-Wallis H test with Tukey's multiple comparison test. * p < 0.05, and **** p < 0.0001.

This final model shows consistent weight loss in mice with AML engraftment which is independent of food consumption. Furthermore, AML engraftment also results in loss of adipose tissue, particularly at the late stages of the disease. Together this shows that there is marked systemic metabolic changes when AML engrafts in the BM.

3.3 AML alters availability and composition of FA in the peripheral blood

AML is highly reliant on FA for metabolism and this project aims to elucidate alterations in FA metabolism in the liver. It was firstly important to investigate whether AML engraftment caused changes to the available FA in the serum. To do this serum was isolated from the final model described above. A terminal bleed was taken at sacrifice of each mouse and stored until all samples were collected (Figure 3.13A). The FFA assay kit showed that the serum of mice engrafted with MN1 cells had significantly elevated FFA when compared to controls. The serum from mice engrafted with HOXA9/MEIS1 cells did not show any difference in the serum FFA when compared with the controls (Figure 3.13B). This indicates that AML engraftment may alter whole system lipid metabolism as more FA in the serum suggests increased secretion and decreased uptake of FA from the liver.

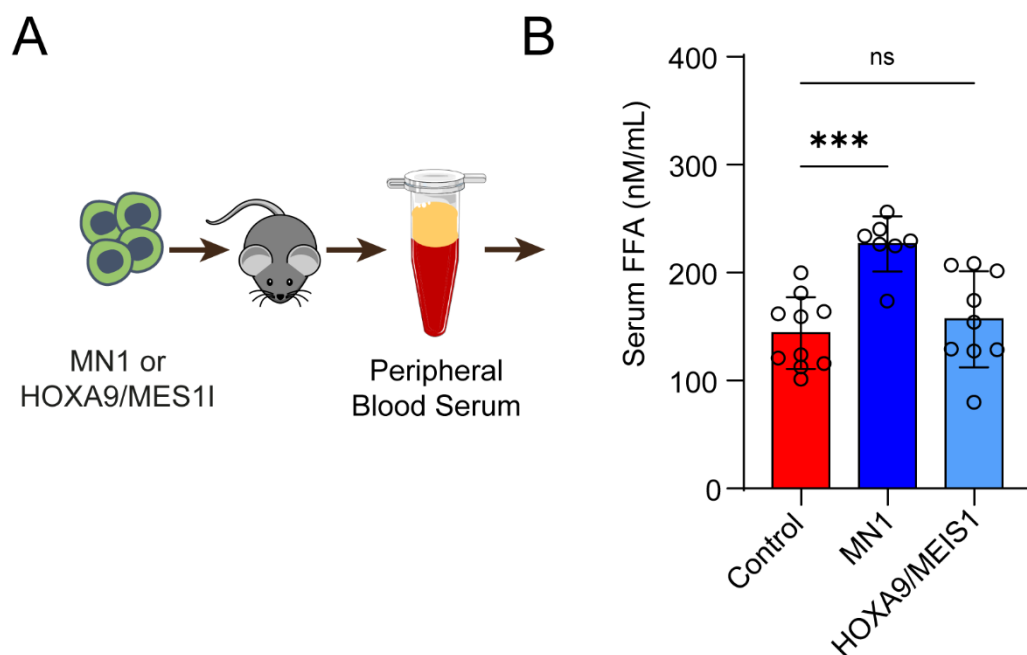


Figure 3.13 MN1 engraftment increased serum FFA.

A) Schematic of experiment. Peripheral blood was collected at sacrifice from mice engrafted with MN1 (n=7) or HOXA9/MEIS1 (n=9) cells or control mice (n=10). Serum was isolated from the blood for analysis. B) FFA were analysed by ELISA kit. Data are expressed as mean \pm SD. Statistical significance was calculated using Kruskal-Wallis H test with Tukey's multiple comparison test. *** $p < 0.001$, and ns = non-significant.

The previous assay is a good indicator of the total FA in the serum but is not very specific. To further investigate aberrant serum FA two random samples from each condition were chosen for analysis by mass spectrometry. Dr Le Gall ran and analysed the samples for changes in LCFA. Figure 3.14 shows the LCFA by their carbon chain length. The heat map indicates that both AML engraftments altered the total FA in the serum in the mice. Not only were the total FA levels altered, but the composition of the available FA was also changed. In the controls the most abundant FA was the C18 LCFA, whereas C16 LCFA appeared to have been the most abundant in all the AML samples.

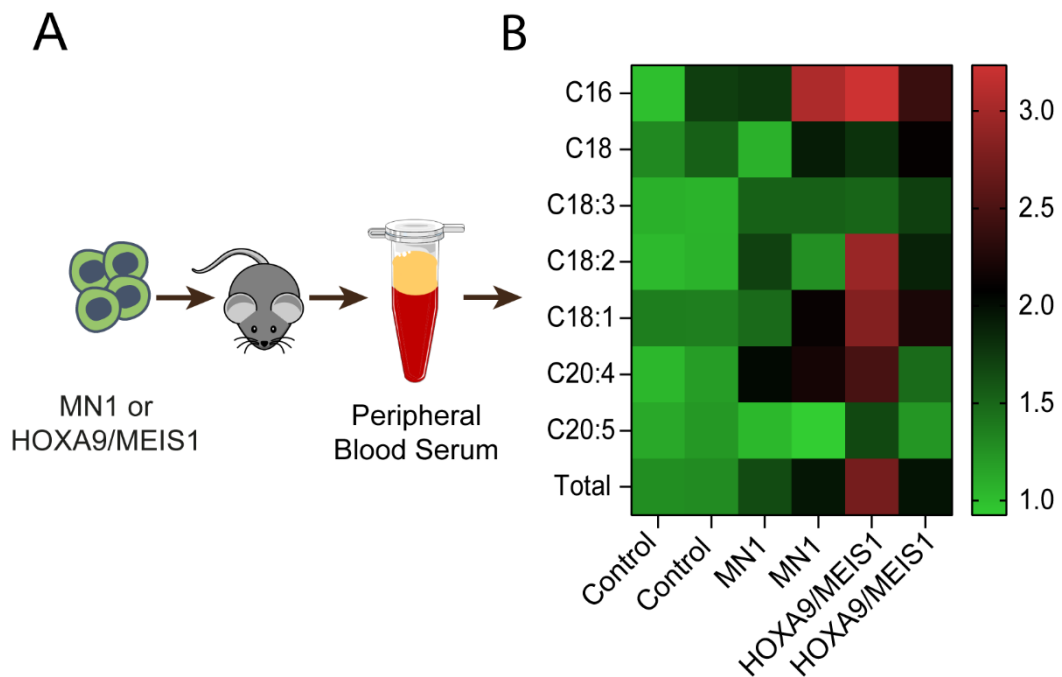


Figure 3.14 Serum long chain fatty acids were elevated in AML engrafted mice.

A) Schematic of experiment. Serum was isolated from the blood taken at sacrifice. The serum from 2 mice from each treatment group (Control, MN1, and HOXA9/MEIS1) were selected for further analysis. B) long chain fatty acids (LCFA) were analysed by mass spectrometry.

Next, remaining serum was available from 6 mice per group and was used to further assess serum metabolic markers (Figure 3.15A). Elevated serum triglycerides are associated with aberrant FA degradation and liver steatosis. However, the ELISA assay kit used indicated that the serum triglycerides were not significantly different between the AML engrafted mice and the control mice (Figure 3.15B). Meanwhile, elevated serum levels of corticosterone are associated with metabolic stress, and these were also not significantly different in mice engrafted with MN1 cells or mice engrafted with HOXA9/MEIS1 cells, when compared to control mice (Figure 3.15C). These data indicate that AML is not inducing a metabolic stress response.

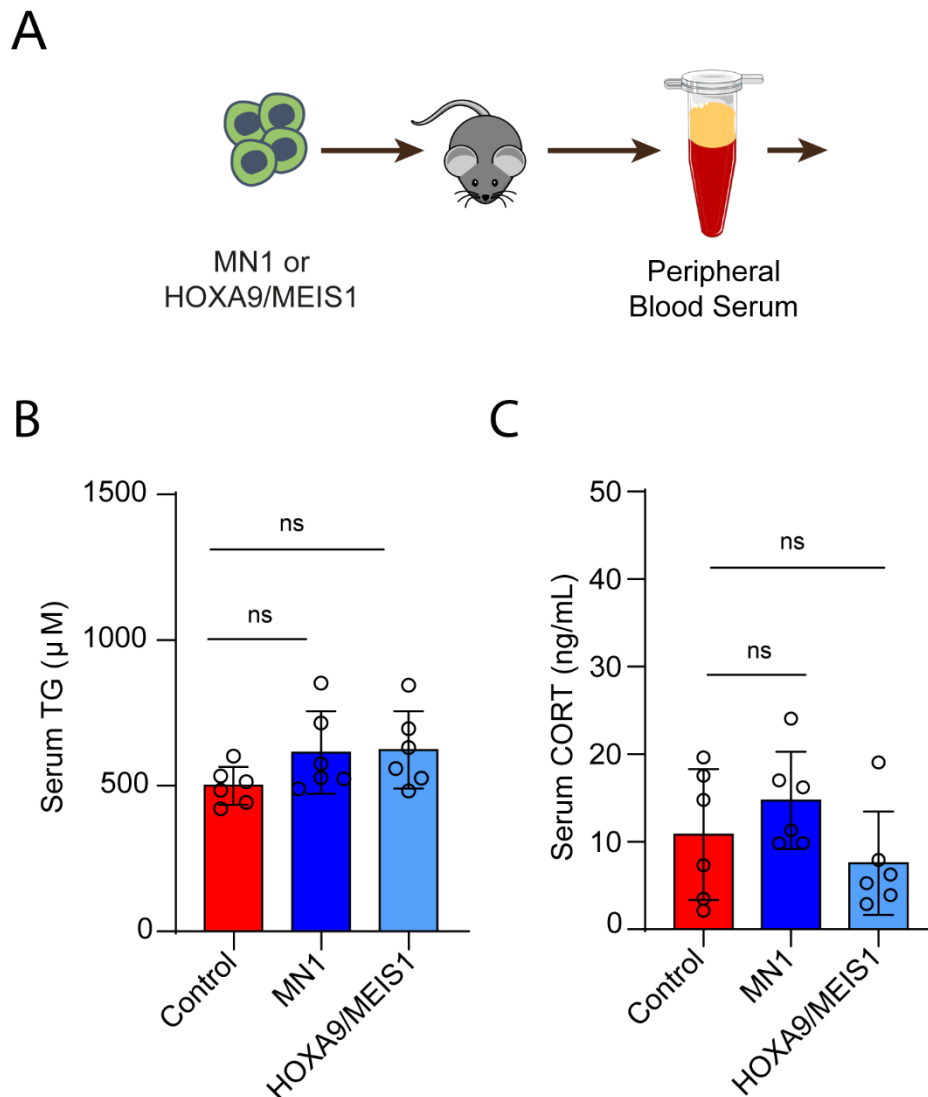


Figure 3.15 AML did not induce a metabolic stress response.

A) Schematic of experiment. Remaining serum isolated from terminal bleeds of control mice or mice engrafted with either MN1 or HOXA9/MEIS1 cells (n=6) was further analysed for B) serum triglycerides (TG) and C) serum corticosterone (CORT). Data are expressed as mean \pm SD. Statistical significance was calculated using Kruskal-Wallis H test with Tukey's multiple comparison test. ns= non-significant.

Both the mass spectrometry data and the FFA assay confirm that there is aberrant FFA levels in the serum of mice engrafted with AML cells. This further suggests that AML affects metabolism outside of the immediate BM niche within which it resides. The data also shows that AML influences these changes whilst maintaining a fine balance in avoiding activation of the metabolic stress response, which would potentially have an anti-tumoural effect.

3.4 Summary

In this first results chapter, I have confirmed that AML induces weight loss and fat pad reduction in a murine model. I have shown that this occurs in late stages of tumour progression and requires each animal to reach the symptomatic phase of the disease. Moreover, I have shown that the rapid weight loss is not associated with changes in food consumption. I have shown that adipose tissue is also lost during AML progression. Furthermore, mice engrafted with both models of AML exhibited altered serum FA levels. This included both the total available FA but also showed altered composition of the LCFA found. Whilst FA were changed in the blood serum, other metabolic markers such as glucose and ketones were not altered in response to AML engraftment. Interestingly corticosterone levels were also maintained in mice engrafted with AML, indicating that AML is able to alter the metabolic state of the mice and avoid activating the stress response.

4. AML in the bone marrow alter FA metabolism in the liver.

4.1 Introduction

During AML progression it is widely accepted that patients lose weight, however this has generally been attributed to the intense chemotherapy regimens alone and in some cases, in combination with stem cell allograft that are used to treat the disease (373, 374). In the previous chapter I have shown that AML progression results in systemic metabolic changes. Mice engrafted with AML lose overall bodyweight as well as experiencing a loss of adipose tissue, in the inguinal and gonadal fat pads, all without any form of intervention. This is supported by more recent studies, outlining that AML itself can cause cachexia in human patients (157, 158), which my findings corroborate in mice. AML is known to utilise FA metabolism for proliferation and survival, and FA metabolism has also been implicated in chemoresistance (33, 375). Our group and other have shown that AML acts on cells within the BM niche to increase the supply of FA from adipocytes within the yellow marrow (33, 188, 235). However, this store is likely to run out as the AML proliferates and expands its coverage of the BM. It can therefore be suggested that AML is accessing FA from the blood supply to the BM. This is supported by evidence in the previous chapter where mice engrafted with AML has elevated serum FA levels.

The liver is considered the metabolic hub of the body, processing endogenous and dietary nutrients. It functions to maintain homeostasis of serum levels of glucose and FA (305). Lipid flux is at the heart of the livers function and when dysregulated it is associated with a number of different liver diseases (318). Hepatocytes remove excess FA from the blood as dietary fats reach the liver from the intestines or circulating lipoproteins return unused (313). These FA that are taken up can be used by the hepatocytes for metabolism or they can be stored, via lipogenesis as LD, for later use or secreted back into the serum during times of stress (229, 336). Hepatocytes respond to signals such as hormones and cytokines to reduce the uptake of serum FA and/or increase release of FA into the serum as FFA, VLDL, and other forms of FA (296, 312). It has been previously shown that some cancers act on the liver to increase FA availability in the serum and subsequently improving the malignant growth (250, 343, 346).

Our understanding of both AML reliance on FA metabolism and liver lipid flux, makes the liver an attractive target to investigate systemic FA metabolic changes in response to AML progression. In this chapter bulk RNAseq of livers from mice engrafted with AML cells will confirm whether metabolism pathways are downregulated in comparison to controls, specifically pathways associated with FA metabolism. Once established, the experiments in this chapter will confirm reduced genetic expression both *in vivo* and *in vitro*. Furthermore, this chapter will elucidate whether FA uptake and respiration are altered in a cell-cell independent manner. These findings aim to support the hypothesis that AML alters liver FA metabolism resulting in increased FA availability in the serum.

4.2 Bulk RNA sequencing confirms aberrant metabolic pathways in the livers of mice engrafted with AML.

AML is known for its metabolic plasticity and high reliance on metabolites for its survival and proliferation (369). During its progression the tumour commandeers the metabolites of the BM, depleting the reserves and therefore requiring nutrients from the blood stream (114). The liver is the major hub for metabolism and dissemination of metabolites, namely FA, into the blood for the rest of the body and is therefore where this project focuses (320). Once the model was confirmed for AML induced weight loss and fat pad reduction I dissected out the livers which were then snap frozen. Whole liver RNA lysates were isolated from 3 mice in each treatment group; control, MN1, or HOXA9/MEIS1 engrafted and sent to Novogene (Cambridge UK) for bulk RNAseq. Samples were processed and analysed by Novogene. Analysis was performed produced differentially expressed genes (DEGs) from fragments per kilobase of transcript per million (fpkm) and were further used for Kegg pathway enrichment. Primary analysis was performed by Novogene however, I am responsible for interpretation and validation of the provided data. Volcano plots of the Bulk RNAseq from mice engrafted with AML both show that there are genes that are differentially regulated when compared with control livers (Figure 4.1).

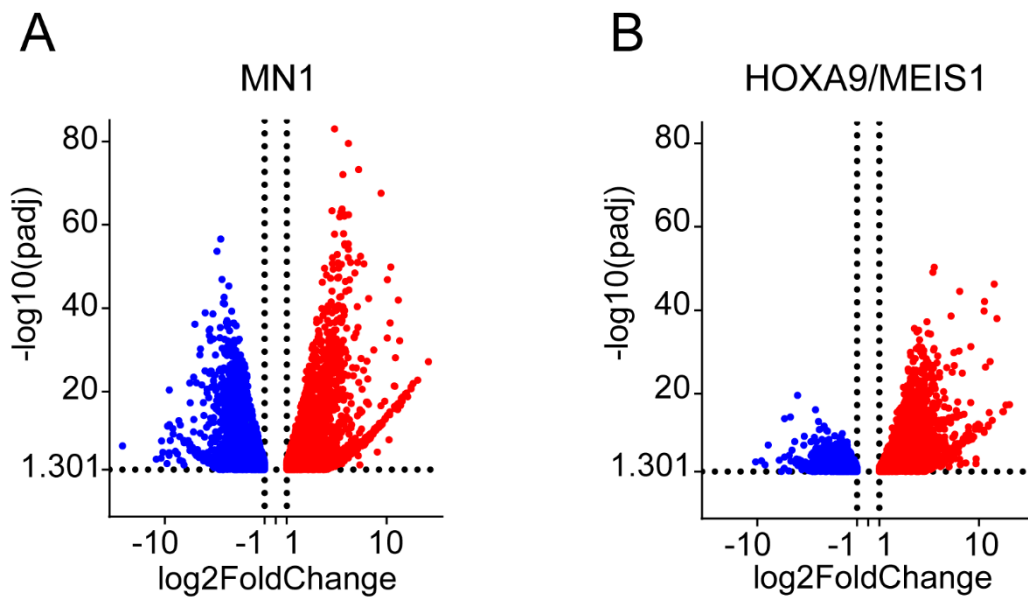
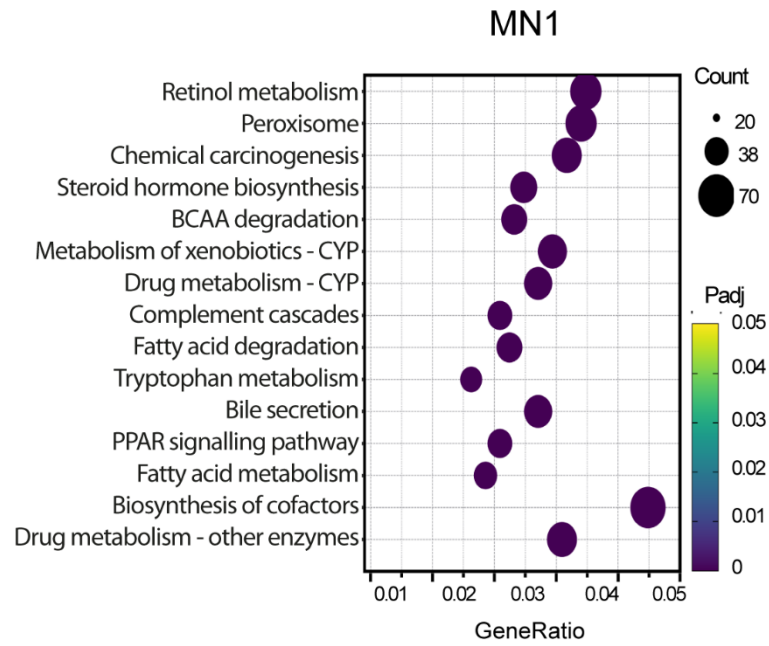


Figure 4.1 Bulk RNAseq shows alteration in mouse liver gene expression in response to AML.

Volcano plots of RNA from whole liver lysates from mice engrafted with A) MN1 cells or B) HOXA9/MEIS1 cells, compared to controls (n=3).

Kegg pathway enrichment data shows how differentially regulated cellular pathways are. Within a known cellular pathway, it is calculated how many of the genes are differentially regulated in comparison to the controls. This was then used to indicate the top pathways that were up or down regulated. This project is focussing on FA metabolism within the liver and pathways associated with this were within the top 15 down regulated pathways for both MN1 (Figure 4.2A) and HOXA9/MEIS1 (Figure 4.2B) engrafted mice. The pathways included are FA metabolism, FA degradation and PPAR signalling pathway. These indicate that AML downregulates liver FA metabolism.

A



B

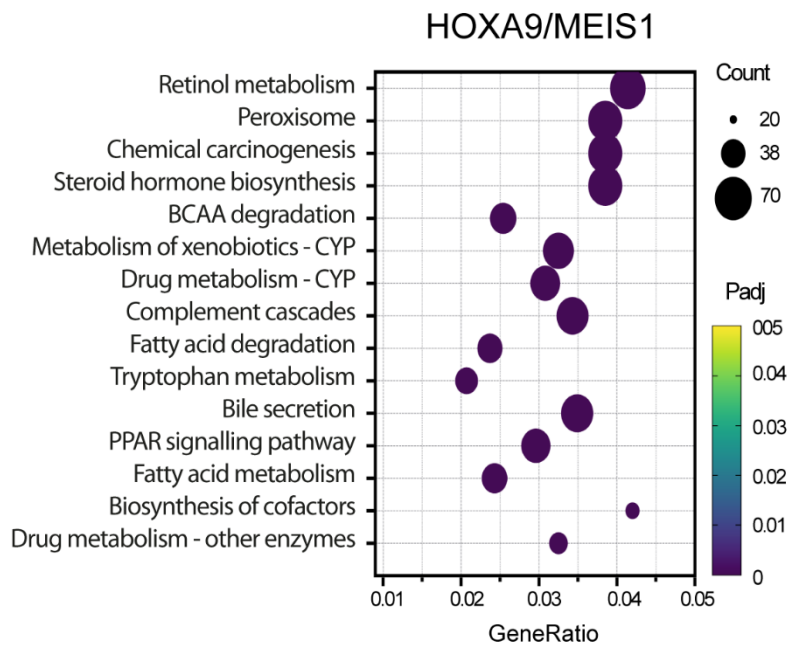


Figure 4.2 FA metabolism pathways among the most significantly downregulated in mice engrafted with AML.

Kegg enrichment and pathway analysis of bulk RNAseq from whole liver lysates of mice engrafted with A) MN1 cells or B) HOXA9/MEIS1 cells, compared to controls (n=3).

The pathways of FA metabolism, degradation and the PPAR signalling pathway were among the most downregulated in the Kegg pathway enrichment data. From these pathways genes highlighted by Novogene were chosen. Log₂(fpmk +1) of the gene is presented as a heat map in (Figure 4.3). This shows that genes associated with the selected pathways are less abundant in whole liver RNA lysates from AML engrafted mice when visualised next to controls further cementing that AML down regulates FA metabolism genes within the liver.

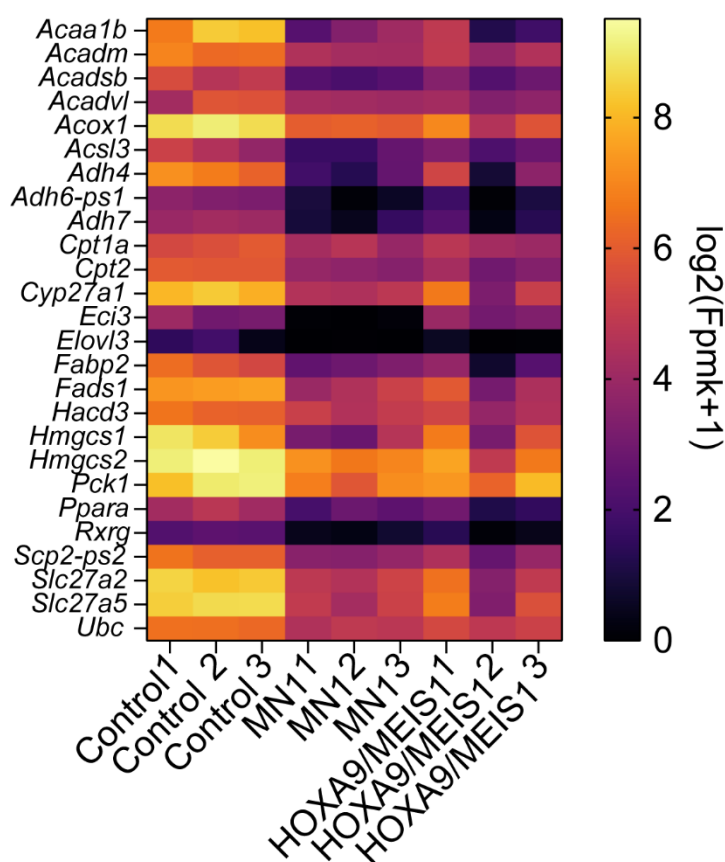


Figure 4.3 Genes associated with fatty acid metabolism pathways are dysregulated in mice engrafted with AML.

Heat map of differential gene expression for genes associated with FA metabolism pathways highlighted by Kegg enrichment. Data is of bulk RNAseq from whole liver lysates of mice engrafted with MN1 cells or HOXA9/MEIS1 cells, compared to controls (n=3).

4.3 Genes associated with FA metabolism are downregulated in the livers of AML engrafted mice.

The sequencing data from the livers of mice with MN1 or HOXA9/MEIS1 engraftment provided a starting point for further investigating the downregulation of liver FA metabolism in response to AML. It is known that extramedullary AML can home to the liver (376), and therefore it is important to investigate whether the changes seen are from the tissue resident cells or whether there is a possibility of sample contamination by infiltrating AML. C57Bl/6 mice were engrafted with MN1 cells (1×10^6) for 5 weeks and livers were isolated at sacrifice. Immune cells were isolated from liver lobes using a collagenase protocol. Immune cells were analysed by flow cytometry for GFP⁺ AML cells (Figure 4.4A). Less than 5% of immune cells in the livers were AML cells in the AML engrafted samples (n=6) (Figure 4.4B). This suggests that gene alterations seen in the bulk RNAseq, and the subsequent experiments, are from the cells of the liver, predominantly hepatocytes as the major cell type present, and not contamination with AML cells.

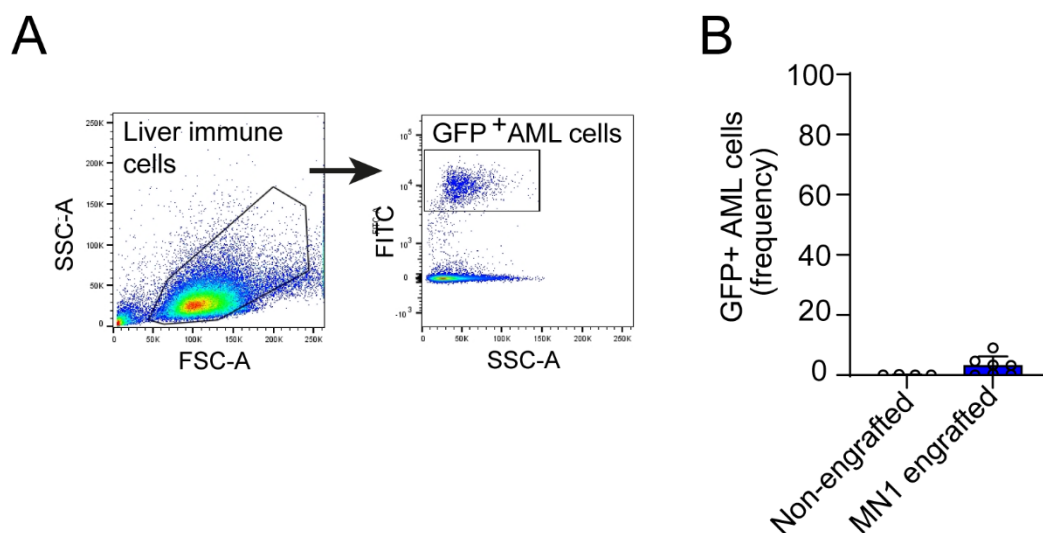


Figure 4.4 MN1 cells have very low engraftment in the liver.

A) Flow cytometry strategy to isolate AML population B) engraftment of GFP⁺ MN1 cells in the liver of mice (n=6), which was not significant when compared with mice that did not have bone marrow engraftment (n=4). Data are expressed as mean \pm SD.

To confirm that AML induced down regulation of liver FA metabolism genes, genes were selected from Figure 4.3 to investigate different stages of FA metabolism (Figure 4.5). FA uptake is demonstrated by *Slc27a2* expression, which is also known as *Fatp2* and will be the name used to refer to the gene/protein in this thesis, transfer of FA from the cytosol into the mitochondria is performed by *Cpt1a*, *Acadm* represents FAO, and *Hmgcs2* is the rate limiting step of ketogenesis. To confirm the sequencing data the gene for the FA scavenger receptor, *Cd36*, is also included further analysis. It was not implicated as significantly down regulated in the bulk RNAseq, suggesting it may be controlled or circumvented via a different mechanism.

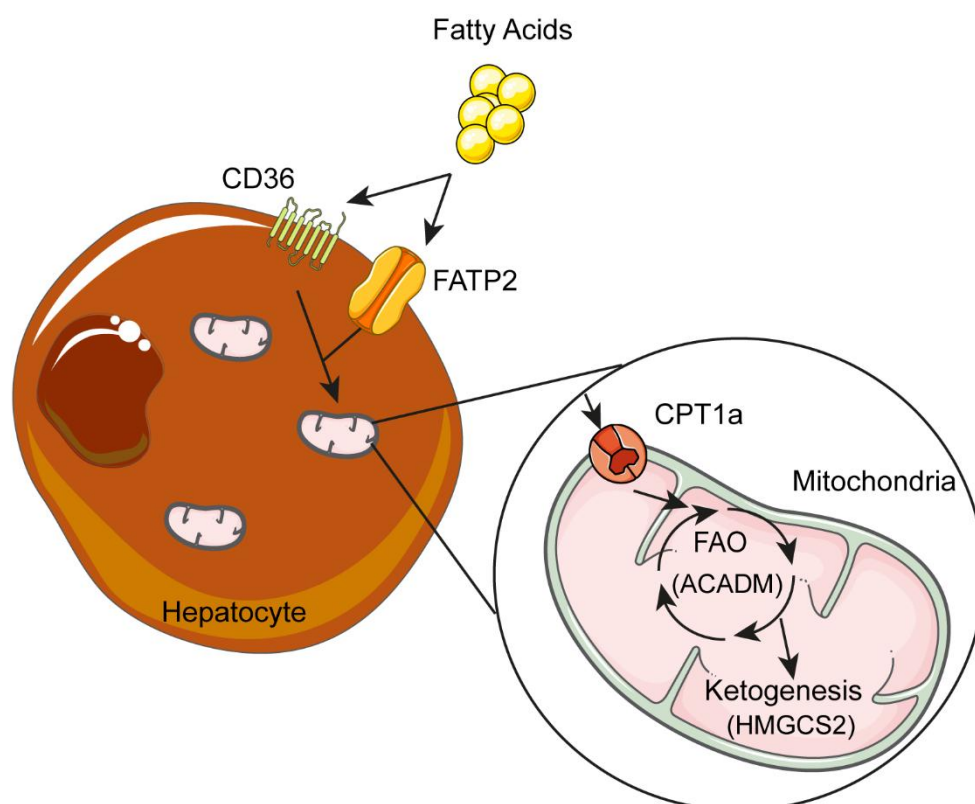


Figure 4.5 Proteins/genes associated with FA metabolism.

Schematic of FA entering hepatocytes via the scavenger receptor CD36 or FATP2. FA enter the mitochondria via CPT1a before undergoing FAO, which utilises the ACADM protein. During periods of starvation FA are used for ketogenesis, of which HMGCS2 is a rate limiting enzyme.

From the experiment which confirmed the model of AML induced metabolic changes, livers were isolated at sacrifice and snap frozen. Whole liver RNA lysates were analysed by RT-qPCR for the genes outlined in Figure 4.5. Analysis shows that all four of the genes highlighted in Figure 4.3 were downregulated in livers of mice engrafted with MN1 (n=7) or HOXA9/MEIS1 cells (n=8) when compared with control mouse livers (n=10). However, *Cd36*, which was not highlighted by sequencing data, was not significantly altered (Figure 4.6). These data show that multiple stages of liver FA metabolism are down regulated by AML engraftment in the BM.

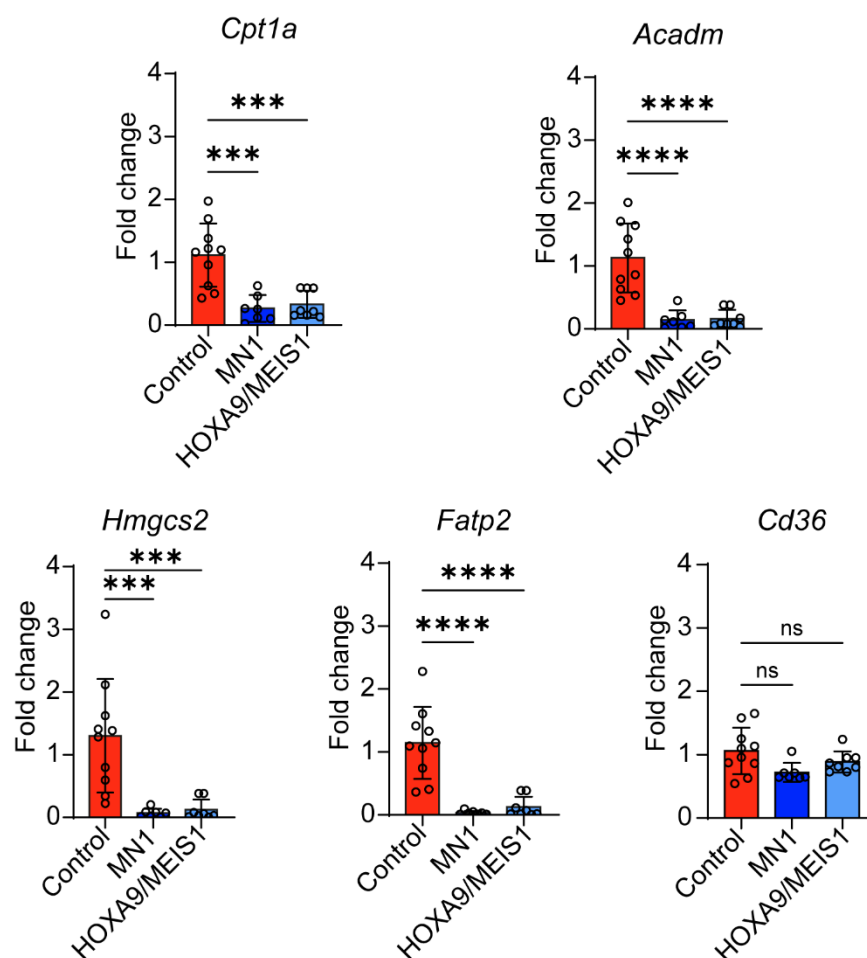


Figure 4.6 Genes associated with FA metabolism are down regulated in the liver of mice engrafted with AML.

Gene expression of *Cpt1a*, *Acadm*, *Hmgcs2*, *Fatp2*, and *Cd36*. Analysis was performed on whole liver lysates from control mice (n=10), or mice engrafted with either MN1 cells (n=7), or HOXA9/MEIS1 cells (n=8) for 4 weeks. Data are expressed as mean \pm SD. Statistical significance was calculated using Kruskal-Wallis H test with Tukey's multiple comparison test. *** p < 0.001, **** p < 0.0001, and ns = non-significant.

Next, it was investigated whether MN1 engraftment alters liver FA metabolism gene expression in early tumourigenesis as well as during late-stage disease. C57Bl/6 mice were IV injected with MN1 cells (1×10^6) for 2 and 4 weeks (Figure 4.7A). Engraftment of GFP⁺ cells was confirmed to increase with time (Figure 4.7B). Livers were isolated at sacrifice and whole liver RNA lysates were analysed by RT-qPCR. Genes associated with different stages of FA metabolism were downregulated at both time points of MN1 engraftment (Figure 4.7C). These data showed that AML downregulates FA metabolism genes even at early stages of tumour development and continues in latter stages.

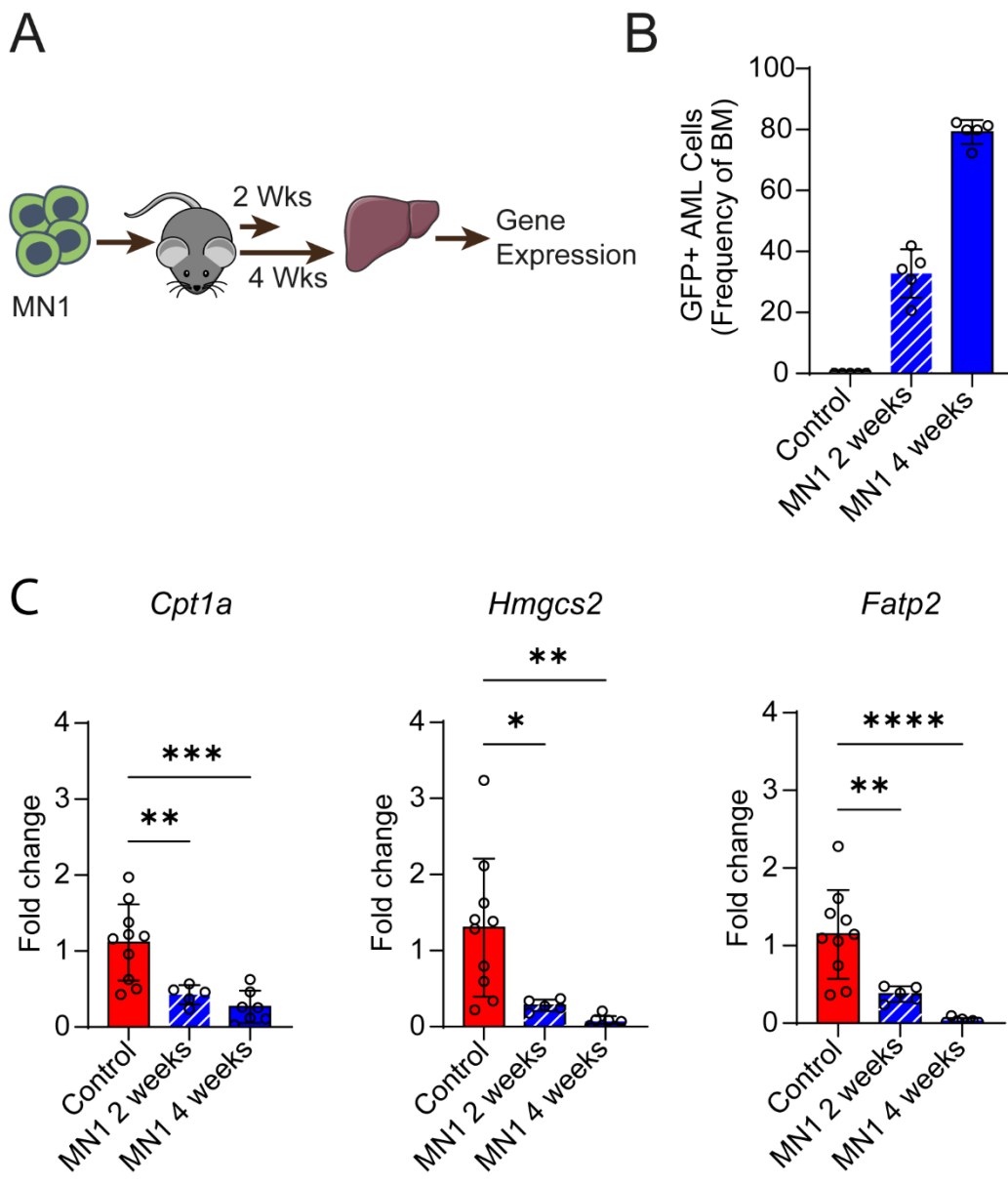


Figure 4.7 MN1 engraftment downregulates liver FA metabolism genes within 2 weeks of engraftment.

A) Schematic of experimental design. Mice were IV injected with MN1 cells (1×10^6) and monitored for 2 or 4 weeks prior to sacrifice. B) Engraftment was quantified using flow cytometry. C) Gene expression of *Cpt1a*, *Hmgcs2*, and *Fatp2* for whole liver lysates of mice engrafted for 2 or 4 weeks ($n=5$), compared to control mice ($n=10$). Data are expressed as mean \pm SD. Statistical significance was calculated using Kruskal-Wallis H test with Tukey's multiple comparison test. * $p < 0.05$, ** $p < 0.01$ *** $p < 0.001$, and **** $p < 0.0001$.

4.4 Engraftment of AML reduces murine FATP2 protein expression *in vivo*.

FA uptake is highly important for the function of the liver allowing for storage, *de novo* lipogenesis and metabolism, this is carried out predominantly by the hepatocytes (313). One of the key genes outlined by the sequencing data was *Slc27a2/Fatp2*. FATP2 is a transmembrane protein, one of its key functions is as a LCFA transporter. It is important for maintaining lipid homeostasis within the cell, transporting FA through the cytoplasm for storage or breakdown (377). *Fatp2* has been linked with liver diseases such as NAFLD and type 2 diabetes (378, 379). It has been shown that knock-down of *Fatp2* reduces the uptake of LCFA in the liver (380). Studies in rats have also shown that high fat diets contribute to increased *Fatp2* expression that leads to insulin resistance (381). *Fatp2* is highly important in hepatocytes to maintain their lipid flux that so crucially contributes to their function in removing FA from the blood stream. It is therefore a desirable target to investigate whether AML alters FA uptake by hepatocytes *in vivo*. For this experiment livers were isolated at sacrifice from the confirmed model. Mice engrafted with MN1 or HOXA9/MEIS1 cells (1×10^6) were monitored and sacrificed individually at the first sign of their illness. Liver lobes were fixed in formaldehyde for later processing. Sectioning and staining were performed by Alyssa Polski-Deleve and analysis by me. For the first attempt of this staining slides were stained for FATP2 (red) and DAPI (blue) for the nuclei (Figure 4.8). It can be visualised in that there are some small circular cells which have stained bright red. These are clearly not the hepatocytes as they are too small and circular. One explanation for this may be that they are infiltrating AML cells which are known to have high FATP2 expression. The decision was made not to analysis this set of images as it would be almost impossible to exclude the small round cells and therefore would not be representative of any changes to hepatocyte FATP2 protein expression.

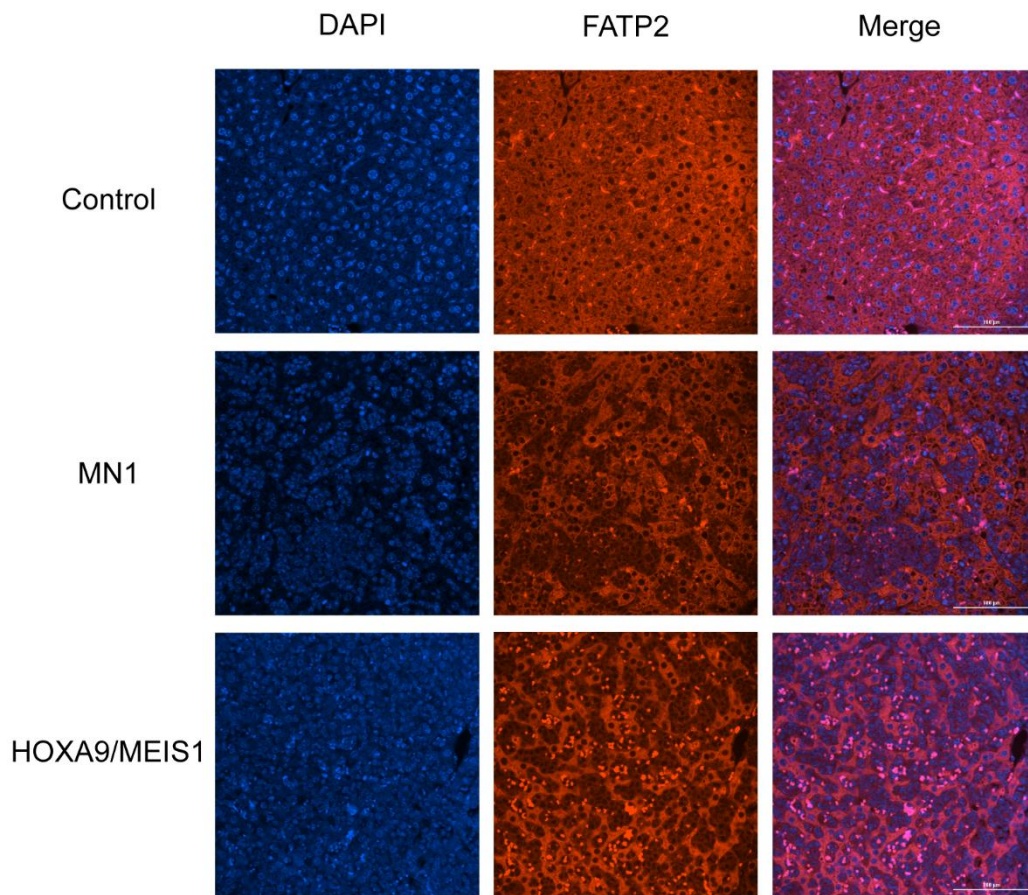


Figure 4.8 Immunofluorescence-stained liver histology samples for FATP2.

Representative images of immunofluorescent staining of livers from control mice and mice engrafted with MN1 cells or HOXA9/MEIS1 cells. Blue = DAPI, Red = FATP2.

Figure 4.4 suggests that the bright red cells are not AML cells, but they may in fact be other immune cells such as Kupffer cells. I therefore suggested to Alyssa that for the next round of staining she should use CD45 to stain for immune cells (green). In the merged representative images in Figure 4.9 it can be seen that the bright red cells stained for FATP2 correspond with the green stained CD45⁺ cells. This optimisation allows for downstream analysis as these cells can be masked out of the analysis for FATP2 intensity. They also add an interesting further analysis to investigate whether there are any changes in the number of immune cells within the liver sections.

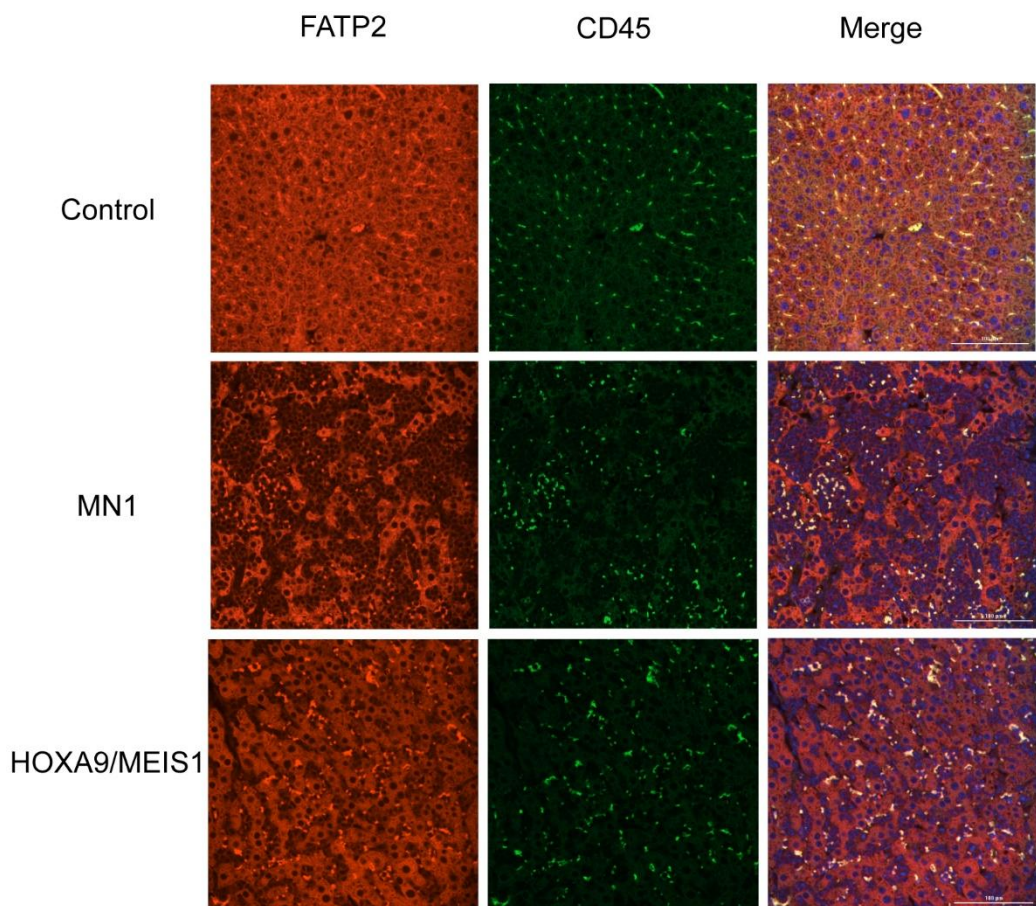


Figure 4.9 Immunofluorescence-staining of liver histology samples for Fatp2 and CD45.

Representative images of immunofluorescent staining of livers from control mice and mice engrafted with MN1 cells or HOXA9/MEIS1 cells. Red = FATP2, Green = CD45, and Blue = DAPI.

Analysis of the image set was performed by creating a pipeline in CellProfiler. For analysis 3 images were taken per section (corresponding to 1 mouse each) for control, MN1 or HOXA9/MEIS1 engrafted mice (n=7). Images were run through a threshold to remove non-specific background staining. A mask was created of the Cd45⁺ cells and used to remove the immune cells from the FATP2 images (Figure 4.10A). From the masked FATP2 stained images the intensity of red staining was measured and showed that there was significantly less FATP2 protein in the livers of mice engrafted with AML (Figure 4.10B). The masked image created from the CD45⁺ cells could then be used to count the number of objects created and thus the average number of immune cells per mouse liver (Figure 4.10C). There was no significant difference in the number of immune cells between control mice and mice with AML. It is interesting to note that 2 of the MN1 engrafted mice showed no CD45⁺ cells. It is uncertain as to why this may occur. Analysis of these images shows that AML in the BM alters liver protein expression of *Fatp2 in vivo*, suggesting that it decreases hepatocyte FA uptake *in vivo*. This matches with previous data showing a downregulation in *Fatp2* gene expression, along with the expression of other genes involved in FA metabolism, in response to AML engraftment.

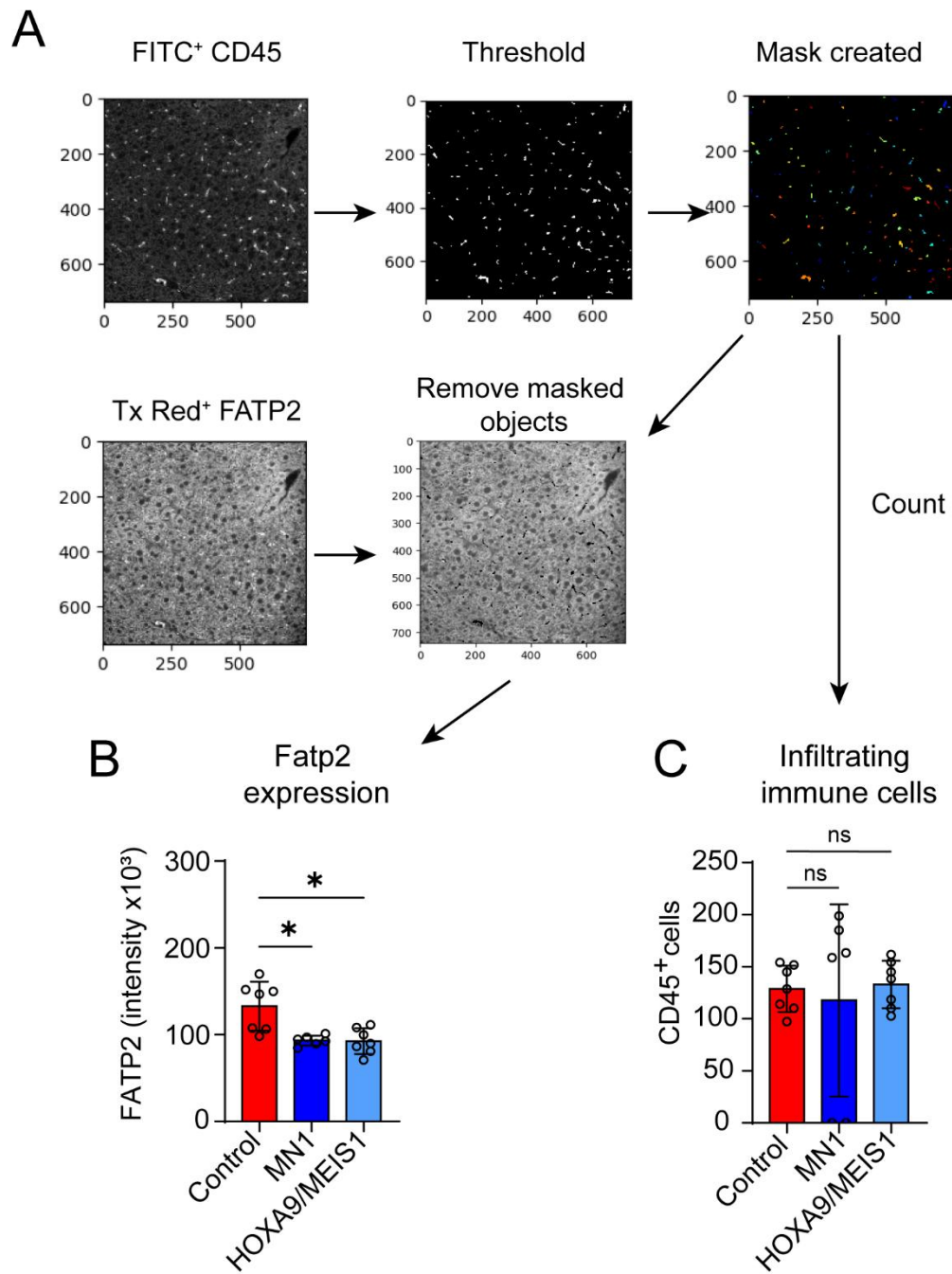


Figure 4.10 FATP2 protein levels are decreased in mice engrafted with AML.

A) CellProfiler strategy used to analyse images of immunofluorescent stained liver sections. B) intensity of FATP2 staining was calculated and C) infiltrating CD45⁺ immune cells counted for control mice compared with mice engrafted with MN1 cells or HOXA9/MEIS1 cells (n=7). Data are expressed as mean \pm SD. Statistical significance was calculated using Kruskal-Wallis H test with Tukey's multiple comparison test. * $p < 0.05$, and ns = non-significant.

4.5 AML downregulates FA metabolism genes in a cell-cell independent manner.

AML clearly induces weight and fat loss in a murine model and down regulates FA metabolism in the liver of these mice, both at a genetic level and protein levels. Further investigation is required to confirm that AML induces these systemic changes and not a compensatory mechanism within the whole organism. Therefore, to confirm that it is an AML dependant mechanism, experiments were performed *in vitro* to isolate the potential effect. All experiments using primary murine hepatocytes were isolated and plated on to 24 well plates by Dr Naiara Beraza and Dr Paula Ruiz from 2-3 C57BL/6 mice (aged 8-12 weeks) which were then pooled.

The first experiment utilised primary murine hepatocytes (1×10^5 /well) and MN1 cells in a transwell (5×10^4). Transwells were used as data from Figure 4.4 shows that AML does not engraft in the liver and therefore the separation provided by the transwell is more physiologically relevant than putting the MN1 cells directly on the hepatocytes. Cells were cultured together for 24hours followed by removal of the trans-wells and RNA lysis of the hepatocytes (n=4) (Figure 4.11A). Hepatocyte RNA was used to perform RT-qPCR and showed significant down regulation of *Cpt1a*, *Acadm* and *Hmgcs2* in hepatocytes treated with MN1 trans-wells compared to controls. As expected, *Cd36* did not show any alterations (Figure 4.11B). This confirms that AML is able to alter liver FA metabolism gene expression in a cell-cell independent mechanism.

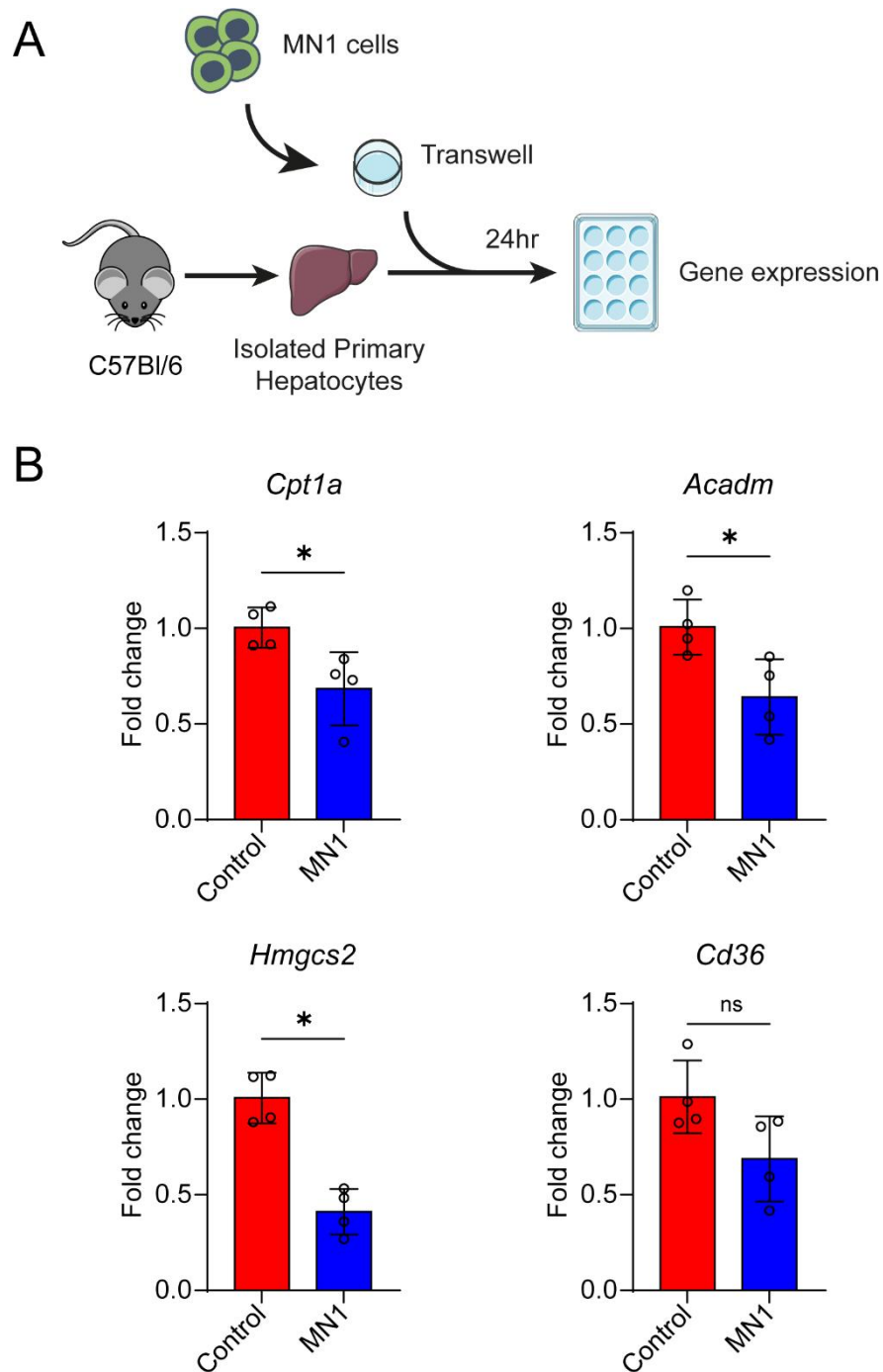


Figure 4.11 FA metabolism is down regulated in primary murine hepatocytes cultured with MN1 cells in transwells.

A) Schematic of experimental design. Primary hepatocytes isolated from C57Bl/6 mice were cultured with MN1 cells in transwells for 24hrs. MN1 cells were washed off prior to RNA lysis of hepatocytes for gene analysis compared to controls (n=3) B) Gene expression of *Cpt1a*, *Acadm*, *Hmgcs2*, and *Cd36*. Data are expressed as mean \pm SD. Statistical significance was calculated using Mann-Whitney U test. * $p < 0.05$, and ns = non-significant.

Transwells are costly so the next experiment aimed to see whether effects on FA metabolism genes could be achieved with media conditioned by the AML cells. To produce conditioned media, 1×10^6 AML cells/mL were cultured in their standard media excluding cytokines (DMEM, 10% FBS, and 1% P/S) for 24hrs. Double centrifugation removed all cells and debris before use. At the beginning of the experiment half the media was removed from each of the wells containing primary murine hepatocytes. This was replaced with conditioned media or control media. For the controls, the media added only contained 5% FBS, this was to simulate the approximate amount of FBS consumed by the AML cells during their growth phase of conditioning the media. In an ideal situation lipidomics would have been performed to correct for the appropriate FBS concentration. The experiment to test conditioned media cultured primary murine hepatocytes with control media or MN1 conditioned media for 24 or 16hrs (n=4). At the end of the experiment all media was removed, and RNA was isolated from the hepatocytes (Figure 4.12A). RT-qPCR of hepatocyte RNA shows that although *Cpt1a*, and *Acadm* are not downregulated at 24hrs, at 16hrs *Cpt1a*, *Acadm* and *Hmgcs2* are all downregulated by the conditioned media. Consistent with other experiments, *Cd36* was not downregulated by MN1 conditioned media (Figure 4.12B). These data show that AML is secreting a molecule that is acting on hepatocytes to downregulate genes associated with FA metabolism. Conditioned media was effective and mediating these changes at 16hrs.

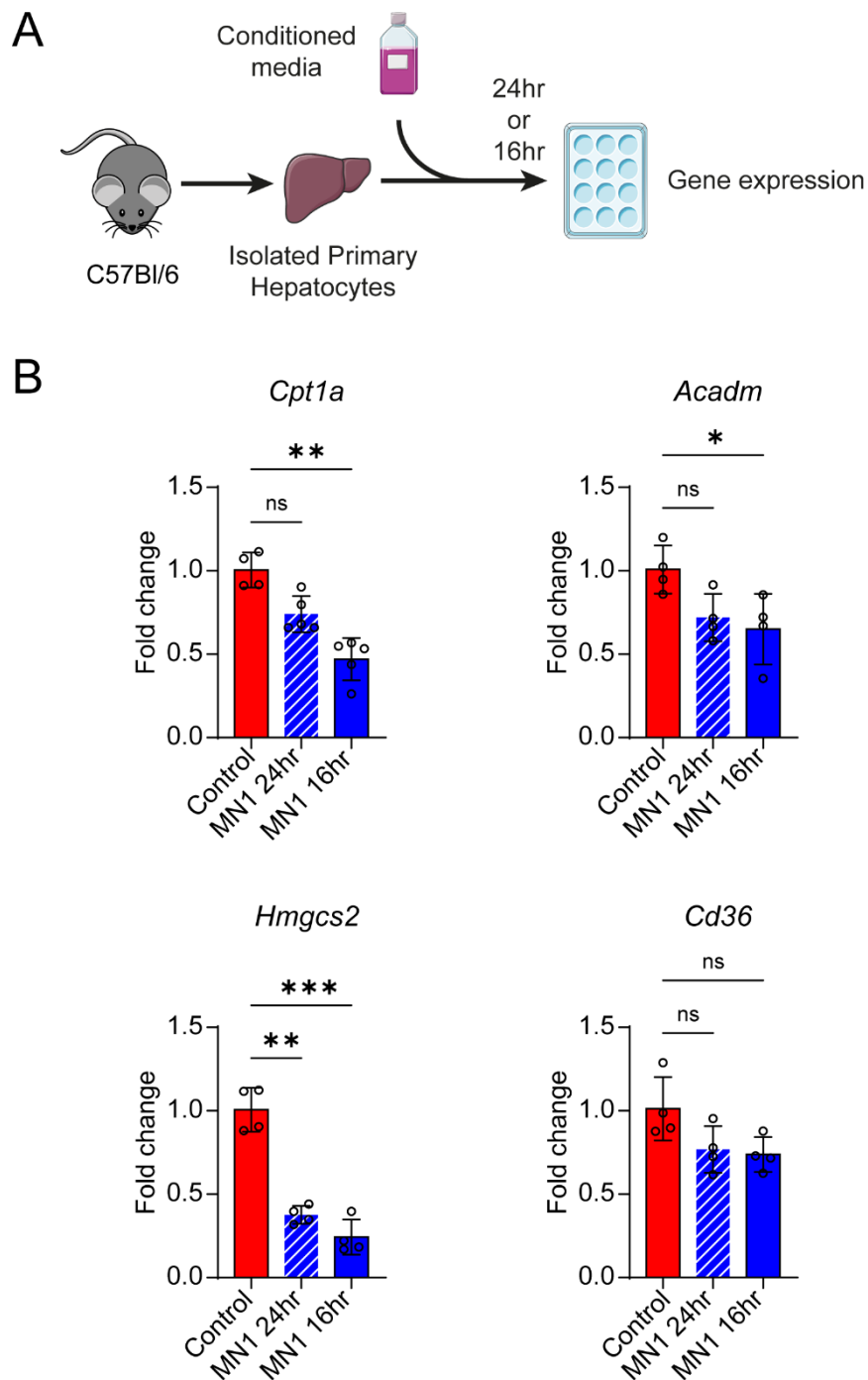


Figure 4.12 FA metabolism genes were altered in primary murine hepatocytes treated with AML conditioned media.

A) Schematic of experimental design. Primary hepatocytes isolated from C57Bl/6 mice were cultured with MN1 conditioned media for 16hrs or 24hrs (n=4). RNA lysates were analysed for gene expression and compared against controls (n=4). B) Gene expression of *Cpt1a*, *Acadm*, *Hmgcs2*, and *Cd36*. Data are expressed as mean \pm SD. Statistical significance was calculated using Kruskal-Wallis H test with Tukey's multiple comparison test. * $p < 0.01$, and ns = non-significant.

Isolating and plating primary hepatocytes is time consuming and limited by the availability of mice and Dr Baraza's time. Therefore, the next step was to investigate whether a murine hepatocyte cell line could be used to investigate the FA metabolic changes mediated by AML secreted factors. The cell line chosen was the 'Alpha mouse liver 12' (AML12) cells. This cell line is isolated from a 12-week-old male wild type mouse (271). This experiment utilised the same seeding density and conditioned media as the previous. AML12s were cultured with conditioned media or control media (n=5) for 16hrs prior to RNA extraction (Figure 4.13A). RT-qPCR shows no significant difference in any of the selected FA metabolism genes (Figure 4.13B). These data suggest that the AML12s are not a sufficient model for further use in this project and therefore primary hepatocytes were used. Limitations on receiving primary murine hepatocytes meant that subsequent experiments had to be carefully planned to gain the most output from the provided 24 well plates.

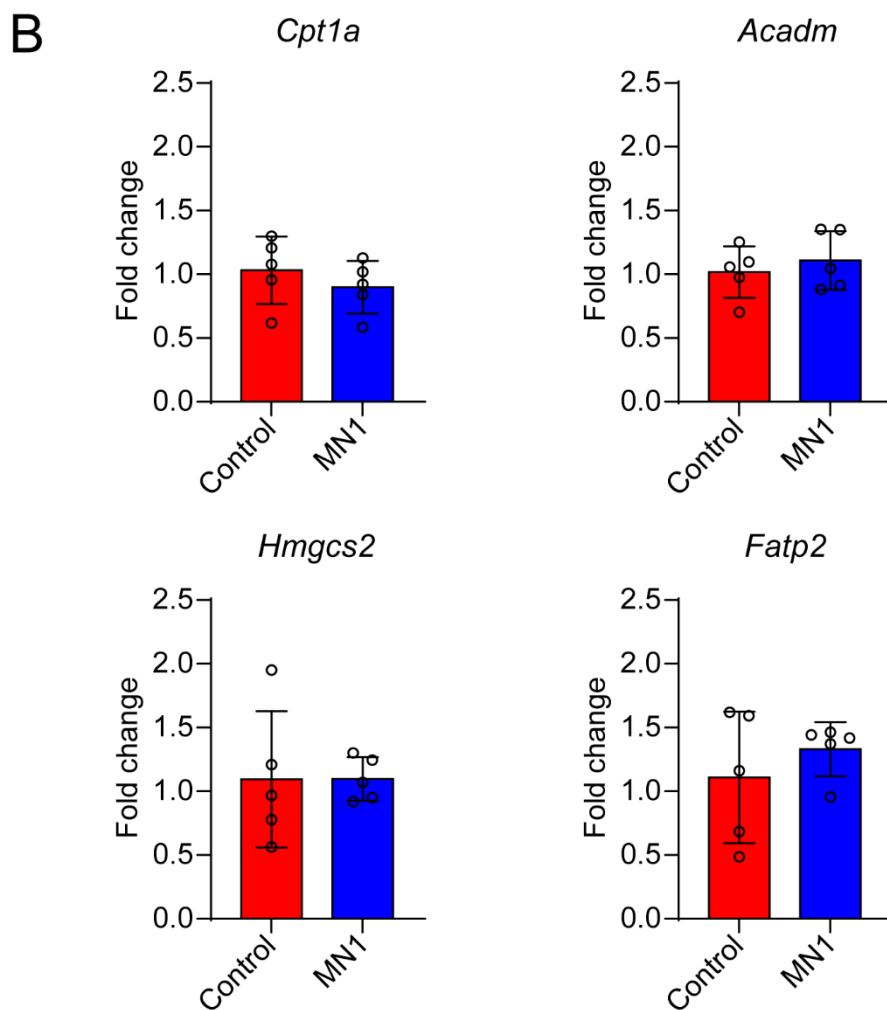
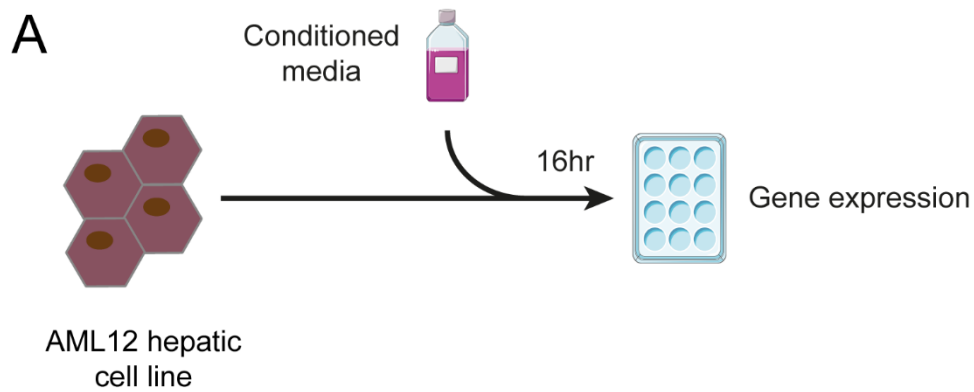


Figure 4.13 FA metabolism genes were not altered in AML12 liver cells treated with AML conditioned media.

A) Schematic of experimental design. Alpha male liver cells 12 (AML12) cells were cultured with or without MN1 conditioned media for 16hrs (n=5). B) Gene expression of *Cpt1a*, *Acadm*, *Hmgcs2*, and *Fatp2*. Data are expressed as mean \pm SD. Statistical significance was calculated using Mann-Whitney U test. ns = non-significant.

MN1 conditioned media downregulated hepatocyte FA metabolism genes at both 16 and 24hrs, confirming that cell-cell contact is not required to induce these changes. The next experiment investigated whether conditioned media, from both MN1 and HOXA9/MEIS1 cell lines, alters FA metabolism in primary murine hepatocytes at 16hrs. Media was conditioned by MN1 or HOXA9/MEIS1 cells as previously described and added to the primary hepatocytes at the beginning of the experiment. After 16hrs the conditioned media was removed, and RNA was isolated from the hepatocytes. RT-qPCR shows that gene expression of FA metabolism genes *Cpt1a*, *Hmgcs2*, and *Fatp2* were downregulated in comparison to control treated cells (Figure 4.14). Interestingly, although not downregulated in other experiments and not implicated in the bulk RNAseq, *Cd36* was significantly lower in hepatocytes treated with the AML conditioned media in comparison to control hepatocytes. It is unclear as to why this occurred. These data show that both AML cell lines downregulate genes at different stages of FA metabolism within hepatocytes via a cell-cell independent mechanism.

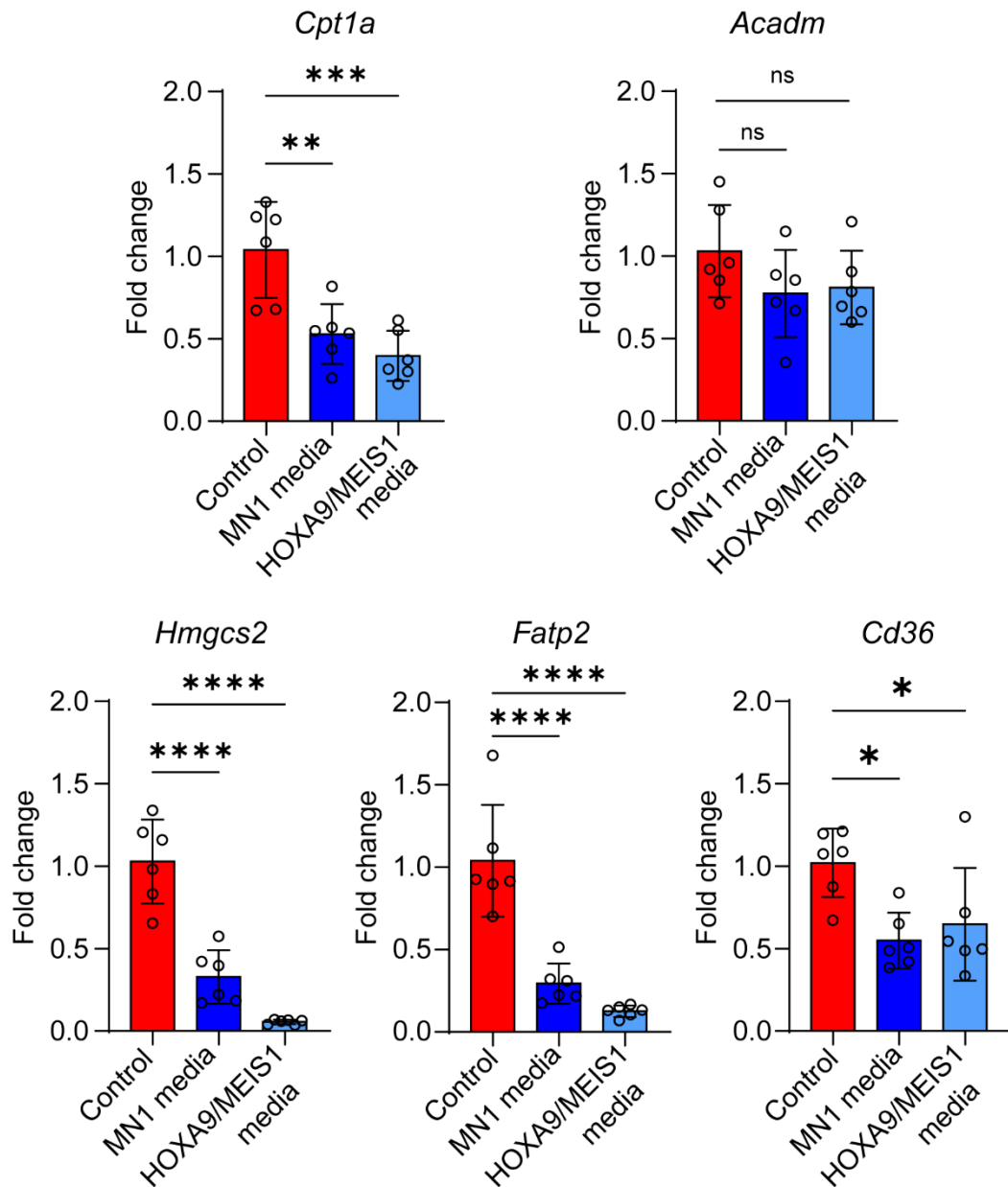


Figure 4.14 FA metabolism genes were altered in primary murine hepatocytes treated with AML conditioned media.

Primary hepatocytes isolated from C57Bl/6 mice were cultured with control media, MN1 or HOXA9/MEIS1 conditioned media for 16hrs (n=6). Gene expression of *Cpt1a*, *Acadm*, *Hmgcs2*, *Fatp2*, and *Cd36*. Data are expressed as mean \pm SD. Statistical significance was calculated using Kruskal-Wallis H test with Tukey's multiple comparison test. * p < 0.05, ** p < 0.01, *** p < 0.001, **** p < 0.0001, and ns = non-significant.

4.6 AML conditioned media reduces primary hepatocyte OCR.

It has been shown that FA metabolism plays a key role in the functionality of both AML blasts and hepatocytes (236, 305, 312). AML is a highly proliferative disease and therefore must access further metabolites than those it is able to pilfer from cells within its' niche via cell-cell interactions and cytokine release (114, 382-384). To assess whether AML in the BM is able to alter FA metabolism capacity in the mitochondria of hepatocytes seahorse metabolic flux analysis was used. This functional assay measures OCR and ECAR of cells, which are representative of OXPHOS and glycolysis. Hepatocytes isolated from C57Bl/6 mice were pretreated for 16hrs with control media or media conditioned by MN1 or HOXA9/MEIS1 cells as described above (Figure 4.15A). To assess the ability of the hepatocytes to metabolise FA, the test was performed with palmitic acid (palm) rather than the standard glucose in the seahorse base media. During the experiment timed injections of Oligomycin (2 μ M), carbonyl cyanide-4-(trifluoromethoxy) phenylhydrazone (FCCP) (1 μ M), and Rotenone + antimycin A (0.5 μ M), are added to the culture plate in accordance with the manufacturer's instructions. The ability of these drugs to alter OCR allows for measurements for basal and maximal respiration (Figure 4.15B).

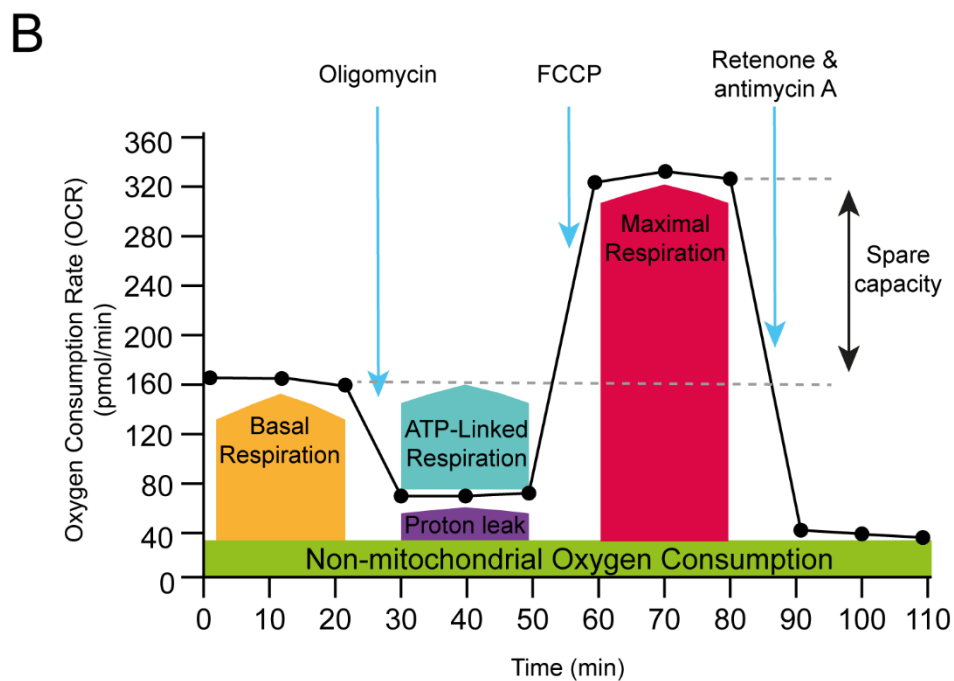
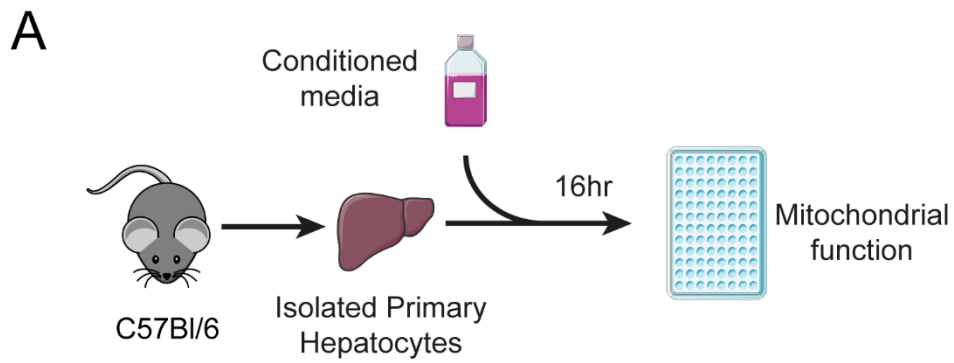


Figure 4.15 Seahorse metabolic flux mitostress kit was used to assess oxygen consumption rate.

A) Schematic of experimental design. Primary hepatocytes isolated from C57Bl/6 mice were cultured with MN1 or HOXA9/MIES1 conditioned media or control media for 16hrs (n=6). B) schematic of seahorse metabolic flux mitostress test.

In this experiment hepatocytes were pooled from 2 C57Bl/6 mice (10 weeks) and plated directly on to the seahorse culture plate (1×10^4 /well). Hepatocytes were treated with conditioned media from either cell line or control media for 16 hours followed by replacement of the media with palm - seahorse base media. The seahorse mito stress kit shows that both MN1 and HOXA9/MEIS1 conditioned media altered the OCR of hepatocytes (Figure 4.16A & B). Analysis showed that both AML conditioned medias caused reduced basal respiration (Figure 4.16C) as well as reduced maximal respiration (Figure 4.16D) in the presence of abundant FA, compared to controls. These data show that AML conditioned media reduces the capability of the hepatocytes to utilise the FA for metabolism and respiration, thus suggesting that AML in the BM may act on liver hepatocytes *in vivo* to alter FA metabolism capabilities.

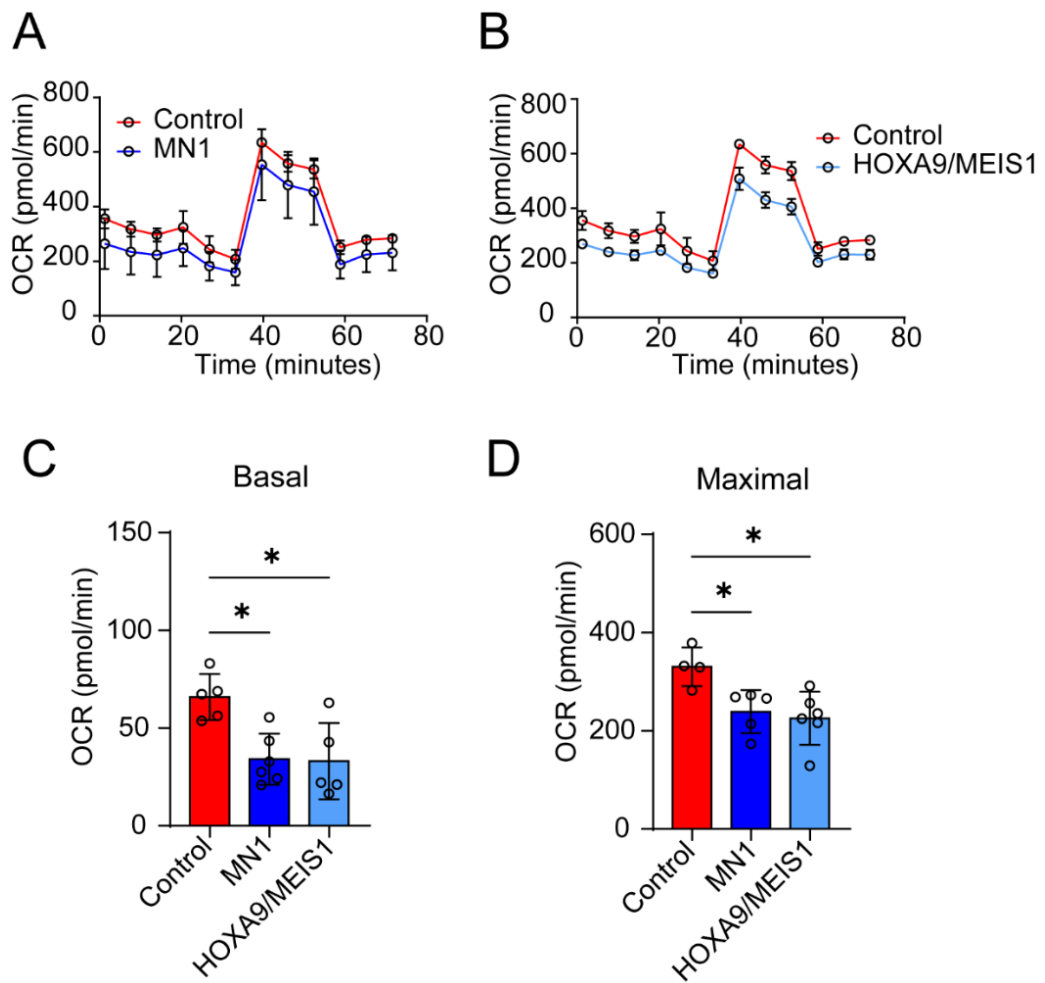


Figure 4.16 Oxygen consumption rate was altered in primary murine hepatocytes treated with AML conditioned media.

Seahorse metabolic flux mitostress kit analysis of primary hepatocytes treated for 16hrs with A) MN1 conditioned media (n= 5) or B) HOXA9/MEIS1 conditioned media (n=6) compared to control treated hepatocytes (n=4). C) Basal and D) Maximal respiration were calculated from plots. Data are expressed as mean \pm SD. Statistical significance was calculated using Kruskal-Wallis H test with Tukey's multiple comparison test. * p < 0.05.

4.7 AML conditioned media reduces primary hepatocyte FA uptake.

One of the major roles of hepatocytes is the uptake of FA from the plasma and the subsequent storage to prevent lipotoxicity (274). Reducing plasma FA reduces the availability of FA to other cells in the body, reducing lipotoxicity and promoting the use of glucose. The uptake and storage of FA by hepatocytes changes with the metabolic demands of the body which can be altered by dietary intake or by stimuli such as infection or disease (296). The next experiments aim to test whether AML impacts these pathways to reduce FA uptake by hepatocytes, with the potential of increasing the availability of FA for its own uptake when the blood reaches the BM. To investigate whether AML in the BM reduces hepatocyte FA uptake, hepatocytes were isolated and pooled from 2 C57Bl/6 mice and cultured for 16hrs in AML conditioned medias. In the final hour of incubation LCFA-BODIPY C12 was added to the media (1 μ M). DAPI nuclei dye (5 μ M) was added for 1 minute before the media was removed and the cells imaged in fresh control media (Figure 4.17). Images from this experiment were not analysed. Due to the addition of fresh media for imaging, uptake and use of the LCFA-BODIPY C12 continued during the imaging which would likely change results. Images were also taken using a bright field filter and were not of high enough quality to easily make out the cell membranes of the hepatocytes. This would have made analysis challenging and therefore further optimisation of the protocol was required.

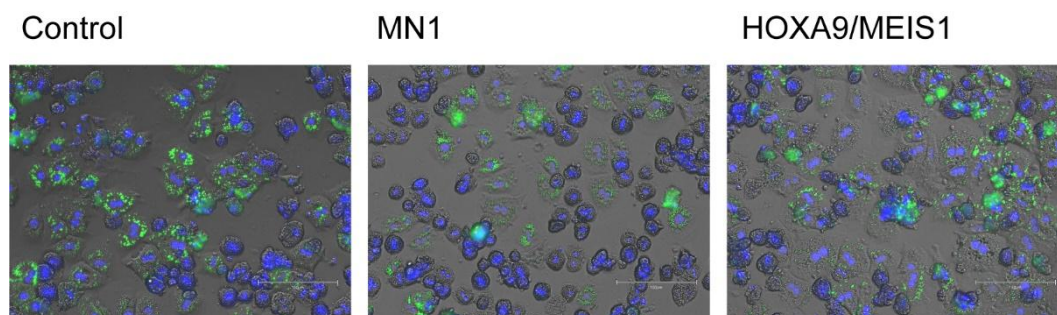


Figure 4.17 Primary murine hepatocytes differentially take up LCFA BODIPY C12 in response to AML conditioned media.

Representative images of primary hepatocyte isolated from C57Bl/6 mice were treated for 16hrs with control media or media conditioned by MN1 or HOXA9/MEIS1 cells. In the last hour LCFA BODIPY C12 was added. Cells were washed and fresh media added for imaging. Blue = DAPI, and Green = LCFA BODIPY C12.

To improve upon the previous experiment incubation with the conditioned media and LCFA-BODIPY C12 remained the same. After the full 16hours all media was removed and the hepatocytes were fixed with formaldehyde (4%, 7.4pH) for 20 minutes, this prevented any further uptake or utilisation of the LCFA-BODIPY C12. Blocking and staining with Phalloidin (1:800) prevented background, non-specific staining and stained the actin cytoskeleton to more easily visualise the cell structure of the hepatocytes for further analysis. Several washes with PBS and imaging the wells with fresh PBS further improved the image quality, removing non-specific staining, thus making this set of images better for analysis (Figure 4.18).

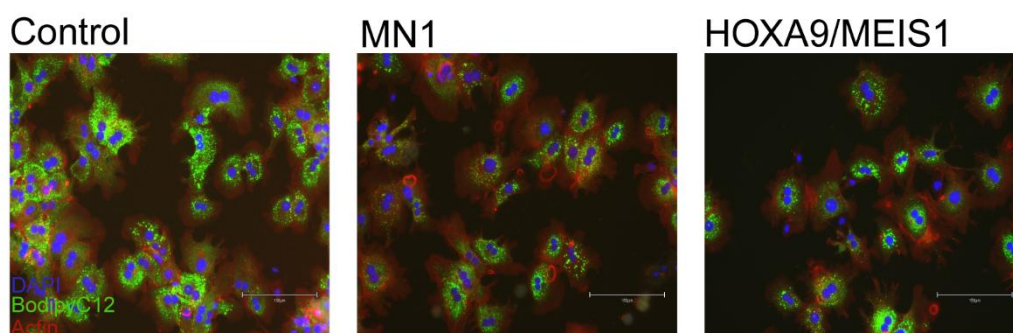


Figure 4.18 Visibly less LCFA-BODIPY C12 taken up by hepatocytes pretreated with AML conditioned media.

Representative images of primary hepatocytes isolated from C57Bl/6 mice pre-treated with control media or media conditioned by MN1 cells or HOXA9/MEIS1 cells for 16hrs, prior to addition of LCFA-BODIPY C12. Blue = DAPI, Red = β -actin, and Green = LCFA-BODIPY C12.

Images from the above experiment were analysed by creating a pipeline in CellProfiler. Images were run through a threshold to remove any lingering background staining. The DAPI channel was used to identify the nuclei. Hepatocytes are often multi-nucleated, and it was therefore important to assess what quantified a cell. The nuclei were masked and expanded to fill the rough size indicated by the β -actin staining. This mask was added to the LCFA-BODIPY C12 images on the FITC channel, and only signal within these masks was measured to give the intensity of LCFA-BODIPY C12 taken up by the treated hepatocytes (Figure 4.19A). Results show that both MN1 and HOXA9/MEIS1 conditioned medias significantly reduced the uptake of LCFA-BODIPY C12 when compared with controls (Figure 4.19B). This further supports the previous data in this project, suggesting that BM AML alter FA uptake by hepatocytes, disrupting the normal function.

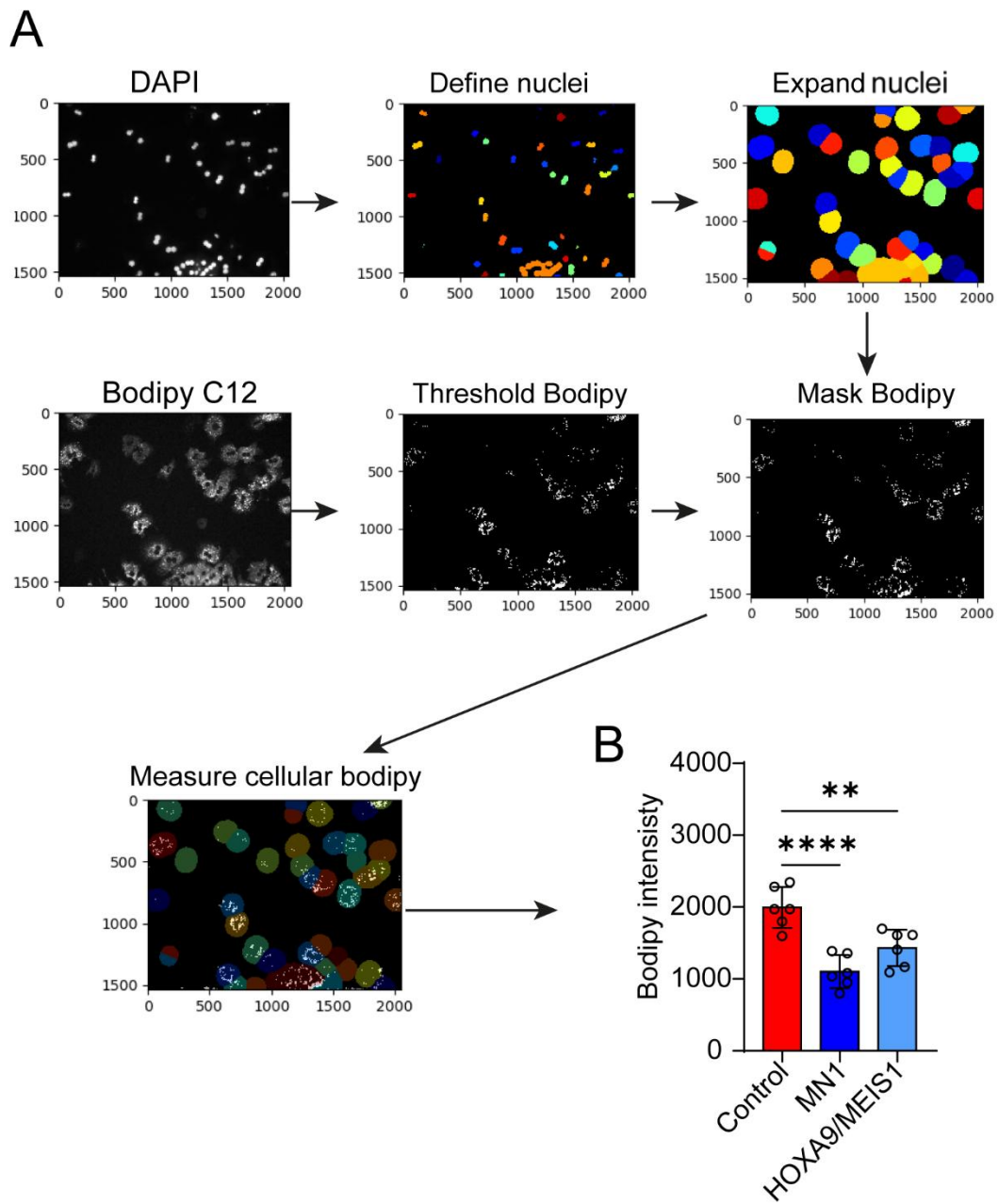


Figure 4.19 LCFA-BODIPY C12 uptake is decreased in primary hepatocytes treated with AML conditioned media.

A) CellProfiler pipeline used to analyse images of immunofluorescent stained primary hepatocytes. B) Intensity of LCFA-BODIPY C12 in wells with primary murine hepatocytes treated for 16hrs with control media or media conditioned by MN1 cells or HOXA9/MEIS1 cells (n=6). Data are expressed as mean \pm SD. Statistical significance was calculated using Kruskal-Wallis H test with Tukey's multiple comparison test. ** $p < 0.01$, and **** $p < 0.0001$.

4.8 Summary

In this chapter I have shown that AML engraftment in the BM alters liver metabolism pathways. Bulk RNAseq of the livers showed that FA metabolic pathways were among the most downregulated. RT-qPCR analysis has shown both *in vivo* and *in vitro* that genes associated with different stages of FA metabolism are downregulated in response to AML secreted factors. Flow cytometry of the liver immune cells further confirms that this is a cell-cell independent mechanism. Functional analysis and immunofluorescent imaging of hepatocyte FA uptake indicates that inhibition of gene expression is carrying over to protein production. AML causes reduced Fatp2 protein expression *in vivo* and *in vitro* AML conditioned media reduces hepatocyte FA uptake capacity. Furthermore, by altering the FA uptake by the hepatocytes, AML conditioned media also reduces the FA metabolism and respiration by the hepatocytes. These data support the hypothesis that AML alters FA metabolism in the liver, the next chapter aims to elucidate the mechanism by which AML in the BM is able to act on the liver.

5. AML secreted HGF inhibits PPAR α mediated liver FA metabolism.

5.1 Introduction

During cycles of feeding and fasting the liver receives a multitude of signals to regulate the uptake, breakdown, synthesis, storage, and release of FA (269). Different cell types have been shown to release cytokines in times of stress to signal an increased need for FA to enter the serum and increase availability as a source of energy (385, 386). For example, to keep up with the demand for new immune cells, during an infection HSC upregulate all forms of metabolism, thus requiring an increase in metabolites (38). It is known that HSC, like AML blasts, are metabolically plastic and reprogramme BMSC to access metabolites, but in severe cases such as sepsis, this is not sufficient and mobilisation of metabolites from around the body is required (11, 387). The liver is the master regulator of circulating FA and as such it is imperative that it can respond body's requirements (269). Sepsis induces an inflammatory response, causing systemic release of pro-inflammatory cytokines such as IL-1 β , IL-6, and TNF α (388, 389), as well as elevating other cytokines such as HGF (390). The listed cytokines can act on the liver to alter metabolism. During sepsis reduced liver PPAR α signalling aids in a starvation response, elevating serum FFA (391). Some malignancies have also been shown to alter liver metabolism. For example, in colorectal cancer release of IL-6 acts on the liver, improving metabolite availability for use by the tumour (250). Other cancers, such as ovarian cancer, lung cancer and lymphoma are implicated to have high serum FA, which is often indicative of a poorer prognosis (346, 392, 393). While not widely researched, it could be suggested that increased serum FA is linked to altered liver FA metabolism.

In the previous chapter I established that AML acts on the liver to alter FA metabolism. I showed that AML conditioned media also downregulates liver FA metabolism genes and impairs FA uptake in primary murine hepatocytes. This suggests that AML releases factor(s) into the blood that act on the liver. In this next chapter I aim to elucidate the factor(s) that AML releases, and which of these can alter liver FA metabolism. Once I ascertain the factor(s), I aim to investigate whether liver FA metabolism can be restored via these factors. Furthermore, I aim to understand the mechanism by which AML released factor(s) act on hepatic cells and whether altering the liver metabolic state can impede AML survival and progression.

5.2 AML secreted HGF and IL-1 β downregulates FA metabolism genes in hepatocytes.

The experiments from the previous chapters have shown that AML acts on the liver, via secreted factors, to downregulate FA metabolism genes, reduce FA uptake, and increase serum levels of FFA for the tumour to access from the blood supply in the BM. We know it is a secreted factor that is acting on the liver as FIGURE 4.4 shows that there is <5% engraftment of AML blasts in the liver. This is further supported *in vitro* by media conditioned by AML cells downregulating FA metabolism in primary murine hepatocytes. Therefore, the next step was to investigate the factor/s which AML secretes, which are involved in FA metabolism. For this Proteome Profiler Cytokine Arrays were performed on control mouse serum, serum from mice engrafted with MN1 or HOXA9/MEIS1 cells (as described in the confirmed model), and media conditioned by MN1 cells or HOXA9/MEIS1 cells (Figure 5.1A). Pathway analysis of the cytokines from the array kit were used to create heat maps for FAO, OXPHOS, and Glycolysis. G-CSF, HGF, and IL-1 β were all elevated on the arrays treated with MN1 (Figure 5.1B) or HOXA9/MEIS1 (Figure 5.1C) mouse serum or conditioned media when compared to control mouse serum. Interestingly IL-6, a target that was expected to be high in AML conditions, was not elevated in either AML mouse serums, and was only slightly elevated in HOXA9/MEIS1 conditioned media. This experiment highlighted 3 AML secreted cytokines to take forward for further investigation.

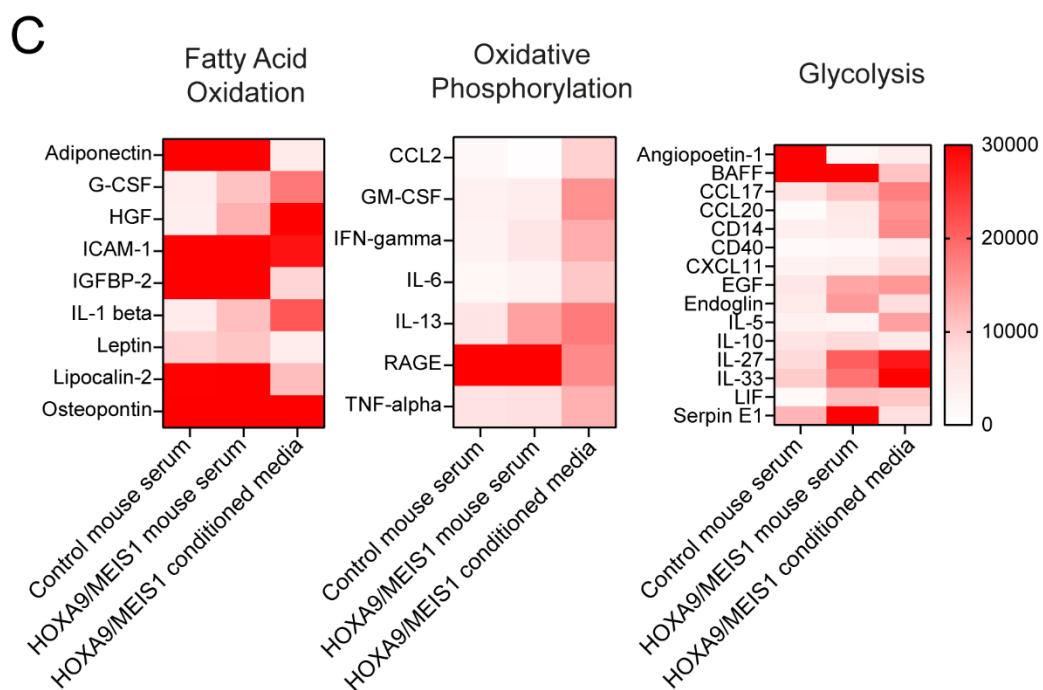
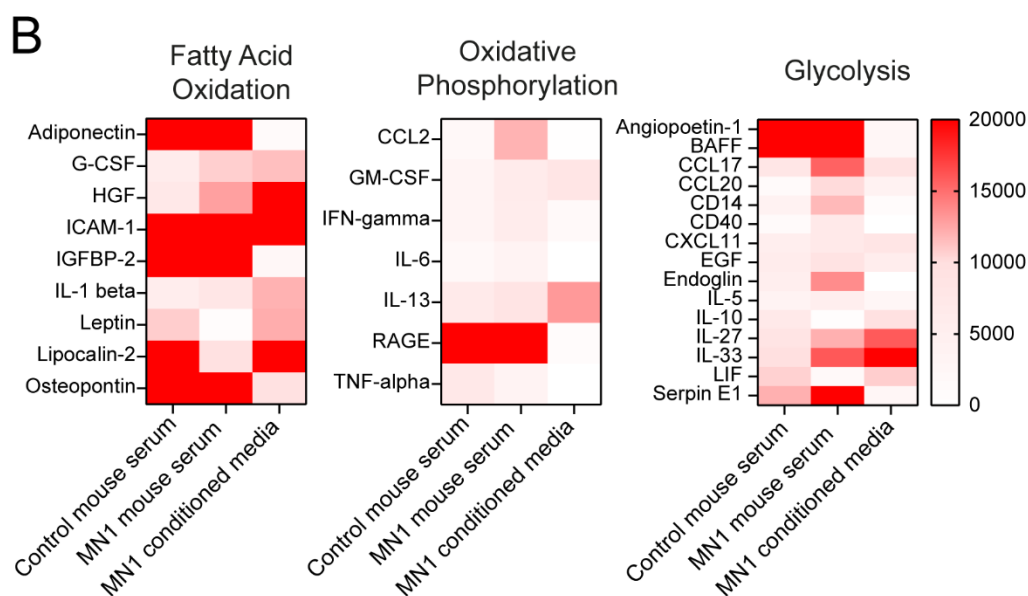
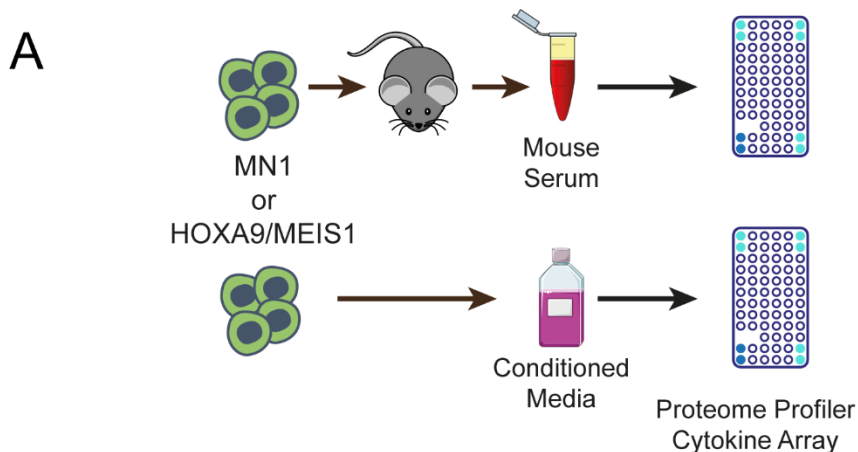


Figure 5.1 Cytokines associated with FA metabolism are elevated in response to AML.

A) Schematic of experimental design. Serum from control mice or mice engrafted with MN1 or HOXA9/MEIS1 cells, or conditioned media from both cell lines were used to perform a proteome profiler cytokine array. Heat maps were produced for cytokines involved in FAO, OXPHOS, and glycolysis. Data is of the chemiluminescence for B) MN1 and C) HOXA9/MEIS1 serum and conditioned media vs control mouse serum.

Next, primary hepatocytes isolated and pooled from 2 C57Bl/6 mice were incubated with G-CSF (100ng/mL), IL-1 β (10ng/mL), or HGF (20ng or 200 ng/mL). HGF was given at 2 doses as it is known to have pro- and anti-mitotic effects at low and high doses (394). After 16hrs of incubation media was removed and RNA isolated from the hepatocytes was used to perform RT-qPCR. Analysis shows that G-CSF had no significant effect on the FA metabolism genes, and therefore was not taken forward for any further experiments (Figure 5.2A). Both IL-1 β and HGF (at both doses) treated hepatocytes downregulated 3 of the 4 tested FA metabolism genes when compared to control treated hepatocytes (Figure 5.2B & C).

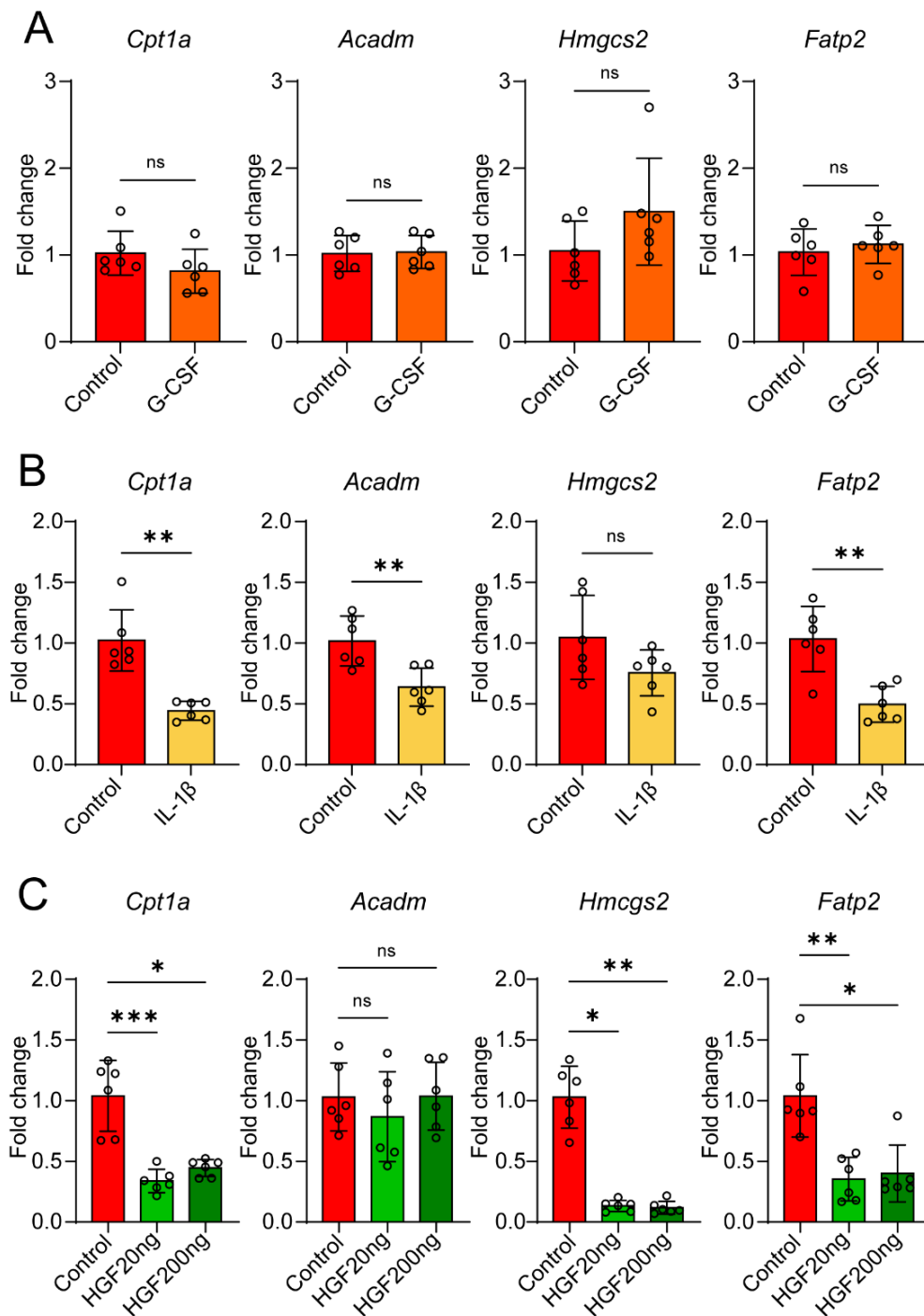


Figure 5.2 Primary murine hepatocyte FA metabolism genes are downregulated by IL-1 β and HGF.

Gene expression of *Cpt1a*, *Acadm*, *Hmgcs2*, and *Fatp2*. Analysis was performed on RNA lysates from C57Bl/6 primary hepatocytes. Hepatocytes were treated for 16hrs with A) G-CSF (100ng/mL), B) IL-1 β (10ng/mL), or C) HGF (20ng/mL or 200ng/mL) and compared with hepatocytes treated with control media (n=6). Data are expressed as mean \pm SD. Statistical significance was calculated using Mann-Whitney U test or Kruskal-Wallis H test with Tukey's multiple comparison test. * p < 0.05, ** p < 0.01 *** p < 0.001, and ns = non-significant.

The previous experiment shows that both IL-1 β and HGF significantly downregulate the expression of genes at different stages of FA metabolism. Although elevated in AML literature has shown that IL-1 β is found at lower concentrations in the blood than the dose given in the last experiment (395). Thus, a more clinically relevant dose of 1ng/mL was added to the primary hepatocytes for the next experiment. RT-qPCR of the RNA from hepatocytes treated for 16hrs with the IL-1 β show that *Cpt1a*, *Hmgcs2*, and *Fatp2* but not *Acadm* are significantly down regulated by the lower dose of IL-1 β when compared with control treated hepatocytes (Figure 5.3).

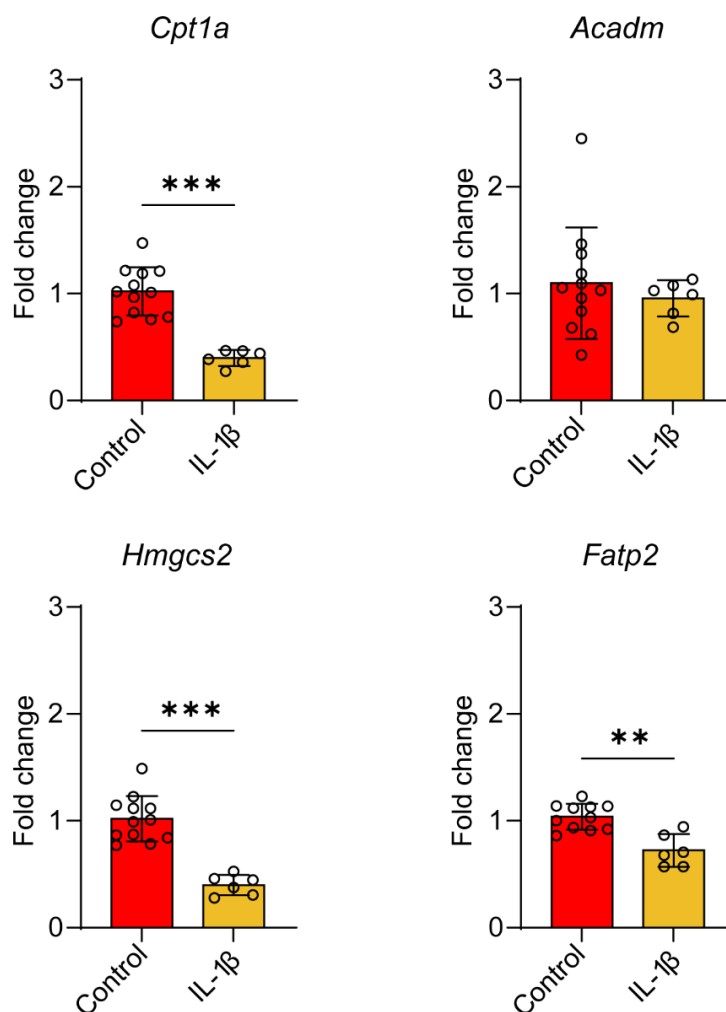


Figure 5.3 Low dose of IL-1 β downregulates primary hepatocyte FA genes.

Gene expression of *Cpt1a*, *Acadm*, *Hmgcs2*, and *Fatp2* for primary murine hepatocytes treated for 16hrs with IL-1 β (1ng/mL) vs controls (n=6). Data are expressed as mean \pm SD. Statistical significance was calculated using Mann-Whitney U test t. ** p < 0.01, *** p < 0.001, and ns = non-significant.

The next experiment aimed to investigate whether inhibition of IL-1 β would rescue the expression of FA metabolism genes in hepatocytes treated with IL-1 β (Figure 5.4A), MN1 conditioned media (Figure 5.4B) or HOXA9/MEIS1 conditioned media (Figure 5.4C) or each in combination with mAb when compared to control treated hepatocytes. RT-qPCR analysis shows that there is no change when the neutralising monoclonal IL-1 β antibody was added to any of the treatment conditions. This is inconclusive as it suggests that the mAb is not working as it is designed to. It would be expected that the mAb would have an inhibitory effect on the IL-1 β , as it is designed against the cytokine. It can therefore not be concluded whether blocking IL-1 β would have a restorative effect on FA metabolism gene expression in primary hepatocytes treated with MN1 or HOXA9/MEIS1 conditioned media. Further testing of the antibody or use of another inhibitor would be required for confirmation.

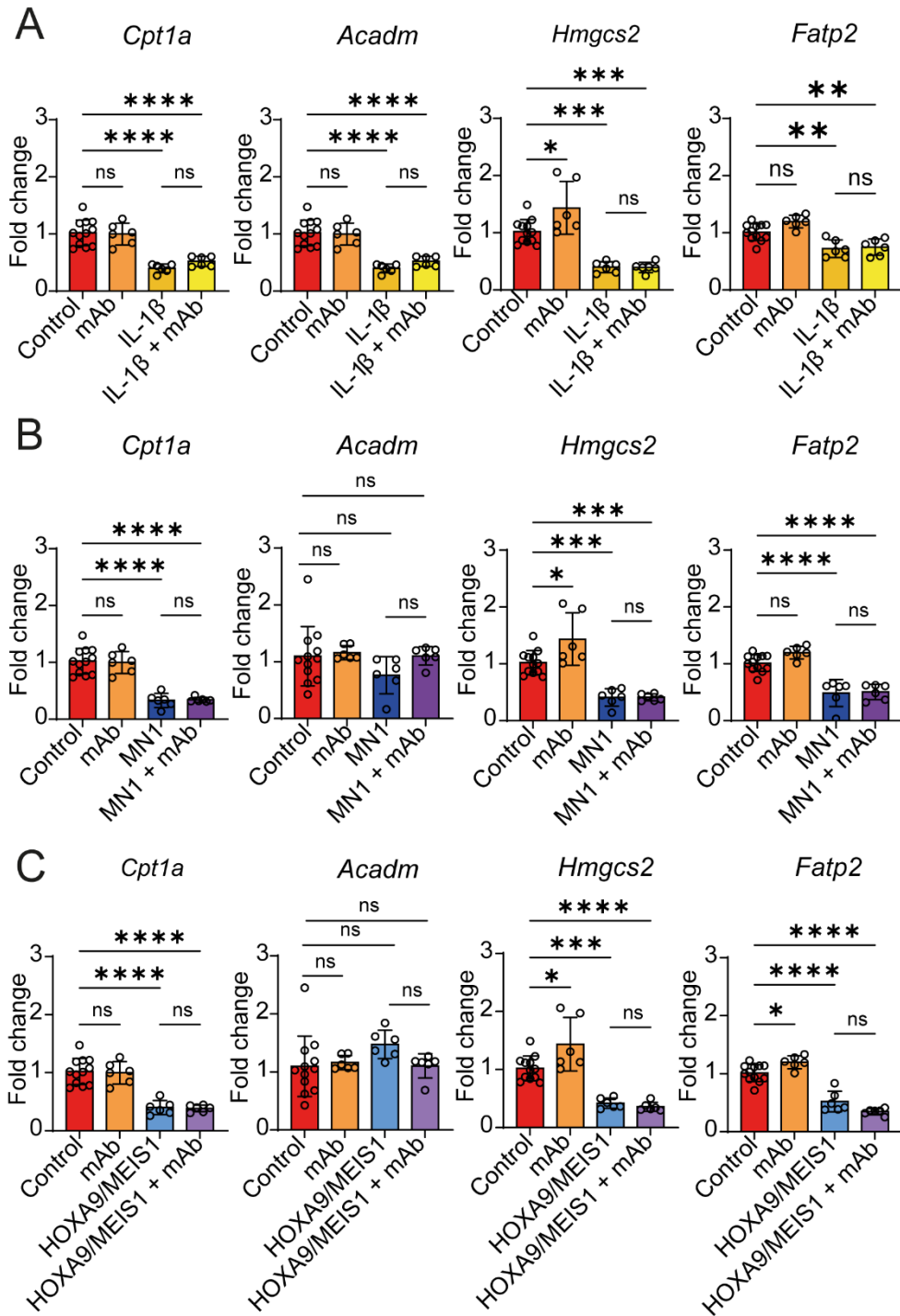


Figure 5.4 Mouse IL-1 β monoclonal antibody (mAb) did not rescue FA metabolism genes in hepatocytes.

Gene expression of *Cpt1a*, *Acadm*, *Hmgcs2*, and *Fatp2*. Primary murine hepatocytes were treated for 16hrs with mAb (5 μ g/mL), IL-1 β (1ng/mL), media conditioned by MN1 cells or HOXA9/MEIS1 cells and in combination (n=6) and compared with controls (n=12). Data are expressed as mean \pm SD. Statistical significance was calculated using or Kruskal-Wallis H test with Tukey's multiple comparison test. * p < 0.05, ** p < 0.01, *** p < 0.001, **** p < 0.0001 and ns = non-significant.

Additionally, due to limitations around primary hepatocyte supply, while experiments were conducted for IL-1 β , so too were further experiments for HGF. Similar to IL-1 β , serum levels of HGF are not regularly found in concentrations given in the prior experiment (396, 397). Therefore, the more relevant dose of 10ng/mL was given to primary hepatocytes for 16hrs. RT-qPCR from the treated hepatocytes confirmed that HGF significantly downregulated the expression of *Cpt1a*, *Hmgcs2* and *Fatp2* when compared with controls (Figure 5.5).

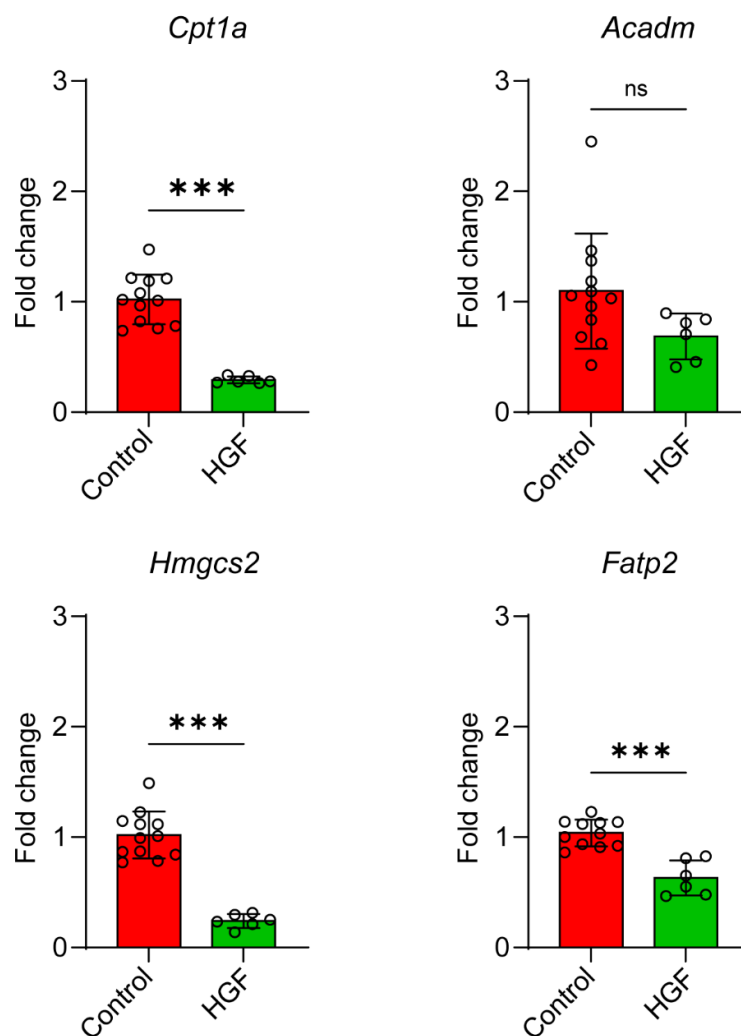


Figure 5.5 Low dose HGF downregulates primary hepatocyte FA genes.

Gene expression of *Cpt1a*, *Acadm*, *Hmgcs2*, and *Fatp2* for primary murine hepatocytes treated for 16hrs with HGF (10ng/mL) vs controls (n=6). Data are expressed as mean \pm SD. Statistical significance was calculated using Mann-Whitney U test t. *** p < 0.001, and ns = non-significant.

The next experiment aimed to show that by inhibiting HGF with crizotinib FA metabolism gene expression could be returned to control levels in primary murine hepatocytes. For this, hepatocytes were treated for 16hrs with control media, crizotinib (100nM) HGF (10ng/mL), MN1 conditioned media, HOXA9/MEIS1 conditioned media, or the treatments were given in combination with crizotinib. RT-qPCR data analysis from the primary hepatocytes shows that when crizotinib is added in combination with HGF it has a restorative effect on the FA gene expression. Data shows significantly elevated expression of *Cpt1a*, *Acadm*, *Hmgcs2*, and *Fatp2* when compared to HGF treated hepatocytes (Figure 5.6A). This effect was not seen in MN1 conditioned media treated hepatocytes (Figure 5.6B) or HOXA9/MEIS1 conditioned media treated hepatocytes (Figure 5.6C).

In this section I have shown that AML blasts secrete HGF and IL-1 β which act on primary murine hepatocytes, downregulating genes at different stages of FA metabolism. However, I observe that crizotinib inhibits HGF induced gene regulation whereas the IL-1 β inhibitor did not appear to work biologically. Moreover, both crizotinib or IL-1 β did not reverse the effect of MN1 or HOXA9/MEIS1 conditioned media on hepatocyte gene expression. This may suggest that these cytokines work in combination to act on the liver.

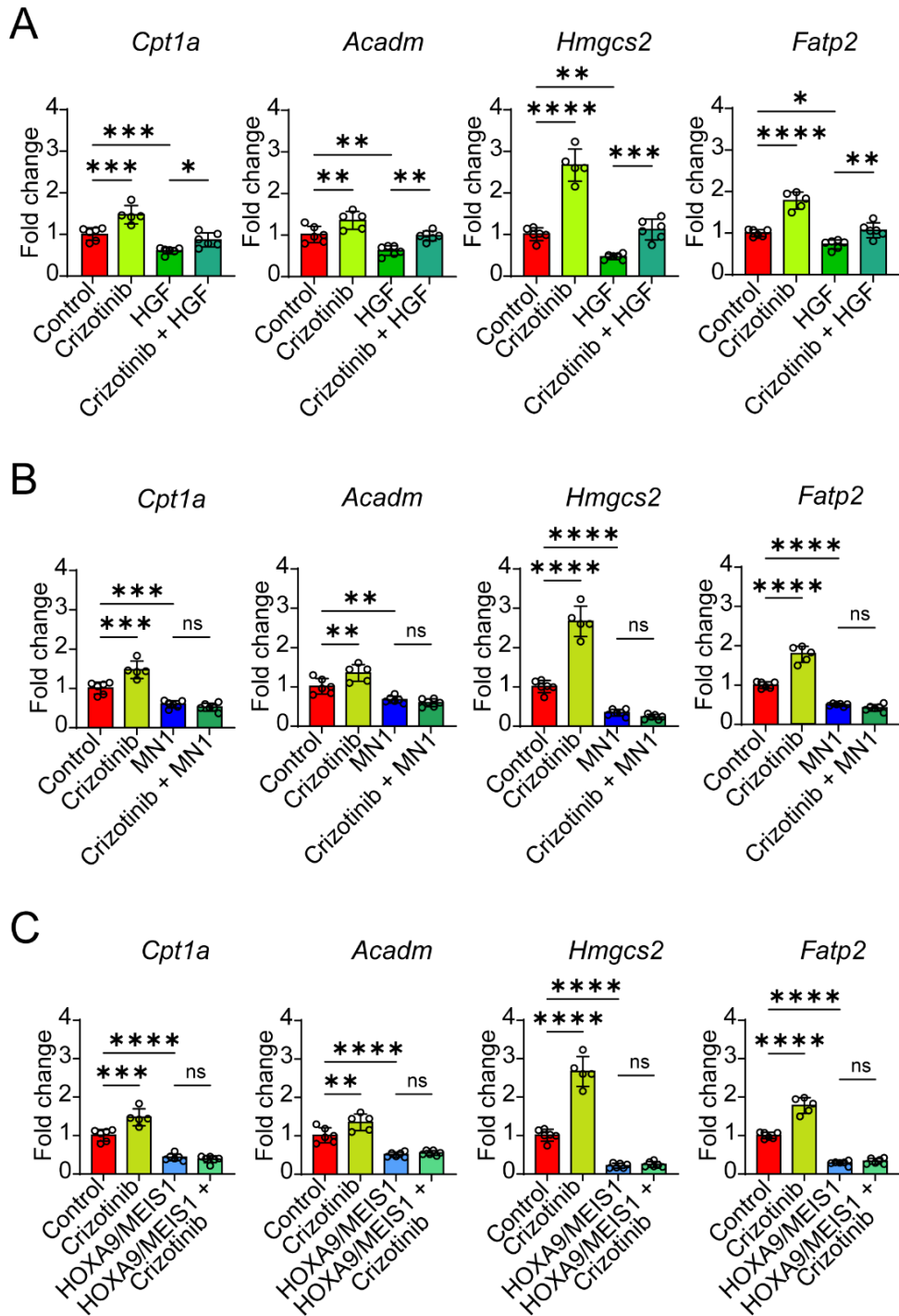


Figure 5.6 Crizotinib rescued FA metabolism expression in HGF treated primary hepatocytes.

Gene expression of *Cpt1a*, *Acadm*, *Hmgcs2*, and *Fatp2*. Primary murine hepatocytes were treated for 16hrs with control media (n=6), crizotinib (100nM) (n=5), A) HGF (10ng/mL) (n=6), B) MN1 conditioned media (n=6), C) HOXA9/MEIS1 conditioned media (n=6). Each treatment was also given in combination with crizotinib (n=6). Data are expressed as mean \pm SD. Statistical significance was calculated using or Kruskal-Wallis H test with Tukey's multiple comparison test. * p < 0.05, ** p < 0.01, *** p < 0.001, and **** p < 0.0001.

5.3 HGF reduces hepatocyte FA uptake and metabolism.

It is known that both HGF and IL-1 β play a role in FA metabolism (247, 398-400) and the previous experiments have confirmed this. Both act to inhibit or activate downstream effectors which result in downregulation of pathways involved in FA uptake and lipogenesis (398, 401, 402). Figure 5.1 shows that both AML models in this project release HGF and IL-1 β , to further investigate how these cytokines affect the FA functionality of hepatocytes assays to analyse uptake and respiration were performed. First primary hepatocytes isolated and pooled from 2 C57Bl/6 mice were treated with HGF (10ng/mL), IL-1 β (1ng/mL) or control media for 16hrs. In the final hour LCFA BODIPY C12 was added to the wells (1 μ M), media was removed and the cells washed before fixing and permeabilising for staining with phalloidin (1:800). The wells were then imaged (Figure 5.7A) and analysed using the same pipeline as Figure 4.19. Interestingly, analysis shows that HGF treatment significantly reduced the uptake of LCFA BODIPY C12 by hepatocytes (Figure 5.7B) however, treatment with IL-1 β did not have the same affect, showing no significant difference when compared with control treated cells (Figure 5.7C). These data suggest that it is predominantly HGF released by AML which is acting on the liver to reduce FA uptake, thus increasing serum FFA.

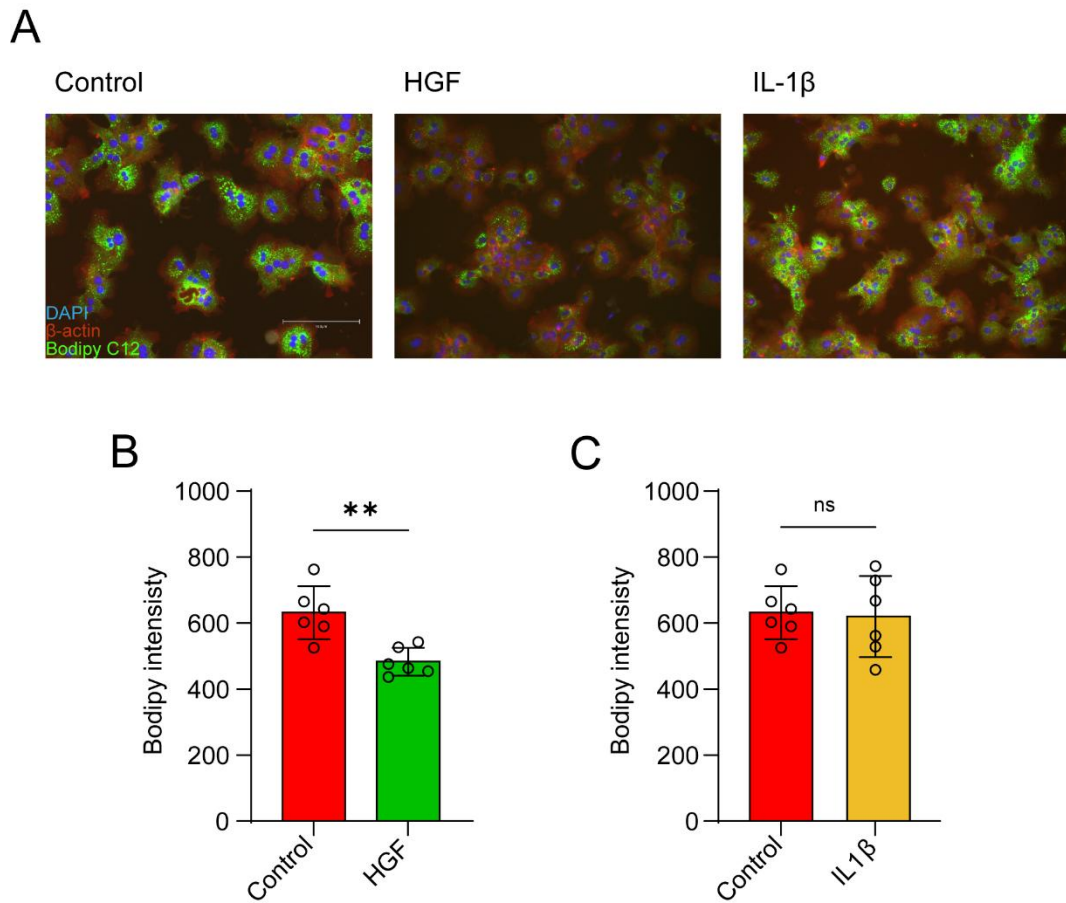


Figure 5.7 Stimulation with HGF reduced LCFA BODIPY C12 uptake in primary hepatocytes.

A) Representative images of primary murine hepatocytes were pre-treated for 16hrs with IL-1 β (1ng/mL), HGF (10ng/mL), or control media (n=6). LCFA BODIPY C12 (green) was added for 1hr, followed by fixing and further staining with DAPI (blue), and β -actin (red). LCFA BODIPY C12 fluorescence intensity was analysed for B) HGF and C) IL-1 β treated cells compared to controls. Data are expressed as mean \pm SD. Statistical significance was calculated using Mann-Whitney U test. ** p < 0.001, and ns = non-significant.

The last experiment showed that HGF reduced FA uptake in primary hepatocytes and so was further used to stimulate primary hepatocytes to investigate changes in respiration. Seahorse metabolic flux mitostress kit showed that HGF treatment for 16hrs (10ng/mL) reduced OCR, in comparison to control treatment, of primary hepatocytes in seahorse base media with palmitic acid as a replacement for glucose (Figure 5.8A). Analysis of the data showed that HGF significantly reduced both basal (Figure 5.8B) and maximal (Figure 5.8C) respiration of the primary hepatocytes. These data show that HGF can reduce hepatocyte capacity for uptake and use of FA, in keeping with what was seen in AML treatment.

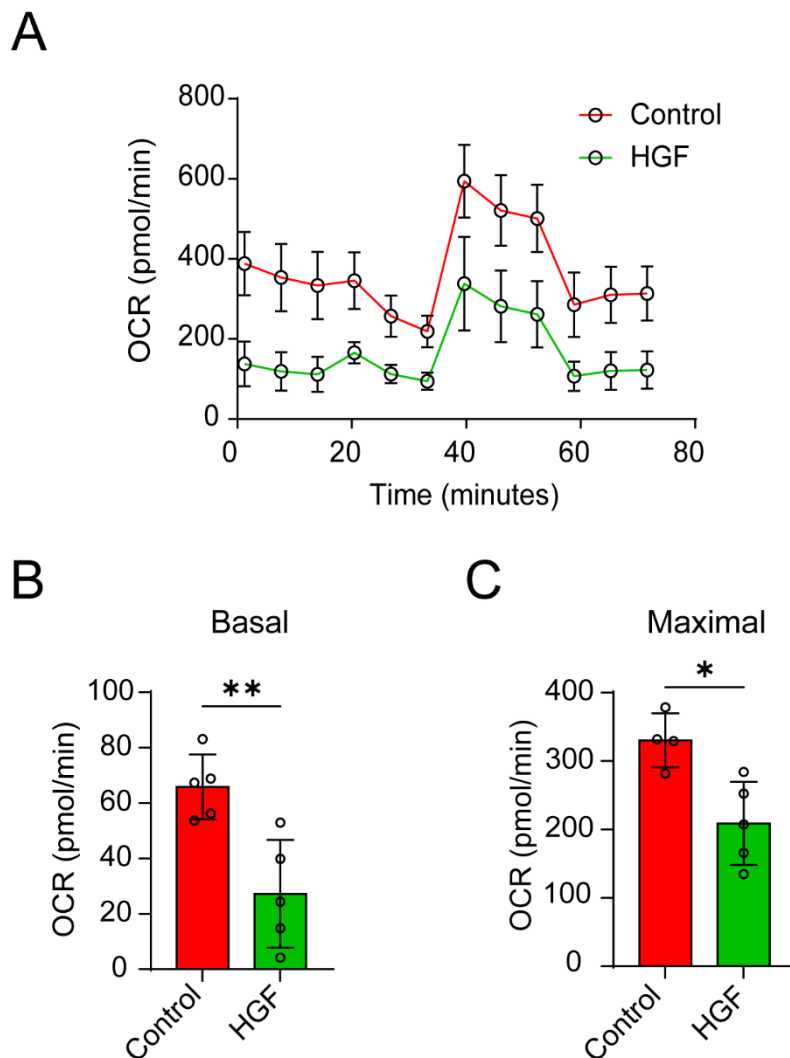


Figure 5.8 HGF stimulation reduced OCR in primary hepatocytes.

A) Seahorse metabolic flux mitostress kit analysis of primary hepatocytes treated for 16hrs with HGF (n= 5) control treated hepatocytes (n=5). B) Basal and C) Maximal respiration were calculated from plots. Data are expressed as mean \pm SD. Statistical significance was calculated using Mann-Whitney test. * $p < 0.05$, ** $p < 0.01$.

After performing experiments which suggest that both HGF and IL-1 β can inhibit different mechanisms of liver FA metabolism it was important to confirm that they are present in the serum of mice with AML. This is important as Figure 5.1 is only one replicate and therefore could be an outlier. Therefore, serum was isolated from blood taken at sacrifice from C57Bl/6 mice engrafted with MN1 or HOXA9/MEIS1 cells (1×10^6) at the time point where they first showed signs of illness, or control mice. Samples were frozen at -20°C until analysis could be performed. R&D Elisa assay kits showed that HGF was significantly elevated in the serum of mice engrafted with AML when compared to control serum (Figure 5.9A). However, analysis for the IL-1 β levels in the serum showed a large spread in the data for each condition and thus no significant difference with the levels present (Figure 5.9B). This is interesting as the half-life of HGF is much shorter than IL-1 β , at ~ 4 minutes and ~ 21 minutes respectively (403, 404). This suggests that HGF is produced in higher quantities and more consistently than IL-1 β . However, the detectable limit of the IL-1 β ELISA maybe the problem.

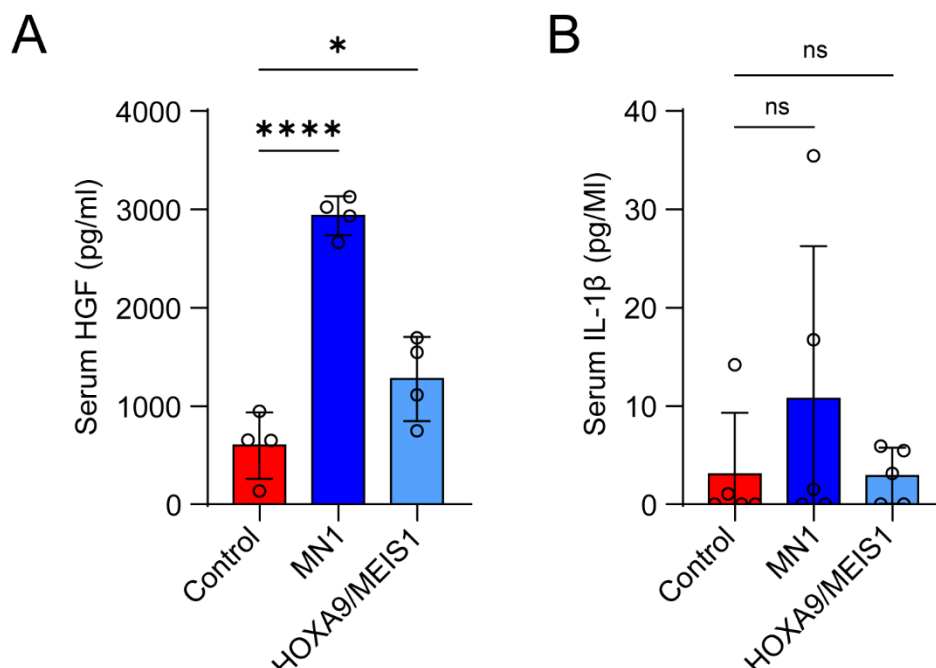


Figure 5.9 Serum HGF is significantly increased in mice engrafted with AML

Serum was isolated at sacrifice from mice engrafted with MN1 cells or HOXA9/MEIS1 cells (1×10^6) as they showed first signs of illness. Serum from mice was used to perform Elisa for A) HGF and B) IL-1 β and compared against control mouse serum ($n=4$). Data are expressed as mean \pm SD. Statistical significance was calculated using Mann-Whitney U test. * $p < 0.05$, **** $p < 0.0001$, and ns = non-significant.

Finally, to ensure that the findings are clinically relevant serum HGF levels were tested in human serum samples kindly given by patients with confirmed AML and control patients. Blood was collected from patients at the Norfolk and Norwich University Hospital by Dr Charlotte Hellmich, and the serum isolate by me. Serum was stored at -20°C until there were 7 replicates for both groups. Analysis of an Elisa assay kit shows that some AML patients had elevated HGF in their serum (Figure 5.10).

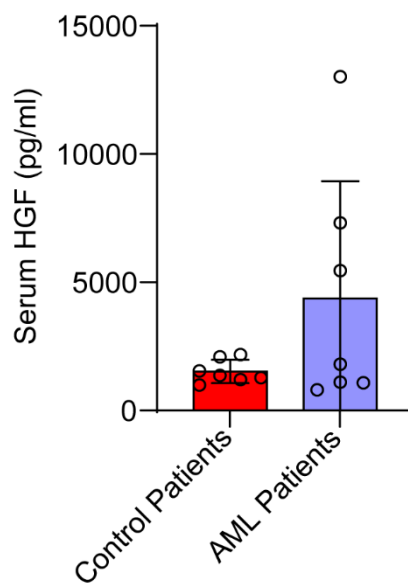


Figure 5.10 HGF is elevated in the serum of some AML patients.

Serum was isolated from patient with confirmed AML diagnosis and control patients. Serum levels of HGF was quantified using ELISA Data are expressed as mean \pm SD. Statistical significance was calculated using Mann-Whitney U test. ns = non-significant.

Table 5.1 outlines the sex, age, HGF serum levels, blast levels and confirmed mutation for the patient samples. This is a small cohort and therefore nothing conclusive can be drawn from it. Only 3 of the cohort are female, the average age of the AML patients is 70.71 years, whereas the control cohort has an average of over 10 years younger at 59.71 years. There is no correlation between the highest blast percentage and serum HGF levels. It is of interest that 2 of the samples with the highest HGF levels have tp53 mutations, while the sample with the highest serum HGF is of unknown mutation. As previously stated, this is too small a cohort to draw conclusions but shows that some human AML patients have elevated serum HGF.

Table 5.1 Patient details for collected samples.

Confirmed AML and control patients, at the Norfolk and Norwich University Hospital, consented to donate blood samples for research purposes. Presented is the patient; age, sex, confirmed mutation, % blasts in BM samples, and serum HGF levels.

Number	Age	Sex	Confirmed mutation	Blasts present (%)	Serum HGF (pg/mL)
AML 1	77	M	<i>CEBPA, IDH2, SRSF2</i>	15	1807.253
AML 2	63	M	<i>TP53</i>	68	7314.36
AML 3	73	M	<i>TP53</i>	80	5457.238
AML 4	57	F	<i>Trisomy 8 and FLT3, TKD</i>	88	811.8028
AML 5	80	M	not specified	70	13016.34
AML 6	60	M	<i>DDX41</i>	66	1112.018
AML 7	85	M	not specified	48	1080.944
Control 1	82	M	N/A	N/A	1281.614
Control 2	61	M	N/A	N/A	996.4099
Control 3	66	F	N/A	N/A	1201.82
Control 4	47	M	N/A	N/A	2095.356
Control 5	45	M	N/A	N/A	2183.05
Control 6	40	M	N/A	N/A	1541.537
Control 7	77	F	N/A	N/A	1362.988

5.4 *In vivo* stimulation with HGF or IL-1 β downregulates FA metabolism genes in mouse livers.

After confirming *in vitro* that both HGF and IL-1 β down regulate gene at different stages of FA metabolism in primary hepatocytes, the next step was to test this *in vivo*. This shows whether the cytokines found in the serum have an effect in the whole system or whether there are compensatory measures to respond to excess stimulation. To achieve this C57Bl/6 received an IP injection of HGF (0.1mg/kg), IL-1 β (0.025mg/kg), or vehicle control (PBS) at 6 or 3hrs before sacrifice. Livers were isolated from the mice for RNA extraction (Figure 5.11A). RT-qPCR of the isolated liver RNA for *Cpt1a*, *Acadm*, *Hmgcs2*, and *Fatp2* showed no significant difference at either 6 or 3 hours of HGF (Figure 5.11B) or IL-1 β (Figure 5.11C) stimulation when compared to the livers from mice which received the vehicle control. The low n number may account partially for this as there is a wide range of fold change for some of the genes and it also reduces the power of statistical analysis.

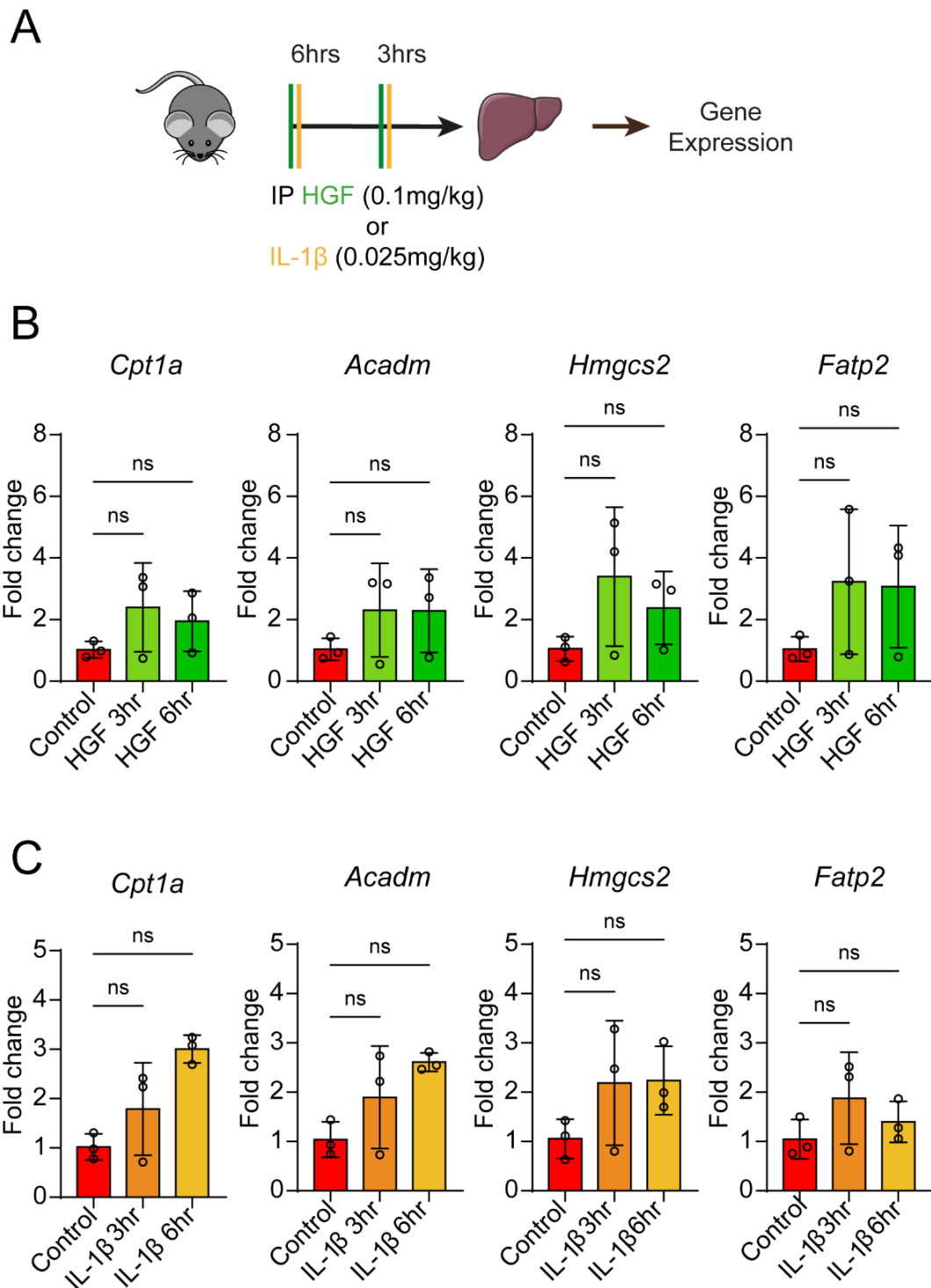


Figure 5.11 Mice stimulated with HGF and IL-1 β did not have altered liver FA metabolism genes.

A) Schematic of experimental design. C57Bl/6 mice received intraperitoneal injections of B) HGF (0.1mg/kg) or C) IL-1 β (0.025mg/kg) for 6hrs or 3 hrs prior to sacrifice. Whole liver RNA lysates were analysed for gene expression of *Cpt1a*, *Acadm*, *Hmgcs2*, and *Fatp2*. Data are expressed as mean \pm SD. Statistical significance was calculated using Kruskal-Wallis H test with Tukey's multiple comparison test ns = non-significant.

One reason the previous experiment may not have garnered the results expected may have been the duration with which the cytokine treatments were left for. The half-lives of both cytokines are relatively short (395, 405), and the amount of both HGF and IL-1 β suggest a more continuous and consistent release of them into the serum, which is not well represented by one acute dose. To mimic a more sustained production of the cytokines C57Bl/6 mice were IP injected every hour for 6hrs with HGF (0.1mg/kg) or vehicle control. Mice were sacrificed 15 minutes after the final injection. The same was initially planned for IL-1 β dosing (0.025mg/kg) however this was not well tolerated by the mice and so they received 2 IP injections an hour apart and sacrificed after a further 4.25 hours with the other treatment groups. This reaction is likely to have been caused by the inflammatory response that IL-1 β can cause. RNA was isolated from the livers of these mice for gene expression analysis (Figure 5.12A). Figure 5.12B shows that gene expression of *Cpt1a*, *Acadm*, *Hmgcs2*, and *Fatp2* is significantly reduced in the mice treated with sustained HGF treatment. The dual treatment doses of IL-1 β caused a significant reduction in expression of *Acadm*, *Hmgcs2*, and *Fatp2* but not *Cpt1a* (Figure 5.12C). These data show that both HGF and IL-1 β do downregulate liver FA metabolism genes during sustained dosing.

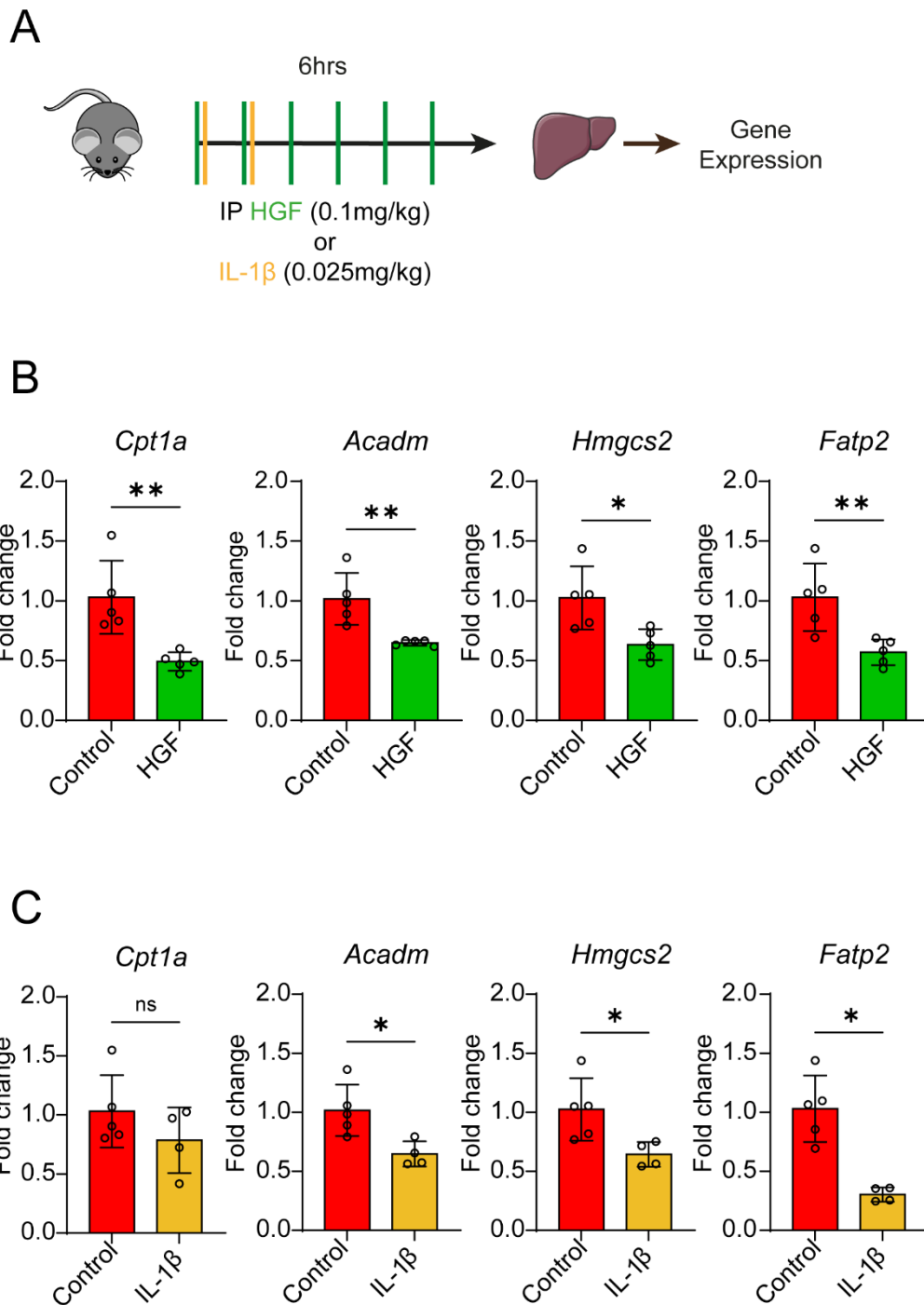


Figure 5.12 Repeated stimulation of HGF and IL-1 β downregulated FA metabolism genes in mouse livers.

A) Schematic of experimental design. C57Bl/6 mice received repeated intraperitoneal injections of cytokines and were sacrificed at 6hrs followed by analysis of whole liver RNA lysates for gene expression of *Cpt1a*, *Acadm*, *Hmgcs2*, and *Fatp2*. B) HGF (0.1mg/kg) was injected every hour for 6hrs. C) IL-1 β (0.025mg/kg) was injected at hour 0 and 1 prior to sacrifice at hour 6. Data are expressed as mean \pm SD. Statistical significance was calculated with Mann-Whitney test. * $p < 0.05$, ** $p < 0.01$, and ns = non-significant.

5.5 AML HGF KD rescues liver FA metabolism *in vivo*.

Both *in vivo* and *in vitro* data showed that HGF acts on the liver to down regulate genes at different stages of FA metabolism, reduce FA uptake, and reduce the use of FA for respiration by hepatocytes. Figure 5.9 confirms that the AML models used in this project release HGF. The next step was to investigate whether inhibiting the serum HGF would rescue the liver FA metabolism. For this, C57Bl/6 mice were injected with MN1 cells (1×10^6). 14 days post IV injection mice received OG Crizotinib or vehicle control and were monitored for a further 24hrs before sacrifice. The livers of the mice were isolated for gene expression analysis (Figure 5.13A). RT-qPCR for *Cpt1a*, *Acadm*, *Hmgcs2*, and *Fatp2* showed downregulation between controls and MN1 engrafted mice, as expected. There was no significant difference between control mice and mice which received crizotinib only, although there was a downward trend in expression of *Hmgcs2*, and *Fatp2* which was unexpected. There was no restorative effect of Crizotinib treatment with MN1 engraftment. When compared to the gene expression of liver from MN1 engrafted mice, the Crizotinib treatment made no significant difference and left the mice with significantly reduced expression of *Acadm*, *Hmgcs2*, and *Fatp2* when compared with controls (Figure 5.13B). These data suggest that Crizotinib inhibition of HGF was not sufficient to rescue the alterations of FA metabolism caused by HGF released by AML.

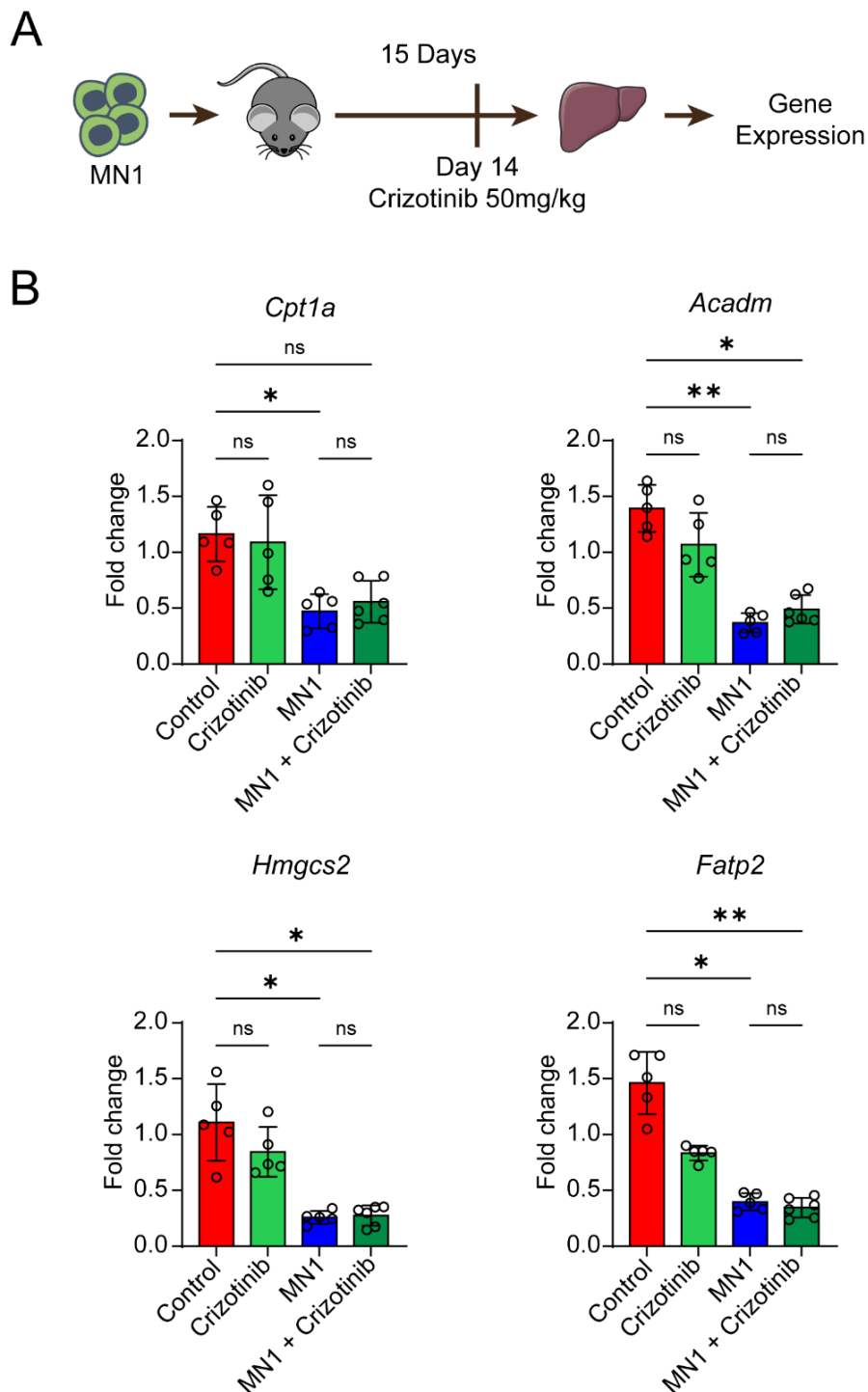


Figure 5.13 Crizotinib treatment did not restore mouse liver FA metabolism.

A) Schematic of experimental design. C57Bl/6 mice were injected with MN1 cells (1×10^6) and monitored for 14 days. Mice received OG of crizotinib (50mg/kg) or vehicle control and monitored for 24 hrs. Livers were isolated for further analysis. B) Gene expression of *Cpt1a*, *Acadm*, *Hmgcs2*, and *Fatp2* for control mice (n=5), crizotinib (n=5), MN1 engrafted mice (n=5), and MN1 engrafted mice with crizotinib (n=6). Data are expressed as mean \pm SD. Statistical significance was calculated using Kruskal-Wallis H test with Tukey's multiple comparison test. * p < 0.05, ** p < 0.01, and ns = non-significant.

Next, rather than inhibiting HGF the aim was to KD the production of HGF by AML cells. MN1 cells were cultured with shHGF or shCon lentivirus (as described in methods) to create MN1^{+FF HGF KD} or MN1^{+FF con KD} cell lines (Figure 5.14). It should be noted that these MN1 cells still have the GFP tag and the FF tag. RT-qPCR of these cells show that a significant reduction of *Hgf* mRNA was achieved, resulting in around 40% KD (Figure 5.14B). The aim of the next *in vivo* experiment was to see whether HGF KD would reduce the uptake of FA by the tumour. This was achieved with the FF tag and the use of FFA tagged with luciferin (FFA-SS-Luci). C57Bl/6 mice were IV injected with MN1^{+FF HGF KD} or MN1^{+FF con KD} cells (1x10⁶). On day 15 mice received an IV injection of FFA-SS-Luci (3mg/kg) and were left for 15minutes before live *in vivo* imaging. While anaesthetised mice received an IP injection of D-luciferin salt (150mg/kg) and left for 5 minutes before repeating live *in vivo* imaging, to confirm engraftment, followed by sacrifice. Livers were isolated for further analysis (Figure 5.14C).

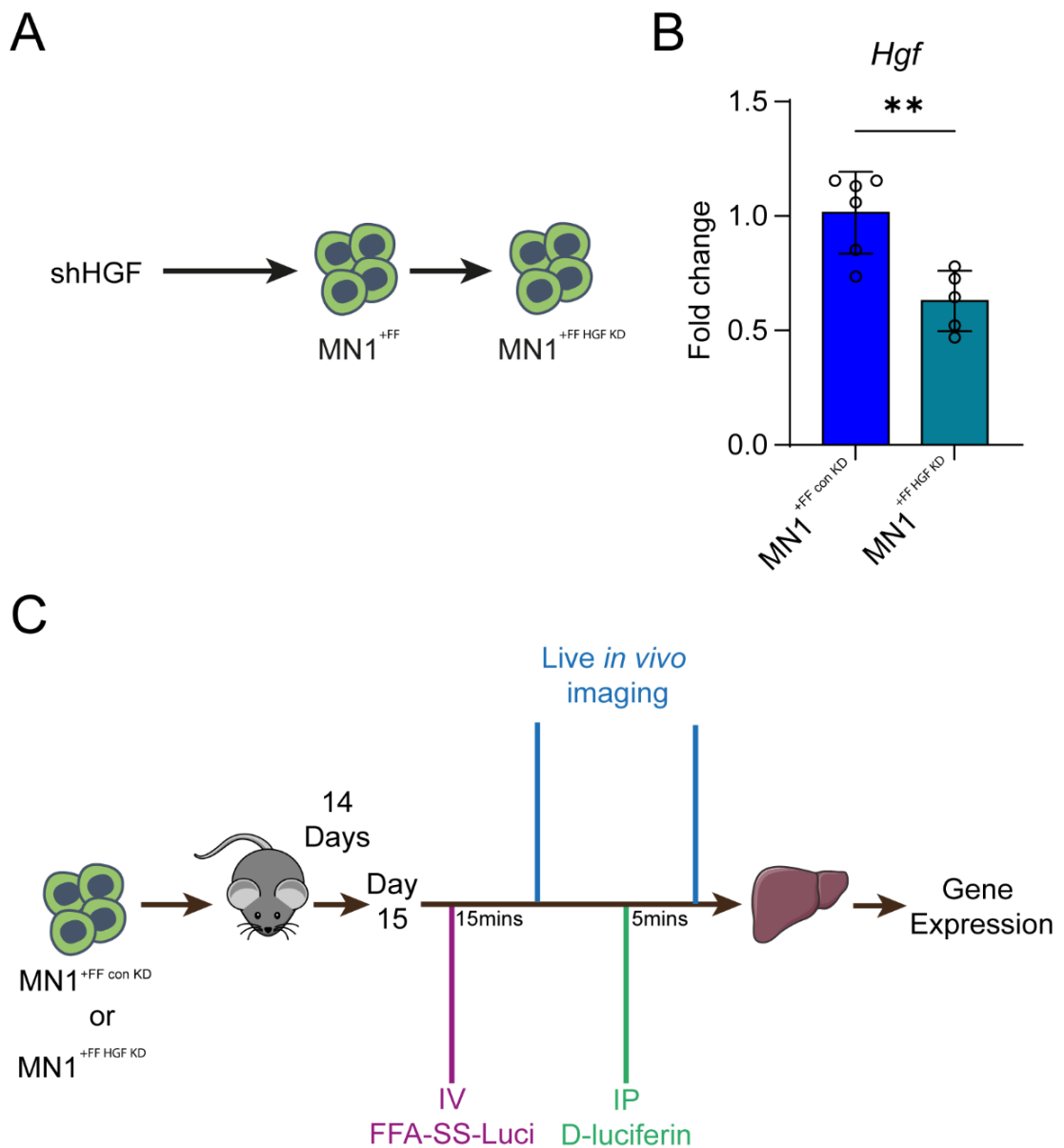


Figure 5.14 HGF KD was used to assess alterations in tumoural FA uptake.

A) Schematic of experimental design. MN1^{+FF} cells were cultured with shHGF lentivirus to obtain KD of HGF (MN1^{+FF KD HGF}). B) Gene expression *Hgf* for MN1^{+FF KD HGF} vs for MN1^{+FF con HGF} (n=5). C) schematic of experimental design using HGF KD. Mice were engrafted with MN1^{+FF KD HGF} vs for MN1^{+FF con HGF} cells (1x10⁶) and monitored for 14days. Mice were intravenously injected with LCFA conjugated luciferin and left for 15minutes prior to live *in vivo* imaging for FA uptake by the tumour. While anaesthetised mice received an intraperitoneal injection of D-luciferin and *in vivo* live imaging was performed after 5 minutes to confirm engraftment prior to sacrifice Data are expressed as mean ± SD. Statistical significance was calculated using Mann-Whitney U test. ** p < 0.01.

It would have been desirable to investigate if HGF KD in engrafted AML cells resulted in increased FA uptake in the livers of engrafted mice. Unfortunately, this was outside of the scope of this project. The designed experiment investigates the inverse, whether KD of HGF in the blasts subsequently reduces the blasts uptake of FA. First the live *in vivo* images after the IP injection of D-luciferin and flow cytometry for the GFP⁺ cells in the BM confirm that there was no significant difference in the engraftment of MN1^{+FF HGF KD} or MN1^{+FF con KD} cells (Figure 5.15A+B). This allowed for direct comparisons between the treatment groups. Analysis of the live *in vivo* images (Figure 5.15C), taken after IV injection with FFA-SS-Luci, shows that mice engrafted with MN1^{+FF HGF KD} had significantly reduced FA uptake in comparison to MN1^{+FF con KD} engrafted mice (Figure 5.15D). This shows reduced FA uptake by the tumour and suggests that reduced HGF reduces the available FA for the AML cells to utilise.

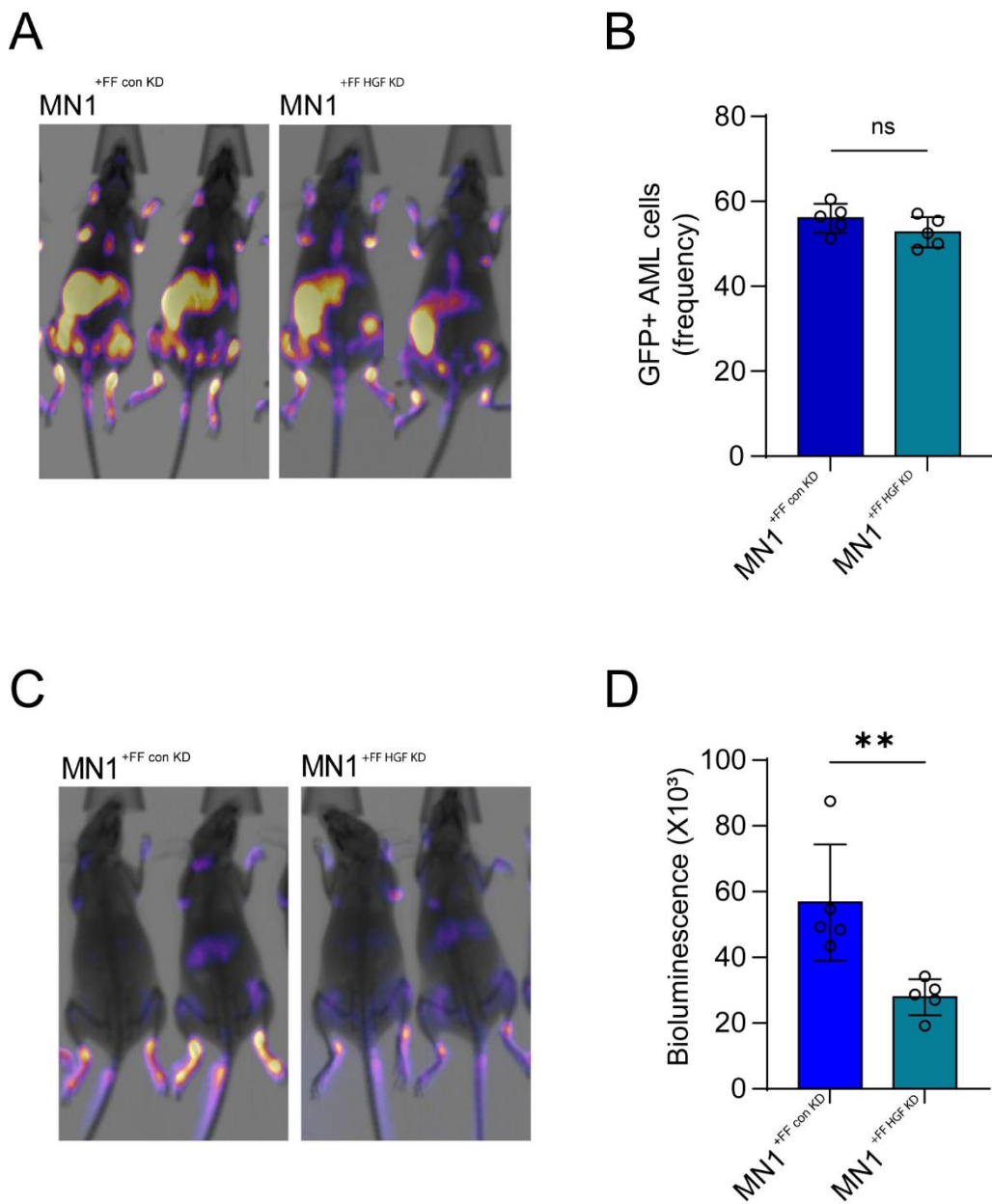


Figure 5.15 HGF KD reduced tumoural LCFA uptake.

A) Representative images of live *in vivo* imaging of mice engrafted with MN1+FF KD HGF (n=6) vs for MN1+FF con HGF (n=6) cells (1×10^6) after IP injection with D-luciferin. B) Engraftment was further confirmed using flow cytometry C) Representative images of live *in vivo* imaging of mice engrafted with MN1+FF KD HGF (n=6) vs for MN1+FF con HGF (n=6) cells (1×10^6) after IV injection with LCFA conjugated luciferin. D) LCFA uptake was quantified from bioluminescence images using Fiji ImageJ. Data are expressed as mean \pm SD. Statistical significance was calculated using Mann-Whitney U test. ** p < 0.01, and ns = non-significant.

Livers from mice engrafted with MN1^{+FF HGF KD} or MN1^{+FF con KD} cells and control mice were isolated at sacrifice and extracted RNA was used to perform RT-qPCR for *Cpt1a*, *Acadm*, *Hmgcs2*, and *Fatp2*. Results show that HGF KD in engrafted MN1 cells has a positive effect on the liver gene expression of *Cpt1a*, and *Fatp2* where gene expression is significantly higher in the liver of mice engrafted with MN1^{+FF HGF KD} cells when compared to the livers of mice engrafted with MN1^{+FF con KD} cells. However, for *Cpt1a* the gene expression is still significantly lower than what is seen in control mouse livers. Interestingly, although engraftment of MN1^{+FF HGF KD} cells did not significantly increase expression of *Acadm* or *Hmgcs2*, in comparison to MN1^{+FF con KD} engraftment, the liver gene expression in these mice is not significantly lower than the expression of *Acadm*, and *Hmgcs2* in control mouse livers (Figure 5.16) The data from this *in vivo* KD experiment show that that HGF-KD in AML cells engrafted into mice improves liver FA metabolism gene expression. Furthermore, the tumour in these mice has reduced FA uptake. This suggests that improved liver FA metabolism reduces available FA for AML blasts in the BM to utilise for survival and proliferation.

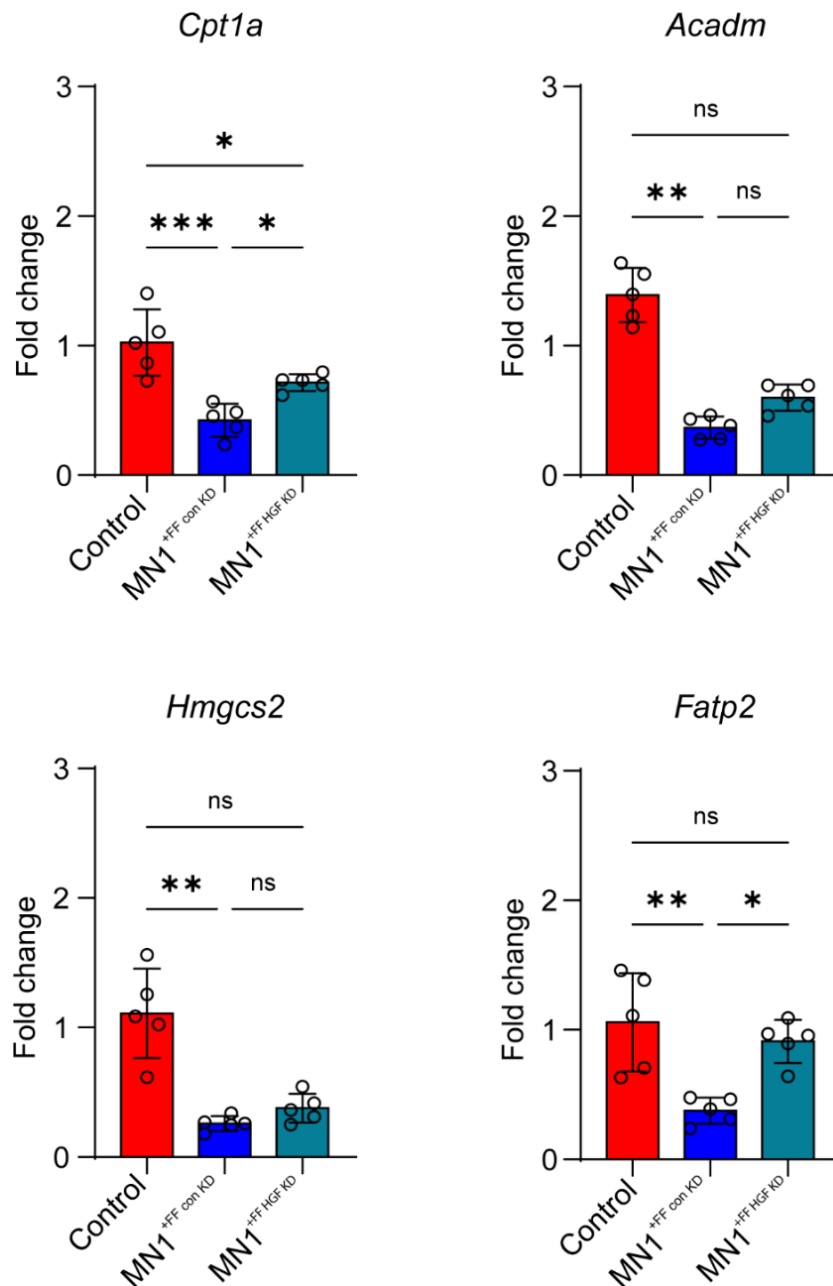


Figure 5.16 HGF KD partially rescued liver FA metabolism gene expression.

Gene expression of whole liver lysates from mice engrafted with MN1^{+FF} KD HGF (n=6), MN1^{+FF} con HGF (n=6) cells (1x10⁶), and control mice (n=6) for *Cpt1a*, *Acadm*, *Hmgcs2*, and *Fatp2*. Data are expressed as mean \pm SD. Statistical significance was calculated using Kruskal-Wallis H test with Tukey's multiple comparison test. * p < 0.05, ** p < 0.01, *** p < 0.001, **** p < 0.0001, and ns = non-significant.

5.6 AML secreted HGF acts on PPAR α to reduce liver FA metabolism.

The final aim of this project was to investigate the mechanism by which AML secreted HGF acts on the liver to inhibit FA metabolism. Kegg enrichment pathway analysis of the RNAseq for livers of AML engrafted mice, highlighted PPAR pathways as significantly downregulated. PPARs are transcription factors which act on genes involved in pathways such as proliferation, migration, and FA metabolism. One of the main groups of activators is FA, creating a positive feedback loop (223). The predominant PPAR found in the liver is PPAR α , and it is a transcription factor for genes such as *Cpt1a* and *Fatp2* (314). HGF has been shown to inhibit lipid accumulation and cholesterol overload in a number of cell types, including hepatocytes (406-409), and has been used to aid with treatments for insulin resistance as it can upregulate glucose transport proteins (410, 411).

Little research has been done to connect these pathways in the context of FA metabolism and therefore the first experiments aimed to investigate whether HGF secreted by AML or recombinant murine HGF significantly reduced *Ppara* expression in the liver. To test this *in vivo* the previous models were used. Mice engrafted with MN1 or HOXA9/MEIS1 cells were monitored until the first signs of illness, at which point they were sacrificed and their livers isolated (Figure 5.17A). RT-qPCR of the extracted DNA shows significantly reduced *Ppara* for both MN1 or HOXA9/MEIS1 engrafted mice in comparison to controls (Figure 5.17B). Mice that received sustained HGF IP injections (6x0.01mg/kg) also had significantly reduced liver *Ppara* expression when compared with controls (Figure 5.17C+D). The third model utilised the MN1^{+FF} HGF^{KD} and MN1^{+FF} con^{KD} cells to test whether KD of HGF in the AML cells could restore liver *Ppara* expression. Although expression was still significantly lower than control mice, MN1^{+FF} HGF^{KD} engrafted mice had significantly higher *Ppara* expression than MN1^{+FF} con^{KD} engrafted mice (Figure 5.17E+F).

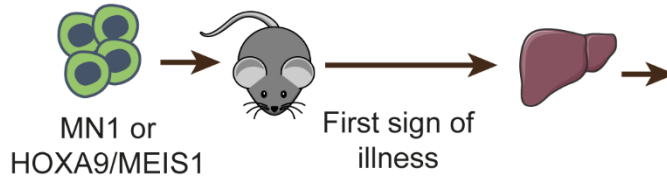
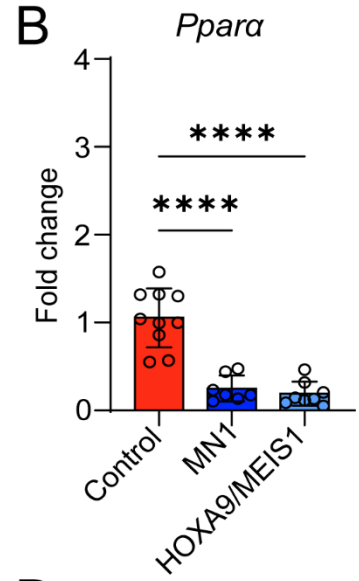
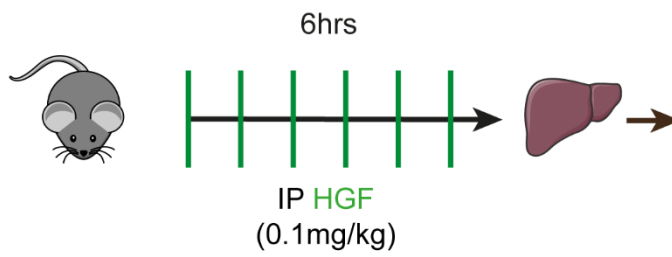
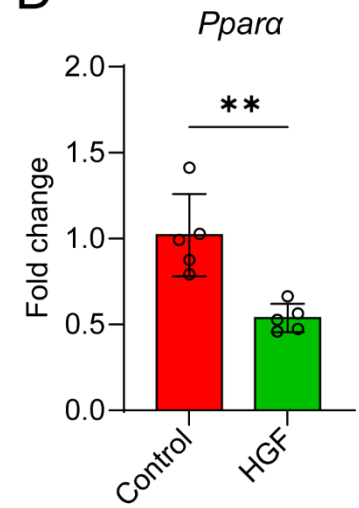
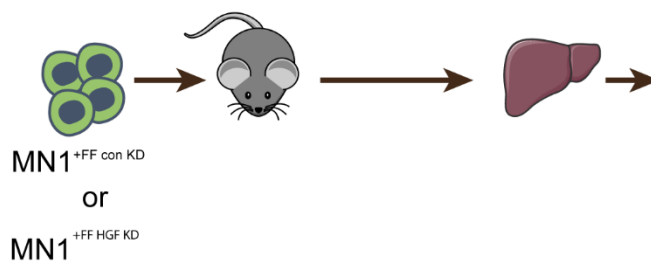
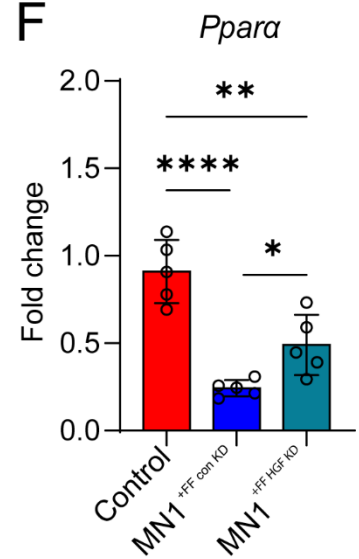
A**B****C****D****E****F**

Figure 5.17 *Ppara* expression is downregulated by AML and HGF *in vivo*.

A) Mice were engrafted with MN1 (n=7) or HOXA9/MIES1 (n=8) cells (1×10^6) and monitored until the individual first sign of illness. B) liver *Ppara* expression was analysed and compared with controls (n=10). C) Mice received IP injections of HGF (0.1mg/kg) or vehicle control every hour for 6 hours (n=5). D) *Ppara* gene expression of whole liver lysates E) mice were engrafted with MN1^{+FF KD HGF} or MN1^{+FF con HGF} cells (1×10^6 , n=6). E) Gene expression for *Ppara* was further compared with control mice (n=6). Data are expressed as mean \pm SD. Statistical significance was calculated using Kruskal-Wallis H test with Tukey's multiple comparison test or Mann-Whitney U test. * p < 0.05, ** p < 0.01, and **** p < 0.0001.

Next, down regulation of *Ppara* expression was confirmed *in vitro* using primary murine hepatocytes. Cells were cultured with recombinant HGF or AML conditioned media for 16hrs, followed by RNA extraction (Figure 5.18A). RT-qPCR confirmed that hepatocyte *Ppara* was significantly reduced by AML conditioned medias, in comparison to control media (Figure 5.18B). Expression was also significantly reduced in primary hepatocytes treated with HGF when compared with control hepatocytes (Figure 5.18C). The data from these experiments confirm that *Ppara* RNA expression is inhibited *in vivo* and *in vitro* by AML secreted cytokines, of which HGF has been shown to be a major contributor. This effect can be moderately rescued by the *Hgf*-KD in MN1 AML cells, thus providing another potential target for inhibiting the effect of AML secreted HGF on the liver.

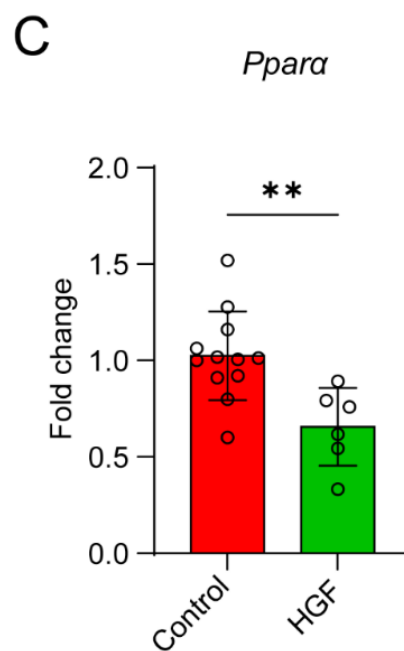
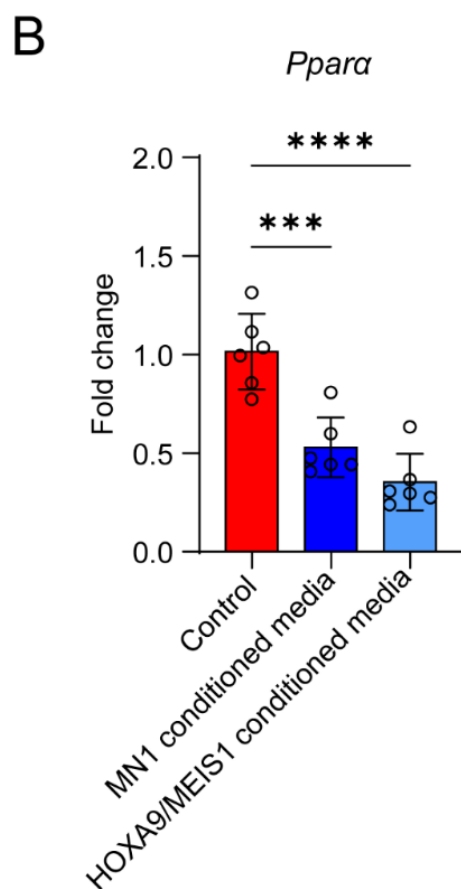
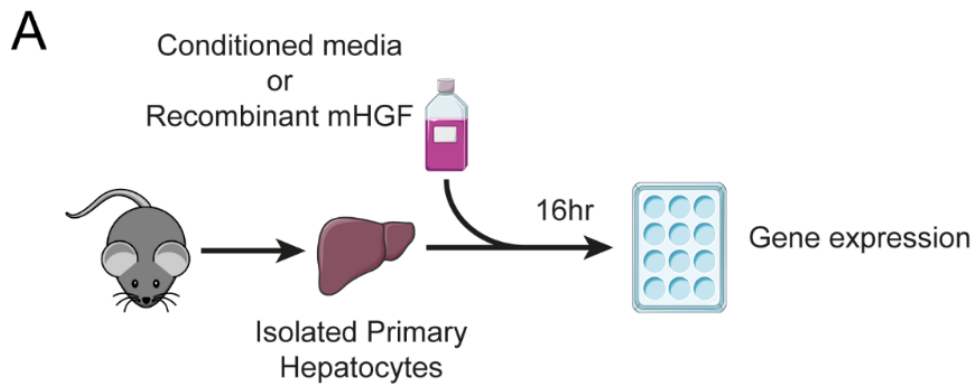


Figure 5.18 *Ppara* downregulated in primary hepatocytes by AML conditioned media and recombinant HGF.

A) Schematic of experiments. Primary hepatocytes isolated from C57Bl/6 mice were pretreated for 16hrs with B) MN1, HOXA9/MIES1 conditioned media, or control media (n=6) followed by analysis of gene expression for *Ppara*. C) *Ppara* gene expression of primary hepatocyte pretreated for 16hrs with HGF (10ng/mL). Data are expressed as mean \pm SD. Statistical significance was calculated using Kruskal-Wallis H test with Tukey's multiple comparison test or Mann-Whitney U test. ** p < 0.01, and **** p < 0.0001.

5.7 PPAR α agonism impairs AML progression by rescuing liver FA metabolism.

The previous experiments have shown us that HGF inhibits *Ppara* expression in vitro, HGF inhibitors are not readily available and genetic manipulation is both expensive and difficult to develop due to the need for it to be targeted. Conversely there are a number of PPAR agonists already used in treatments (412). One of these is the fenofibrate, which is PPAR α specific. As a readily available drug it was used to investigate whether agonism of PPAR α ameliorates the effect of AML secreted HGF. This was firstly tested in vitro, primary murine hepatocytes culture plates were set up with control media, fenofibrate (10 μ M), MN1 or HOXA9/MEIS1 conditioned media, or recombinant HGF (10ng/mL), and combinations of fenofibrate with these treatments. RT-qPCR data shows that PPAR α agonism rescues the expression of *Cpt1a*, *Acadm*, and *Hmgcs2* when fenofibrate is added to MN1 conditioned media treatment on primary hepatocytes (Figure 5.19A). Fenofibrate in combination with HOXA9/MEIS1 conditioned media only significantly improved the expression of *Hmgcs2*, although there is an upward trend for the expression of *Cpt1a* (Figure 5.19B). Similar to the combination with MN1 conditioned media, fenofibrate rescued the expression of *Cpt1a*, *Acadm*, and *Hmgcs2* in primary hepatocytes treated with HGF (Figure 5.19C). It is of interest that fenofibrate alone only upregulated expression of *Acadm* and *Hmgcs2*. This may be due to the duration of the experiment. Both *Acadm* and *Hmgcs2* are expressed within the mitochondria of cells and are involved in latter stages of FA metabolism, whereas *Fatp2* and *Cpt1a* are involved in the uptake and transport of FA. Another reason may be that the primary hepatocytes treated with fenofibrate have had no stress stimuli and therefore are likely to have sufficient LD. Thus, feedback loops may induce downregulation of *Fatp2* and *Cpt1a* to prevent further uptake and toxicity that FA accumulation can cause. These data are promising in showing that PPAR α agonism could be used to restore liver FA metabolism to impede AML progression.

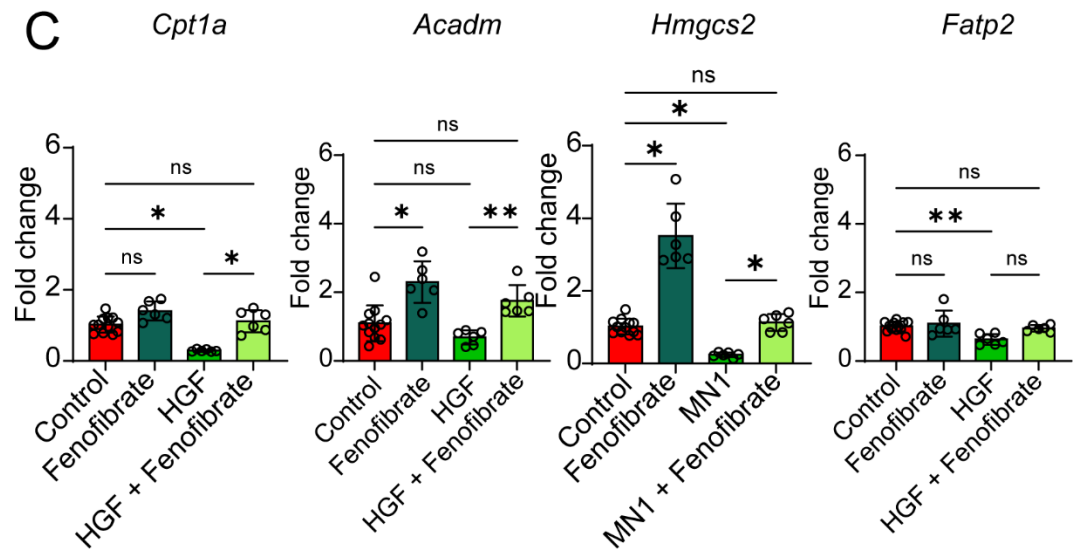
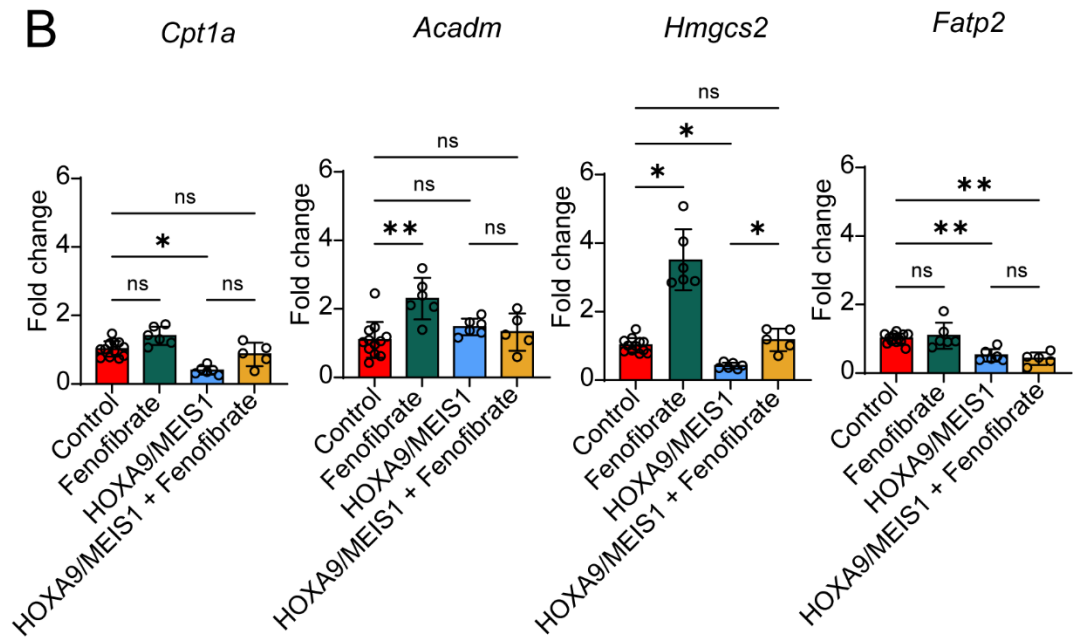
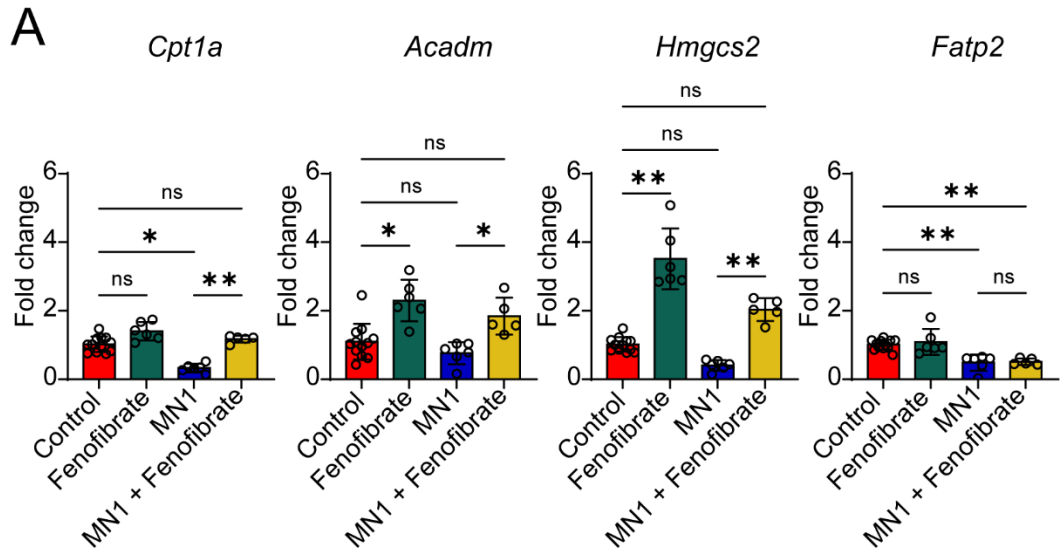


Figure 5.19 Agonism of *Ppara* rescues some FA metabolism gene expression in primary hepatocytes stimulated with AML conditioned media or HGF.

Gene expression of *Cpt1a*, *Acadm*, *Hmgcs2*, and *Fatp2*. A) Primary murine hepatocytes were treated for 16hrs with control media (n = 12), fenofibrate (10 μ M/mL), MN1 conditioned media, or in combination (n = 6). B) Primary murine hepatocytes were treated for 16hrs with control media (n = 12), fenofibrate (10 μ M/mL), HOXA9/MIES1 conditioned media, or in combination (n = 6). C) Primary murine hepatocytes were treated for 16hrs with control media (n = 12), fenofibrate (10 μ M/mL), HGF (10ng/mL), or in combination (n = 6). Data are expressed as mean \pm SD. Statistical significance was calculated using or Kruskal-Wallis H test with Tukey's multiple comparison test. * p < 0.05, *** p < 0.001, **** p < 0.0001 and ns = non-significant.

Before any *in vivo* experiments could take place, it was important to ascertain whether fenofibrate itself was toxic to MN1 AML cells. To do this MN1 cells were cultured in rising concentrations of fenofibrate (0, 1, 10, and 50 μ M) for 24hrs. A cell viability assay confirmed that fenofibrate is non-toxic to MN1 cells (Figure 5.20). For further *in vivo* experiments this shows that any differences in engraftment, FA metabolism and gene expression is due to the actions of the drug and not because of toxicity to the AML cells.

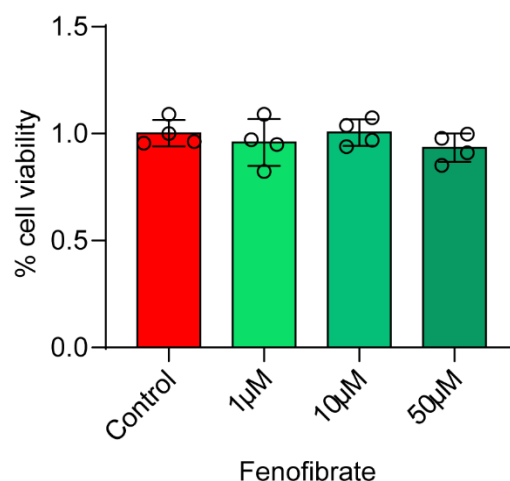


Figure 5.20 Fenofibrate is not toxic to MN1 cells.

MN1 cells were cultured for 24hrs with rising concentrations of fenofibrate (0, 1, 10, and 50 μ M). Cell titre glo assay was performed to assess viability. Data are expressed as mean \pm SD. Statistical significance was calculated using or Kruskal-Wallis H test with Tukey's multiple comparison test.

Next, C57Bl/6 mice were injected with MN1 cells (1×10^6) and monitored, mice were given OG fenofibrate (50mg/kg) or vehicle control for 7 days and sacrificed 24hrs following the final dose (Figure 5.21A). Flow cytometry of the BM for GFP⁺ MN1 cells shows that PPAR α agonism by fenofibrate treatment significantly reduced the engraftment of MN1 cells (Figure 5.21B). Flow cytometry of the GFP⁺ population was also used to assess the neutral lipid content, after incubation with lipidtox (1x). The results show that MN1 cells from mice treated with fenofibrate had less neutral lipid content than MN1 cells from mice treated with the vehicle control (Figure 5.21C). These data show that PPAR α agonism reduces AML engraftment and reduces the storage of neutral lipids, thus suggesting reduced uptake by the AML blasts.

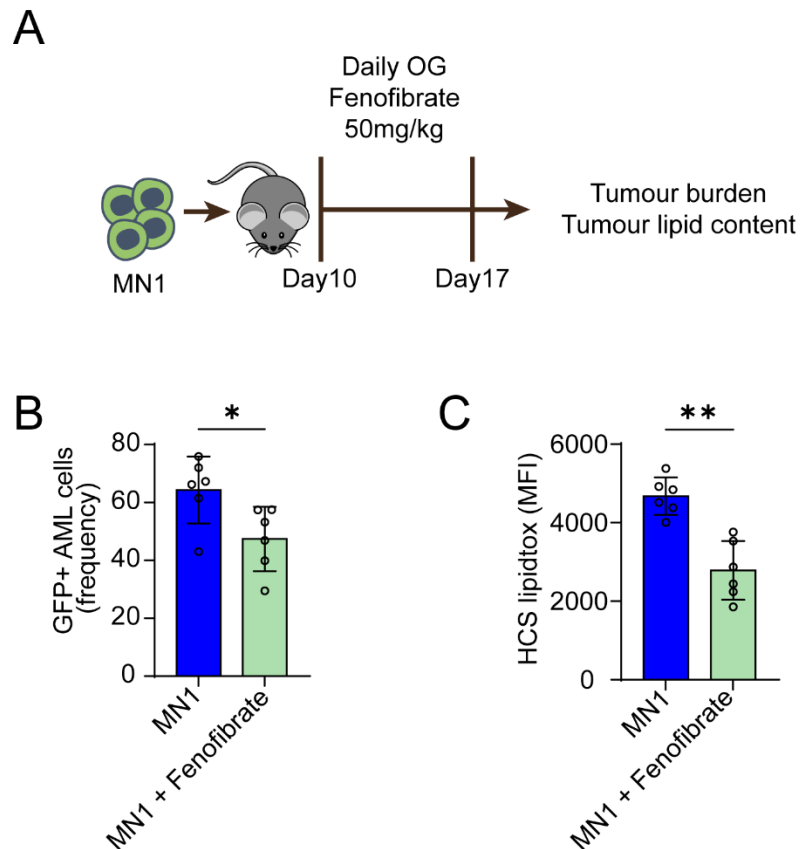


Figure 5.21 Fenofibrate treatment reduces AML engraftment and neutral lipid storage.

A) Schematic of experimental design. Mice were engrafted with MN1 cells (1×10^6) and given daily OG fenofibrate (50mg/kg) or vehicle control ($n=6$) for 7 days from day 10. Mice were sacrificed 24hrs after the final dose. B) Flow cytometry of the BM for the GFP⁺ MN1 cells. C) Flow cytometry of the GFP⁺ BM population for HSC lipidtox (1x) neutral lipid staining (MFI). Data are expressed as mean \pm SD. Statistical significance was calculated using Mann Whitney U test. * $p < 0.05$, and ** $p < 0.01$.

To investigate whether PPAR α agonism by fenofibrate treatment had a restorative effect on the livers of mice with MN1 engraftment, livers were isolated for RNA extraction and RT-qPCR analysis for *Cpt1a*, *Fatp2*, and *Ppara*. Gene expression shows that when mice engrafted with MN1 cells were treated with fenofibrate, there was a significant increase in the expression of *Fatp2*, and *Ppara* when compared to MN1 engrafted mice treated with a vehicle control (Figure 5.22). This shows that PPAR α agonism can suppress the alterations induced by AML secreted HGF. Further analysis of the isolated livers would be valuable to ascertain whether more genes involved in the FA metabolism pathway can be rescued by PPAR α agonism during AML progression.

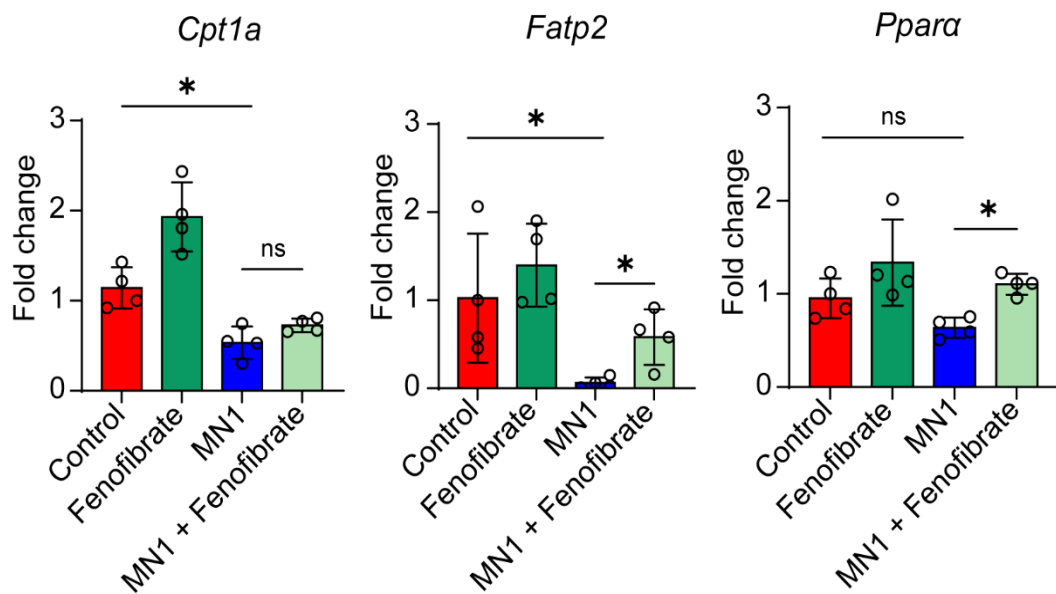


Figure 5.22 Fenofibrate treatment rescues liver FA metabolism genes.

Livers were isolated from control mice or mice engrafted with MN1 cells (1×10^6) that were given daily OG fenofibrate (50mg/kg) or vehicle control (n=4) for 7 days from day 10 post injection. RT-qPCR of extracted RNA was performed for *Cpt1a*, *Fatp2*, and *Ppara*. Data are expressed as mean \pm SD. Statistical significance was calculated using Mann Whitney U test.

* $p < 0.05$, and ns – non-significant.

Finally, serum was isolated from the mice treated with either vehicle control or fenofibrate, in the presence or absence of MN1 engraftment, upon sacrifice. The serum was analysed for LCFA using mass spectrometry. Statistical analysis of the total FFA shows that PPAR α agonism with fenofibrate significantly reduced the FFA content in MN1 engrafted mice, similar to levels seen in control mice. It is interesting to note that the composition of the serum, in regard to the LCFA that make it up, is altered by MN1 engraftment. MN1 engraftment causes C20.5 to be the most abundant LCFA in the serum, whereas in control mice have the greatest abundance of C18.2, unlike the MN1 engrafted, fenofibrate treated mice which had proportionally more C16 (Figure 5.23).

These last experiments show that the alterations to liver FA metabolism induced by AML engraftment in mice, can be restored by PPAR α agonism. Fenofibrate resulted in reduced availability of FA in the serum for AML blasts to utilise. Therefore, blasts had to metabolise their neutral lipid stores for survival, which stalled engraftment and progression. These data show a potential new target for therapeutics to slow AML progression.

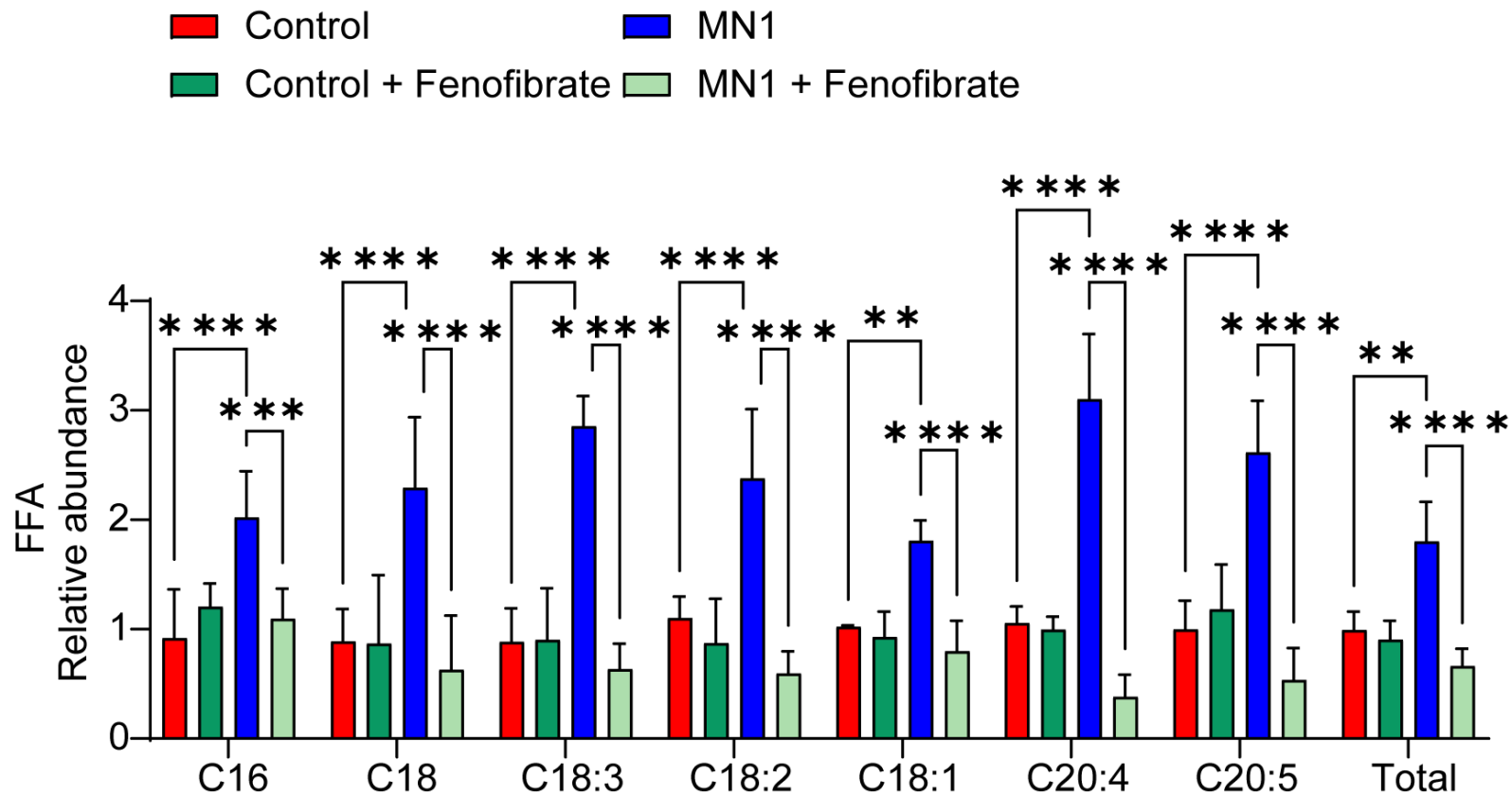


Figure 5.23 Fenofibrate treatment restored serum FFA in mice engrafted with AML.

Serum was isolated from control mice or mice engrafted with MN1 cells (1×10^6) that were given daily OG fenofibrate (50mg/kg) or vehicle control (n=4) for 7 days from day 10 post injection. Serum was analysed by mass spectrometry for different length LCFA as well as total FFA. Data are expressed as mean \pm SD. Statistical significance was calculated using Kruskal-Wallis H test with Tukey's multiple comparison test. ** p < 0.01, *** p < 0.001, and **** p < 0.0001.

5.8 Summary

In this chapter the data has established that the two models of AML used in this project secrete HGF and IL-1 β , which act on primary hepatocytes to down regulate FA metabolism genes at multiple steps of the pathways. HGF was found to reduce uptake of FA by primary hepatocytes and when given *in vivo* a sustained dose time also down regulated genes associated with FA metabolism. Further investigation is required to see whether pharmacological inhibition of HGF or IL-1 β can have a restorative effect of FA metabolism both *in vivo* and *in vitro*. The data showed that *Hgf* KD in murine AML blasts impeded tumour uptake of LCFA *in vivo* and had a restorative effect on gene expression in the liver. Together sequencing data from Chapter 4 and RT-qPCR data, of extracted livers and primary hepatocytes stimulated with AML or HGF, showed that downregulation in liver FA metabolism was associated with PPAR α . Agonism of PPAR α with fenofibrate was able to rescue gene expression in primary hepatocytes after stimulation with HGF or MN1 conditioned media and had a modest effect in the livers of MN1 engrafted mice. Moreover, fenofibrate treatment reduced serum FFA availability, resulting in AML blasts accumulating significantly less intracellular neutral lipids and stalling progression of the tumour. These data identify that although AML is a BM malignancy, benefit can be drawn from looking at other organs of the body. Further research into improving liver FA metabolism may lead to new combination treatments for improvements to quality of life and prognosis.

6. Discussion

6.1 General discussion

AML is a fatal haematological malignancy which remains incurable despite decades of research and improvements to treatments. The current treatments utilise intensive chemotherapy regimens and stem cell allografts (161). This removes the majority of the AML cells; however, relapse is common due to some cells being resistant and remaining within specialised BM niches. Not only are there specialised niches which protect the blasts, but it has been well documented that AML remodels the niche to create a more permissive niche. The metabolic plasticity and hijacking of normal HSC processes allows the blasts to access increased FA, AA and mitochondria (33, 209, 219). Recent advances have created strategies such as the BCL-2 inhibitor (venetoclax) in combination with hypomethylating agents (168). This targets the acquired mitochondria to induce apoptosis within the specialised niches, with the aim to further remove lingering blasts. However, research by Stevens et al, has shown that AML blasts can be resistant to this strategy by utilising FA metabolism (375). As such, the present study into how AML acquires more FA is timely. Before performing this study, current literature shows that AML expands within the BM, greatly reducing the available FA within the niche and therefore acquires FA from the serum, where they are significantly elevated during disease progression (233). It has also been shown that AML has aberrant production of cytokines such as HGF and IL-1 β . These cytokines have been shown to mediate growth, survival, and metastasis of AML within the BM (395, 413). However, little research has been performed to look at the systemic effect of these secreted cytokines. This further highlights the potential of therapeutics against these cytokines, both directly against AML progression and targeting systemic metabolic alterations to further slow AML growth and to improve patient comfort. Understanding how AML influences the liver, which is the major organ that controls serum fatty acids, to access FA may illuminate new druggable targets for novel therapies.

In this thesis I have shown that AML induces systemic metabolic changes and specifically alters FA metabolism in the liver. I have investigated the mechanism by which AML secreted HGF acts on the liver to downregulate genes associated with FA metabolism and reduces FA uptake, resulting in increased serum FA.

6.2 Key findings

6.2.1 AML alone induces systemic metabolic alteration in a murine model.

In this thesis I have shown that AML engraftment in mice induces systemic metabolic changes. Importantly, I have shown that AML alone causes animal weight loss and raises serum FA.

Studies have investigated the metabolic plasticity of AML and the role it has on AML progression. Multiple studies have focused on targeting AML metabolism as a method for delaying disease progression, specifically the ability of AML to hijack functions of healthy HSC, wherein the tumour is able to reprogramme cells of the BM niche (203, 204, 217, 236, 414). Research has shown that not only is AML able to hijack BMSC for their mitochondria, but it is also able to induce lipolysis of BM adipocytes (209, 232). In conjunction with this, it has been shown that AML is able to alter which metabolic pathway is dominant to improve treatment resistance (369). An increasing body of evidence is showing that that metabolic changes caused by AML are not isolated to the BM. Research has shown that AML induces a cachectic phenotype, causing the loss of body mass predominantly in muscle mass and often including the loss of fat (157, 158). I find that progression of MN1 and HOXA9/MEIS1 cell engraftment in a murine model induced loss of total body weight, as well as showing a reduction in the weight of fat pads. Supporting the research indicating that AML, independent of chemotherapy, induces weight loss. Moreover, studies have shown that patients with a greater loss of weight or a lower starting weight respond worse to treatments and have a poorer prognosis (374, 415). These findings support the notion that AML induces systemic metabolic changes.

The importance of FA metabolism has been highlighted by studies investigating the role of FA uptake proteins expressed by AML (236, 238). BM adipocytes have previously been shown to be essential for the survival and proliferation of AML. Lipolysis of these adipocytes is imperative for the supply of FA to the tumour for metabolism and production of cellular membranes (188). Blasts have been shown to upregulate CD36 and FATPs to increase FA uptake, blockade of these processes impairs proliferation and presents an attractive target for therapeutics (33, 235, 416). However, evidence suggests that rapid AML expansion leads to patients presenting

in clinics with minimal BM adipose tissue (189, 417). This suggests that in later stages of AML progression, blasts access FA from other fat deposits within the body. This is supported by data in this project showing that AML engrafted mice have reduced inguinal and gonadal fat pads in comparison to controls. It is unclear what signal, and mechanism induces the lipolysis of these fat deposits, and was unfortunately outside of the scope of this project. National statistics indicate that the average person within the population is getting larger, with an increased incidence of obesity (418). Studies have shown that there is an increased correlation between obesity and the development of AML (419), as well as a multitude of other malignancies (420). Obesity has not only been shown to confer higher chance of developing a malignancy but has also been shown to increase the risk of dying from the cancer (421). Furthermore, studies have shown that obese patients diagnosed with AML have a worse prognosis than their counterparts with healthy BMI measurements (422). Obese patients have increase adipose tissue and thus a greater source of FA for malignancy progression. These results indicate the importance of investigating systemic metabolic changes when targeting cancer metabolism.

The significance of serum FFA has been exemplified in studies outlining the negative correlation between elevated serum FFA and AML progression and patient prognosis (233). Similarly, elevated serum FFA has been implicated in other malignancies, including lung cancer (392), ovarian cancer (350), and B-cell lymphoma (393). These studies further confirm the requirement of FA from outside of the immediate niche and highlight the importance of investigating systemic alterations to FA metabolism. In this study I have shown both by ELISA and mass spectrometry, that AML progression resulted in elevated serum FFA. Furthermore, lipidomic analysis of the serum FFA showed that the proportions of different length FA in the serum was different between control mice and AML engrafted mice. These data may be useful for investigating which FA AML has a higher dependency on, and whether this is of benefit to more targeted therapies. This study has shown that even without the addition of AML treatments, such as chemotherapies, AML induces metabolic changes outside of the BM microenvironment.

6.2.2 BM resident AML downregulates liver FA metabolism.

In this study I have shown that AML engrafted in the bone marrow acts on the liver to downregulate FA metabolism, including FA uptake and FAO.

As outlined above, AML is highly reliant of FA for survival and proliferation. Once resources are used up in the BM, the mechanism by which FA are acquired is more complex. The liver is the master regulator of FA metabolism in the body, responding to different signals to maintain homeostasis or during a stress response, such as infection (423). During fasting and feeding the liver undergoes cycles of taking up, storing, synthesising, breaking down, and releasing FA to match with the demands of the body (269). Studies have shown that this process can be disrupted by metabolic diseases like NAFLD and diabetes, where excess storage of FA causes toxicity and systemic inflammation (318, 335). These result in reduced capacity to take up FA and downregulate the expression of FAO genes and are also associated with elevated serum FFA (424). In this study bulk RNAseq and RT-qPCR of liver samples have similarly shown that engrafted AML downregulates FA metabolism and degradation pathways, despite there being little to no infiltration of AML into the liver. This alteration to liver FA metabolism highlights the importance of researching the liver in more than just liver diseases and drug metabolism.

The importance of metabolism in the progression and prognosis of malignancies cannot be overlooked. High metabolic plasticity is a hallmark of cancers and is an area of research for developing more targeted and tolerable therapies (425). Some examples are: Etomoxir, which inhibits FOA by blocking CPT1 (426); Metformin, although a drug initially developed for the treatment of diabetes it can also target cancer cell mitochondria function (427). However, these treatments only target the metabolism within all cells and still affect healthy cells. Studies have shown that pancreatic and colorectal cancer can both alter host liver FA metabolism, as well as enhancing their own metabolism (250). Here I have shown that AML conditioned media reduces FA uptake in primary hepatocytes as well as downregulating FA metabolism genes. These studies show the potential of malignancies to induce systemic metabolic changes. Like AML other cancers have high serum FFA comparative to normal levels, this indicates that these other cancers may also induce liver metabolic changes. This highlights the importance of the liver when investigating FA metabolism in cancer research.

The function of liver FA metabolism is reliant on efficient uptake and secretion of FA. One of the important uptake proteins is FATP2. In this study immunofluorescent staining of liver sections showed that the level of FATP2 protein expression was significantly lower in mice with AML, compared to controls. Studies have shown that FATP2 is overexpressed in a number of malignant cell types such as breast cancer and colorectal cancer (230, 377). However, the effect of these tumours on liver FATP2 expression has largely not been studied. In liver diseases, such as NAFLD, hepatocyte FATP2 protein levels are reduced and uptake of FA into the liver is reduced and secretion of FA into the serum is increased (377). Reduced hepatic FA uptake results in higher serum FA which can be utilised by cancer cells for metabolism and constructing cellular membranes for growth and proliferation. Furthermore, reduced hepatocyte FA uptake decreases FAO, and ketone body production (248). Both were seen in the analysis of liver gene expression of *Hmgcs2* and *Acadm*, both of which were significantly down regulated in AML engrafted mice. These results highlight that AML has the potential to alter pathways in other organs, rather than just cells within the immediate niche. Providing the potential for further therapeutic targeting.

It has been shown that during the course of diseases such as NAFLD, hepatocytes are unable to respond as efficiently to their metabolic demands for respiration. The metabolic injury further promotes progression of the disease, creating a cycle of increased metabolic stress and liver injury (428, 429). In this study I used the Seahorse metabolic flux mitostress kit to show that AML conditioned media also disrupts the metabolic response of hepatocytes. This is supported by some rare case studies in which patients have been reported to exhibit liver injury or failure as an early presentation of their AML (430-432). It is almost impossible to know whether liver damage is likely at later stages of the disease progression, as patients are put on to treatment regimens such as chemotherapy, which are widely acknowledged to cause some liver damage (433, 434). However, this is an interesting result as it hints that there are other mechanisms by which the liver damage is occurring, and these may be targetable for therapeutics.

6.2.3 AML secreted HGF downregulates liver FA metabolism via a PPAR α mechanism.

One of the major aims of research projects is to identify the mechanism of an observation. In my thesis I have shown that AML in the BM secretes both HGF and IL-1 β which act on the liver to reduce gene expression of FA metabolism genes, although only HGF acted to reduce LCFA uptake. I have identified that HGF enacts these effects via the downregulation of the PPAR α signalling pathway.

The cells of the body are constantly communicating with each other via cell-cell interactions and/or secretion of molecules such as cytokines (435). One of the key functions of the liver is the ability to respond to these signals within the blood (436, 437). The *in vivo* and *in vitro* investigation of AML's impact on the liver, in this study, showed that AML secretes factors into the blood which are able to act on the liver. Cytokine analysis of the serum from mice engrafted with AML and of media conditioned with AML blasts highlighted HGF and IL-1 β . This is supported by previous studies which have shown that human AML secretes HGF (413, 438) and IL-1 β (395), however studies have primarily investigate the role of these cytokines within the niche as both play a role in the infiltration and progression of AML. Furthermore, studies show that HGF and IL-1 β have the capacity to act on the liver and alter FA metabolism (402, 409). I have shown that stimulating mice and primary hepatocytes with HGF and IL-1 β gene expression of liver FA metabolism, at different stages of the pathways, is downregulated. Moreover, as in other studies (409), stimulating hepatocytes with HGF reduced cellular LCFA uptake. These results indicate the importance of HGF secretion by AML blasts. Not only is it shown to advance the tumour in the BM, but now in this study it has been shown to aid in the access to FA via interaction with the liver.

Research has shown that the PPAR signalling pathways are imperative for FA metabolism in health and in disease (223). Likewise, the balance between PPAR α , β , and γ signalling can provide different responses (439). Downregulation of PPAR α in AML confers protection against apoptosis, as well as improving FA synthesis (440). Conversely, PPAR γ is upregulated in AML blasts and improves FA storage and promotes the tumour microenvironment via anti-inflammatory regulation (441). Changes to and balance of PPAR expression is known to be important for the function of HSC during homeostasis and infection response, altering haematopoieses and FA

metabolism (442). During sepsis it has also been shown that serum levels of HGF are elevated and may be secreted with other growth factors in the liver by migratory HSC (443, 444). In this study I have shown that HGF downregulated the expression of *Ppara* in hepatocytes, both *in vivo* and *in vitro*. This corroborated with the bulk RNA sequencing of livers from AML engrafted mice and gene analysis for *Ppara* in hepatocytes treated with AML conditioned media. These results suggest that the inhibitory effect of AML on liver FA metabolism may act via downregulation of the PPAR α pathway. Not only is higher serum HGF found in sepsis, but so too is disruption to liver FA metabolism and PPAR signalling, resulting in impaired lipid metabolism in the liver (391, 443). This may suggest that during sepsis HGF secretion is not only beneficial for liver regeneration and angiogenesis (445), but may also act on the liver to induce higher serum FA for use by other cells in the body, including HSC in the BM. The data produced for this project, with other studies, further support the evidence of HGF production by AML as a potential target for drug development.

Research also shows that other tumours such as gliomas (446), breast cancer (447), and lung cancer (448) secrete HGF. These studies show that HGF has been implicated in proliferation, migration and tumour metabolism but research has not investigated the effect of HGF systemically, especially on the liver. As these cancers are often associated with high serum FA and body weight loss, it may be an interesting area for future research. This further highlights the potential of HGF as a target for therapeutics, not just to delay tumour progression but also to normalise systemic metabolism, specifically FA metabolism in the liver.

6.2.4 HGF KD in AML blasts has a restorative effect on AML induced downregulation of liver FA metabolism.

In this thesis I have shown that altered liver FA metabolism can be rescued via KD of HGF in AML blasts. Furthermore, data showed that HGF KD in engrafted MN1 cells reduced their LCFA in the BM.

HGF as a molecule was also separately discovered in non-hepatic tissues as Scatter Factor (SF), it was initially thought to be produced by hepatocytes, and only during development (449). Over the last few decades further research into this molecule, and its receptor C-MET, have shown that it has multiple roles such as suppressing apoptosis (450), liver regeneration (451), ECM breakdown (452), and development of other tissues such as neurones and kidneys (453, 454). As mentioned above HGF has also been implicated to increase the motility and invasion of tumours including AML. Therefore, treatments have been developed with the aim to improve regeneration via increased HGF or conversely to block the HGF/C-MET pathway to impair cell invasion (455). This study found that AML cells secrete HGF and confirmed that this alters liver FA metabolism. There is currently no murine blocking or neutralising antibody for HGF, thus a knockdown was used. I have shown that knockdown of *Hgf* in AML blasts restricts their uptake of FA when engrafted into mice. This may contribute to slower progression of the disease and better survival; however further investigation is required. *Hgf* knockdown in AML blasts engrafted into the BM of mice also restored the gene expression of some FA metabolism associated genes in the liver of these mice. Analysis of primary human serum samples corroborates with previous studies that show that some patients present with elevated HGF (456). This further highlights HGF targeted therapies in combination with traditional treatments for the treatment of AML. Studies have already started to investigate blockade or neutralisation of the HGF/C-MET pathway for other cancer treatments. Anti-HGF antibodies, C-MET inhibitors and *HGF* gene silencing treatments have reached clinical trials for cancers such as lung cancer, pancreatic cancer, and breast cancer, often in combination with chemotherapies or immunomodulators (457-459) Sadly they could not be used in this study as they have been shown not to bind mouse HGF. These studies show that there are already human anti-HGF treatments which may be safe for the treatment of AML. However, it should be noted that the aggressive nature of AML may mean that blockade of HGF may be of more benefit during consolidation treatment as it may not benefit the patients at an induction stage.

6.2.5 PPAR α agonism slows AML engraftment and rescues liver FA metabolism.

The final part of this project showed that the commercially available PPAR α agonist fenofibrate can restore serum FFA levels, moderately rescue liver FA metabolism gene expression, and reduces both AML engraftment and neutral lipid content.

Not only has it been outlined in cancer cells but impaired PPAR α pathway activation is involved in diseases including Alzheimer's and liver steatosis (401, 460) Therefore, research and medical trials have already produced agonists such as fenofibrate, and other agonists which are less specific and agonise other isoforms of PPAR (412). PPAR α is the most abundant isoform in the liver and is involved in upregulating genes associated with FA metabolism (314), this makes it an attractive target for many diseases involved in dysregulated liver metabolism. In this study I showed that liver Ppar α gene expression is downregulated by AML engrafted in the BM, as well as by the factor it secretes: HGF. Moreover, I showed that *in vivo* agonism of PPAR α with fenofibrate in AML engrafted mice and on primary hepatocytes treated with conditioned media or HGF, moderately rescued liver FA metabolism gene expression, although further genetic analysis would be of benefit for *in vivo* studies. High serum FFA is a marker of AML progression (233) and as such it was a positive result to serum FA levels significantly lower after fenofibrate treatment and more closely resembling control levels. These results show that PPAR α agonism during AML engraftment can restore liver FA metabolism. This has the potential to impede AML associated weight loss (158), improving patient tolerance of other treatments and quality of life.

FA have been shown to be used by AML blasts both for metabolism and as building blocks for other cellular processes (369, 461). This includes the use of FA to make cell membrane for extracellular vesicles, which have been shown to be important for offloading non-functional mitochondria and other metabolic waste (214). In this study I showed that agonism with fenofibrate resulted in lower neutral lipid content in the engrafted AML blasts. This is supported by research which that agonism of PPAR α disrupts lipid storage and synthesis (412, 440). This suggests that systemic PPAR α agonism, as seen by OG of fenofibrate, both reduces the available FFA in the serum, but also disrupts AML FA metabolism and export of vesicles as the reduced stores are not replenished. Furthermore, FA metabolism has been shown to be a

mechanism by which AML is resistant to Venetoclax, which targets mitochondrial proteins to induce apoptosis (462). To this end, research by Xie, et al has investigated synergising Venetoclax with PPAR α agonist Chiglitazar to resensitise AML blasts to the targeted therapy (463). These results and the results in this project supports the notion that PPAR α agonism could have a dual affect as a therapeutic, target both AML blasts and liver metabolism. Further investigation is required to which market PPAR α agonist has the best efficacy and whether this could be combined with other therapeutics.

Having found that PPAR α agonism slowed AML engraftment and restored serum FFA, as well as some liver FA metabolism gene expression, it must be considered when this treatment may be of benefit. During this study fenofibrate was administered 10 days after IV injection with MN1 cells, at which point Figure 4.7 suggests that engraftment would have been <40% of the BM. This may not be representative of the level of AML in the BM of patients at initial presentation at the clinics. The average % blasts in BM biopsies from the human patients in this study was 62.1% (15%-88%), although criteria for diagnosis recommends >20% (464). This suggests that further research into the timings for administering fenofibrate may be of benefit. The aggressive nature of AML dictates that induction therapies are highly intensive in the aim to achieve remission (162). These, primarily, chemotherapy and hypomethylating agents, in combination, are often unable to fully accomplish clearance, and therefore consolidation treatments are required to maintain remission and prevent relapse (179). The use of fenofibrate may have a potential in induction therapy to slow weight loss by restoring liver FA metabolism. However, as an anti-AML treatment it may be better suited as a consolidation treatment in combination with targeted therapeutics such as Venetoclax (168, 463). Some patients are too frail to tolerate intensive chemotherapies and so induction treatment with Venetoclax has been introduced (465). The combination of Venetoclax and fenofibrate as induction treatment may sensitise blasts to Venetoclax and prevent further frailty by reducing weight loss caused by aberrant liver metabolism.

6.3 Limitations

There are several limitations that restricted this project. These relate to *in vivo* and *in vitro* studies, as well as difficulties in acquiring and processing primary human samples. This project aimed to balance the use of *in vivo* models, with planning in accordance with the 3Rs (Replacement, Reduction and Refinement) and Home Office guidelines, and *in vitro* work for which the acquisition of primary hepatocytes was limited and sporadic. Experiments were planned with the utmost care to ensure the largest data output possible while not compromising on statistical power. However, there were occasions where plans had to encompass ideas for the next stages of the project at the same time as the previous step, for example testing the recombinant proteins at the same time as the inhibitors, despite being unclear of their success in downregulating liver FA metabolism. Although this process was successful in achieving statistical significance in the results it meant that more in depth time courses or dose curves could not be performed. The irregular notice and limited supply of primary hepatocytes also made it impossible to use LSK cells to make control conditioned media. These would have been a more biologically relevant comparison to the AML conditioned media but unfortunately require availability of mice for isolation and an extended period of time to culture and further condition control media.

During the analysis of *in vitro* studies investigating the inhibition of IL-1 β on primary hepatocytes treated with AML conditioned media or IL-1 β itself, it became clear that the neutralising antibody was most likely not working as expected. This could be seen by the lack of change caused by the mAb when added to the hepatocytes in combination with recombinant murine IL-1 β . It would have been of benefit to test the antibody further to see if it would have an inhibitory effect on cells we know produce IL-1 β , for example bone marrow derived macrophages. This would have been informative about the viability of the antibody. Alternatively, with more time, I would have liked to test another IL-1 β inhibitor. One method would have been to use recombinant murine IL-1Ra, an endogenous inhibitor of the IL-1 β family (466). Without being able to fully investigate the inhibition of IL-1 β *in vitro* or *in vivo*, it cannot be ruled out that HGF and IL-1 β secreted by AML blasts work in combination to downregulate FA metabolism in the liver. This would have been of interest as both HGF and IL-1 β have been shown to act on PPAR signalling pathways (391, 467). It could be suggested that the concentrations of HGF and IL-1 β may have differing

effects on this signalling pathway, however it could also be suggested that they are mediating an effect via different mechanisms. Therefore, it could be suggested that both HGF and IL-1 β are required for the downregulation of liver FA metabolism seen in AML. It would be of interest to try inhibition of both cytokines in an AML model.

Another limitation of this project was the partial success of the *Hgf* knockdown in MN1 cells. Although multiple MOI were tested to reach a more potent knockdown, it was only successful in reducing *Hgf* expression to 60% in the MN1 blasts. While the results were still promising, with statistical significance, it potentially would have been clearer, with more confident conclusions, had there been a more substantial knockdown. This would have allowed for further testing, including a survival curve that could have brought further strength to evidence that blocking AML secreted HGF improves FA metabolism in the liver and has the potential to prolong survival. An alternative to the shRNA lentivirus that was used would be to use a lentivirus conjugated to a co-transfection such as an antibiotic-resistant promoter. Once the knockdown protocol has been administered, an antibiotic such as neomycin can be added to the media (468). This selection pressure will kill any cell without the integrated knockdown, selecting for only cells with the knockdown and likely achieving a much lower over gene expression from a sample of the remaining cells.

The *in vivo* experiment that utilised the generated *Hgf* knockdown MN1 cells also had its own limitations. It was not ideal to test the FA uptake of engrafted AML cells as the investigation was the effect on the liver. However, this was used as a proxy measurement as the optimal experiment would have required additional mouse strains, which was outside the scope of this project. To test whether *Hgf* knockdown in the engrafted cells restored liver FA metabolism, it would have been ideal to have a mouse strain with a liver specific luciferase tag. This could be achieved using a liver specific Cre mouse line such as Albumin-Cre and a mouse strain with firefly luciferase preceded by a LoxP-stop-LoxP cassette. When these mice strains are crossed, successful Cre recombination would result in liver specific luciferase expression (469). With this new mouse strain, it would be possible to use the FFA-ss-luc to visualise the FA uptake in the liver of these mice with live *in vivo* imaging. Engraftment with AML cells without the firefly luciferase tag would allow for imaging of AML mediated changes to the FA uptake in the liver.

Finally, there was a limitation to the number of primary human AML samples that could be collected. Despite the hard work of Dr Hellmich samples are understandably

limited by the number of patients being diagnosed, those that are happy to consent to their samples being used for research, and the time available to doctors and nurses performing blood tests and/or BM aspirates. More primary samples would have allowed for more robust analysis due to the heterogeneity of patients. Increase statistical power would have allowed for definitive conclusions whereas, with the limited number of samples available, no clear conclusions can be drawn from analysis of the samples. Furthermore, samples are precious and had to be used sparingly, thus more samples would have allowed for further testing for other parameters such as lipidomic analysis. Although it has been shown that both HGF and IL-1 β can be elevated in human samples (395, 413), it remains to be investigated if certain mutations associated with these. Moreover, it would be of interest to see whether these patients have altered liver function markers, serum FFA and if serum samples similarly downregulate FA metabolism genes in human liver cell lines.

6.4 Future work

While this project achieved all the primary objectives there are new questions that have arisen from this research. This study advances our understanding of how AML alters liver metabolism to access FA from outside the niche however, there remains aspects which are unknown or unclear.

Firstly, it would be of interest to see whether HGF and IL-1 β act to alter liver FA metabolism. Inhibition of HGF with Crizotinib and knockdown of *Hgf* in the AML blasts did not fully restore FA metabolism in the livers of AML engrafted mice. This suggests that other molecules may be acting alongside HGF to affect the liver. Data in this thesis has shown that IL-1 β does alter liver FA metabolism, although it did not cause downregulation of FA uptake by hepatocytes, whereas HGF affected both gene expression and function of the hepatocytes. It is known that IL-1 β has an inhibitory effect on PPAR signalling pathways and therefore it may be involved in the downregulation of *Ppara* seen in this project (467). To test the combination of IL-1 β and HGF, recombinant proteins could first be used on primary hepatocytes, as well as combined inhibition before further being tested *in vivo*. These experiments would help to answer whether AML secreted IL-1 β plays a role in downregulating liver FA metabolism and if this effect is in combination with HGF.

Although this study showed that some human patients with AML also had elevated serum HGF, no conclusions could be drawn from this small dataset. It would be beneficial to increase the sample size to improve the statistical power to ascertain whether some AML mutations secrete HGF. However, this would require a significantly larger pool of patients which could take a long time to collect. A potential alternative would be to use online data sets of AML patients such as Bloodspot (470) or The Cancer Genome Atlas (471). This way much larger sequencing data sets could be used to create a much greater statistical power to elucidate which AML mutations increase HGF expression and secretion.

This study found that both the MN1 and HOXA9/MEIS1 murine AML cell lines secreted HGF that acted to impair liver lipid metabolism. To further consolidate the data shown in this thesis, it would be beneficial to investigate another model type. One possible model would be to use a patient derived xenograft (pdx) model. After confirmation that the patient mutation results in elevated HGF secretion, AML blasts can be isolated from BM aspirates and engrafted into immunodeficient mice, such as

NSG mice (472). A humanised model will aid in confirming that AML secreted HGF downregulates liver FA metabolism and will be more relevant to human studies. This model would also need to be tested *in vitro* on human hepatocytes. Sadly, the HepG2 cell line is not a good model for this study as it is an immortalised cell line from hepatocellular carcinoma and therefore will not act in the same manner as healthy cells (271). Another model would be to test the potential of media conditioned by patient AML blasts on induced pluripotent stem cells (iPSC) that have been differentiated into hepatocytes (473). This humanised model is more likely to act like healthy hepatocytes and could be used to further discover if human AML similarly downregulates FA metabolism in human hepatocytes.

It is well documented that AML occurs predominantly in older patients and increasing evidence indicates that obesity confers a predisposition to and alters treatment response in malignancies, including AML (182, 422). This project has only investigated the effects of AML engraftment on healthy young adult mice. The data from these experiments is a good starting place but it would potentially be more biologically relevant to use aged mice and/or mice placed on a high fat diet to mimic obesity. Utilising these models would provide better insight in to whether aging or obesity alter the changes to FA metabolism caused by AML engraftment in the BM. Obesity itself causes systemic changes to metabolism and comes with an excess of adipose deposits (474). It would therefore be interesting to interrogate whether the altered energetic state effects the potential for downregulating FA metabolism genes in the liver and whether these occur at different time points. Furthermore, obesity can also induce liver damage (291) and this may have an interesting effect on the efficacy of the cytokines released by AML in the BM. Aging would also be interesting to model to further the work of this study. Aging not only causes frailty but also influences metabolism and tolerance of treatments (475). This may alter the liver response to AML cytokine release, as well as potentially altering the response to interventions such as the fenofibrate. It is important to use models which are likely to be seen in human patient populations as these experiments may be more accurate in representing the potential druggable targets.

The bulk RNA sequencing, performed for this study, is a huge source of information which could further inform research into the effect of AML on the liver. Due to the scope of this project only the pathways and genes involved in FA metabolism were used, especially those that were downregulated. This resulted in much of the

sequencing data being largely ignored. Future work could be informed by the use of this data. For example, high on the list of significantly downregulated pathways was drug metabolism. It has previously been shown in infectious diseases and liver tumours, that cytochrome P450 mediated drug metabolism can be impaired (476, 477). These data suggest that multitude of factors which contribute to patient response to drugs may also include their disease type. Making it a potentially interested area to investigate. It should also be noted that this project did not study any of the pathways that were upregulated in the liver in response to AML engraftment. The volcano plots (Figure 4.1) for both show that there are a large number of proteins which are significantly upregulated in the livers of mice engrafted with AML when compared to control mouse livers. Further use of the bulk RNA sequencing data could be of benefit to future research, this would allow the dataset to be more exploratory in informing projects of the alterations caused by AML, in the BM, on the liver.

Finally, emerging research has shown that AML induces changes in other organs of the host such as the heart (478, 479). Cancer-related heart failure has long been attributed to the use of chemotherapies (480). However, further studies have shown that the incidence of heart failure in cancer patients differs between cancer type, those with haematologic malignancies had the highest rate of failure in the studies performed by Wang, L. et al and Hibler, E. et al (481, 482). Furthermore, leukaemia patients have presented with cardiac alterations prior to treatment with chemotherapies (483). This suggests that AML directly contributes to cancer-related heart failure. Cardiac tissues utilise FA for metabolism over other metabolites (484), and this study has shown that AML secretes cytokines which can alter FA metabolism. It would therefore be of interest to see whether the hearts of mice engrafted with AML have altered FA metabolism gene expression and whether HGF similarly alters the expression. This research could greatly improve our understanding of AML action on the wider system outside of the BM niche, with the potential to find new druggable targets to improve treatments for patients.

6.5 Conclusions

In this thesis I have shown that AML induces cachexia, independent to treatment with chemotherapy. I determined that AML progression causes bodyweight loss, leads to reduce fat pad size, and results in high serum FA. Moreover, I have demonstrated that AML downregulates FA metabolism genes within the liver and slows the uptake of LCFA. This investigation confirmed that alterations are cell-cell independent and highlighted HGF secreted by AML cells. I showed that HGF similarly downregulates liver FA metabolism and LCFA uptake. Interestingly I found that some human patients, diagnosed with AML, have elevated serum HGF. Furthermore, my data demonstrates that knockdown of *Hgf* in AML blasts can rescue FA metabolism in the liver and reduce FA uptake in the AML blasts. Importantly, I established that the mechanism by which HGF, secreted by AML blasts, downregulates FA metabolism in the liver, is via the PPAR α signalling pathway. Lastly, I showed that agonising this pathway, with currently available drugs, could rescue serum FA levels and restore FA metabolism gene expression. I confirmed that PPAR α agonism slowed tumour progression and discovered that it depleted blast neutral lipid content. This study is another example of how AML is capable of hijacking healthy processes. I have highlighted important mechanisms by which AML alters liver FA metabolism to improve survival and progression. Although unlikely to provide any curative drugs, this research may aid in the discovery of drugs which could be used in combination with new and current treatments which to slow or prevent weight loss and improve the clearance of AML blasts to prolong disease-free periods.

7. References

1. Doulatov S, Notta F, Laurenti E, Dick JE. Hematopoiesis: a human perspective. *Cell Stem Cell*. 2012;10(2):120-36.
2. Balistreri CR, Garagnani P, Madonna R, Vaiserman A, Melino G. Developmental programming of adult haematopoiesis system. *Ageing Res Rev*. 2019;54:100918.
3. Christensen JL, Wright DE, Wagers AJ, Weissman IL. Circulation and chemotaxis of fetal hematopoietic stem cells. *PLoS Biol*. 2004;2(3):E75.
4. Dzierzak E, Medvinsky A, de Bruijn M. Qualitative and quantitative aspects of haematopoietic cell development in the mammalian embryo. *Immunol Today*. 1998;19(5):228-36.
5. Dzierzak E. Ontogenic emergence of definitive hematopoietic stem cells. *Curr Opin Hematol*. 2003;10(3):229-34.
6. Morrison SJ, Scadden DT. The bone marrow niche for haematopoietic stem cells. *Nature*. 2014;505(7483):327-34.
7. Alamo IG, Kannan KB, Loftus TJ, Ramos H, Efron PA, Mohr AM. Severe trauma and chronic stress activates extramedullary erythropoiesis. *J Trauma Acute Care Surg*. 2017;83(1):144-50.
8. Laurenti E, Göttgens B. From haematopoietic stem cells to complex differentiation landscapes. *Nature*. 2018;553(7689):418-26.
9. Marlein R, Chris, Rushworth A, Stuart. *Bone Marrow*. LS John Wiley & Sons, Ltd, Chichester. 2018.
10. Cipolleschi MG, Dello Sbarba P, Olivotto M. The role of hypoxia in the maintenance of hematopoietic stem cells. *Blood*. 1993;82(7):2031-7.
11. Chen Z, Guo Q, Song G, Hou Y. Molecular regulation of hematopoietic stem cell quiescence. *Cell Mol Life Sci*. 2022;79(4):218.
12. Notta F, Doulatov S, Laurenti E, Poeppl A, Jurisica I, Dick JE. Isolation of single human hematopoietic stem cells capable of long-term multilineage engraftment. *Science*. 2011;333(6039):218-21.
13. Chao MP, Seita J, Weissman IL. Establishment of a normal hematopoietic and leukemia stem cell hierarchy. *Cold Spring Harb Symp Quant Biol*. 2008;73:439-49.
14. Paudel S, Ghimire L, Jin L, Jeanson D, Jeyaseelan S. Regulation of emergency granulopoiesis during infection. *Front Immunol*. 2022;13:961601.
15. Bonaud A, Lemos JP, Espéli M, Balabanian K. Hematopoietic Multipotent Progenitors and Plasma Cells: Neighbors or Roommates in the Mouse Bone Marrow Ecosystem? *Front Immunol*. 2021;12:658535.
16. Velten L, Haas SF, Raffel S, Blaszkiewicz S, Islam S, Hennig BP, et al. Human haematopoietic stem cell lineage commitment is a continuous process. *Nat Cell Biol*. 2017;19(4):271-81.
17. Simsek T, Kocabas F, Zheng J, Deberardinis RJ, Mahmoud AI, Olson EN, et al. The distinct metabolic profile of hematopoietic stem cells reflects their location in a hypoxic niche. *Cell Stem Cell*. 2010;7(3):380-90.
18. Takubo K, Goda N, Yamada W, Iriuchishima H, Ikeda E, Kubota Y, et al. Regulation of the HIF-1alpha level is essential for hematopoietic stem cells. *Cell Stem Cell*. 2010;7(3):391-402.
19. Zhang CC, Sadek HA. Hypoxia and metabolic properties of hematopoietic stem cells. *Antioxid Redox Signal*. 2014;20(12):1891-901.
20. Florencio-Silva R, Sasso GR, Sasso-Cerri E, Simões MJ, Cerri PS. Biology of Bone Tissue: Structure, Function, and Factors That Influence Bone Cells. *Biomed Res Int*. 2015;2015:421746.

21. Shafat MS, Gnaneswaran B, Bowles KM, Rushworth SA. The bone marrow microenvironment - Home of the leukemic blasts. *Blood Rev.* 2017;31(5):277-86.
22. Kumar R, Godavarthy PS, Krause DS. The bone marrow microenvironment in health and disease at a glance. *J Cell Sci.* 2018;131(4).
23. Chiarilli MG, Delli Pizzi A, Mastrodicasa D, Febo MP, Cardinali B, Consorte B, et al. Bone marrow magnetic resonance imaging: physiologic and pathologic findings that radiologist should know. *Radiol Med.* 2021;126(2):264-76.
24. Gurkan UA, Akkus O. The mechanical environment of bone marrow: a review. *Ann Biomed Eng.* 2008;36(12):1978-91.
25. Marenzana M, Arnett TR. The Key Role of the Blood Supply to Bone. *Bone Res.* 2013;1(3):203-15.
26. Maryanovich M, Takeishi S, Frenette PS. Neural Regulation of Bone and Bone Marrow. *Cold Spring Harb Perspect Med.* 2018;8(9).
27. Wilson A, Trumpp A. Bone-marrow haematopoietic-stem-cell niches. *Nat Rev Immunol.* 2006;6(2):93-106.
28. Ding L, Morrison SJ. Haematopoietic stem cells and early lymphoid progenitors occupy distinct bone marrow niches. *Nature.* 2013;495(7440):231-5.
29. Islam A, Glomski C, Henderson ES. Bone lining (endosteal) cells and hematopoiesis: a light microscopic study of normal and pathologic human bone marrow in plastic-embedded sections. *Anat Rec.* 1990;227(3):300-6.
30. Nakamura Y, Arai F, Iwasaki H, Hosokawa K, Kobayashi I, Gomei Y, et al. Isolation and characterization of endosteal niche cell populations that regulate hematopoietic stem cells. *Blood.* 2010;116(9):1422-32.
31. Fröbel J, Landspersky T, Percin G, Schreck C, Rahmig S, Ori A, et al. The Hematopoietic Bone Marrow Niche Ecosystem. *Front Cell Dev Biol.* 2021;9:705410.
32. Birbrair A, Frenette PS. Niche heterogeneity in the bone marrow. *Ann N Y Acad Sci.* 2016;1370(1):82-96.
33. Shafat MS, Oellerich T, Mohr S, Robinson SD, Edwards DR, Marlein CR, et al. Leukemic blasts program bone marrow adipocytes to generate a protumoral microenvironment. *Blood.* 2017;129(10):1320-32.
34. Cho DS, Schmitt RE, Dasgupta A, Ducharme AM, Doles JD. ACUTE AND SUSTAINED ALTERATIONS TO THE BONE MARROW IMMUNE MICROENVIRONMENT FOLLOWING POLYMICROBIAL INFECTION. *Shock.* 2022;58(1):45-55.
35. Binder M, Szalat RE, Talluri S, Fulciniti M, Avet-Loiseau H, Parmigiani G, et al. Bone marrow stromal cells induce chromatin remodeling in multiple myeloma cells leading to transcriptional changes. *Nat Commun.* 2024;15(1):4139.
36. Greenbaum A, Hsu YM, Day RB, Schuettelpelz LG, Christopher MJ, Borgerding JN, et al. CXCL12 in early mesenchymal progenitors is required for haematopoietic stem-cell maintenance. *Nature.* 2013;495(7440):227-30.
37. Itkin T, Gur-Cohen S, Spencer JA, Schajnovitz A, Ramasamy SK, Kusumbe AP, et al. Distinct bone marrow blood vessels differentially regulate haematopoiesis. *Nature.* 2016;532(7599):323-8.
38. Crane GM, Jeffery E, Morrison SJ. Adult haematopoietic stem cell niches. *Nat Rev Immunol.* 2017;17(9):573-90.
39. Méndez-Ferrer S, Michurina TV, Ferraro F, Mazloom AR, Macarthur BD, Lira SA, et al. Mesenchymal and haematopoietic stem cells form a unique bone marrow niche. *Nature.* 2010;466(7308):829-34.
40. Gao Q, Wang L, Wang S, Huang B, Jing Y, Su J. Bone Marrow Mesenchymal Stromal Cells: Identification, Classification, and Differentiation. *Front Cell Dev Biol.* 2021;9:787118.
41. Pittenger MF. Mesenchymal stem cells from adult bone marrow. *Methods Mol Biol.* 2008;449:27-44.

42. Sitnicka E, Ruscetti FW, Priestley GV, Wolf NS, Bartelmez SH. Transforming growth factor beta 1 directly and reversibly inhibits the initial cell divisions of long-term repopulating hematopoietic stem cells. *Blood*. 1996;88(1):82-8.
43. Marote A, Santos D, Mendes-Pinheiro B, Serre-Miranda C, Anjo SI, Vieira J, et al. Cellular Aging Secretes: a Comparison of Bone-Marrow-Derived and Induced Mesenchymal Stem Cells and Their Secretome Over Long-Term Culture. *Stem Cell Rev Rep*. 2023;19(1):248-63.
44. Wu J, Zhang W, Ran Q, Xiang Y, Zhong JF, Li SC, et al. The Differentiation Balance of Bone Marrow Mesenchymal Stem Cells Is Crucial to Hematopoiesis. *Stem Cells Int*. 2018;2018:1540148.
45. Anthony BA, Link DC. Regulation of hematopoietic stem cells by bone marrow stromal cells. *Trends Immunol*. 2014;35(1):32-7.
46. Pesce M, Di Carlo A, De Felici M. The c-kit receptor is involved in the adhesion of mouse primordial germ cells to somatic cells in culture. *Mech Dev*. 1997;68(1-2):37-44.
47. Shin JY, Hu W, Naramura M, Park CY. High c-Kit expression identifies hematopoietic stem cells with impaired self-renewal and megakaryocytic bias. *J Exp Med*. 2014;211(2):217-31.
48. Tzeng YS, Li H, Kang YL, Chen WC, Cheng WC, Lai DM. Loss of Cxcl12/Sdf-1 in adult mice decreases the quiescent state of hematopoietic stem/progenitor cells and alters the pattern of hematopoietic regeneration after myelosuppression. *Blood*. 2011;117(2):429-39.
49. Levesque JP, Winkler IG. Mobilization of hematopoietic stem cells: state of the art. *Curr Opin Organ Transplant*. 2008;13(1):53-8.
50. Li H, Ghazanfari R, Zacharaki D, Lim HC, Scheduling S. Isolation and characterization of primary bone marrow mesenchymal stromal cells. *Ann N Y Acad Sci*. 2016;1370(1):109-18.
51. García-García A, de Castillejo CL, Méndez-Ferrer S. BMSCs and hematopoiesis. *Immunol Lett*. 2015;168(2):129-35.
52. Omatsu Y, Sugiyama T, Kohara H, Kondoh G, Fujii N, Kohno K, et al. The essential functions of adipo-osteogenic progenitors as the hematopoietic stem and progenitor cell niche. *Immunity*. 2010;33(3):387-99.
53. Ding L, Saunders TL, Enikolopov G, Morrison SJ. Endothelial and perivascular cells maintain haematopoietic stem cells. *Nature*. 2012;481(7382):457-62.
54. Kunisaki Y, Bruns I, Scheiermann C, Ahmed J, Pinho S, Zhang D, et al. Arteriolar niches maintain haematopoietic stem cell quiescence. *Nature*. 2013;502(7473):637-43.
55. Komori T. Regulation of osteoblast differentiation by Runx2. *Adv Exp Med Biol*. 2010;658:43-9.
56. Galán-Díez M, Kousteni S. The osteoblastic niche in hematopoiesis and hematological myeloid malignancies. *Curr Mol Biol Rep*. 2017;3(2):53-62.
57. Chitteti BR, Cheng YH, Streicher DA, Rodriguez-Rodriguez S, Carlesso N, Srour EF, et al. Osteoblast lineage cells expressing high levels of Runx2 enhance hematopoietic progenitor cell proliferation and function. *J Cell Biochem*. 2010;111(2):284-94.
58. Calvi LM, Adams GB, Weibrecht KW, Weber JM, Olson DP, Knight MC, et al. Osteoblastic cells regulate the haematopoietic stem cell niche. *Nature*. 2003;425(6960):841-6.
59. Zhang J, Niu C, Ye L, Huang H, He X, Tong WG, et al. Identification of the haematopoietic stem cell niche and control of the niche size. *Nature*. 2003;425(6960):836-41.
60. Aguila HL, Mun SH, Kalinowski J, Adams DJ, Lorenzo JA, Lee SK. Osteoblast-specific overexpression of human interleukin-7 rescues the bone mass

phenotype of interleukin-7-deficient female mice. *J Bone Miner Res.* 2012;27(5):1030-42.

61. Zhu J, Garrett R, Jung Y, Zhang Y, Kim N, Wang J, et al. Osteoblasts support B-lymphocyte commitment and differentiation from hematopoietic stem cells. *Blood.* 2007;109(9):3706-12.

62. Chitteti BR, Cheng YH, Kacena MA, Srour EF. Hierarchical organization of osteoblasts reveals the significant role of CD166 in hematopoietic stem cell maintenance and function. *Bone.* 2013;54(1):58-67.

63. Yu VW, Saez B, Cook C, Lotinun S, Pardo-Saganta A, Wang YH, et al. Specific bone cells produce DLL4 to generate thymus-seeding progenitors from bone marrow. *J Exp Med.* 2015;212(5):759-74.

64. Del Fattore A, Teti A, Rucci N. Bone cells and the mechanisms of bone remodelling. *Front Biosci (Elite Ed).* 2012;4(6):2302-21.

65. Buck HV, Stains JP. Osteocyte-mediated mechanical response controls osteoblast differentiation and function. *Front Physiol.* 2024;15:1364694.

66. Christopher MJ, Rao M, Liu F, Woloszynek JR, Link DC. Expression of the G-CSF receptor in monocytic cells is sufficient to mediate hematopoietic progenitor mobilization by G-CSF in mice. *J Exp Med.* 2011;208(2):251-60.

67. Grigoriadis AE, Wang ZQ, Cecchini MG, Hofstetter W, Felix R, Fleisch HA, et al. c-Fos: a key regulator of osteoclast-macrophage lineage determination and bone remodeling. *Science.* 1994;266(5184):443-8.

68. Takayanagi H, Kim S, Koga T, Nishina H, Isshiki M, Yoshida H, et al. Induction and activation of the transcription factor NFATc1 (NFAT2) integrate RANKL signaling in terminal differentiation of osteoclasts. *Dev Cell.* 2002;3(6):889-901.

69. Roy M, Roux S. Rab GTPases in Osteoclastic Bone Resorption and Autophagy. *Int J Mol Sci.* 2020;21(20).

70. Morel A, Douat C, Blangy A, Vives V. Bone resorption by osteoclasts involves fine tuning of RHOA activity by its microtubule-associated exchange factor GEF-H1. *Front Physiol.* 2024;15:1342024.

71. Scheller EL, Troiano N, Vanhoutan JN, Bouxsein MA, Fretz JA, Xi Y, et al. Use of osmium tetroxide staining with microcomputerized tomography to visualize and quantify bone marrow adipose tissue in vivo. *Methods Enzymol.* 2014;537:123-39.

72. Cawthorn WP, Scheller EL, Learman BS, Parlee SD, Simon BR, Mori H, et al. Bone marrow adipose tissue is an endocrine organ that contributes to increased circulating adiponectin during caloric restriction. *Cell Metab.* 2014;20(2):368-75.

73. Yeung DK, Griffith JF, Antonio GE, Lee FK, Woo J, Leung PC. Osteoporosis is associated with increased marrow fat content and decreased marrow fat unsaturation: a proton MR spectroscopy study. *J Magn Reson Imaging.* 2005;22(2):279-85.

74. Ambrosi TH, Scialdone A, Graja A, Gohlke S, Jank AM, Bocian C, et al. Adipocyte Accumulation in the Bone Marrow during Obesity and Aging Impairs Stem Cell-Based Hematopoietic and Bone Regeneration. *Cell Stem Cell.* 2017;20(6):771-84.e6.

75. Robert AW, Marcon BH, Dallagiovanna B, Shigunov P. Adipogenesis, Osteogenesis, and Chondrogenesis of Human Mesenchymal Stem/Stromal Cells: A Comparative Transcriptome Approach. *Front Cell Dev Biol.* 2020;8:561.

76. Wang H, Leng Y, Gong Y. Bone Marrow Fat and Hematopoiesis. *Front Endocrinol (Lausanne).* 2018;9:694.

77. Rendina-Ruedy E, Rosen CJ. Lipids in the Bone Marrow: An Evolving Perspective. *Cell Metab.* 2020;31(2):219-31.

78. Belaid-Choucair Z, Lepelletier Y, Poncin G, Thiry A, Humblet C, Maachi M, et al. Human bone marrow adipocytes block granulopoiesis through neuropilin-1-

- induced granulocyte colony-stimulating factor inhibition. *Stem Cells*. 2008;26(6):1556-64.
79. Miharada K, Hiroyama T, Sudo K, Nagasawa T, Nakamura Y. Lipocalin 2 functions as a negative regulator of red blood cell production in an autocrine fashion. *FASEB J*. 2005;19(13):1881-3.
80. Naveiras O, Nardi V, Wenzel PL, Hauschka PV, Fahey F, Daley GQ. Bone-marrow adipocytes as negative regulators of the haematopoietic microenvironment. *Nature*. 2009;460(7252):259-63.
81. Zhou BO, Yu H, Yue R, Zhao Z, Rios JJ, Naveiras O, et al. Bone marrow adipocytes promote the regeneration of stem cells and haematopoiesis by secreting SCF. *Nat Cell Biol*. 2017;19(8):891-903.
82. Li Z, MacDougald OA. Stem cell factor: the bridge between bone marrow adipocytes and hematopoietic cells. *Haematologica*. 2019;104(9):1689-91.
83. Cuminetti V, Arranz L. Bone Marrow Adipocytes: The Enigmatic Components of the Hematopoietic Stem Cell Niche. *J Clin Med*. 2019;8(5).
84. Li Z, Bowers E, Zhu J, Yu H, Hardij J, Bagchi DP, et al. Lipolysis of bone marrow adipocytes is required to fuel bone and the marrow niche during energy deficits. *Elife*. 2022;11.
85. Mistry JJ, Hellmich C, Moore JA, Jibril A, Macaulay I, Moreno-Gonzalez M, et al. Free fatty-acid transport via CD36 drives β -oxidation-mediated hematopoietic stem cell response to infection. *Nat Commun*. 2021;12(1):7130.
86. Mistry JJ, Bowles K, Rushworth SA. HSC-derived fatty acid oxidation in steady-state and stressed hematopoiesis. *Exp Hematol*. 2023;117:1-8.
87. Hassanshahi M, Hassanshahi A, Khabbazi S, Su YW, Xian CJ. Bone marrow sinusoidal endothelium as a facilitator/regulator of cell egress from the bone marrow. *Crit Rev Oncol Hematol*. 2019;137:43-56.
88. Barnhouse V, Petrikas N, Crosby C, Zoldan J, Harley B. Perivascular Secretome Influences Hematopoietic Stem Cell Maintenance in a Gelatin Hydrogel. *Ann Biomed Eng*. 2021;49(2):780-92.
89. Iga T, Kobayashi H, Kusumoto D, Sanosaka T, Fujita N, Tai-Nagara I, et al. Spatial heterogeneity of bone marrow endothelial cells unveils a distinct subtype in the epiphysis. *Nat Cell Biol*. 2023;25(10):1415-25.
90. Mendelson A, Frenette PS. Hematopoietic stem cell niche maintenance during homeostasis and regeneration. *Nat Med*. 2014;20(8):833-46.
91. Winkler IG, Barbier V, Nowlan B, Jacobsen RN, Forristal CE, Patton JT, et al. Vascular niche E-selectin regulates hematopoietic stem cell dormancy, self renewal and chemoresistance. *Nat Med*. 2012;18(11):1651-7.
92. Rafii S, Shapiro F, Pettengell R, Ferris B, Nachman RL, Moore MA, et al. Human bone marrow microvascular endothelial cells support long-term proliferation and differentiation of myeloid and megakaryocytic progenitors. *Blood*. 1995;86(9):3353-63.
93. Himburg HA, Termini CM, Schlusser L, Kan J, Li M, Zhao L, et al. Distinct Bone Marrow Sources of Pleiotrophin Control Hematopoietic Stem Cell Maintenance and Regeneration. *Cell Stem Cell*. 2018;23(3):370-81.e5.
94. Hao J, Zhou H, Nemes K, Yen D, Zhao W, Bramlett C, et al. Membrane-bound SCF and VCAM-1 synergistically regulate the morphology of hematopoietic stem cells. *J Cell Biol*. 2021;220(10).
95. Shapouri-Moghaddam A, Mohammadian S, Vazini H, Taghadosi M, Esmaeili SA, Mardani F, et al. Macrophage plasticity, polarization, and function in health and disease. *J Cell Physiol*. 2018;233(9):6425-40.
96. Heideveld E, van den Akker E. Digesting the role of bone marrow macrophages on hematopoiesis. *Immunobiology*. 2017;222(6):814-22.

97. Davies LC, Jenkins SJ, Allen JE, Taylor PR. Tissue-resident macrophages. *Nat Immunol.* 2013;14(10):986-95.
98. Kaur S, Raggatt LJ, Batoon L, Hume DA, Levesque JP, Pettit AR. Role of bone marrow macrophages in controlling homeostasis and repair in bone and bone marrow niches. *Semin Cell Dev Biol.* 2017;61:12-21.
99. Chow A, Lucas D, Hidalgo A, Méndez-Ferrer S, Hashimoto D, Scheiermann C, et al. Bone marrow CD169+ macrophages promote the retention of hematopoietic stem and progenitor cells in the mesenchymal stem cell niche. *J Exp Med.* 2011;208(2):261-71.
100. Rosales C. Neutrophil: A Cell with Many Roles in Inflammation or Several Cell Types? *Front Physiol.* 2018;9:113.
101. Stark MA, Huo Y, Burcin TL, Morris MA, Olson TS, Ley K. Phagocytosis of apoptotic neutrophils regulates granulopoiesis via IL-23 and IL-17. *Immunity.* 2005;22(3):285-94.
102. Casanova-Acebes M, Pitaval C, Weiss LA, Nombela-Arrieta C, Chèvre R, A-González N, et al. Rhythmic modulation of the hematopoietic niche through neutrophil clearance. *Cell.* 2013;153(5):1025-35.
103. Wang H, He J, Xu C, Chen X, Yang H, Shi S, et al. Decoding Human Megakaryocyte Development. *Cell Stem Cell.* 2021;28(3):535-49.e8.
104. Bruns I, Lucas D, Pinho S, Ahmed J, Lambert MP, Kunisaki Y, et al. Megakaryocytes regulate hematopoietic stem cell quiescence through CXCL4 secretion. *Nat Med.* 2014;20(11):1315-20.
105. de Graaf CA, Metcalf D. Thrombopoietin and hematopoietic stem cells. *Cell Cycle.* 2011;10(10):1582-9.
106. Abkowitz JL, Chen J. Studies of c-Mpl function distinguish the replication of hematopoietic stem cells from the expansion of differentiating clones. *Blood.* 2007;109(12):5186-90.
107. Fox N, Priestley G, Papayannopoulou T, Kaushansky K. Thrombopoietin expands hematopoietic stem cells after transplantation. *J Clin Invest.* 2002;110(3):389-94.
108. Qian H, Buza-Vidas N, Hyland CD, Jensen CT, Antonchuk J, Månsson R, et al. Critical role of thrombopoietin in maintaining adult quiescent hematopoietic stem cells. *Cell Stem Cell.* 2007;1(6):671-84.
109. Alvarez MB, Xu L, Childress PJ, Maupin KA, Mohamad SF, Chitteti BR, et al. Megakaryocyte and Osteoblast Interactions Modulate Bone Mass and Hematopoiesis. *Stem Cells Dev.* 2018;27(10):671-82.
110. Oburoglu L, Tardito S, Fritz V, de Barros SC, Merida P, Craveiro M, et al. Glucose and glutamine metabolism regulate human hematopoietic stem cell lineage specification. *Cell Stem Cell.* 2014;15(2):169-84.
111. Hui S, Ghergurovich JM, Morscher RJ, Jang C, Teng X, Lu W, et al. Glucose feeds the TCA cycle via circulating lactate. *Nature.* 2017;551(7678):115-8.
112. Luo ST, Zhang DM, Qin Q, Lu L, Luo M, Guo FC, et al. The Promotion of Erythropoiesis via the Regulation of Reactive Oxygen Species by Lactic Acid. *Sci Rep.* 2017;7:38105.
113. Kolditz CI, Langin D. Adipose tissue lipolysis. *Curr Opin Clin Nutr Metab Care.* 2010;13(4):377-81.
114. Maynard RS, Hellmich C, Bowles KM, Rushworth SA. Acute Myeloid Leukaemia Drives Metabolic Changes in the Bone Marrow Niche. *Front Oncol.* 2022;12:924567.
115. Mistry JJ, Marlein CR, Moore JA, Hellmich C, Wojtowicz EE, Smith JGW, et al. ROS-mediated PI3K activation drives mitochondrial transfer from stromal cells to hematopoietic stem cells in response to infection. *Proc Natl Acad Sci U S A.* 2019;116(49):24610-9.

116. UK Bc. Facts and information about blood cancer <https://bloodcancer.org.uk/news/blood-cancer-facts/August> 2022 [Available from: <https://bloodcancer.org.uk/news/blood-cancer-facts/>].
117. Zhang N, Wu J, Wang Q, Liang Y, Li X, Chen G, et al. Global burden of hematologic malignancies and evolution patterns over the past 30 years. *Blood Cancer J.* 2023;13(1):82.
118. Mitra A, Barua A, Huang L, Ganguly S, Feng Q, He B. From bench to bedside: the history and progress of CAR T cell therapy. *Front Immunol.* 2023;14:1188049.
119. Fuertes T, Álvarez-Corrales E, Gómez-Escolar C, Ubieto-Capella P, Serrano-Navarro Á, de Molina A, et al. miR-28-based combination therapy impairs aggressive B cell lymphoma growth by rewiring DNA replication. *Cell Death Dis.* 2023;14(10):687.
120. Mirzaie M, Gholizadeh E, Miettinen JJ, Ianevski F, Ruokoranta T, Saarela J, et al. Designing patient-oriented combination therapies for acute myeloid leukemia based on efficacy/toxicity integration and bipartite network modeling. *Oncogenesis.* 2024;13(1):11.
121. Lewis WD, Lilly S, Jones KL. Lymphoma: Diagnosis and Treatment. *Am Fam Physician.* 2020;101(1):34-41.
122. Weniger MA, Küppers R. Molecular biology of Hodgkin lymphoma. *Leukemia.* 2021;35(4):968-81.
123. Singh R, Shaik S, Negi BS, Rajguru JP, Patil PB, Parihar AS, et al. Non-Hodgkin's lymphoma: A review. *J Family Med Prim Care.* 2020;9(4):1834-40.
124. Nassef Kadry Naguib Roufaiel M, Wells JW, Steptoe RJ. Impaired T-Cell Function in B-Cell Lymphoma: A Direct Consequence of Events at the Immunological Synapse? *Front Immunol.* 2015;6:258.
125. Le K, Sun J, Khawaja H, Shibata M, Maggirwar SB, Smith MR, et al. Mantle cell lymphoma polarizes tumor-associated macrophages into M2-like macrophages, which in turn promote tumorigenesis. *Blood Adv.* 2021;5(14):2863-78.
126. Flowers CR, Leonard JP, Nastoupil LJ. Novel immunotherapy approaches to follicular lymphoma. *Hematology Am Soc Hematol Educ Program.* 2018;2018(1):194-9.
127. Raab MS, Podar K, Breitkreutz I, Richardson PG, Anderson KC. Multiple myeloma. *Lancet.* 2009;374(9686):324-39.
128. Chanan-Khan AA, San Miguel JF, Jagannath S, Ludwig H, Dimopoulos MA. Novel therapeutic agents for the management of patients with multiple myeloma and renal impairment. *Clin Cancer Res.* 2012;18(8):2145-63.
129. Rosko A, Giralt S, Mateos MV, Dispenzieri A. Myeloma in Elderly Patients: When Less Is More and More Is More. *Am Soc Clin Oncol Educ Book.* 2017;37:575-85.
130. Cancer Stat Facts: Myeloma: National Institutes of Health. Surveillance, Epidemiology, and End Results Program.; 2020 [Available from: <https://seer.cancer.gov/statfacts/html/mulmy.html>].
131. Lust JA, Lacy MQ, Zeldenrust SR, Witzig TE, Moon-Tasson LL, Dinarello CA, et al. Reduction in C-reactive protein indicates successful targeting of the IL-1/IL-6 axis resulting in improved survival in early stage multiple myeloma. *Am J Hematol.* 2016;91(6):571-4.
132. Akhmetzyanova I, McCarron MJ, Parekh S, Chesi M, Bergsagel PL, Fooksman DR. Dynamic CD138 surface expression regulates switch between myeloma growth and dissemination. *Leukemia.* 2020;34(1):245-56.
133. Rajkumar SV, Kumar S. Multiple myeloma current treatment algorithms. *Blood Cancer J.* 2020;10(9):94.

134. Sheykhasan M, Ahmadih-Yazdi A, Vicidomini R, Poondla N, Tanzadehpanah H, Dirbaziyan A, et al. CAR T therapies in multiple myeloma: unleashing the future. *Cancer Gene Ther.* 2024;31(5):667-86.
135. Manier S, Ingegnere T, Escure G, Prodhomme C, Nudel M, Mitra S, et al. Current state and next-generation CAR-T cells in multiple myeloma. *Blood Rev.* 2022;54:100929.
136. Li H, Zhao L, Sun Z, Yao Y, Li L, Wang J, et al. Prolonged hematological toxicity in patients receiving BCMA/CD19 CAR-T-cell therapy for relapsed or refractory multiple myeloma. *Front Immunol.* 2022;13:1019548.
137. Ottensmeier C. The classification of lymphomas and leukemias. *Chem Biol Interact.* 2001;135-136:653-64.
138. Bakst R, Powers A, Yahalom J. Diagnostic and Therapeutic Considerations for Extramedullary Leukemia. *Curr Oncol Rep.* 2020;22(7):75.
139. Szczepański T, van der Velden VH, van Dongen JJ. Classification systems for acute and chronic leukaemias. *Best Pract Res Clin Haematol.* 2003;16(4):561-82.
140. Onciu M. Acute lymphoblastic leukemia. *Hematol Oncol Clin North Am.* 2009;23(4):655-74.
141. Chiarini F, Lonetti A, Evangelisti C, Buontempo F, Orsini E, Cappellini A, et al. Advances in understanding the acute lymphoblastic leukemia bone marrow microenvironment: From biology to therapeutic targeting. *Biochim Biophys Acta.* 2016;1863(3):449-63.
142. Chiu M, Taurino G, Dander E, Bardelli D, Fallati A, Andreoli R, et al. ALL blasts drive primary mesenchymal stromal cells to increase asparagine availability during asparaginase treatment. *Blood Adv.* 2021;5(23):5164-78.
143. Juarez J, Bradstock KF, Gottlieb DJ, Bendall LJ. Effects of inhibitors of the chemokine receptor CXCR4 on acute lymphoblastic leukemia cells in vitro. *Leukemia.* 2003;17(7):1294-300.
144. Vilchis-Ordoñez A, Contreras-Quiroz A, Vadillo E, Dorantes-Acosta E, Reyes-López A, Quintela-Nuñez del Prado HM, et al. Bone Marrow Cells in Acute Lymphoblastic Leukemia Create a Proinflammatory Microenvironment Influencing Normal Hematopoietic Differentiation Fates. *Biomed Res Int.* 2015;2015:386165.
145. Hawkins ED, Duarte D, Akinduro O, Khorshed RA, Passaro D, Nowicka M, et al. T-cell acute leukaemia exhibits dynamic interactions with bone marrow microenvironments. *Nature.* 2016;538(7626):518-22.
146. Döhner H, Weisdorf DJ, Bloomfield CD. Acute Myeloid Leukemia. *N Engl J Med.* 2015;373(12):1136-52.
147. Stelmach P, Trumpp A. Leukemic stem cells and therapy resistance in acute myeloid leukemia. *Haematologica.* 2023;108(2):353-66.
148. Sasaki K, Ravandi F, Kadia TM, DiNardo CD, Short NJ, Borthakur G, et al. De novo acute myeloid leukemia: A population-based study of outcome in the United States based on the Surveillance, Epidemiology, and End Results (SEER) database, 1980 to 2017. *Cancer.* 2021;127(12):2049-61.
149. Liu H. Emerging agents and regimens for AML. *J Hematol Oncol.* 2021;14(1):49.
150. Haferlach T. Advancing leukemia diagnostics: Role of Next Generation Sequencing (NGS) in acute myeloid leukemia. *Hematol Rep.* 2020;12(Suppl 1):8957.
151. Ley TJ, Miller C, Ding L, Raphael BJ, Mungall AJ, Robertson A, et al. Genomic and epigenomic landscapes of adult de novo acute myeloid leukemia. *N Engl J Med.* 2013;368(22):2059-74.
152. Stirewalt DL, Radich JP. The role of FLT3 in haematopoietic malignancies. *Nat Rev Cancer.* 2003;3(9):650-65.

153. Papaemmanuil E, Gerstung M, Bullinger L, Gaidzik VI, Paschka P, Roberts ND, et al. Genomic Classification and Prognosis in Acute Myeloid Leukemia. *N Engl J Med*. 2016;374(23):2209-21.
154. Mishra SR, Rawal L, Othman MAK, Thatai A, Sarkar A, Lal V, et al. Complex rearrangement in acute myeloid leukemia M2 with RUNX1/RUNX1T1 fusion involving chromosomes 8, 17 and 21. *Mol Cytogenet*. 2021;14(1):28.
155. Kamath-Loeb AS, Shen JC, Schmitt MW, Kohn BF, Loeb KR, Estey EH, et al. Accurate detection of subclonal variants in paired diagnosis-relapse acute myeloid leukemia samples by next generation Duplex Sequencing. *Leuk Res*. 2022;115:106822.
156. Tomaszewski EL, Fickley CE, Maddux L, Krupnick R, Bahceci E, Paty J, et al. The Patient Perspective on Living with Acute Myeloid Leukemia. *Oncol Ther*. 2016;4(2):225-38.
157. Campelj DG, Timpani CA, Rybalka E. Cachectic muscle wasting in acute myeloid leukaemia: a sleeping giant with dire clinical consequences. *J Cachexia Sarcopenia Muscle*. 2022;13(1):42-54.
158. Rashidi A. Cachexia during anti-leukemia chemotherapy: it is not "just" the chemo. *Haematologica*. 2024.
159. Döhner H, Estey E, Grimwade D, Amadori S, Appelbaum FR, Büchner T, et al. Diagnosis and management of AML in adults: 2017 ELN recommendations from an international expert panel. *Blood*. 2017;129(4):424-47.
160. Khoury JD, Solary E, Abla O, Akkari Y, Alaggio R, Apperley JF, et al. The 5th edition of the World Health Organization Classification of Haematolymphoid Tumours: Myeloid and Histiocytic/Dendritic Neoplasms. *Leukemia*. 2022;36(7):1703-19.
161. Bertoli S, Tavitian S, Huynh A, Borel C, Guenounou S, Luquet I, et al. Improved outcome for AML patients over the years 2000-2014. *Blood Cancer J*. 2017;7(12):635.
162. Döhner H, Wei AH, Appelbaum FR, Craddock C, DiNardo CD, Dombret H, et al. Diagnosis and management of AML in adults: 2022 recommendations from an international expert panel on behalf of the ELN. *Blood*. 2022;140(12):1345-77.
163. He P, Liang J, Zhang W, Lin S, Wu H, Li Q, et al. Hematopoietic Stem Cell Transplantation for Acute Myeloid Leukemia: An Overview of Systematic Reviews. *Int J Clin Pract*. 2022;2022:1828223.
164. Murphy T, Yee KWL. Cytarabine and daunorubicin for the treatment of acute myeloid leukemia. *Expert Opin Pharmacother*. 2017;18(16):1765-80.
165. Larrosa-Garcia M, Baer MR. FLT3 Inhibitors in Acute Myeloid Leukemia: Current Status and Future Directions. *Mol Cancer Ther*. 2017;16(6):991-1001.
166. Souers AJ, Levenson JD, Boghaert ER, Ackler SL, Catron ND, Chen J, et al. ABT-199, a potent and selective BCL-2 inhibitor, achieves antitumor activity while sparing platelets. *Nat Med*. 2013;19(2):202-8.
167. Roberts AW. Therapeutic development and current uses of BCL-2 inhibition. *Hematology Am Soc Hematol Educ Program*. 2020;2020(1):1-9.
168. DiNardo CD, Pratz KW, Letai A, Jonas BA, Wei AH, Thirman M, et al. Safety and preliminary efficacy of venetoclax with decitabine or azacitidine in elderly patients with previously untreated acute myeloid leukaemia: a non-randomised, open-label, phase 1b study. *Lancet Oncol*. 2018;19(2):216-28.
169. Guy DG, Uy GL. Bispecific Antibodies for the Treatment of Acute Myeloid Leukemia. *Curr Hematol Malig Rep*. 2018;13(6):417-25.
170. Kubicka E, Lum LG, Huang M, Thakur A. Bispecific antibody-targeted T-cell therapy for acute myeloid leukemia. *Front Immunol*. 2022;13:899468.
171. Mehta NK, Pfluegler M, Meetze K, Li B, Sindel I, Vogt F, et al. A novel IgG-based FLT3xCD3 bispecific antibody for the treatment of AML and B-ALL. *J Immunother Cancer*. 2022;10(3).

172. Boucher JC, Shrestha B, Vishwasrao P, Leick M, Cervantes EV, Ghafoor T, et al. Bispecific CD33/CD123 targeted chimeric antigen receptor T cells for the treatment of acute myeloid leukemia. *Mol Ther Oncolytics*. 2023;31:100751.
173. Ladikou EE, Sivaloganathan H, Pepper A, Chevassut T. Acute Myeloid Leukaemia in Its Niche: the Bone Marrow Microenvironment in Acute Myeloid Leukaemia. *Curr Oncol Rep*. 2020;22(3):27.
174. Barbier V, Erhani J, Fiveash C, Davies JM, Tay J, Tallack MR, et al. Endothelial E-selectin inhibition improves acute myeloid leukaemia therapy by disrupting vascular niche-mediated chemoresistance. *Nat Commun*. 2020;11(1):2042.
175. Cheng J, Li Y, Liu S, Jiang Y, Ma J, Wan L, et al. CXCL8 derived from mesenchymal stromal cells supports survival and proliferation of acute myeloid leukemia cells through the PI3K/AKT pathway. *FASEB J*. 2019;33(4):4755-64.
176. Pal D, Blair H, Parker J, Hockney S, Beckett M, Singh M, et al. hiPSC-derived bone marrow milieu identifies a clinically actionable driver of niche-mediated treatment resistance in leukemia. *Cell Rep Med*. 2022;3(8):100717.
177. Miraki-Moud F, Anjos-Afonso F, Hodby KA, Griessinger E, Rosignoli G, Lillington D, et al. Acute myeloid leukemia does not deplete normal hematopoietic stem cells but induces cytopenias by impeding their differentiation. *Proc Natl Acad Sci U S A*. 2013;110(33):13576-81.
178. Garrido SM, Appelbaum FR, Willman CL, Banker DE. Acute myeloid leukemia cells are protected from spontaneous and drug-induced apoptosis by direct contact with a human bone marrow stromal cell line (HS-5). *Exp Hematol*. 2001;29(4):448-57.
179. Heasman SA, Zaitseva L, Bowles KM, Rushworth SA, Macewan DJ. Protection of acute myeloid leukaemia cells from apoptosis induced by front-line chemotherapeutics is mediated by haem oxygenase-1. *Oncotarget*. 2011;2(9):658-68.
180. Palani HK, Ganesan S, Balasundaram N, Venkatraman A, Korula A, Abraham A, et al. Ablation of Wnt signaling in bone marrow stromal cells overcomes microenvironment-mediated drug resistance in acute myeloid leukemia. *Sci Rep*. 2024;14(1):8404.
181. Salazar-Terreros MJ, Vernot JP. In Vitro and In Vivo Modeling of Normal and Leukemic Bone Marrow Niches: Cellular Senescence Contribution to Leukemia Induction and Progression. *Int J Mol Sci*. 2022;23(13).
182. Hellmich C, Moore JA, Bowles KM, Rushworth SA. Bone Marrow Senescence and the Microenvironment of Hematological Malignancies. *Front Oncol*. 2020;10:230.
183. Ruiz-Aparicio PF, Vernot JP. Bone Marrow Aging and the Leukaemia-Induced Senescence of Mesenchymal Stem/Stromal Cells: Exploring Similarities. *J Pers Med*. 2022;12(5).
184. Ladikou EE, Chevassut T, Pepper CJ, Pepper AG. Dissecting the role of the CXCL12/CXCR4 axis in acute myeloid leukaemia. *Br J Haematol*. 2020;189(5):815-25.
185. Rettig MP, Anstas G, DiPersio JF. Mobilization of hematopoietic stem and progenitor cells using inhibitors of CXCR4 and VLA-4. *Leukemia*. 2012;26(1):34-53.
186. Nervi B, Ramirez P, Rettig MP, Uy GL, Holt MS, Ritchey JK, et al. Chemosensitization of acute myeloid leukemia (AML) following mobilization by the CXCR4 antagonist AMD3100. *Blood*. 2009;113(24):6206-14.
187. Tabe Y, Yamamoto S, Saitoh K, Sekihara K, Monma N, Ikeo K, et al. Bone Marrow Adipocytes Facilitate Fatty Acid Oxidation Activating AMPK and a Transcriptional Network Supporting Survival of Acute Monocytic Leukemia Cells. *Cancer Res*. 2017;77(6):1453-64.

188. Samudio I, Harmancey R, Fiegl M, Kantarjian H, Konopleva M, Korchin B, et al. Pharmacologic inhibition of fatty acid oxidation sensitizes human leukemia cells to apoptosis induction. *J Clin Invest*. 2010;120(1):142-56.
189. Boyd AL, Reid JC, Salci KR, Aslostovar L, Benoit YD, Shapovalova Z, et al. Acute myeloid leukaemia disrupts endogenous myelo-erythropoiesis by compromising the adipocyte bone marrow niche. *Nat Cell Biol*. 2017;19(11):1336-47.
190. Ayala F, Dewar R, Kieran M, Kalluri R. Contribution of bone microenvironment to leukemogenesis and leukemia progression. *Leukemia*. 2009;23(12):2233-41.
191. Oster W, Cicco NA, Klein H, Hirano T, Kishimoto T, Lindemann A, et al. Participation of the cytokines interleukin 6, tumor necrosis factor-alpha, and interleukin 1-beta secreted by acute myelogenous leukemia blasts in autocrine and paracrine leukemia growth control. *J Clin Invest*. 1989;84(2):451-7.
192. Zhang J, Ye J, Ma D, Liu N, Wu H, Yu S, et al. Cross-talk between leukemic and endothelial cells promotes angiogenesis by VEGF activation of the Notch/Dll4 pathway. *Carcinogenesis*. 2013;34(3):667-77.
193. Fiedler W, Graeven U, Ergün S, Verago S, Kilic N, Stockschräder M, et al. Vascular endothelial growth factor, a possible paracrine growth factor in human acute myeloid leukemia. *Blood*. 1997;89(6):1870-5.
194. Chao MP, Takimoto CH, Feng DD, McKenna K, Gip P, Liu J, et al. Therapeutic Targeting of the Macrophage Immune Checkpoint CD47 in Myeloid Malignancies. *Front Oncol*. 2019;9:1380.
195. Lin F, Xiong M, Hao W, Song Y, Liu R, Yang Y, et al. A Novel Blockade CD47 Antibody With Therapeutic Potential for Cancer. *Front Oncol*. 2020;10:615534.
196. Zhang W, Huang Q, Xiao W, Zhao Y, Pi J, Xu H, et al. Advances in Anti-Tumor Treatments Targeting the CD47/SIRP α Axis. *Front Immunol*. 2020;11:18.
197. Al-Matary YS, Botezatu L, Opalka B, Hönes JM, Lams RF, Thivakaran A, et al. Acute myeloid leukemia cells polarize macrophages towards a leukemia supporting state in a Growth factor independence 1 dependent manner. *Haematologica*. 2016;101(10):1216-27.
198. Moore JA, Mistry JJ, Hellmich C, Horton RH, Wojtowicz EE, Jibril A, et al. LC3-associated phagocytosis in bone marrow macrophages suppresses acute myeloid leukemia progression through STING activation. *J Clin Invest*. 2022;132(5).
199. WARBURG O. On the origin of cancer cells. *Science*. 1956;123(3191):309-14.
200. Suganuma K, Miwa H, Imai N, Shikami M, Gotou M, Goto M, et al. Energy metabolism of leukemia cells: glycolysis versus oxidative phosphorylation. *Leuk Lymphoma*. 2010;51(11):2112-9.
201. Poulain L, Sujobert P, Zylbersztejn F, Barreau S, Stuani L, Lambert M, et al. High mTORC1 activity drives glycolysis addiction and sensitivity to G6PD inhibition in acute myeloid leukemia cells. *Leukemia*. 2017;31(11):2326-35.
202. Song K, Li M, Xu X, Xuan LI, Huang G, Liu Q. Resistance to chemotherapy is associated with altered glucose metabolism in acute myeloid leukemia. *Oncol Lett*. 2016;12(1):334-42.
203. Grenier A, Poulain L, Mondesir J, Jacquelin A, Bosc C, Stuani L, et al. AMPK-PERK axis represses oxidative metabolism and enhances apoptotic priming of mitochondria in acute myeloid leukemia. *Cell Rep*. 2022;38(1):110197.
204. Mesbahi Y, Trahair TN, Lock RB, Connerty P. Exploring the Metabolic Landscape of AML: From Haematopoietic Stem Cells to Myeloblasts and Leukaemic Stem Cells. *Front Oncol*. 2022;12:807266.
205. Cheng Z, Ristow M. Mitochondria and metabolic homeostasis. *Antioxid Redox Signal*. 2013;19(3):240-2.

206. Fernie AR, Carrari F, Sweetlove LJ. Respiratory metabolism: glycolysis, the TCA cycle and mitochondrial electron transport. *Curr Opin Plant Biol.* 2004;7(3):254-61.
207. Moschoi R, Imbert V, Nebout M, Chiche J, Mary D, Prebet T, et al. Protective mitochondrial transfer from bone marrow stromal cells to acute myeloid leukemic cells during chemotherapy. *Blood.* 2016;128(2):253-64.
208. Guo X, Can C, Liu W, Wei Y, Yang X, Liu J, et al. Mitochondrial transfer in hematological malignancies. *Biomark Res.* 2023;11(1):89.
209. Marlein CR, Zaitseva L, Piddock RE, Robinson SD, Edwards DR, Shafat MS, et al. NADPH oxidase-2 derived superoxide drives mitochondrial transfer from bone marrow stromal cells to leukemic blasts. *Blood.* 2017;130(14):1649-60.
210. Mistry JJ, Moore JA, Kumar P, Marlein CR, Hellmich C, Pillinger G, et al. Daratumumab inhibits acute myeloid leukaemia metabolic capacity by blocking mitochondrial transfer from mesenchymal stromal cells. *Haematologica.* 2021;106(2):589-92.
211. Farber M, Chen Y, Arnold L, Möllmann M, Boog-Whiteside E, Lin YA, et al. Targeting CD38 in acute myeloid leukemia interferes with leukemia trafficking and induces phagocytosis. *Sci Rep.* 2021;11(1):22062.
212. Naik J, Themeli M, de Jong-Korlaar R, Ruiters RWJ, Poddighe PJ, Yuan H, et al. CD38 as a therapeutic target for adult acute myeloid leukemia and T-cell acute lymphoblastic leukemia. *Haematologica.* 2019;104(3):e100-e3.
213. Fu HZ, Xiaomei., He S, Li J, Liu Y. CX43-Mediated Mitochondria Transfer from Bone Marrow Stromal Cells Promotes the Stemness of Leukemia Stem Cells. *Blood.* 2022;140.
214. Glytsou C, Chen X, Zacharioudakis E, Al-Santli W, Zhou H, Nadorp B, et al. Mitophagy Promotes Resistance to BH3 Mimetics in Acute Myeloid Leukemia. *Cancer Discov.* 2023;13(7):1656-77.
215. Nguyen TD, Shaid S, Vakhrusheva O, Koschade SE, Klann K, Thölken M, et al. Loss of the selective autophagy receptor p62 impairs murine myeloid leukemia progression and mitophagy. *Blood.* 2019;133(2):168-79.
216. Wei Z, Liu X, Cheng C, Yu W, Yi P. Metabolism of Amino Acids in Cancer. *Front Cell Dev Biol.* 2020;8:603837.
217. Jacque N, Ronchetti AM, Larrue C, Meunier G, Birsén R, Willems L, et al. Targeting glutaminolysis has antileukemic activity in acute myeloid leukemia and synergizes with BCL-2 inhibition. *Blood.* 2015;126(11):1346-56.
218. Cormerais Y, Massard PA, Vucetic M, Giuliano S, Tambutté E, Durivault J, et al. The glutamine transporter ASCT2 (SLC1A5) promotes tumor growth independently of the amino acid transporter LAT1 (SLC7A5). *J Biol Chem.* 2018;293(8):2877-87.
219. Jones CL, Stevens BM, D'Alessandro A, Reisz JA, Culp-Hill R, Nemkov T, et al. Inhibition of Amino Acid Metabolism Selectively Targets Human Leukemia Stem Cells. *Cancer Cell.* 2018;34(5):724-40.e4.
220. Yang L, Venneti S, Nagrath D. Glutaminolysis: A Hallmark of Cancer Metabolism. *Annu Rev Biomed Eng.* 2017;19:163-94.
221. Rinaldo P, Matern D, Bennett MJ. Fatty acid oxidation disorders. *Annu Rev Physiol.* 2002;64:477-502.
222. de Carvalho CCCR, Caramujo MJ. The Various Roles of Fatty Acids. *Molecules.* 2018;23(10).
223. Grygiel-Górniak B. Peroxisome proliferator-activated receptors and their ligands: nutritional and clinical implications--a review. *Nutr J.* 2014;13:17.
224. Krey G, Braissant O, L'Horsset F, Kalkhoven E, Perroud M, Parker MG, et al. Fatty acids, eicosanoids, and hypolipidemic agents identified as ligands of

peroxisome proliferator-activated receptors by coactivator-dependent receptor ligand assay. *Mol Endocrinol.* 1997;11(6):779-91.

225. Varga T, Czimmerer Z, Nagy L. PPARs are a unique set of fatty acid regulated transcription factors controlling both lipid metabolism and inflammation. *Biochim Biophys Acta.* 2011;1812(8):1007-22.

226. Hegarty BD, Furler SM, Oakes ND, Kraegen EW, Cooney GJ. Peroxisome proliferator-activated receptor (PPAR) activation induces tissue-specific effects on fatty acid uptake and metabolism in vivo--a study using the novel PPARalpha/gamma agonist tesaglitazar. *Endocrinology.* 2004;145(7):3158-64.

227. Wagner N, Wagner KD. Peroxisome Proliferator-Activated Receptors and the Hallmarks of Cancer. *Cells.* 2022;11(15).

228. Armstrong EH, Goswami D, Griffin PR, Noy N, Ortlund EA. Structural basis for ligand regulation of the fatty acid-binding protein 5, peroxisome proliferator-activated receptor β/δ (FABP5-PPAR β/δ) signaling pathway. *J Biol Chem.* 2014;289(21):14941-54.

229. Zhong Q, Zhao S, Yu B, Wang X, Matyal R, Li Y, et al. High-density lipoprotein increases the uptake of oxidized low density lipoprotein via PPAR γ /CD36 pathway in inflammatory adipocytes. *Int J Biol Sci.* 2015;11(3):256-65.

230. Shang K, Ma N, Che J, Li H, Hu J, Sun H, et al. SLC27A2 mediates FAO in colorectal cancer through nongenetic crosstalk regulation of the PPARs pathway. *BMC Cancer.* 2023;23(1):335.

231. Ong KT, Mashek MT, Davidson NO, Mashek DG. Hepatic ATGL mediates PPAR- α signaling and fatty acid channeling through an L-FABP independent mechanism. *J Lipid Res.* 2014;55(5):808-15.

232. Tabe Y, Konopleva M, Andreeff M. Fatty Acid Metabolism, Bone Marrow Adipocytes, and AML. *Front Oncol.* 2020;10:155.

233. Khalid A, Siddiqui AJ, Huang JH, Shamsi T, Musharraf SG. Alteration of Serum Free Fatty Acids are Indicators for Progression of Pre-leukaemia Diseases to Leukaemia. *Sci Rep.* 2018;8(1):14883.

234. Ye H, Adane B, Khan N, Sullivan T, Minhajuddin M, Gasparetto M, et al. Leukemic Stem Cells Evade Chemotherapy by Metabolic Adaptation to an Adipose Tissue Niche. *Cell Stem Cell.* 2016;19(1):23-37.

235. Zhang Y, Guo H, Zhang Z, Lu W, Zhu J, Shi J. IL-6 promotes chemoresistance via upregulating CD36 mediated fatty acids uptake in acute myeloid leukemia. *Exp Cell Res.* 2022;415(1):113112.

236. Åbacka H, Masoni S, Poli G, Huang P, Gusso F, Granchi C, et al. SMS121, a new inhibitor of CD36, impairs fatty acid uptake and viability of acute myeloid leukemia. *Sci Rep.* 2024;14(1):9104.

237. Lu W, Wan Y, Li Z, Zhu B, Yin C, Liu H, et al. Growth differentiation factor 15 contributes to marrow adipocyte remodeling in response to the growth of leukemic cells. *J Exp Clin Cancer Res.* 2018;37(1):66.

238. Tabe Y, Saitoh K, Yang H, Sekihara K, Yamatani K, Ruvolo V, et al. Inhibition of FAO in AML co-cultured with BM adipocytes: mechanisms of survival and chemosensitization to cytarabine. *Sci Rep.* 2018;8(1):16837.

239. Stanger BZ. Cellular homeostasis and repair in the mammalian liver. *Annu Rev Physiol.* 2015;77:179-200.

240. Jungermann K, Katz N. Functional specialization of different hepatocyte populations. *Physiol Rev.* 1989;69(3):708-64.

241. Boyer JL, Soroka CJ. Bile formation and secretion: An update. *J Hepatol.* 2021;75(1):190-201.

242. Kubes P, Jenne C. Immune Responses in the Liver. *Annu Rev Immunol.* 2018;36:247-77.

243. Kozeniecki M, Ludke R, Kerner J, Patterson B. Micronutrients in Liver Disease: Roles, Risk Factors for Deficiency, and Recommendations for Supplementation. *Nutr Clin Pract*. 2020;35(1):50-62.
244. Alves-Bezerra M, Cohen DE. Triglyceride Metabolism in the Liver. *Compr Physiol*. 2017;8(1):1-8.
245. Umpleby AM, Shojaee-Moradie F, Fielding B, Li X, Marino A, Alsini N, et al. Impact of liver fat on the differential partitioning of hepatic triacylglycerol into VLDL subclasses on high and low sugar diets. *Clin Sci (Lond)*. 2017;131(21):2561-73.
246. Lee SH, Veeriah V, Levine F. Liver fat storage is controlled by HNF4 α through induction of lipophagy and is reversed by a potent HNF4 α agonist. *Cell Death Dis*. 2021;12(6):603.
247. Kaibori M, Kwon AH, Oda M, Kamiyama Y, Kitamura N, Okumura T. Hepatocyte growth factor stimulates synthesis of lipids and secretion of lipoproteins in rat hepatocytes. *Hepatology*. 1998;27(5):1354-61.
248. Azzu V, Vacca M, Virtue S, Allison M, Vidal-Puig A. Adipose Tissue-Liver Cross Talk in the Control of Whole-Body Metabolism: Implications in Nonalcoholic Fatty Liver Disease. *Gastroenterology*. 2020;158(7):1899-912.
249. Younossi Z, Anstee QM, Marietti M, Hardy T, Henry L, Eslam M, et al. Global burden of NAFLD and NASH: trends, predictions, risk factors and prevention. *Nat Rev Gastroenterol Hepatol*. 2018;15(1):11-20.
250. Flint TR, Janowitz T, Connell CM, Roberts EW, Denton AE, Coll AP, et al. Tumor-Induced IL-6 Reprograms Host Metabolism to Suppress Anti-tumor Immunity. *Cell Metab*. 2016;24(5):672-84.
251. Kmieć Z. Introduction — Morphology of the Liver Lobule.

In: Cooperation of Liver Cells in Health and Disease. *Advances in Anatomy Embryology and Cell Biology*. Berlin, Heidelberg: Springer; 2001.

252. Nguyen-Lefebvre AT, Horuzsko A. Kupffer Cell Metabolism and Function. *J Enzymol Metab*. 2015;1(1).
253. Doulatov S, Notta F, Eppert K, Nguyen LT, Ohashi PS, Dick JE. Revised map of the human progenitor hierarchy shows the origin of macrophages and dendritic cells in early lymphoid development. *Nat Immunol*. 2010;11(7):585-93.
254. Bykov I, Ylipaasto P, Eerola L, Lindros KO. Phagocytosis and LPS-stimulated production of cytokines and prostaglandin E2 is different in Kupffer cells isolated from the periportal or perivenous liver region. *Scand J Gastroenterol*. 2003;38(12):1256-61.
255. Corbitt N, Kimura S, Isse K, Specht S, Chedwick L, Rosborough BR, et al. Gut bacteria drive Kupffer cell expansion via MAMP-mediated ICAM-1 induction on sinusoidal endothelium and influence preservation-reperfusion injury after orthotopic liver transplantation. *Am J Pathol*. 2013;182(1):180-91.
256. Bykov I, Ylipaasto P, Eerola L, Lindros KO. Functional Differences between Periportal and Perivenous Kupffer Cells Isolated by Digitonin-Collagenase Perfusion. *Comp Hepatol*. 2004;3 Suppl 1(Suppl 1):S34.
257. Thurman RG, Bradford BU, Iimuro Y, Knecht KT, Connor HD, Adachi Y, et al. Role of Kupffer cells, endotoxin and free radicals in hepatotoxicity due to prolonged alcohol consumption: studies in female and male rats. *J Nutr*. 1997;127(5 Suppl):903S-6S.
258. Terpstra V, van Berkel TJ. Scavenger receptors on liver Kupffer cells mediate the in vivo uptake of oxidatively damaged red blood cells in mice. *Blood*. 2000;95(6):2157-63.

259. Cogliati B, Yashaswini CN, Wang S, Sia D, Friedman SL. Friend or foe? The elusive role of hepatic stellate cells in liver cancer. *Nat Rev Gastroenterol Hepatol*. 2023;20(10):647-61.
260. Puche JE, Saiman Y, Friedman SL. Hepatic stellate cells and liver fibrosis. *Compr Physiol*. 2013;3(4):1473-92.
261. Geerts A. History, heterogeneity, developmental biology, and functions of quiescent hepatic stellate cells. *Semin Liver Dis*. 2001;21(3):311-35.
262. Huang Z, Liu Y, Qi G, Brand D, Zheng SG. Role of Vitamin A in the Immune System. *J Clin Med*. 2018;7(9).
263. Liu C, Li J, Xiang X, Guo L, Tu K, Liu Q, et al. PDGF receptor- α promotes TGF- β signaling in hepatic stellate cells via transcriptional and posttranscriptional regulation of TGF- β receptors. *Am J Physiol Gastrointest Liver Physiol*. 2014;307(7):G749-59.
264. Garbuzenko DV. Pathophysiological mechanisms of hepatic stellate cells activation in liver fibrosis. *World J Clin Cases*. 2022;10(12):3662-76.
265. Lee Y, Leslie J, Yang Y, Ding L. Hepatic stellate and endothelial cells maintain hematopoietic stem cells in the developing liver. *J Exp Med*. 2021;218(3).
266. Yu MC, Chen CH, Liang X, Wang L, Gandhi CR, Fung JJ, et al. Inhibition of T-cell responses by hepatic stellate cells via B7-H1-mediated T-cell apoptosis in mice. *Hepatology*. 2004;40(6):1312-21.
267. Ishibashi H, Nakamura M, Komori A, Migita K, Shimoda S. Liver architecture, cell function, and disease. *Semin Immunopathol*. 2009;31(3):399-409.
268. Martini T, Naef F, Tchorz JS. Spatiotemporal Metabolic Liver Zonation and Consequences on Pathophysiology. *Annu Rev Pathol*. 2023;18:439-66.
269. Trefts E, Gannon M, Wasserman DH. The liver. *Curr Biol*. 2017;27(21):R1147-R51.
270. Iyanagi T. Molecular mechanism of phase I and phase II drug-metabolizing enzymes: implications for detoxification. *Int Rev Cytol*. 2007;260:35-112.
271. Castell JV, Jover R, Martínez-Jiménez CP, Gómez-Lechón MJ. Hepatocyte cell lines: their use, scope and limitations in drug metabolism studies. *Expert Opin Drug Metab Toxicol*. 2006;2(2):183-212.
272. Mizoi K, Arakawa H, Yano K, Koyama S, Kojima H, Ogihara T. Utility of Three-Dimensional Cultures of Primary Human Hepatocytes (Spheroids) as Pharmacokinetic Models. *Biomedicines*. 2020;8(10).
273. Hart SN, Wang S, Nakamoto K, Wesselman C, Li Y, Zhong XB. Genetic polymorphisms in cytochrome P450 oxidoreductase influence microsomal P450-catalyzed drug metabolism. *Pharmacogenet Genomics*. 2008;18(1):11-24.
274. Schulze RJ, Schott MB, Casey CA, Tuma PL, McNiven MA. The cell biology of the hepatocyte: A membrane trafficking machine. *J Cell Biol*. 2019;218(7):2096-112.
275. Belinskaia DA, Voronina PA, Goncharov NV. Integrative Role of Albumin: Evolutionary, Biochemical and Pathophysiological Aspects. *J Evol Biochem Physiol*. 2021;57(6):1419-48.
276. Rhyu J, Yu R. Newly discovered endocrine functions of the liver. *World J Hepatol*. 2021;13(11):1611-28.
277. Heinz S, Braspenning J. Measurement of Blood Coagulation Factor Synthesis in Cultures of Human Hepatocytes. *Methods Mol Biol*. 2015;1250:309-16.
278. Enjolras N, Plantier JL, Rodriguez MH, Rea M, Attali O, Vinciguerra C, et al. Two novel mutations in EGF-like domains of human factor IX dramatically impair intracellular processing and secretion. *J Thromb Haemost*. 2004;2(7):1143-54.
279. Wolberg AS, Sang Y. Fibrinogen and Factor XIII in Venous Thrombosis and Thrombus Stability. *Arterioscler Thromb Vasc Biol*. 2022;42(8):931-41.

280. Paulusma CC, Lamers WH, Broer S, van de Graaf SFJ. Amino acid metabolism, transport and signalling in the liver revisited. *Biochem Pharmacol.* 2022;201:115074.
281. Darshan D, Vanoaica L, Richman L, Beermann F, Kühn LC. Conditional deletion of ferritin H in mice induces loss of iron storage and liver damage. *Hepatology.* 2009;50(3):852-60.
282. Ehltling C, Wolf SD, Bode JG. Acute-phase protein synthesis: a key feature of innate immune functions of the liver. *Biol Chem.* 2021;402(9):1129-45.
283. Castell JV, Gómez-Lechón MJ, David M, Hirano T, Kishimoto T, Heinrich PC. Recombinant human interleukin-6 (IL-6/BSF-2/HSF) regulates the synthesis of acute phase proteins in human hepatocytes. *FEBS Lett.* 1988;232(2):347-50.
284. Crispe IN. Hepatocytes as Immunological Agents. *J Immunol.* 2016;196(1):17-21.
285. Guillén MI, Gómez-Lechón MJ, Nakamura T, Castell JV. The hepatocyte growth factor regulates the synthesis of acute-phase proteins in human hepatocytes: divergent effect on interleukin-6-stimulated genes. *Hepatology.* 1996;23(6):1345-52.
286. Carrera-Silva EA, Guiñazu N, Pellegrini A, Cano RC, Arocena A, Aoki MP, et al. Correction: Importance of TLR2 on Hepatic Immune and Non-Immune Cells to Attenuate the Strong Inflammatory Liver Response During *Trypanosoma cruzi* Acute Infection. *PLoS Negl Trop Dis.* 2023;17(11):e0011738.
287. Zheng M, Tian Z. Liver-Mediated Adaptive Immune Tolerance. *Front Immunol.* 2019;10:2525.
288. Qian S, Wang Z, Lee Y, Chiang Y, Bonham C, Fung J, et al. Hepatocyte-induced apoptosis of activated T cells, a mechanism of liver transplant tolerance, is related to the expression of ICAM-1 and hepatic lectin. *Transplant Proc.* 2001;33(1-2):226.
289. Venkatakrishnan B, Zlotnick A. The Structural Biology of Hepatitis B Virus: Form and Function. *Annu Rev Virol.* 2016;3(1):429-51.
290. Suhail M, Abdel-Hafiz H, Ali A, Fatima K, Damanhoury GA, Azhar E, et al. Potential mechanisms of hepatitis B virus induced liver injury. *World J Gastroenterol.* 2014;20(35):12462-72.
291. Legaki AI, Moustakas II, Sikorska M, Papadopoulos G, Velliou RI, Chatzigeorgiou A. Hepatocyte Mitochondrial Dynamics and Bioenergetics in Obesity-Related Non-Alcoholic Fatty Liver Disease. *Curr Obes Rep.* 2022;11(3):126-43.
292. Ma X, Qian H, Chen A, Ni HM, Ding WX. Perspectives on Mitochondria-ER and Mitochondria-Lipid Droplet Contact in Hepatocytes and Hepatic Lipid Metabolism. *Cells.* 2021;10(9).
293. Lewis GF, Carpentier AC, Pereira S, Hahn M, Giacca A. Direct and indirect control of hepatic glucose production by insulin. *Cell Metab.* 2021;33(4):709-20.
294. Wasserman DH. Four grams of glucose. *Am J Physiol Endocrinol Metab.* 2009;296(1):E11-21.
295. Tokarz VL, MacDonald PE, Klip A. The cell biology of systemic insulin function. *J Cell Biol.* 2018;217(7):2273-89.
296. Habegger KM. Cross Talk Between Insulin and Glucagon Receptor Signaling in the Hepatocyte. *Diabetes.* 2022;71(9):1842-51.
297. Marušić M, Paić M, Knobloch M, Liberati Pršo AM. NAFLD, Insulin Resistance, and Diabetes Mellitus Type 2. *Can J Gastroenterol Hepatol.* 2021;2021:6613827.
298. Albahrani AA, Greaves RF. Fat-Soluble Vitamins: Clinical Indications and Current Challenges for Chromatographic Measurement. *Clin Biochem Rev.* 2016;37(1):27-47.

299. Licata A, Zerbo M, Como S, Cammilleri M, Soresi M, Montalto G, et al. The Role of Vitamin Deficiency in Liver Disease: To Supplement or Not Supplement? *Nutrients*. 2021;13(11).
300. Peng KY, Barlow CK, Kammoun H, Mellett NA, Weir JM, Murphy AJ, et al. Stable Isotopic Tracer Phospholipidomics Reveals Contributions of Key Phospholipid Biosynthetic Pathways to Low Hepatocyte Phosphatidylcholine to Phosphatidylethanolamine Ratio Induced by Free Fatty Acids. *Metabolites*. 2021;11(3).
301. Song Y, Liu J, Zhao K, Gao L, Zhao J. Cholesterol-induced toxicity: An integrated view of the role of cholesterol in multiple diseases. *Cell Metab*. 2021;33(10):1911-25.
302. Ruiz-Núñez B, Dijck-Brouwer DA, Muskiet FA. The relation of saturated fatty acids with low-grade inflammation and cardiovascular disease. *J Nutr Biochem*. 2016;36:1-20.
303. Kapoor B, Kapoor D, Gautam S, Singh R, Bhardwaj S. Dietary Polyunsaturated Fatty Acids (PUFAs): Uses and Potential Health Benefits. *Curr Nutr Rep*. 2021;10(3):232-42.
304. Britton KA, Massaro JM, Murabito JM, Kreger BE, Hoffmann U, Fox CS. Body fat distribution, incident cardiovascular disease, cancer, and all-cause mortality. *J Am Coll Cardiol*. 2013;62(10):921-5.
305. Hodson L, Gunn PJ. The regulation of hepatic fatty acid synthesis and partitioning: the effect of nutritional state. *Nat Rev Endocrinol*. 2019;15(12):689-700.
306. Pereyra AS, McLaughlin KL, Buddo KA, Ellis JM. Medium-chain fatty acid oxidation is independent of l-carnitine in liver and kidney but not in heart and skeletal muscle. *Am J Physiol Gastrointest Liver Physiol*. 2023;325(4):G287-G94.
307. Hidalgo MA, Carretta MD, Burgos RA. Long Chain Fatty Acids as Modulators of Immune Cells Function: Contribution of FFA1 and FFA4 Receptors. *Front Physiol*. 2021;12:668330.
308. Li H, Yu XH, Ou X, Ouyang XP, Tang CK. Hepatic cholesterol transport and its role in non-alcoholic fatty liver disease and atherosclerosis. *Prog Lipid Res*. 2021;83:101109.
309. Alabi A, Xia XD, Gu HM, Wang F, Deng SJ, Yang N, et al. Membrane type 1 matrix metalloproteinase promotes LDL receptor shedding and accelerates the development of atherosclerosis. *Nat Commun*. 2021;12(1):1889.
310. Cedó L, Fernández-Castillejo S, Rubió L, Metso J, Santos D, Muñoz-Aguayo D, et al. Phenol-Enriched Virgin Olive Oil Promotes Macrophage-Specific Reverse Cholesterol Transport In Vivo. *Biomedicines*. 2020;8(8).
311. Juarez D, Fruman DA. Targeting the Mevalonate Pathway in Cancer. *Trends Cancer*. 2021;7(6):525-40.
312. Heida A, Gruben N, Catrysse L, Koehorst M, Koster M, Kloosterhuis NJ, et al. The hepatocyte IKK:NF- κ B axis promotes liver steatosis by stimulating de novo lipogenesis and cholesterol synthesis. *Mol Metab*. 2021;54:101349.
313. Sanders FW, Griffin JL. De novo lipogenesis in the liver in health and disease: more than just a shunting yard for glucose. *Biol Rev Camb Philos Soc*. 2016;91(2):452-68.
314. Burri L, Thoresen GH, Berge RK. The Role of PPAR α Activation in Liver and Muscle. *PPAR Res*. 2010;2010.
315. Fernández-Alvarez A, Alvarez MS, Gonzalez R, Cucarella C, Muntané J, Casado M. Human SREBP1c expression in liver is directly regulated by peroxisome proliferator-activated receptor alpha (PPAR α). *J Biol Chem*. 2011;286(24):21466-77.
316. Vida M, Serrano A, Romero-Cuevas M, Pavón FJ, González-Rodríguez A, Gavito AL, et al. IL-6 cooperates with peroxisome proliferator-activated receptor- α

- ligands to induce liver fatty acid binding protein (LFABP) up-regulation. *Liver Int.* 2013;33(7):1019-28.
317. Diehl KL, Vorac J, Hofmann K, Meiser P, Unterweger I, Kuerschner L, et al. Kupffer Cells Sense Free Fatty Acids and Regulate Hepatic Lipid Metabolism in High-Fat Diet and Inflammation. *Cells.* 2020;9(10).
318. Gluchowski NL, Becuwe M, Walther TC, Farese RV. Lipid droplets and liver disease: from basic biology to clinical implications. *Nat Rev Gastroenterol Hepatol.* 2017;14(6):343-55.
319. Renne MF, Hariri H. Lipid Droplet-Organelle Contact Sites as Hubs for Fatty Acid Metabolism, Trafficking, and Metabolic Channeling. *Front Cell Dev Biol.* 2021;9:726261.
320. Mashek DG. Hepatic fatty acid trafficking: multiple forks in the road. *Adv Nutr.* 2013;4(6):697-710.
321. Horton JD, Goldstein JL, Brown MS. SREBPs: activators of the complete program of cholesterol and fatty acid synthesis in the liver. *J Clin Invest.* 2002;109(9):1125-31.
322. Nisticò C, Pagliari F, Chiarella E, Fernandes Guerreiro J, Marafioti MG, Aversa I, et al. Lipid Droplet Biosynthesis Impairment through DGAT2 Inhibition Sensitizes MCF7 Breast Cancer Cells to Radiation. *Int J Mol Sci.* 2021;22(18).
323. Greenberg AS, Egan JJ, Wek SA, Garty NB, Blanchette-Mackie EJ, Londos C. Perilipin, a major hormonally regulated adipocyte-specific phosphoprotein associated with the periphery of lipid storage droplets. *J Biol Chem.* 1991;266(17):11341-6.
324. Seebacher F, Zeigerer A, Kory N, Krahmer N. Hepatic lipid droplet homeostasis and fatty liver disease. *Semin Cell Dev Biol.* 2020;108:72-81.
325. Wilfling F, Haas JT, Walther TC, Farese RV. Lipid droplet biogenesis. *Curr Opin Cell Biol.* 2014;29:39-45.
326. Orlicky DJ, Libby AE, Bales ES, McMahan RH, Monks J, La Rosa FG, et al. Perilipin-2 promotes obesity and progressive fatty liver disease in mice through mechanistically distinct hepatocyte and extra-hepatocyte actions. *J Physiol.* 2019;597(6):1565-84.
327. Zhang X, Su L, Sun K. Expression status and prognostic value of the perilipin family of genes in breast cancer. *Am J Transl Res.* 2021;13(5):4450-63.
328. Cao Q, Ruan H, Wang K, Song Z, Bao L, Xu T, et al. Overexpression of PLIN2 is a prognostic marker and attenuates tumor progression in clear cell renal cell carcinoma. *Int J Oncol.* 2018;53(1):137-47.
329. Mashek DG. Hepatic lipid droplets: A balancing act between energy storage and metabolic dysfunction in NAFLD. *Mol Metab.* 2021;50:101115.
330. Kaushik S, Cuervo AM. Degradation of lipid droplet-associated proteins by chaperone-mediated autophagy facilitates lipolysis. *Nat Cell Biol.* 2015;17(6):759-70.
331. Lass A, Zimmermann R, Haemmerle G, Riederer M, Schoiswohl G, Schweiger M, et al. Adipose triglyceride lipase-mediated lipolysis of cellular fat stores is activated by CGI-58 and defective in Chanarin-Dorfman Syndrome. *Cell Metab.* 2006;3(5):309-19.
332. Wu JW, Wang SP, Alvarez F, Casavant S, Gauthier N, Abed L, et al. Deficiency of liver adipose triglyceride lipase in mice causes progressive hepatic steatosis. *Hepatology.* 2011;54(1):122-32.
333. Cui W, Sathyanarayan A, Lopresti M, Aghajan M, Chen C, Mashek DG. Lipophagy-derived fatty acids undergo extracellular efflux via lysosomal exocytosis. *Autophagy.* 2021;17(3):690-705.
334. Gilham D, Alam M, Gao W, Vance DE, Lehner R. Triacylglycerol hydrolase is localized to the endoplasmic reticulum by an unusual retrieval sequence where it

participates in VLDL assembly without utilizing VLDL lipids as substrates. *Mol Biol Cell*. 2005;16(2):984-96.

335. Geng Y, Faber KN, de Meijer VE, Blokzijl H, Moshage H. How does hepatic lipid accumulation lead to lipotoxicity in non-alcoholic fatty liver disease? *Hepatol Int*. 2021;15(1):21-35.

336. Cotter DG, Ercal B, Huang X, Leid JM, d'Avignon DA, Graham MJ, et al. Ketogenesis prevents diet-induced fatty liver injury and hyperglycemia. *J Clin Invest*. 2014;124(12):5175-90.

337. Cotter DG, Ercal B, d'Avignon DA, Dietzen DJ, Crawford PA. Impairments of hepatic gluconeogenesis and ketogenesis in PPAR α -deficient neonatal mice. *Am J Physiol Endocrinol Metab*. 2014;307(2):E176-85.

338. Mooli RGR, Ramakrishnan SK. Emerging Role of Hepatic Ketogenesis in Fatty Liver Disease. *Front Physiol*. 2022;13:946474.

339. Ramakrishnan S, Mooli RGR, Han Y, Fiorenza E, Kumar S, Bello F, et al. Hepatic ketogenesis regulates lipid homeostasis via ACSL1-mediated fatty acid partitioning. *Res Sq*. 2023.

340. Pawlak M, Lefebvre P, Staels B. Molecular mechanism of PPAR α action and its impact on lipid metabolism, inflammation and fibrosis in non-alcoholic fatty liver disease. *J Hepatol*. 2015;62(3):720-33.

341. Fukao T, Lopaschuk GD, Mitchell GA. Pathways and control of ketone body metabolism: on the fringe of lipid biochemistry. *Prostaglandins Leukot Essent Fatty Acids*. 2004;70(3):243-51.

342. Vallejo FA, Shah SS, de Cordoba N, Walters WM, Prince J, Khatib Z, et al. The contribution of ketone bodies to glycolytic inhibition for the treatment of adult and pediatric glioblastoma. *J Neurooncol*. 2020;147(2):317-26.

343. Shukla SK, Gebregiworgis T, Purohit V, Chaika NV, Gunda V, Radhakrishnan P, et al. Metabolic reprogramming induced by ketone bodies diminishes pancreatic cancer cachexia. *Cancer Metab*. 2014;2:18.

344. Hopkins BD, Pauli C, Du X, Wang DG, Li X, Wu D, et al. Publisher Correction: Suppression of insulin feedback enhances the efficacy of PI3K inhibitors. *Nature*. 2018;563(7731):E24.

345. Malla J, Zahra A, Venugopal S, Selvamani TY, Shoukrie SI, Selvaraj R, et al. What Role Do Inflammatory Cytokines Play in Cancer Cachexia? *Cureus*. 2022;14(7):e26798.

346. Zhang L, Han L, He J, Lv J, Pan R, Lv T. A high serum-free fatty acid level is associated with cancer. *J Cancer Res Clin Oncol*. 2020;146(3):705-10.

347. Yang B, Ren XL, Fu YQ, Gao JL, Li D. Ratio of n-3/n-6 PUFAs and risk of breast cancer: a meta-analysis of 274135 adult females from 11 independent prospective studies. *BMC Cancer*. 2014;14:105.

348. Llorente A, Skotland T, Sylv  n T, Kauhanen D, R  g T, Orłowski A, et al. Molecular lipidomics of exosomes released by PC-3 prostate cancer cells. *Biochim Biophys Acta*. 2013;1831(7):1302-9.

349. Mika A, Kobiela J, Czumaj A, Chmielewski M, Stepnowski P, Sledzinski T. Hyper-Elongation in Colorectal Cancer Tissue - Cerotic Acid is a Potential Novel Serum Metabolic Marker of Colorectal Malignancies. *Cell Physiol Biochem*. 2017;41(2):722-30.

350. Li J, Condello S, Thomes-Pepin J, Ma X, Xia Y, Hurley TD, et al. Lipid Desaturation Is a Metabolic Marker and Therapeutic Target of Ovarian Cancer Stem Cells. *Cell Stem Cell*. 2017;20(3):303-14.e5.

351. Swierczynski J, Hebanowska A, Sledzinski T. Role of abnormal lipid metabolism in development, progression, diagnosis and therapy of pancreatic cancer. *World J Gastroenterol*. 2014;20(9):2279-303.

352. Wang G, Li J, Bojmar L, Chen H, Li Z, Tobias GC, et al. Tumour extracellular vesicles and particles induce liver metabolic dysfunction. *Nature*. 2023;618(7964):374-82.
353. Baldrige D, Wangler MF, Bowman AN, Yamamoto S, Schedl T, Pak SC, et al. Model organisms contribute to diagnosis and discovery in the undiagnosed diseases network: current state and a future vision. *Orphanet J Rare Dis*. 2021;16(1):206.
354. Poh WT, Stanslas J. The new paradigm in animal testing - "3Rs alternatives". *Regul Toxicol Pharmacol*. 2024;153:105705.
355. Vandamme TF. Rodent models for human diseases. *Eur J Pharmacol*. 2015;759:84-9.
356. Tuttle AH, Philip VM, Chesler EJ, Mogil JS. Comparing phenotypic variation between inbred and outbred mice. *Nat Methods*. 2018;15(12):994-6.
357. Walrath JC, Hawes JJ, Van Dyke T, Reilly KM. Genetically engineered mouse models in cancer research. *Adv Cancer Res*. 2010;106:113-64.
358. Mohanty S, Heuser M. Mouse Models of Frequently Mutated Genes in Acute Myeloid Leukemia. *Cancers (Basel)*. 2021;13(24).
359. Blanchard Z, Brown EA, Ghazaryan A, Welm AL. PDX models for functional precision oncology and discovery science. *Nat Rev Cancer*. 2024.
360. McCormack E, Bruserud O, Gjertsen BT. Review: genetic models of acute myeloid leukaemia. *Oncogene*. 2008;27(27):3765-79.
361. Lekanne Deprez RH, Riegman PH, Groen NA, Warringa UL, van Biezen NA, Molijn AC, et al. Cloning and characterization of MN1, a gene from chromosome 22q11, which is disrupted by a balanced translocation in a meningioma. *Oncogene*. 1995;10(8):1521-8.
362. Shafik RE, Hassan NM, El Meligui YM, Shafik HE. The Meningioma 1 (MN1) Gene is an Independent Poor Prognostic Factor in Adult Egyptian Acute Myeloid Leukemia Patients. *Asian Pac J Cancer Prev*. 2017;18(3):609-13.
363. Sharma A, Jyotsana N, Gabdoulline R, Heckl D, Kuchenbauer F, Slany RK, et al. Meningioma 1 is indispensable for mixed lineage leukemia-rearranged acute myeloid leukemia. *Haematologica*. 2020;105(5):1294-305.
364. Heuser M, Argiropoulos B, Kuchenbauer F, Yung E, Piper J, Fung S, et al. MN1 overexpression induces acute myeloid leukemia in mice and predicts ATRA resistance in patients with AML. *Blood*. 2007;110(5):1639-47.
365. Grosveld GC. MN1, a novel player in human AML. *Blood Cells Mol Dis*. 2007;39(3):336-9.
366. Shenoy US, Adiga D, Alhedyan F, Kabekkodu SP, Radhakrishnan R. HOXA9 transcription factor is a double-edged sword: from development to cancer progression. *Cancer Metastasis Rev*. 2024;43(2):709-28.
367. Zhou X, Lu R. HOXA9/MEIS1 targets in leukemia: reinforced signaling networks and therapeutic opportunities. *Haematologica*. 2023;108(5):1205-7.
368. Almosailleakh M, Schwaller J. Murine Models of Acute Myeloid Leukaemia. *Int J Mol Sci*. 2019;20(2).
369. Kreitz J, Schönfeld C, Seibert M, Stolp V, Alshamleh I, Oellerich T, et al. Metabolic Plasticity of Acute Myeloid Leukemia. *Cells*. 2019;8(8).
370. Akinduro O, Weber TS, Ang H, Haltalli MLR, Ruivo N, Duarte D, et al. Proliferation dynamics of acute myeloid leukaemia and haematopoietic progenitors competing for bone marrow space. *Nat Commun*. 2018;9(1):519.
371. Pievani A, Donsante S, Tomasoni C, Corsi A, Dazzi F, Biondi A, et al. Acute myeloid leukemia shapes the bone marrow stromal niche. *Haematologica*. 2021;106(3):865-70.

372. Terao Y, Nakayama Y, Abo M, Otobe Y, Suzuki M, Kojima I, et al. Changes in skeletal muscle function during chemotherapy and related factors in patients with acute leukemia. *Support Care Cancer*. 2024;32(8):512.
373. Keng MK, Sidana S, Mukherjee S, Elson P, Seastone DJ, Nazha A, et al. The Degree and Effect Of Weight Loss In Acute Myeloid Leukemia Patients Receiving Induction and Post-Remission Chemotherapy. *Blood*. 2013;122(3889).
374. Tamaki M, Nakasone H, Nakamura Y, Kawamura M, Kawamura S, Takeshita J, et al. Body Weight Loss Before Allogeneic Hematopoietic Stem Cell Transplantation Predicts Survival Outcomes in Acute Leukemia Patients. *Transplant Cell Ther*. 2021;27(4):340.e1-.e6.
375. Stevens BM, Jones CL, Pollyea DA, Culp-Hill R, D'Alessandro A, Winters A, et al. Fatty acid metabolism underlies venetoclax resistance in acute myeloid leukemia stem cells. *Nat Cancer*. 2020;1(12):1176-87.
376. Barisas DAG, Choi K. Extramedullary hematopoiesis in cancer. *Exp Mol Med*. 2024.
377. Qiu P, Wang H, Zhang M, Peng R, Zhao Q, Liu J. FATP2-targeted therapies - A role beyond fatty liver disease. *Pharmacol Res*. 2020;161:105228.
378. Ipsen DH, Lykkesfeldt J, Tveden-Nyborg P. Molecular mechanisms of hepatic lipid accumulation in non-alcoholic fatty liver disease. *Cell Mol Life Sci*. 2018;75(18):3313-27.
379. Khan S, Gaivin R, Abramovich C, Boylan M, Calles J, Schelling JR. Fatty acid transport protein-2 regulates glycemic control and diabetic kidney disease progression. *JCI Insight*. 2020;5(15).
380. Falcon A, Doege H, Fluitt A, Tsang B, Watson N, Kay MA, et al. FATP2 is a hepatic fatty acid transporter and peroxisomal very long-chain acyl-CoA synthetase. *Am J Physiol Endocrinol Metab*. 2010;299(3):E384-93.
381. Chabowski A, Żendzian-Piotrowska M, Konstantynowicz K, Pankiewicz W, Mikłosz A, Łukaszuk B, et al. Fatty acid transporters involved in the palmitate and oleate induced insulin resistance in primary rat hepatocytes. *Acta Physiol (Oxf)*. 2013;207(2):346-57.
382. Arévalo C, Rojas L, Santamaria M, Molina L, Arbeláez L, Sánchez P, et al. Untargeted metabolomic and lipidomic analyses reveal lipid dysregulation in the plasma of acute leukemia patients. *Front Mol Biosci*. 2023;10:1235160.
383. Li Y, Moysich KB, Baer MR, Weiss JR, Brasure J, Graham S, et al. Intakes of selected food groups and beverages and adult acute myeloid leukemia. *Leuk Res*. 2006;30(12):1507-15.
384. Rezae A, Fakak R, Alexander KG, Constantinou C. The Overlooked Association Between Nutrition and the Development of Acute Myeloid Leukaemia: A Scoping Review. *Curr Nutr Rep*. 2024;13(2):113-25.
385. Shi J, Fan J, Su Q, Yang Z. Cytokines and Abnormal Glucose and Lipid Metabolism. *Front Endocrinol (Lausanne)*. 2019;10:703.
386. Lee NK, Sowa H, Hinoi E, Ferron M, Ahn JD, Confavreux C, et al. Endocrine regulation of energy metabolism by the skeleton. *Cell*. 2007;130(3):456-69.
387. Filippi MD. Hungry Hematopoietic Stem Cells during Bacterial Infection: Fatty Acid for Food. *Immunometabolism*. 2022;4(2).
388. Beyer D, Hoff J, Sommerfeld O, Zipprich A, Gaßler N, Press AT. The liver in sepsis: molecular mechanism of liver failure and their potential for clinical translation. *Mol Med*. 2022;28(1):84.
389. Muniz-Santos R, Lucieri-Costa G, de Almeida MAP, Moraes-de-Souza I, Brito MADS, Silva AR, et al. Lipid oxidation dysregulation: an emerging player in the pathophysiology of sepsis. *Front Immunol*. 2023;14:1224335.

390. Peng F, Liang C, Chang W, Sun Q, Xie J, Qiu H, et al. Prognostic Significance of Plasma Hepatocyte Growth Factor in Sepsis. *J Intensive Care Med.* 2022;37(3):352-8.
391. Van Wyngene L, Vanderhaeghen T, Timmermans S, Vandewalle J, Van Looveren K, Souffriau J, et al. Hepatic PPAR α function and lipid metabolic pathways are dysregulated in polymicrobial sepsis. *EMBO Mol Med.* 2020;12(2):e11319.
392. Liu J, Mazzone PJ, Cata JP, Kurz A, Bauer M, Mascha EJ, et al. Serum free fatty acid biomarkers of lung cancer. *Chest.* 2014;146(3):670-9.
393. Fan L, Lin Q, Huang X, Fu D, Huang H. Prognostic significance of pretreatment serum free fatty acid in patients with diffuse large B-cell lymphoma in the rituximab era: a retrospective analysis. *BMC Cancer.* 2021;21(1):1255.
394. Gómez-Lechón MJ, Castelli J, Guillén I, O'Connor E, Nakamura T, Fabra R, et al. Effects of hepatocyte growth factor on the growth and metabolism of human hepatocytes in primary culture. *Hepatology.* 1995;21(5):1248-54.
395. Carey A, Edwards DK, Eide CA, Newell L, Traer E, Medeiros BC, et al. Identification of Interleukin-1 by Functional Screening as a Key Mediator of Cellular Expansion and Disease Progression in Acute Myeloid Leukemia. *Cell Rep.* 2017;18(13):3204-18.
396. Masuo H, Shimizu A, Motoyama H, Kubota K, Notake T, Yoshizawa T, et al. Impact of endothelial nitric oxide synthase activation on accelerated liver regeneration in a rat ALPPS model. *World J Gastroenterol.* 2023;29(5):867-78.
397. Okui T, Hiasa M, Hata K, Roodman GD, Nakanishi M, Yoneda T. The acid-sensing nociceptor TRPV1 controls breast cancer progression in bone via regulating HGF secretion from sensory neurons. *Res Sq.* 2023.
398. Jing Y, Sun Q, Xiong X, Meng R, Tang S, Cao S, et al. Hepatocyte growth factor alleviates hepatic insulin resistance and lipid accumulation in high-fat diet-fed mice. *J Diabetes Investig.* 2019;10(2):251-60.
399. Matsuki T, Horai R, Sudo K, Iwakura Y. IL-1 plays an important role in lipid metabolism by regulating insulin levels under physiological conditions. *J Exp Med.* 2003;198(6):877-88.
400. Andus T, Holstege A. Cytokines and the liver in health and disease. Effects on liver metabolism and fibrogenesis. *Acta Gastroenterol Belg.* 1994;57(3-4):236-44.
401. Todisco S, Santarsiero A, Convertini P, De Stefano G, Gilio M, Iacobazzi V, et al. PPAR Alpha as a Metabolic Modulator of the Liver: Role in the Pathogenesis of Nonalcoholic Steatohepatitis (NASH). *Biology (Basel).* 2022;11(5).
402. Negrin KA, Roth Flach RJ, DiStefano MT, Matevossian A, Friedline RH, Jung D, et al. IL-1 signaling in obesity-induced hepatic lipogenesis and steatosis. *PLoS One.* 2014;9(9):e107265.
403. Appasamy R, Tanabe M, Murase N, Zarnegar R, Venkataramanan R, Van Thiel DH, et al. Hepatocyte growth factor, blood clearance, organ uptake, and biliary excretion in normal and partially hepatectomized rats. *Lab Invest.* 1993;68(3):270-6.
404. Liu C, Chu D, Kalantar-Zadeh K, George J, Young HA, Liu G. Cytokines: From Clinical Significance to Quantification. *Adv Sci (Weinh).* 2021;8(15):e2004433.
405. Ido A, Moriuchi A, Kim I, Numata M, Nagata-Tsubouchi Y, Hasuike S, et al. Pharmacokinetic study of recombinant human hepatocyte growth factor administered in a bolus intravenously or via portal vein. *Hepatol Res.* 2004;30(3):175-81.
406. Tomita K, Azuma T, Kitamura N, Nishida J, Tamiya G, Oka A, et al. Pioglitazone prevents alcohol-induced fatty liver in rats through up-regulation of c-Met. *Gastroenterology.* 2004;126(3):873-85.
407. Tahara M, Matsumoto K, Nukiwa T, Nakamura T. Hepatocyte growth factor leads to recovery from alcohol-induced fatty liver in rats. *J Clin Invest.* 1999;103(3):313-20.

408. Perdomo G, Martinez-Brocca MA, Bhatt BA, Brown NF, O'Doherty RM, Garcia-Ocaña A. Hepatocyte growth factor is a novel stimulator of glucose uptake and metabolism in skeletal muscle cells. *J Biol Chem*. 2008;283(20):13700-6.
409. Domínguez-Pérez M, Nuño-Lámbarri N, Clavijo-Cornejo D, Luna-López A, Souza V, Bucio L, et al. Hepatocyte Growth Factor Reduces Free Cholesterol-Mediated Lipotoxicity in Primary Hepatocytes by Countering Oxidative Stress. *Oxid Med Cell Longev*. 2016;2016:7960386.
410. Muratsu J, Iwabayashi M, Sanada F, Taniyama Y, Otsu R, Rakugi H, et al. Hepatocyte Growth Factor Prevented High-Fat Diet-Induced Obesity and Improved Insulin Resistance in Mice. *Sci Rep*. 2017;7(1):130.
411. Bertola A, Bonnafous S, Cormont M, Anty R, Tanti JF, Tran A, et al. Hepatocyte growth factor induces glucose uptake in 3T3-L1 adipocytes through a Gab1/phosphatidylinositol 3-kinase/Glut4 pathway. *J Biol Chem*. 2007;282(14):10325-32.
412. Bortolini M, Wright MB, Bopst M, Balas B. Examining the safety of PPAR agonists - current trends and future prospects. *Expert Opin Drug Saf*. 2013;12(1):65-79.
413. Kentsis A, Reed C, Rice KL, Sanda T, Rodig SJ, Tholouli E, et al. Autocrine activation of the MET receptor tyrosine kinase in acute myeloid leukemia. *Nat Med*. 2012;18(7):1118-22.
414. Burt R, Dey A, Aref S, Aguiar M, Akarca A, Bailey K, et al. Activated stromal cells transfer mitochondria to rescue acute lymphoblastic leukemia cells from oxidative stress. *Blood*. 2019;134(17):1415-29.
415. Brauer D, Backhaus D, Pointner R, Vucinic V, Niederwieser D, Platzbecker U, et al. Nutritional Status at Diagnosis and Pre-transplant Weight Loss Impact Outcomes of Acute Myeloid Leukemia Patients Following Allogeneic Stem Cell Transplantation. *Hemasphere*. 2021;5(3):e532.
416. Yang S, Lu W, Zhao C, Zhai Y, Wei Y, Liu J, et al. Leukemia cells remodel marrow adipocytes via TRPV4-dependent lipolysis. *Haematologica*. 2020;105(11):2572-83.
417. Lu W, Weng W, Zhu Q, Zhai Y, Wan Y, Liu H, et al. Small bone marrow adipocytes predict poor prognosis in acute myeloid leukemia. *Haematologica*. 2018;103(1):e21-e4.
418. Keaver L, Xu B, Jaccard A, Webber L. Morbid obesity in the UK: A modelling projection study to 2035. *Scand J Public Health*. 2020;48(4):422-7.
419. Li S, Chen L, Jin W, Ma X, Ma Y, Dong F, et al. Influence of body mass index on incidence and prognosis of acute myeloid leukemia and acute promyelocytic leukemia: A meta-analysis. *Sci Rep*. 2017;7(1):17998.
420. Pati S, Irfan W, Jameel A, Ahmed S, Shahid RK. Obesity and Cancer: A Current Overview of Epidemiology, Pathogenesis, Outcomes, and Management. *Cancers (Basel)*. 2023;15(2).
421. Ramdass V, Caskey E, Sklarz T, Ajmeri S, Patel V, Balogun A, et al. Association Between Obesity and Cancer Mortality: An Internal Medicine Outpatient Clinic Perspective. *J Clin Med Res*. 2021;13(7):377-86.
422. Dhakal P, Lyden E, Lee A, Michalski J, Al-Kadhimi ZS, Maness LJ, et al. Effects of Obesity on Overall Survival of Adults With Acute Myeloid Leukemia. *Clin Lymphoma Myeloma Leuk*. 2020;20(3):e131-e6.
423. Yan J, Li S. The role of the liver in sepsis. *Int Rev Immunol*. 2014;33(6):498-510.
424. Moore MP, Cunningham RP, Meers GM, Johnson SA, Wheeler AA, Ganga RR, et al. Compromised hepatic mitochondrial fatty acid oxidation and reduced markers of mitochondrial turnover in human NAFLD. *Hepatology*. 2022;76(5):1452-65.

425. Tsimberidou AM. Targeted therapy in cancer. *Cancer Chemother Pharmacol*. 2015;76(6):1113-32.
426. McGuffee RM, McCommis KS, Ford DA. Etomoxir: an old dog with new tricks. *J Lipid Res*. 2024;65(9):100604.
427. Li M, Li X, Zhang H, Lu Y. Molecular Mechanisms of Metformin for Diabetes and Cancer Treatment. *Front Physiol*. 2018;9:1039.
428. Carvalho-Gontijo R, Han C, Zhang L, Zhang V, Hosseini M, Mekeel K, et al. Metabolic Injury of Hepatocytes Promotes Progression of NAFLD and AALD. *Semin Liver Dis*. 2022;42(3):233-49.
429. Ajaz S, McPhail MJ, Gnudi L, Trovato FM, Mujib S, Napoli S, et al. Mitochondrial dysfunction as a mechanistic biomarker in patients with non-alcoholic fatty liver disease (NAFLD). *Mitochondrion*. 2021;57:119-30.
430. Sun K, Reynolds RJ, Sheu TG, Tomsula JA, Colton L, Rice L. Acute myeloid leukaemia presenting as acute liver failure-a case report and literature review. *Ecancermedicallscience*. 2019;13:960.
431. Mathews E, Laurie T, O'Riordan K, Nabhan C. Liver involvement with acute myeloid leukemia. *Case Rep Gastroenterol*. 2008;2(1):121-4.
432. Spinelli I, De Santis A, Cesini L, Riminucci M, Corsi A, Forlino M, et al. Acute hepatitis-like presentation with cholestasis of CBFβ-MYH11-positive acute myeloid leukemia in an adult male: a case report. *J Med Case Rep*. 2022;16(1):294.
433. Mudd TW, Guddati AK. Management of hepatotoxicity of chemotherapy and targeted agents. *Am J Cancer Res*. 2021;11(7):3461-74.
434. Fu SH, Flannery AH, Thompson Bastin ML. Acute Hepatotoxicity After High-Dose Cytarabine for the Treatment of Relapsed Acute Myeloid Leukemia: A Case Report. *Hosp Pharm*. 2019;54(3):160-4.
435. Meier-Schellersheim M, Varma R, Angermann BR. Mechanistic Models of Cellular Signaling, Cytokine Crosstalk, and Cell-Cell Communication in Immunology. *Front Immunol*. 2019;10:2268.
436. Gerner RR, Wieser V, Moschen AR, Tilg H. Metabolic inflammation: role of cytokines in the crosstalk between adipose tissue and liver. *Can J Physiol Pharmacol*. 2013;91(11):867-72.
437. Liu Z, Cordoba-Chacon J, Kineman RD, Cronstein BN, Muzumdar R, Gong Z, et al. Growth Hormone Control of Hepatic Lipid Metabolism. *Diabetes*. 2016;65(12):3598-609.
438. Guo JR, Li W, Wu Y, Wu LQ, Li X, Guo YF, et al. Hepatocyte growth factor promotes proliferation, invasion, and metastasis of myeloid leukemia cells through PI3K-AKT and MAPK/ERK signaling pathway. *Am J Transl Res*. 2016;8(9):3630-44.
439. Nunn AV, Bell J, Barter P. The integration of lipid-sensing and anti-inflammatory effects: how the PPARs play a role in metabolic balance. *Nucl Recept*. 2007;5(1):1.
440. Zhou H, Jiang Y, Huang Y, Zhong M, Qin D, Xie C, et al. Therapeutic inhibition of PPARα-HIF1α-PGK1 signaling targets leukemia stem and progenitor cells in acute myeloid leukemia. *Cancer Lett*. 2023;554:215997.
441. Esmaeili S, Salari S, Kaveh V, Ghaffari SH, Bashash D. Alteration of PPAR-GAMMA (PPARG; PPARγ) and PTEN gene expression in acute myeloid leukemia patients and the promising anticancer effects of PPARγ stimulation using pioglitazone on AML cells. *Mol Genet Genomic Med*. 2021;9(11):e1818.
442. Chute JP, Ross JR, McDonnell DP. Minireview: Nuclear receptors, hematopoiesis, and stem cells. *Mol Endocrinol*. 2010;24(1):1-10.
443. Sekine K, Fujishima S, Aikawa N. Plasma hepatocyte growth factor is increased in early-phase sepsis. *J Infect Chemother*. 2004;10(2):110-4.

444. Siapati EK, Roubelakis MG, Vassilopoulos G. Liver Regeneration by Hematopoietic Stem Cells: Have We Reached the End of the Road? *Cells*. 2022;11(15).
445. Mizuno S, Nakamura T. Improvement of sepsis by hepatocyte growth factor, an anti-inflammatory regulator: emerging insights and therapeutic potential. *Gastroenterol Res Pract*. 2012;2012:909350.
446. Lamszus K, Laterra J, Westphal M, Rosen EM. Scatter factor/hepatocyte growth factor (SF/HGF) content and function in human gliomas. *Int J Dev Neurosci*. 1999;17(5-6):517-30.
447. Sheen-Chen SM, Liu YW, Eng HL, Chou FF. Serum levels of hepatocyte growth factor in patients with breast cancer. *Cancer Epidemiol Biomarkers Prev*. 2005;14(3):715-7.
448. Tsuji T, Sakamori Y, Ozasa H, Yagi Y, Ajimizu H, Yasuda Y, et al. Clinical impact of high serum hepatocyte growth factor in advanced non-small cell lung cancer. *Oncotarget*. 2017;8(42):71805-16.
449. Schmidt C, Bladt F, Goedecke S, Brinkmann V, Zschesche W, Sharpe M, et al. Scatter factor/hepatocyte growth factor is essential for liver development. *Nature*. 1995;373(6516):699-702.
450. Kosai K, Matsumoto K, Nagata S, Tsujimoto Y, Nakamura T. Abrogation of Fas-induced fulminant hepatic failure in mice by hepatocyte growth factor. *Biochem Biophys Res Commun*. 1998;244(3):683-90.
451. Ishiki Y, Ohnishi H, Muto Y, Matsumoto K, Nakamura T. Direct evidence that hepatocyte growth factor is a hepatotrophic factor for liver regeneration and has a potent antihepatitis effect in vivo. *Hepatology*. 1992;16(5):1227-35.
452. Wang H, Keiser JA. Hepatocyte growth factor enhances MMP activity in human endothelial cells. *Biochem Biophys Res Commun*. 2000;272(3):900-5.
453. Maina F, Klein R. Hepatocyte growth factor, a versatile signal for developing neurons. *Nat Neurosci*. 1999;2(3):213-7.
454. Little MH, McMahon AP. Mammalian kidney development: principles, progress, and projections. *Cold Spring Harb Perspect Biol*. 2012;4(5).
455. Nakamura T, Sakai K, Matsumoto K. Hepatocyte growth factor twenty years on: Much more than a growth factor. *J Gastroenterol Hepatol*. 2011;26 Suppl 1:188-202.
456. Hjorth-Hansen H, Seidel C, Lamvik J, Børset M, Sundan A, Waage A. Elevated serum concentrations of hepatocyte growth factor in acute myelocytic leukaemia. *Eur J Haematol*. 1999;62(2):129-34.
457. Tarhini AA, Rafique I, Floros T, Tran P, Gooding WE, Villaruz LC, et al. Phase 1/2 study of rilotumumab (AMG 102), a hepatocyte growth factor inhibitor, and erlotinib in patients with advanced non-small cell lung cancer. *Cancer*. 2017;123(15):2936-44.
458. Kim J, Lee TS, Lee MH, Cho IR, Ryu JK, Kim YT, et al. Pancreatic Cancer Treatment Targeting the HGF/c-MET Pathway: The MEK Inhibitor Trametinib. *Cancers (Basel)*. 2024;16(5).
459. Catenacci DVT, Tebbutt NC, Davidenko I, Murad AM, Al-Batran SE, Ilson DH, et al. Rilotumumab plus epirubicin, cisplatin, and capecitabine as first-line therapy in advanced MET-positive gastric or gastro-oesophageal junction cancer (RILOMET-1): a randomised, double-blind, placebo-controlled, phase 3 trial. *Lancet Oncol*. 2017;18(11):1467-82.
460. D'Orio B, Fracassi A, Ceru MP, Moreno S. Targeting PPARalpha in Alzheimer's Disease. *Curr Alzheimer Res*. 2018;15(4):345-54.
461. Mendes M, Monteiro AC, Neto E, Barrias CC, Sobrinho-Simões MA, Duarte D, et al. Transforming the Niche: The Emerging Role of Extracellular Vesicles in Acute Myeloid Leukaemia Progression. *Int J Mol Sci*. 2024;25(8).

462. Lagadinou ED, Sach A, Callahan K, Rossi RM, Neering SJ, Minhajuddin M, et al. BCL-2 inhibition targets oxidative phosphorylation and selectively eradicates quiescent human leukemia stem cells. *Cell Stem Cell*. 2013;12(3):329-41.
463. Xie C, Zhou H, Qin D, Zheng H, Tang Y, Li W, et al. Bcl-2 inhibition combined with PPAR α activation synergistically targets leukemic stem cell-like cells in acute myeloid leukemia. *Cell Death Dis*. 2023;14(8):573.
464. Arber DA, Orazi A, Hasserjian RP, Borowitz MJ, Calvo KR, Kvasnicka HM, et al. International Consensus Classification of Myeloid Neoplasms and Acute Leukemias: integrating morphologic, clinical, and genomic data. *Blood*. 2022;140(11):1200-28.
465. Jen WY, Kantarjian H, Kadia TM, DiNardo CD, Issa GC, Short NJ, et al. Combination therapy with novel agents for acute myeloid leukaemia: Insights into treatment of a heterogenous disease. *Br J Haematol*. 2024.
466. Arend WP, Malyak M, Guthridge CJ, Gabay C. Interleukin-1 receptor antagonist: role in biology. *Annu Rev Immunol*. 1998;16:27-55.
467. Kim MS, Sweeney TR, Shigenaga JK, Chui LG, Moser A, Grunfeld C, et al. Tumor necrosis factor and interleukin 1 decrease RXR α , PPAR α , PPAR γ , LXRA α , and the coactivators SRC-1, PGC-1 α , and PGC-1 β in liver cells. *Metabolism*. 2007;56(2):267-79.
468. Geiling B, Vandal G, Posner AR, de Bruyns A, Dutchak KL, Garnett S, et al. A modular lentiviral and retroviral construction system to rapidly generate vectors for gene expression and gene knockdown in vitro and in vivo. *PLoS One*. 2013;8(10):e76279.
469. Safran M, Kim WY, Kung AL, Horner JW, DePinho RA, Kaelin WG. Mouse reporter strain for noninvasive bioluminescent imaging of cells that have undergone Cre-mediated recombination. *Mol Imaging*. 2003;2(4):297-302.
470. Gislason MH, Demircan GS, Prachar M, Furtwängler B, Schwaller J, Schoof EM, et al. BloodSpot 3.0: a database of gene and protein expression data in normal and malignant haematopoiesis. *Nucleic Acids Res*. 2024;52(D1):D1138-D42.
471. The Cancer Genome Atlas National Cancer Institute2019 [Available from: <https://www.cancer.gov/ccg/research/genome-sequencing/tcga/using-tcga-data>].
472. Hassan N, Yang J, Wang JY. An Improved Protocol for Establishment of AML Patient-Derived Xenograft Models. *STAR Protoc*. 2020;1(3):100156.
473. Gieseck RL, Vallier L, Hannan NR. Generation of Hepatocytes from Pluripotent Stem Cells for Drug Screening and Developmental Modeling. *Methods Mol Biol*. 2015;1250:123-42.
474. Boden G. Obesity and free fatty acids. *Endocrinol Metab Clin North Am*. 2008;37(3):635-46, viii-ix.
475. Mishra M, Wu J, Kane AE, Howlett SE. The intersection of frailty and metabolism. *Cell Metab*. 2024;36(5):893-911.
476. Morgan ET. Impact of infectious and inflammatory disease on cytochrome P450-mediated drug metabolism and pharmacokinetics. *Clin Pharmacol Ther*. 2009;85(4):434-8.
477. Braeuning A, Schwarz M. Regulation of expression of drug-metabolizing enzymes by oncogenic signaling pathways in liver tumors: a review. *Acta Pharm Sin B*. 2020;10(1):113-22.
478. Pan Y, Wang C, Zhou W, Shi Y, Meng X, Muhammad Y, et al. Inhibiting AGTR1 reduces AML burden and protects the heart from cardiotoxicity in mouse models. *Sci Transl Med*. 2024;16(752):eadl5931.
479. Kattih B, Shirvani A, Klement P, Garrido AM, Gabdoulline R, Liebich A, et al. IDH1/2 mutations in acute myeloid leukemia patients and risk of coronary artery disease and cardiac dysfunction-a retrospective propensity score analysis. *Leukemia*. 2021;35(5):1301-16.

480. Trapani D, Zagami P, Nicolò E, Pravettoni G, Curigliano G. Management of Cardiac Toxicity Induced by Chemotherapy. *J Clin Med*. 2020;9(9).
481. Wang L, Tan TC, Halpern EF, Neilan TG, Francis SA, Picard MH, et al. Major Cardiac Events and the Value of Echocardiographic Evaluation in Patients Receiving Anthracycline-Based Chemotherapy. *Am J Cardiol*. 2015;116(3):442-6.
482. Hibler E, Tanaka Y, Akhter N, Murphy K, Perlman K, Lloyd-Jones D, et al. Risk of Incident Heart Failure Among Young Adult Cancer Survivors. *JACC CardioOncol*. 2023;5(4):539-41.
483. Assuncao BMBL, Handschumacher MD, Brunner AM, Yucel E, Bartko PE, Cheng KH, et al. Acute Leukemia is Associated with Cardiac Alterations before Chemotherapy. *J Am Soc Echocardiogr*. 2017;30(11):1111-8.
484. Kerr M, Dodd MS, Heather LC. The 'Goldilocks zone' of fatty acid metabolism; to ensure that the relationship with cardiac function is just right. *Clin Sci (Lond)*. 2017;131(16):2079-94.